Improvement of the Properties of Novel Bioplastics Through Reactive Compatibilization

A Thesis Submitted for the Degree of Doctor of Philosophy

by
Arjang Amini Shahsavarani

Wolfson Centre for Materials Processing and Centre
for Phosphors and Display Materials
Brunel University
September 2016

Abstract

Bioplastics are emerging as most promising materials to replace oil based thermoplastics particularly in packaging. Bioplastics can mitigate and address concerns about the negative role of plastics in the environment creating pollution and depleting resources hence bioplastics can enable an innovative approach toward addressing these issues. However, manufacturing of bioplastic is still costly and their mechanical and thermal properties require extensive development. Therefore there has been substantial interest to improve processing and properties of bioplastics to diminish the environmental impacts caused by continuous use of synthetic polymers of petroleum origin.

In this research, Poly (3-hydroxybutyrate-co-3-hydroxyvalerate) or PHBV and Polybutylene succinate (PBS) composites and blends were developed to improve the properties of PHBV as the matrix polymer and hence produce a novel formulation for product development. Three approaches were studied in this work:

- The effect of talcum powder as a nucleating agent and reinforcing filler.
- The effect of oligomer chain extenders on miscibility, crystallinity, thermal and thermomechanical, mechanical and morphological properties of PHBV/PBS blends.
- The effect of acrylic core-shell impact modifier on crystallinity, thermal and thermomechanical, mechanical and morphological properties of PHBV were also evaluated.

All the above scientific approaches have been studied. It was noticed that talc can change the sluggish crystallinity of PHBV. Talc enhances nucleation of PHBV in the composites which leads to a faster crystallization rate. The heat distortion temperature, crystallinity and the modulus of PHBV/talc composite were also increased.

In the presence of the chain extender (CE) the miscibility conditions of PHBV/PBS blends were changed. The results were supported by calculation of the activation energies. The elongation at break and tensile strength of PHBV/PBS/Chain extender blends increased indicating miscibility change. The possible reaction mechanism between PHBV, PBS and CE are proposed and the results supported by using FTIR. Immiscibility results of the PHBV/PBS blends are supported by SEM images.

Addition of the impact modifier to PHBV reduced the crystallization rate and prolonged crystallization time. It has been found that the shell of impact modifier (PMMA) is partially miscible with PHBV. The absorbed impact energy is improved by the impact modifier but the improvement was not as satisfactory as results noted for PLA. The SEM images showed the average fine dispersion of different sized particles inside the matrix.

Key words: Poly (3-hydroxybutyrate-co-3-hydroxyvalerate) [PHBV], Polybutylene Succinate (PBS), Chain Extender, Talc, Acrylic core-shell impact modifier, biocomposite, Reactive Extrusion

Acknowledgements

I would like to express my deepest appreciation to my supervisors; Professor Karnik Tarverdi and Dr. Peter Allan. They have been my greatest supporter during the intense time of my study. Their practical experiences, considerable patience and utmost knowledge have been richly supporting me in the last four years.

I am using this opportunity to express my gratitude to everyone in Wolfson centre for material processing, and Experimental Technique Centre at Brunel University who supported me throughout my PhD. I am thankful for their aspiring guidance, invaluably constructive criticism and friendly advice during those years. I would like to thank Prof. Paul A. Sermon for the all kind helps during the correction of this thesis. I would like to thank Wolfson's technicians, Mr. Abdul Ghani and Mr. Steve Ferris for their great help. I would like to express my gratitude to Prof. Jack Silver and Brunel University for the kind financial support of my project.

The completion of my PhD could not have been accomplished without the support of my dearest sister Arghavan Amini who always has been a great strength and encourage for me. I would like to use this opportunity and thank my father, Dr. Abbas Amini whose aspiration has always been encouraging me during my work.

I would like to dedicate this work to the memory of my beloved Mother…

List of contents

Chapter 2

Literature Review

Chapter 3

Talc as a nucleating agent and reinforcement filler for PHBV

Chapter 4

Miscibility, crystallinity and mechanical properties of biodegradable blends of PHBV/PBS and its compatibilized blend by chain extender

Chapter 5

Effect of the core-shell structure impact modifier on mechanical, thermal, crystallization and morphology of PHBV

Chapter 6

List of tables

List of figures

List of abbreviations

Abbreviation	Explanations
ABS	Acrylonitrile-Butadiene-Styrene Rubber
CE	Chain Extender
CTE	Coefficient of Thermal Expansion
CP	Chloroprene Rubber
DEFRA	Department for Environment Food & Rural Affairs
EPDM	Ethylene Propylene Diene Monomer (M-class) Rubber
ENR	Epoxidized natural rubber
FTIR	Fourier Transform Infrared
HDPE	High Density Polyethylene
HDT	Heat Distortion Temperature
HIPS	High impact polystyrene
ICI	Imperial Chemical Industries
IM	Impact Modifier
IR	Infrared
LCA	Life Cycle Assessment
LDPE	Low Density Polyethylene
MW	Molecular Weight
PAA	Polyacrylic Acid
PBAT	Polybutyrate Adipate Terephthalate
PB	Polybutadiene
PBA	Polybutyleacrylate
PBS	Polybutylene succinate
PC	Polycarbonate
PEA	Polyethylacrylate
PET	Polyethylene terephthalate
PHA	Polyhydroxyalkanoate
PHB	Poly (hydroxybutyrate)
PHBV	Poly (3-hydroxybutyrate-co-3-hydroxyvalerate)
PLA	Polylactic acid
POM	Polyoxymethylene
PP	Polypropylene
PS	Polystyrene
PVA	Polyvinyl alcohol
PVDF	Poly (Vinylidene Fluoride)
SE:	Sustainable Development
SPC	The Sustainable Packaging Coalition
TPS	Thermoplastic Starch
TPU	Thermoplastic Polyurethane Carboxylated Poly (ϵ -Caprolactone)
XPCL:	

Research Objectives

There were several initial aims for the research in this PhD.

- To design experimental trials with conventional plastic processing machinery such as extrusion, injection moulding and compression moulding with bio-polyesters in order to obtain satisfactory test specimens

- To study thermal, mechanical and morphology of different grades of bio-polyesters and its composites processed in the conventional plastic processing machinery.

- To conduct experimental processing trials with conventional plastic processing machinery as follows:

    1. Compounding of the bio-polyester with the reinforcement filler using twin screw extruder
    2. Compounding of the bio-polyesters using twin screw extruder
    3. Compounding of the bio-polyesters with chain extenders through reactive blending using twin screw extruder
    4. Compounding of the bio-polyesters with the encapsulated core-shell impact modifier through reactive blending using twin screw extruder
    5. injection moulding of the extruded pellets

- Characterizing of the moulded specimens by DSC, TGA, XRD, FTIR, SEM & TEM, DMA, tensile and flexural testing, drop-weight impact testing

- Evaluating the effect of reinforcement filler on the thermal and mechanical properties, crystallinity and morphological properties of bio-polyester composite.

- Investigating the effect of low modulus bio-polyesters on the miscibility, thermal and mechanical properties, crystallinity and morphology of biodegradable compounds.

- Evaluating the effect of chain extenders on the miscibility, thermal and mechanical properties, crystallinity and morphology of bio-polyester compounds.

- Evaluating the effect of the core-shell structure oligomer on the miscibility, thermal and mechanical properties, crystallinity and morphological properties of bio-polyester compounds.

Original contribution to knowledge

The following areas of research that are original contribution to the knowledge are:

- Processing of low cost composite based on Poly (3-hydroxybutyrate-co-3-hydroxyvalerate) PHBV material reinforced by talcum powder as a mineral filler and nucleating agent by twin-screw extrusion and injection moulding processes and the investigation of crystallinity, thermal, thermomechanical, mechanical and morphological properties on a laboratory scale.

- Blending of low cost fully biodegradable compound based on PHBV and polybutylene succinate (PBS) materials by twin-screw extrusion and injection moulding processes and the investigation of crystallinity, thermal, thermomechanical, mechanical, chemical structure and morphological properties of specimens on a laboratory scale.

- Altering the miscibility condition of PHBV/PBS compounds in the presence of a commercial multi-functional oligomer chain extender and the investigation of crystallinity, thermal, thermomechanical, mechanical, structural (chemical) and morphological properties of specimens on a laboratory scale.

- Examination of incorporating commercial core-shell impact modifier in PHBV matrix and the investigation of crystallinity, thermal, thermomechanical, mechanical, structural (chemical) and morphological properties of specimens on a laboratory scale.

Chapter 1

Introduction

1.1 Sustainable development, waste management and polymer issues

"All sustainable design practices are ultimately cost saving, hence always considered, always recommended"
Anonymous

1.1.1 The birth of a concept

In 1970s, the headline of newspapers was full of sentences like the existing pattern of the resource consumption will consequences to a disaster in the world system within the next century. This ideology led to widespread acceptance of the depletion of resources as a central environmental, economic and political issue. However, this pessimistic anticipation has become false and the collapse of the oil prices in 1986 obstructed the era of recourse dreadful. But it was unwittingly good fortune that the policies considered widely after 1973 which have helped address a problem that no one anticipated. But even if environmentalists were wrong in the 1970s about imminent oil depletion, they were right that unchecked growth in petroleum consumption could endanger the planet and new concern over the future of the global environment start to emerge after that era.

In 1982, The International Union for Conservation of Nature and Natural Resources (IUCN) organized the Conservation for Development Centre to support the project which integrates nature conservation in their development policies and over the years they supported the development of the national conservation strategies in the 30 countries. It was the birth of *Sustainable Development* concept.

Later by, the idea of *The Sustainable Development* has become more embraced by the professionals when the World Commission on Environment and Development (WCED), or also known as the Brundtland Commission's defined the term as: "development that meets the needs of the present without compromising the ability of future generations to meet their own needs" (Azapagic, Emsley, and Hamerton, 2003).

Since then, the concept of *The Sustainable Development* has been discussed and elaborated more than any other concept in the strategies from an accurate detailed approach to a holistic abroad approach from the small firms to the international collaboration associations. In spite of all elaboration, the sustainable development consists of three major components; Economy, Society, Environment, figure 1 illustrates the concept:

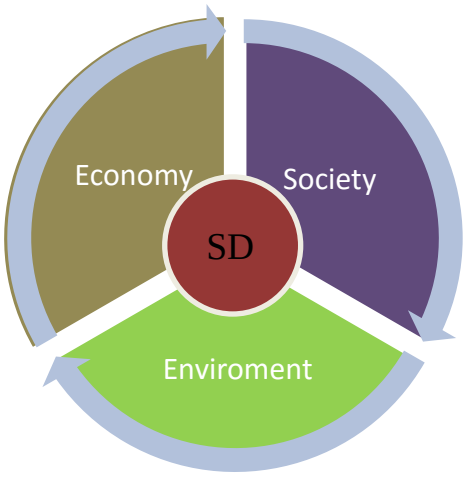

Figure 1-1 Sustainable development components

Figure 1-1 shows that for achieving to a sustainable development, three components should always be fulfilled and satisfied.

Therefore, the concept of the sustainable development has become more and more important to address for any type of strategy. Sustainable development in its holistic approach, require addressing some major issues. Issues like the global inequity and undeniable poverty have tremendous effect on all three components of sustainable development, even equal impact at the environmental damages. Thus the global environment is not only threatened by the climate change or lack of biodiversity, but also there are different complicated aspects which

all connected in a matrix. It is vital to identify the causes of unsustainability and address them with substantial, holistic solutions. For instance, one of major challenges that threaten the daily life of the global environment is waste management.

1.1.2 The price of the crude oil and renewable resources plastics

There is not any doubt that "peak oil" means "peak plastic", since plastics are made mostly from the crude oil or the natural gas. Thus, biopolymers have attracted more attention particularly in the era of resource scarcity. However, the sustainability and the feasibility of biopolymer production have a strong relation with the fluctuation and the production of the fossil fuels and its price.

Bioplastics have low mechanical and thermal properties. These poor performances along with their high prices hinder the expanded usage of these materials as well as the effort for improving their properties.

Global demand for crude oil has risen from 82.5m barrels per day in 2004 to an estimated 87.2m barrels in 2008. Supply has kept pace rising from 83.4m to 87.3m. Demand in emerging economies is up to 5.2m barrels per day of which China accounts for 1.5m.

BP's Statistical Review of the oil market published in June 2008 states that the proven world oil reserves are 1.24 trillion barrels which on current production is sufficient for 41 years.
The price of the all synthetic polymers is a linear function of the price of crude oil. In years, when a barrel of oil cost less than US$40, the use of corn ethanol or soy bean for composite producing sounded fantastic and environmentally friendly approaches but in economic terms, it is definitely unfeasible considering the low price of petroleum based products.

The prediction of oil prices in future is not possible due to the variable factors which can affect the prices such as sudden political movement. However, some kinds of the forecasts could be done based on depletion/extraction of reserves and security of supply. In fact, the world's oil resource not running out in the near future, but rather countries ability to produce high-quality cheap and the economically extractable oil on demand is declining . It is now

clear that the rate at which world oil producers can extract oil is reaching the maximum level possible. This is what is meant by Peak Oil (Kosior, Braganca and Fowler, 2006).

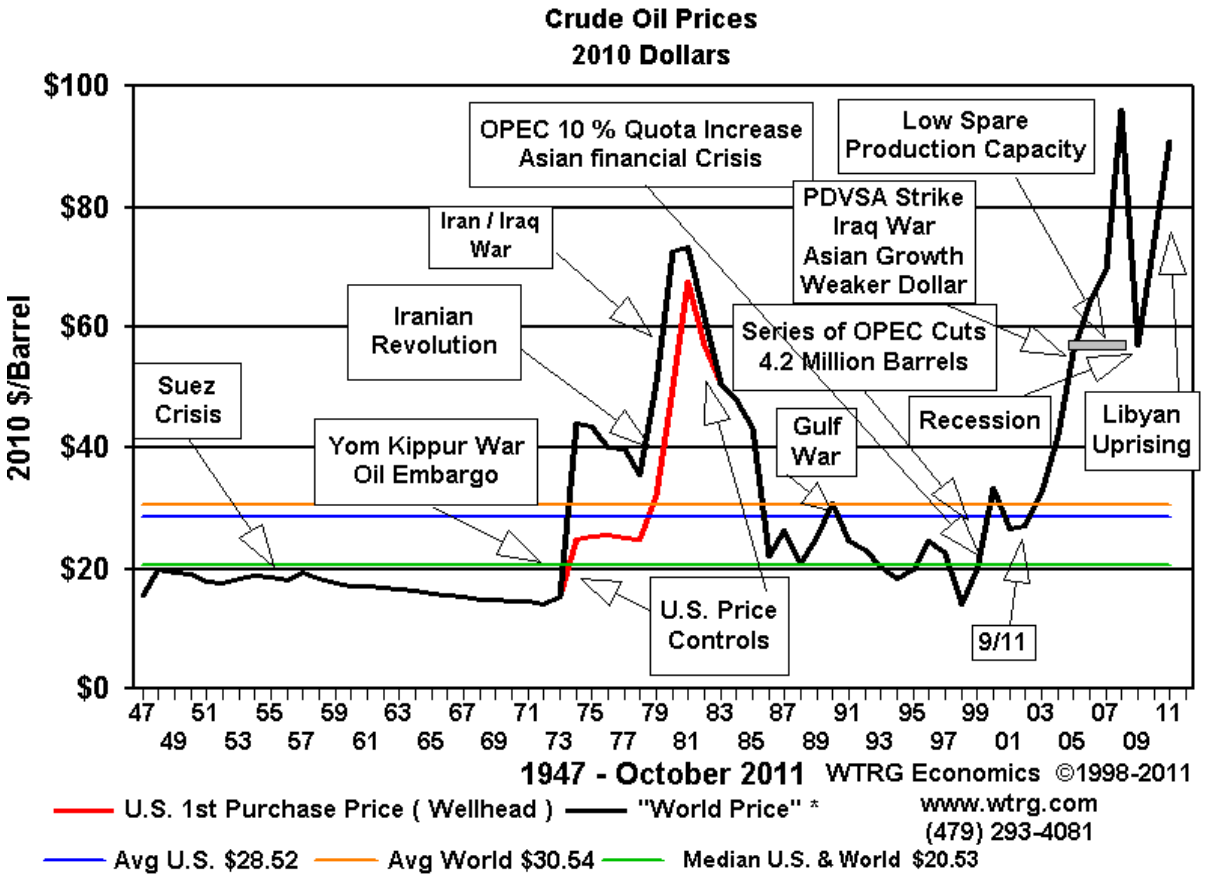

Figure 2-1 the variation of crude oil prices from 1947-Octobre 2011(Kosior, Braganca, Fowler, 2006)

The Optimistic analysers such as Massachusetts Institute of Technology estimate that the oil peak has still future to go because that possible production/depletion of oil is mostly the function of the innovative technical achievement which would allow a better exploitation of using the resources while progressing in times (Kosior, Braganca and Fowler, 2006).

On the other hand, with a pessimistic perspective Association for the Study of Peak Oil and Gas (ASPO) believes that the production already reached the peak at 2004(Figure 2-1)

United State Geological Survey (USGS) has a fair view compared to those at above, which forecasted that there would be enough oil reserves to stand in the current rates of production between years of 2050 to 2100 and peak of oil production would occur around the year 2037.

Government legislation and incentives are driving companies to shift to greener portfolio, and many companies have mandated increased use of "renewably sourced" materials in their products. Moreover, major companies continue to develop their sustainable brand image aimed at the new "circular economy" consumers (i.e., design in bioplastics, product reuse, material recyclability, greenhouse gas footprint reduction) versus the current linear economy (i.e., make, use, discard) which is strongly believed unsustainable (Rosato, 2015).

However, despite the lower oil prices, the renewable market is growing.it seems the link between the oil and the renewable is weakening. Although it is more applicable to renewable resource energy market but it can apply to bio-plastics too. It could be justified by four main reasons:

- They operate in different market: Only 4% of the world's oil reserves are allocated to polymer manufacturing and it accounts for less than 1 percent of power generation in the United States and Canada and not much more in Europe. Oil is mostly used for transportation rather than energy and material conversion and renewable are more for electricity generation.

- The economics of renewables are improving

- The global dynamics of energy are changing

- The science is improving (Nyquist, 2015).

1.1.3 Innovation and sustainability development

"Biodegradable plastics are one of the most innovative materials being developed in the packaging industry. How widespread bioplastics will be used all depends on how strongly society embraces and believes in environmental preservation" (El-Kadi, 2010)

One of the highlight of the DEFRA report in 2011 has been about utter resolution and commitment of coalition government in UK to the sustainability development. Nowadays, it has become obvious that sustainably development (SD) is not just a green movement or a political jest; it is in fact the core of any strategy or policy in the hierarchy of any organisation, private or public comprises the sustainability strategy. It is absolutely vital to define correctly and accurately in order to be efficient. Although it always promote as a holistic approach in strategy, but when it comes in terms of a pragmatic plan, issues are emerging one by one maybe because we can't predict the future accurately. Moreover, changing of some conditions can change the basic assumptions dramatically, for instance something like oil price fluctuation or financial crisis within the last years. However, it is still possible to design a conceptual framework, in a better word, a flowing conceptual framework, and the core of its development belongs to innovation.

The relation between innovation and sustainability is quite complex. The definition of sustainability technically changes all the time because we are becoming more innovative, finding new solutions, and testing new materials that push the envelope all the time on what can be done. However, it makes the definition of sustainability more and more complicated due to the unbalance multicomponent aspects which require satisfying simultaneously.

Sustainability based on definition is a constant stream. When a component changes it should be considered that what it might alter other components and also affect outside of the stream.

Nonetheless, Sustainability's goal achievement has become the next great innovation in business. As sustainability continues to grow in importance for consumers, companies are seeking ways to minimize the environmental impact of everything they do. Even though, the consumers are not asking, industry should be ready to answer "what is sustainability?"(Azapagic, Emsley, and Hamerton, 2003).

SPC (The Sustainable Packaging Coalition) a leading organization for packaging industry, presenting the criteria which addresses board of sustainability and industrial ecology objectives as well as business rules and methods for challenge with environmental concerns through life cycle of packaging. If these criteria are considered carefully packaging materials or generally packaging could be able to transform into a closed loop flow of materials located in a sophisticated system which satisfy three components of sustainability development.
SPC defines those criteria as:

- For individual and communities provide benefit, health throughout its life cycle
- The performance and cost comply with market drive
- Is sourced, manufactured, transported, and recycled using renewable energy;
- Optimizes the use of renewable or recycled source materials;
- Is manufactured using clean production technologies and best practices
- Is made from materials healthy throughout the life cycle
- Is physically designed to optimize materials and energy
- Is sufficiently recovered and utilized closed loop cycles process "(SPC, 2011)

1.1.4 Polymer & Waste management

In 2012, the total waste generated in the 28 countries in Europe by all economic activities and households added up to 2 514 million tonnes; this was slightly higher than in 2010 and 2008 (2 460 million tonnes and 2 427 million tonnes) but lower than in 2004(2 565 million tonnes) (Eurostat, 2016).

There is no doubt that the landfill capacity is decreasing and the impact of municipal buried waste on the environment is undeniable.

Approximately, in industrial countries plastic accounts for 7-8% by weight and nearly 20% by volume of the municipal solid waste (IPCS, 2016)

And when we talk about plastic waste, Packaging industry is in front row. Except paper-based product, packaging materials particularly food packaging products have traditionally been based on non-renewable materials. Until the beginning of the twentieth century, packaging materials and other industrial products were made from biologically derived resources. Twentieth century, was the era of petroleum based products. Now, at the beginning of the twenty-first century, sustainability based thinking, due to economic forces as well as political factors and technological advances, and environmental concerns, the pendulum swing back to the bio plastics.

Today, we can practically guarantee that yesterday's packaging is going to be here in thousand years, but in fact instead of that what we should try to guarantee is that our descendants, our children's children, will be living happily and in harmony with a healthy earth (Ted, 2010).

1.1.5 Marine Debris

A message in a bottle, a familiar image for all of us, remind us our gigantic beautiful oceans and seas are too small where a bottle can travel through, but now world even looks smaller when a familiar product with its famous brand or traces of that slowly comes to the shore in front of our feet far from their birthplaces. Unfortunately for humans, Marine environment worldwide are polluted with man-made debris. Plastic products are dominating the marine debris on a global basis. Given the scale of this problem, a report by the Ellen MacArthur Foundation published in January 2016 predicted that, at the current rate, the world's oceans could contain more plastic than fish by weight by 2050 (Daniel, 2016). Plastic debris is absolutely harmful; it affects the fishing and tourism industry, destroys the marine life, and releases dangerous chemical substances and can represent a threat to human health. Debris in the ocean spreads all over the world from pole to equator and shorelines, estuaries and the sea surface to ocean floor.(Barnes *et al* 2009, Browne *et al* ,2011)
In 2012, The California Department of Toxic Substances Control and California Department of Resources Recycling and Recovery (CalRecycle) published a research study with the

California State University Chico Research Foundation about investigating the biodegradation of polylactic acid (PLA) and polyhydroxyalkanoate (PHA) in the marine environment and to determine any sub chemical intermediates that might be generated during biodegradation. All tests were conducted per (ASTM) standards for biodegradation test method in the marine environment. According to their report After 12 months, the biodegradation results showed 2 types of PHA specimens 52 percent and 82 percent of samples and 52 percent of cellulose sample (positive control) biodegraded into carbon dioxide. Also it was mentioned that for 8 percent conversion of the PLA sample and 6 percent of the low density polyethylene (LDPE) plastic bag (negative control) biodegraded into carbon dioxide. However, neither PLA nor polyethylenes are biodegradable in the marine environment as it has been declared by producers and they just tested for comparison between different types of biopolymers (Calrecycle, 2012).

1.1.6 Bioplastics as innovative materials

In food packaging using biodegradable material still is a hot trend for industry. Companies innovative strategies try to attract the consumer awareness and reducing the carbon footprint based on the legislation pressure from government. However, the terms of sustainability or environmental friendly for biodegradable packaging are still a controversial claim. Therefore, designers tend to focus on the waste reduction and improving of the 3R concept of their products: Renewability, Recyclability and Reusability. With analysis approach of different countries to the use and disposal of the packaging material based on their specific legislative could help having an optimised framework for ending the life of packaging. Countries applying charges on plastic bags in supermarkets have seen a dramatic decline in plastic bag taken from supermarkets and hence UK also expects to witness similar outcome by legalizing 5p charges for plastic bags from Oct 2015. It will be estimated the new law will be altering the economy by delivering savings of £60m in litter clean-up costs and £13m million n in carbon savings (The Guardian, 2015). Furthermore, it should also be considered that how widespread biodegradable plastics will be used all depends on how strongly society embraces and believes in environmental preservation.

Nowadays, with increasing environmental awareness, scientists are trying to develop innovative strategies for the environmental sustainability by using processes and materials with relatively low cost, energy consumption and toxicity, together with high biodegradability. There is a strong motivation within this context to develop innovative bio-based polymer materials.

1.1.7 Life cycle assessment, a holistic & pragmatic approach to the strategies

The best tool for the environmental observance of a product could be life cycle assessment (LCA). Life cycle assessment is a framework to evaluate the environmental impacts caused with all the stages of a product's life from cradle to grave (extraction of raw materials from the earth and ending at the waste products being returned to the earth). The life cycle assessment (LCA) of the polymers from renewable resources is the key to observe their real environmental impacts (considering all direct and indirect impacts), associated feasibility and their social aspects, or in one word their *Sustainability*. Those observations could provide essential information to compare the biopolymers and conventional polymers for any necessary decision made from politician to industrial peoples.

The some LCA study for PHA is reported in literatures:

1. In a study by Kim and Dale (2005) titled “Life Cycle Assessment Study of Biopolymers (Polyhydroxyalkanoates) Derived from No-Tilled Corn”, the different impact of PHA biopolymer is assessed and compared to polystyrene (as a non-environmental friendly common polymer). The study showed that PHA doesn’t provide specific advantages over polystyrene if it is manufactured by the current technology. However, in the near future PHA fermentation technology would improve the fermentation and recovery process and be much more environmental friendly than polystyrene especially by effect of global warming. Although, the issues like photochemical smog, acidification and eutrophication causes by the corn cultivation might not make PHA favourable over polystyrene (Kim and Dale, 2005).

2. The environmental analysis of two petroleum-based polymer, polypropylene and polyethylene with the biologically-based PHA has been compared by Harding *et al*. using life cycle analysis. The study used stems from generated net CO_2 gas of the renewable resource with a cradle-to-grave approach to measure the environmental impact. It compares the findings with similar studies of polypropylene (PP) and polyethylene (PE). The results revealed that, in all of the life cycle categories, PHA is more environmental friendly than PP. Moreover, the energy requirements are significantly lower than those for polyolefin production. PE impacts were lower than PHA values in acidification and eutrophication (Harding et al, 2007).

3. A meta-analysis of 30 life cycle assessments by the nova-institute in Germany in 2012 has shown definite positive results for the bioplastics; PLA and PHA/PHB.

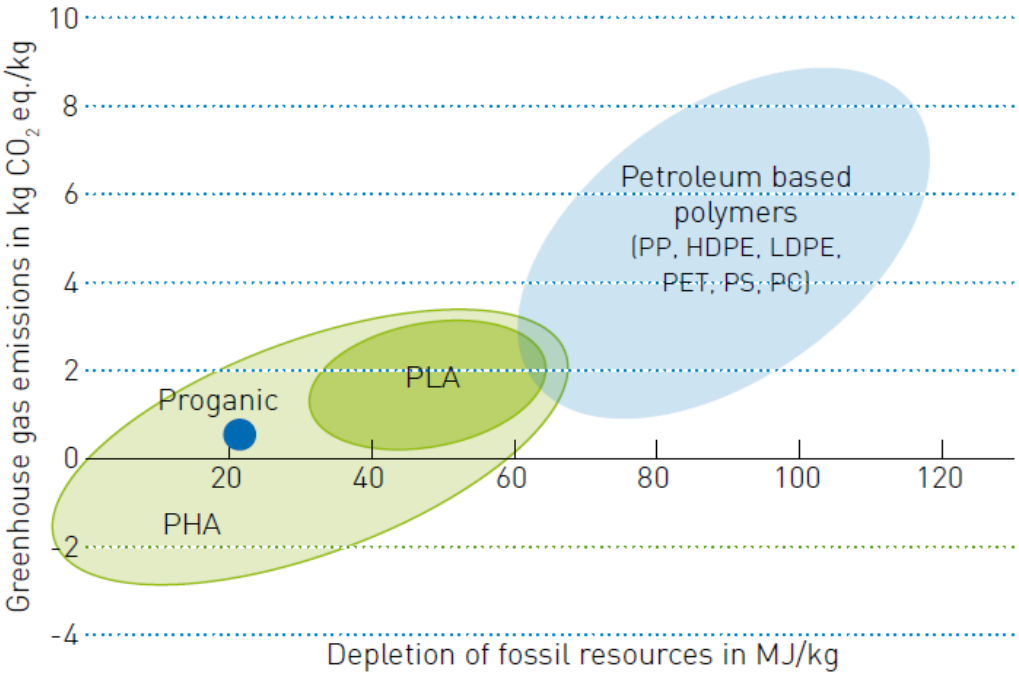

Figure 3-1 Nova-institute meta-analysis of the environmental impacts of biopolymers [PLA, PHA, *Proganic* (a compound of PHA/PLA/minerals)] compare to petroleum-based polymers in fossil resource depletion and climate change: (www.nova-institut.de)

Figure 3-1 shows three ellipses, the upper right contains data of the some conventional petroleum based plastic (PP, HDPE, LDPE, PET, PS, PC), and lower left is ellipses of PLA and PHA with Proganic (a compound of PHA/PLA/minerals). The x axis shows the depletion

of fossil fuel resources in megajouls per kilogram and the y axis is the greenhouse gas emission in kilogram CO_2 equivalent per kilogram plastics. The figure shows that Petrolum based plastics use more than 70 MJ/kg of fossil resources and generate more than 3 kg of CO_2 equivalent per kilogram plastics while for biopolymers both aspects are lower than. The ellipse of the PHA/PHB material exhibits a considerably wider spread of results than the ellipse of PLA. However, those results also depend on which types of renewable resources are used and the methods of production (Nova, 2012).

1.2 Material and experimental work

There has been a growing demand on petroleum-derived plastics and a global dependence on this unsustainable product which increased significantly over the years. However, increasing concern about the rapid depletion of crude oil and the mounting apprehension about the environmental effects of plastic materials have attracted much interest in developing of biologically derived polymers from renewable sources, particularly of the biodegradable class.

1.2.1 Different type of biopolymers

Biopolymers by definition are polymers that are produced by a living organism, such as DNA, RNA, starch, cellulose and proteins (Reference, 2016)

As it shown in Figure 4-1, bioplastics can be classified in three main categories:

- Renewable-resource-based bioplastics: they could be synthesized naturally from plants & animals, or entirely synthesized from renewable resources. Starch, cellulose, proteins, lignin, chitosan, poly lactic acid (PLA) and polyhydroxyalkanoates (PHAs). Recently, with development of new technologies, it has become possible to synthesize some conventional polymers from renewable resources. Polymers like bio-polyethylene(bio-PE) and bio-polypropylene(bio-PP) or poly-butylene succinate (PBS)

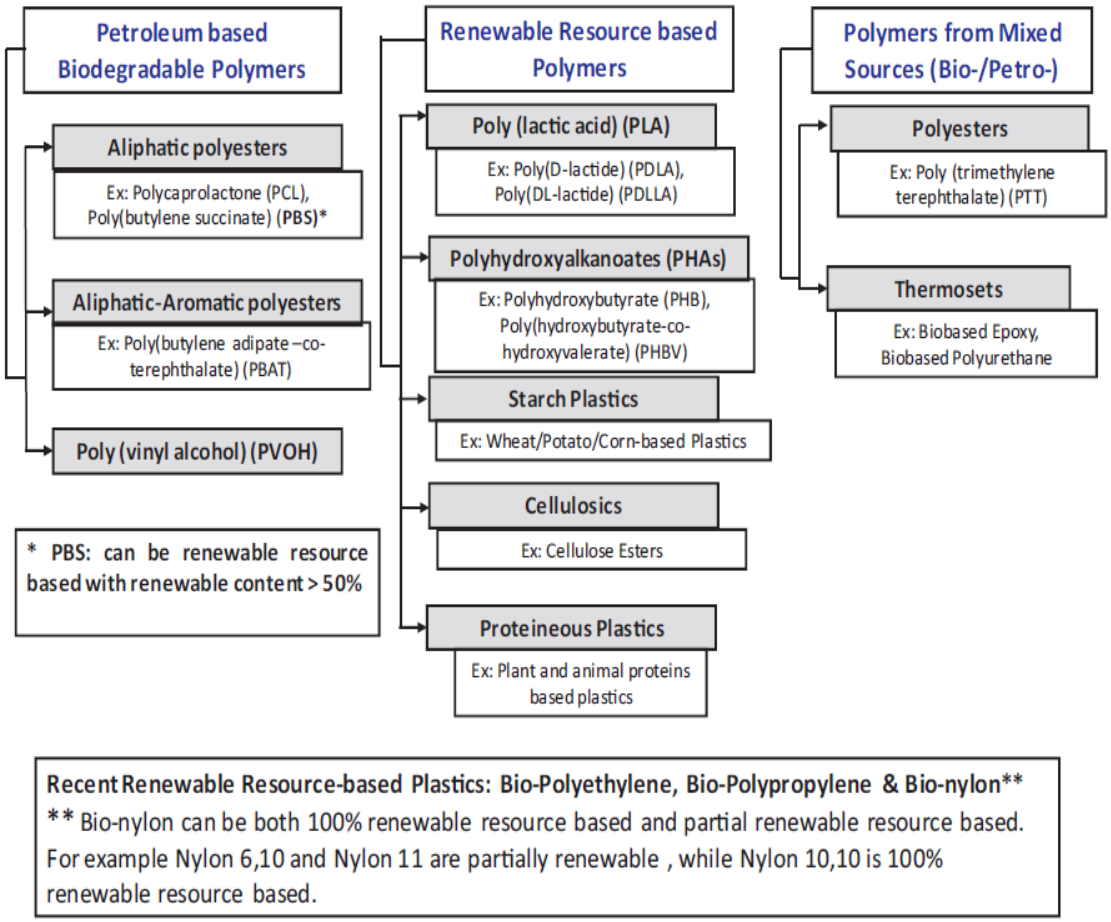

Figure 4-1 - Classification of bioplastics based on their production routes (Reddy et al, 2013)

- Petroleum-based bioplastics: These polymers are synthesized from petroleum resources but are biodegradable at the end of their functionality. Polycaprolactone (PCL) and poly (butylene adipate-co-terephthalate) (PBAT) are included in this category.
- Bioplastics from mixed sources: These are made from combinations of biobased and petroleum monomers; they include polymers like poly (trimethylene terephthalate) (PTT), bio-thermosets and biobased blends (Reddy, Misra, Mohanty, 2012).

The classification of biopolymers based on their manufacturing method is shown in Figure 4-1.

1.2.2 PHA (Polyhydroxyalkanoates)

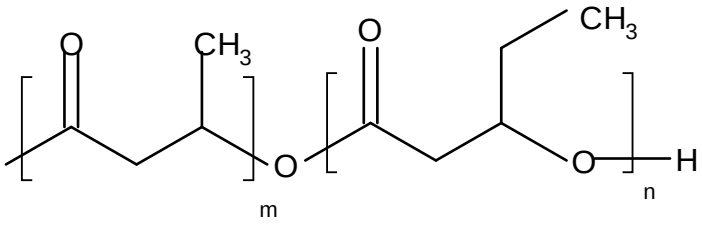

Figure 5-1 Chemical structure of Poly (3-hydroxybutyrate-co-3-hydroxyvalerate) or PHBV

Poly (3-hydroxybutyrate-co-3-hydroxyvalerate) or PHBV (figure 5-1) is categorized under a family of linear bio-polyesters of 3, 4, 5 & 6-hydroxyacids also known as polyhydroxyalkanoates (PHAs). PHAs synthesised by a wide variety of bacteria through the fermentation of sugars, lipids, alkanes, alkenes and alkanoic acids. PHAs are recyclable and they degraded to carbon dioxide and water. In addition, these polymers are biocompatible and therefore they exhibit several medical applications (Philip, Keshavarz, Roy, 2007).

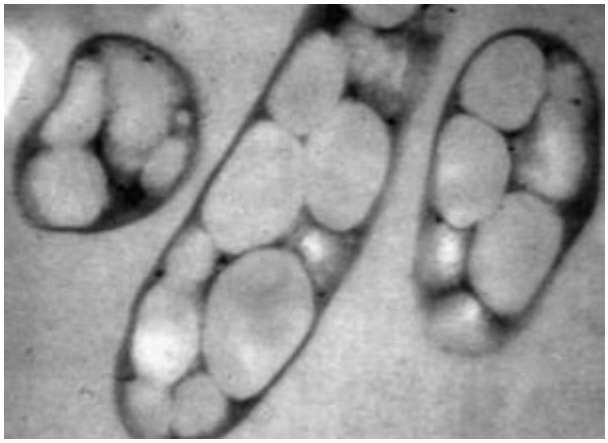

Figure 6-1 TEM images of cells with approximately 60 wt% of P(3HB) after cultivation (Ecobiomaterial, 2016)

1.2.2.1 History

It was first Lemoigne at the Institute Pasteur in 1923 that discovered aerobic spore-forming *Bacillus Megaterium* could accumulate 3-hydroxybutyric acid under the anaerobic conditions. In 1927, a polymer of 3-hydroxybutyric acid was successfully extracted from *Bacillus* using chloroform as solvent. In early 1960's, Baptist and Werber at W.R. Grace & Co. (U.S.A) published several magnificent papers about the production of PHB and patented their works. Resource scarcity era in 1970's, provide a period of tremendous interest in the research & development of bioplastic, ICI (UK) was the first to formulate the conditions for *Alcaligenes latus* to produce P(3HB) up to 70% of its dry cell weight. However, the inherent brittleness of PHB and the high cost and the poor mechanical properties hindered the desire about this bioplastic after the price of the oil also declined dramatically by 1980's. Nonetheless, ICI has stepped forward in developing the PHA's properties by copolymerization of PHB with the other member of PHA's family, PHV (poly3-hydroxyvalerate) and producing PHBV Poly (3-hydroxybutyrate-co-3-hydroxyvalerate) under the commercial name of BIOPOL. The properties of PHBV have been improved comparing to PHB, the lower melting point, the glass transition and the crystallinity, and better elongation at break; those properties change by increasing of the valerat amount. ICI splitted in June1993 and the Zeneca BioProducts branch of ICI started dealing with BIOPOL. Zeneca then sold their BIOPOL technology to Monsanto in April 1996. Metabolix Inc. obtained the licence from Monsanto at 1998. At the same year, following the collaboration between Metabolix Inc. and Children's Hospital, Boston, a new spin off company named Tepha Inc. was initiated (Sharma et al, 2012, Rai and Ray, 2011, Philip, Keshavarz, Roy, 2007)

Now, the big manufacturers of PHA are Metabolix Inc. (U.S.), Meredian Inc. (U.S.), Biomer (Germany), Tianjin GreenBio Materials Co. Ltd (China), and Shenzhen Ecomann Technology Co. Ltd (China). US-based Metabolix and Chinas Shenzhen Ecomann Technology have been more developed than others and expand their product portfolio to a distinguishable level.

MarketsandMarkets, the largest market research firm worldwide in a report called "Polyhydroxyalkanoate (PHA) Market, By Application (Packaging, Food Services, Bio-medical, Agriculture) & Raw Material — Global Trends & Forecasts to 2018" published in

2013 defined and segmented the global PHA market with analysis and forecasting of the global revenue and consumption. PHA market consumption will grow from an estimated 10,000 MT in 2013 to 34,000 MT by 2018, with a CAGR of 27.7% from 2013 to 2018(MarketsandMarkets, 2013).

Figure 7-1- PHBV ENMAT^{TM} Y1000 with 3 *mol%* of hydroxyvalerate (HV) content in white powder form manufactured by Tianan Biologic Material Co. (Ningbo, P. R.China).

Figure 7-1 shows the PHBV ENMAT^{TM} Y1000 with 3 mol% of hydroxyvalerate (HV) content in a very fine white powder form manufactured by Tianan Biologic Material Co. (Ningbo, P. R. China) which was used in this study.

1.2.2.2 Issues associated with the widespread usage of PHAs

PHAs have gained great interest because of their useful properties such as biodegradability for disposable plastic application. They also represent the best candidate for the substitution of some type of the conventional petroleum-derived plastics due to their wide spectrum of properties. However, this material offers an extensive level of challenges due to its chemistry and properties. Some serious drawbacks associated with PHA's have hindered its widespread usage, issues such as narrow processing window, inherent brittleness, low impact resistance

along with its sluggish crystallinity coupled to a rapid thermal degradation that provide challenges for using of material in conventional processing machinery (Philip, Keshavarz, Roy, 2007).

1.2.3 Polybutylene succinate (PBS)

Bionolle ™ by Showa Denko is the first commercially produced PBS polyester in 1993.

Polybutylene succinate (PBS) is a semi-crystalline biodegradable, synthetic polyester. The new technologies provide the ability of producing the PBS from the plant-based renewable resources. It is one of the most suitable materials for processing into films. PBS has an excellent process-ability, and can be processed into melt-blown textile fibres, multifilament, monofilament, flat, and split yarn, and also into injection moulded products. It also can be used to make agricultural films, shopping bags, and compost bags. PBS has similar properties to PET, with 35-45% degree of crystallinity, T_g= -32, T_m= 114-115 ℃. It also has density of 1.26 (g/cm^3), heat distortion temperature (HDT) =97 ℃, and heat of combustion (Kj/g) (Song, Kay, Coles, 2011).

Currently, 35,000 tons of succinic acid is manufactured annually. Estimations predict a rise to 2,000,000 tons per year in 2020 (Song, Kay, Coles, 2011).

Traditionally, succinic acid is synthesized by catalytic hydrogenation of maleic acid which is of fossil origin. Consequently, its cost has been relatively high and linked to the increasing price of fossil fuel feedstocks. Bio-succinic acid is produced by fermentation of starch or oligosaccharides (C-5, C-6 sugars) containing renewable resources. Fermentation is commonly performed by bacteria, but yeast has been used as well for the production of this green chemical (Innovativeindustry, 2011).

Low molecular weight PBS is chemically synthesized through the polycondensation of 1, 4-butandion with succinic acid. Then high molecular weight PBS is obtained by a coupling reaction in the presence of hexamethylene diisocyanate as a chain extender. The chemical structure of PBS is shown in Figure 8-1.

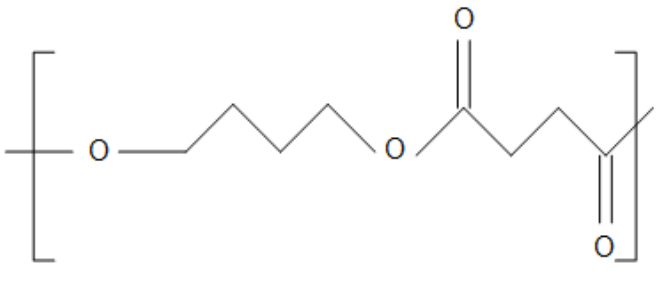

Figure 8-1 the chemical structure of Polybutylene succinate

PBS could be a suitable blend with PHBV due to its mechanical properties, biodegradability and the ability to produce it from renewable resources.

Figure 9-1 Bionolle ™ white pellets from Showa Denko

Figure 9-1 shows the Bionolle ™, white pellets from Showa Denko, Japan which has been used in this study.

1.2.4 Chain extenders

Chain extenders or coupling agents are a variety of additives capable of generating coupling reaction through addition reaction. They can reverse the MW (Molecular Weight) reduction which occurs by the chain hydrolysis of the polyesters and also enhance the melt strength and modify the rheology of the polymers. In principle, their reactive functional group (at least two) reacts with hydroxyl (OH) and carboxyl (COOH) groups in the polyesters and connects the chains to each other. The chemicals such as diepoxides, bis-oxazolines, diisocyanates, dianhydrides, bis-acyllactams, bis-malamides,dicyanates, carbodiimides, diesters, and several commercial chain extenders are among the proposed chain extenders. They are sometimes combined with catalyst to accelerate the reaction or as a masterbach for the other application for polymers (Pfaendner,2016).

There are several studies about the effect of chain extenders as a either compatibilizer or molecular weight enhancer in the blend of polymers. Oxazoline copolymer is reported to react with variety of reagents, such as carboxylic acid, which shows significant compatibilization ability for this functional group through amido-ester linkage (Subramanian, 2013).

Pilla *et al*. studied the effect of oligomeric epoxy-based chain extenders on properties of PLA. According to the study, the addition of Cesa-chain extender improved the molecular weight and also reduced the cell size and therefore, increased the cell density. DSC analysis showed that that the addition of Cesa had separated shoulder in melting peak of PLA into two individual peaks, resulting in a double-melting peak and also PLA degree of crystallinity decreased with the addition of the Cesa-chain extender . Moreover, the thermal stability of PLA is enhanced but DMA showed that storage and loss modulus of PLA hasn't change by addition of the CESA-chain extender. Finally, the mechanical properties of PLA, the tensile strength and the elongation at break were also improved by adding the chain extender, but however, the specific modulus was decreased (Pilla et al, 2008).

Oligomeric epoxy-based chain extenders such as Joncryl-ADR-4368, have been designed to show better dispersion inside the matrix of polymers and also their high amount of functionality group (f_n >4) enhance the narrow windows processibility in compare with their

unimodal telechelic multifunctional counterparts of similar or even lower functionality (f = 3, or 4). Villalobos et al argued that the main reason for these phenomena is reported by many researches with multiple condensation thermoplastics including polyesters, polyamides, polycarbonates, polyurethanes and blends of these, lays on the tailored functionality distribution of the oligomer which delays the onset of gelation (Villalobos, 2006).

Reactive blending and compatibilization of Polyoxymethylene/thermoplastic polyurethane (POM/TPU)) compounds using oligomeric multifunctional chain extenders, Joncryl ADR-4368, as the compatibilizer is reported by Tang et al. it has been stated that the compatibilization of two polymers significantly increases the mechanical properties of blends, such as flexural, tensile modulus mechanism of POM/TPU/CE also impact strength of compounds. SEM images show that Joncryl ADR-4368 can shrink TPU particle size and enhance the interfacial interactions between POM and TPU (Tang, 2012).

Li et al described the general reaction between chain extender and PHBV in Figure 10-1.

1) Epoxy groups in ADR react with carboxylic acid end groups in P (3HB-co-4HB).
2) Epoxy groups in ADR react with hydroxyl end groups in P (3HB-co-4HB).

It has been stated that the complex viscosity magnitude is improved even with a small amount of the CE, and adding more CE (2-6%), the result shows the significant differences in the steady shear viscosity. However, just a small amount of CE coupled with PHBV and the addition of 2-6% could act as plasticisers or lubricants dispersed among the coupled co-polymer chains and decreases viscosity of the blends (Li, 2010).

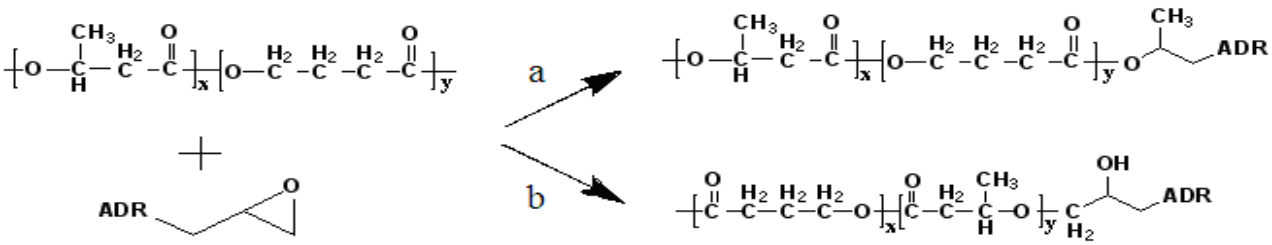

Figure 10-1 The general reaction between chain extender and PHBV

On the other hand, Li declared that for the reactive blending of polylactide acid/thermoplastic starch/multifunctional epoxy-based chain extender masterbach, chain extension resulted in relatively minor differences in the mechanical properties and in the PLA/TPS blend morphology. Although it was discovered that the epoxide group of CE reacts with carboxylic group of PLA and branching phenomena occurred but there are not any evidences about the interfacial role of CE on PLA/TPS compounds according to the morphology study (Li, 2011)

1.2.5 Talcum Powder

Talcum Powder is one of the softest minerals on the planet earth. Talc is an organophilic, water impervious and chemically inert mineral. It is characterized as a hydrated magnesium sheet silicate with the formula $Mg_3\ Si_4O_{10}\ (OH)_2$.

Basically, Fillers are commonly used in modifying different properties of polymers. Inorganic and organic fillers are reported to improve mechanical, thermal and electrical properties of some crystalline polymers, when they are used as reinforcing agents (Psarras, Manolakaki and Tsangaris, 2003).

Among the inorganic fillers, talc is being used for synthesis of the polymeric composites due to its excellent blending nature, thermal resistance, superior electrical resistance, chemical inertness and smooth greasy feel (Parvin, et al 2013).

The crystal structure of Talc is shown in Figure 11-1, a layer of brucite ($Mg\ (OH)_2$) sandwiched between two sheets of silica (SiO_2).

Talc's particles are in lamellar (platy) form, and they exist with variable aspect ratio. The aspect ratio is an important parameter of the fillers and talc's high aspect ratio make it desirable as a filler and inorganic additive for the plastics.

In thermoforming and injection moulding process, the accurate softening point of thermoplastic is sometimes more important than the glass transition temperature due to the variable amount of T_g in transition temperature spectrum. On the other hand, in some

applications, rigidity is desirable at upraised temperature, like plastic car part injection moulding. Basically, the heat distortion temperature (HDT) enhances by the addition of the mineral filler. Some fillers are more effective than others, like talc, and the aspect ratio determines the effectiveness of filler.

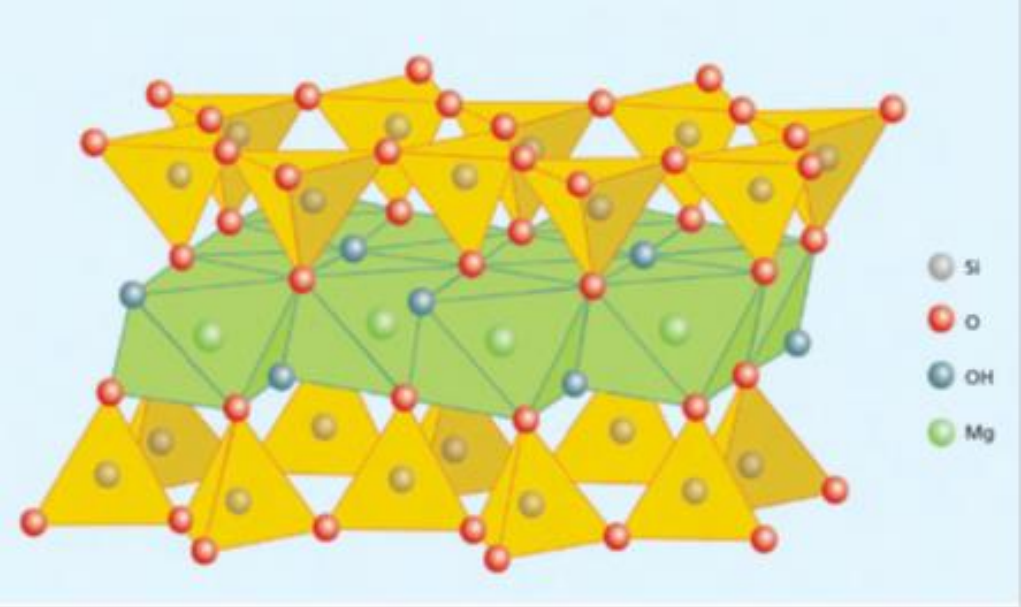

Figure 11-1 The crystal structure of talc (China-talc, 2016)

Talc is considered an active filler; it can increase heat deflection temperature (HDT), and increasing the stiffness (E-modulus). How rigid the polymer after addition of talc becomes, is strongly depended on the aspect ratio of talcum powder. The talc concentration and its fineness condition enhance the thermal conductivity of the polymer (Posch, 2005).

Moreover, in injection moulding process, the shrinkage, warpage and thermal expansion of plastic part can be decreased by incorporating the Talc. Figure 12-1 shows the heat distortion of different filler:

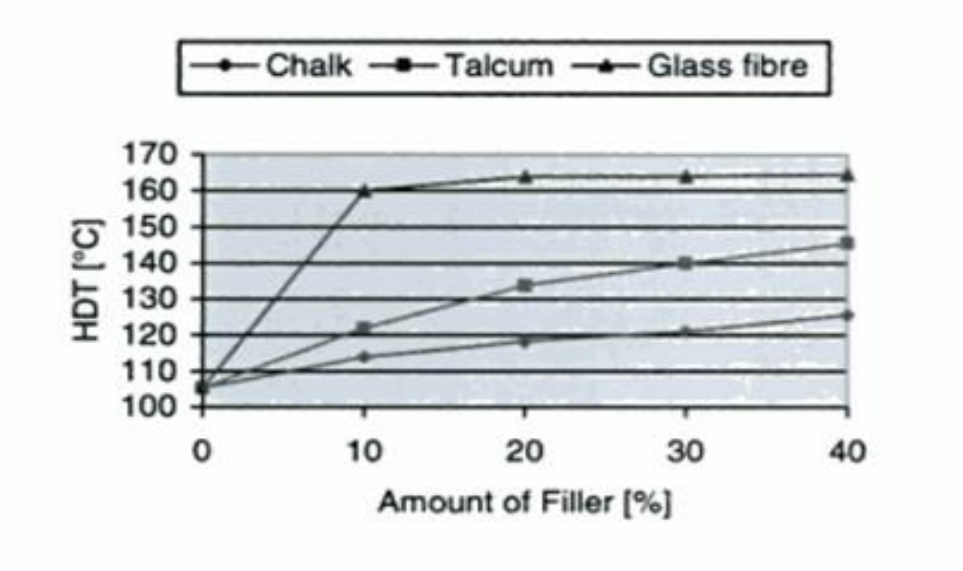

Figure 12-1 The heat distortion (℃) of three different filler; Chalk, Talcum and Glass fiber (Posch, 2005)

1.3 Sample preparation

1.3.1 Twins Screw Extruder

Plastic extrusion is continuous process in which thermoplastic feed stock material in an extruder is transformed into a molten viscous fluid using heat and mechanical shear. Extruders are the most common type of machines in the plastic processing industry. Extruders have a more broad usage than just extrusion operation, for instances injection moulding machines and blow moulding machines also have an extruder.

There are different types of extruders, the most popular are:

- Single-screw extruders

A single screw extrusion basically builds pressure in a polymer melt so it can be extruded through a die or injected into a mould.

- Twin screw extruders

The most common multi-screw extruder in plastic industry is twin-screw extruder. It is very difficult to categorise twin-screw extruders due to versatility of screws. In terms of screw rotation, there are two main types:

1- Co-rotating twin screw extruder: the screws rotate in the same direction.
2- Counter-rotating twin screw extruder: the screws rotate in opposite direction.

The application of extrusion can determine the rotation speed run of extruders. High speed extruders which are primarily used in compounding run at around 200 to 1000 rpm, or higher. For profile extrusion applications the low speed extruders are mostly used which run at about 10 to 40 rpm (Rauwendaal, 2010)

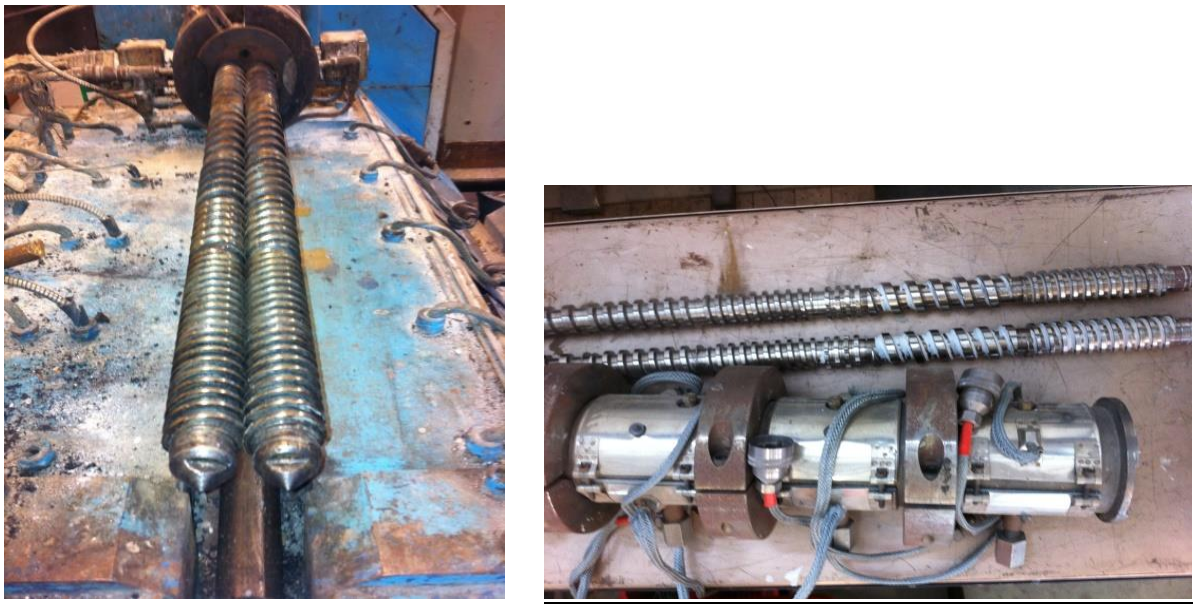

Figure 13-1 Screws and barrel in a typical twin-screw extruder
Left) co-rotating screw
Right) disassembled screws and barrel from a co-rotating twin-screw extruder

Extruders can be distinguished as the extent of intermeshing. The screws can be fully intermeshing or partially intermeshing or exist as non-intermeshing.

1.3.1.1 Extrusion compounding line

In industry, there are several type of extruder used for extrusion compounding such as single screw extruder, twin screw extruder, reciprocating single screw compounder, batch internal mixers, and continues internal mixers. (Rauwendaal, 2010). In this study, a Betol intermeshing co-rotating twin-screw extruder is used (Figure 13-1). The feeders were powder/pellet twin screw feeder and powder/powder twin screw feeder (Figure 14-1).

Figure 14-1 the twin screw feeder

The downstream equipment was a pelletizing system. The pelletizers system (strand pelletizers) cut extruded strands cooled in a water bath (Figure 15-1)

a b

c d

Figure 15-1 Strand pelletizing system consists of a & b) water bath c) pelletiser d) compounded pellets

1.3.2 Injection moulding

Injection moulding is one of the most important processing methods for manufacturing majority of plastic parts. It is a high speed method due to a single procedure which converts resins to the final product. The plastic part with complex geometries can only be produced in injection moulding machines.

Injection moulding machine consists of these components:

- Plasticating/injection unit
- Clamping unit
- Control system
- Tempering devices for the mould

Potsch & Michaeli described the different steps in an injection moulding cycle as:

1. Start of plastication: The screw rotated and conveys the melted material through screw barrel into screw chamber. The screw returns, sliding axially.
2. End of plastication: Screw rotation is off and it is enough material to inject into the mould.
3. Closing the mould: the clamping unit closes the mould
4. Start of injection: the screw moves forward axially without rotation and convey the melted plastic into the mould cavity
5. End of injection and cooling of the moulding: as the mould part cools down, further melt is conveyed into cavity, recover the volume shrinkage
   Meanwhile the step 1 repeats
6. Ejecting of the part: after the part has cooled adequately, the mould opens and finished part is ejected (step 2 is finished and step 3 can start) (Potsch, Michaeli, 1995).

Figure 16–1 Plasticating/injection unit (above), Clamping unit (down) of the injection moulding machine D60NCIII

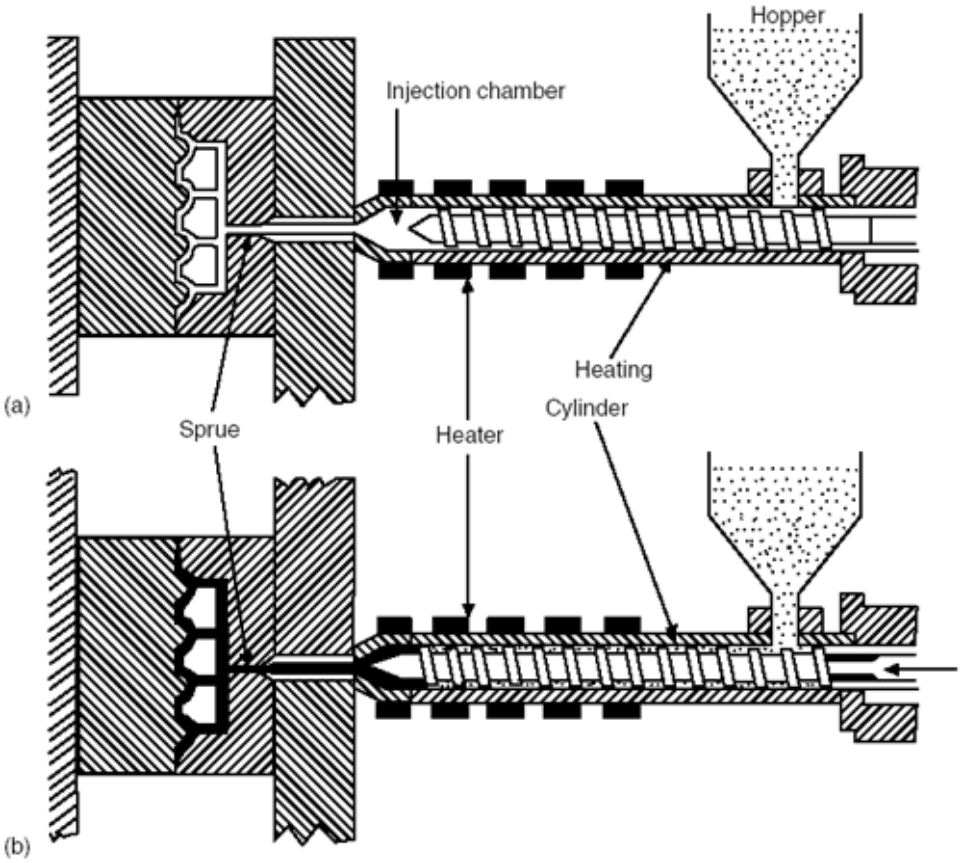

Figure 17–1 A schematic injection moulding plastification and injection procedure, showing the screw (a) in the retracted position and (b) in the forward position (longmoldtechnology, 2009)

Figure 17–1 shows a schematic injection moulding plastification and injection procedure in two positions; the retracted and in the forward positions.

Injection moulding is used in this study to obtain suitable specimens in dumb-shell and plate form for the mechanical testing (Figure18-1).

Figure 18 –1 Dumbshell and Tensile bars of PHBV from injection moulding

1.4 Thermal properties study

Thermal analysis is used to measure many physical and chemical properties and characterize polymers and additives. Table 1-1 shows the three most common thermal analysis techniques, the properties measured by and the recommendation for determining of polymer characteristics with (next page).

1.4.1 DSC

Differential scanning calorimetry (DSC) is a thermal technique that measures temperature and heat flow (enthalpy) changes associated with thermal transition in a material. DSC make it possible to investigate heat absorbed or emitted by a sample during different thermal events, such as glass transition, melting, crystallization, cross-linking, chemical reaction, evaporation, and chemical decomposition. (Naranjo, 2008)

Table 1-1 Main thermal analysis technique and physical properties measured (Naranjo, 2008)

Technique	Property measured	Recommending to determine
Thermogravimetry (TGA/DTG)	$\frac{dm}{dT}$ *or* $\frac{dm}{dt}$ *where* m=mass T=temperature t=time	Chemical stability Thermal stability Chemical composition Moisture content Cross-linking rate
Differential Scanning Calirometry (DSC)	$\frac{dm}{dT}$ *or* $\frac{dH}{dt}$ *where* H=enthalpy, T=temperature t=time	Heat capacity Melting heat Melting temperature Glass transition temp Crystallization temp Crystallinity Degree of Crystallinity Chemical stability Cross-linking rate Cross-linking degree
Dynamic Mechanical Analysis(DMA)	Complex modulus and tan δ under oscillatory loads	Glass transition temp Mechanical stability Elasticity module

Figure 19-1 TA Instruments DSC/Q2000 with Universal Analysis 2000 software

There are three major transition temperatures of polymer that can be evaluated by DSC:

- Glass transition temperature: T_g is registered in the DSC technique as a step in heat flow.
- Melting temperature: T_m is investigated as an endothermic peak in the heat flow.
- Crystallization temperature: T_c is observed as an exothermic peak in heat flow.

Figure 20-1 shows the DSC graphs (first and second cycles) of a PHA resin. The heat of fusion (J/g), melting point ℃, and crystallization peak are shown at graph. When following the first heating curve (below curve) from left to right, there is not a detectable jump or shoulders as T_g, (it will be discussed later in chapter), The first area under the curve that is enclosed between the trend line and the base line can be used for measurement of the amount of heat, ΔH, because the transition is melting (T_m= 176.29°C) it is the heat of fusion, ΔH_f. When following the second cycle (cooling curve at above), the transition occurred in crystallization area and area under the curve that is enclosed between the trend line and the base line is, ΔH_c , the heat of crystallization (T_c =104.7 ℃).

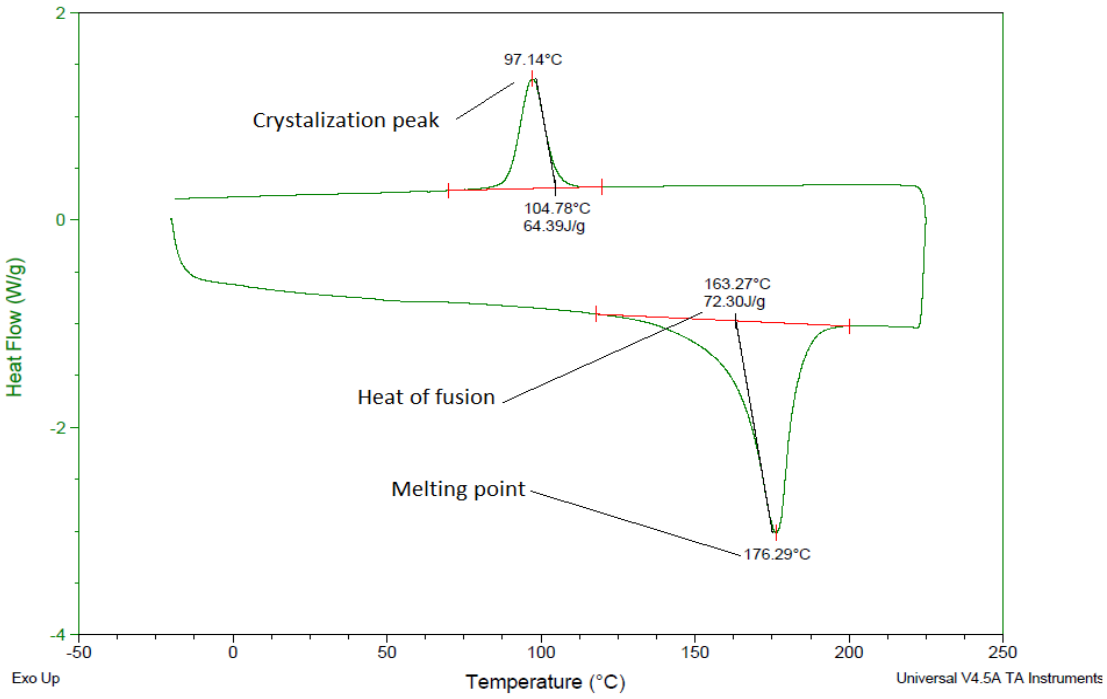

Figure 20-1 The DSC graphs (first and second cycles) of a PHA resin

A 100% crystalline polymer structure doesn't exist. The degree of crystallinity, χ, is measured from the ratio of the heat of fusion of a polymer sample, ΔH_f, and the enthalpy of fusion of a 100% crystalline of that polymer sample:

Equation 1-1) $$\chi = \Delta H_f / \Delta H_{f\%100} \times 100$$

DSC is used in this study for evaluating of the non-isothermal and the isothermal behaviour of the polymer samples (Naranjo, 2008).

1.4.2 TGA

Thermogravimetric analysis is a technique which monitors the altering in mass of a substance as a function of temperature or time as the sample specimen is subjected to a controlled temperature program in a controlled atmosphere. A TGA consists of a sample pan that is supported by a precision balance. That pan takes in a furnace and is heated while the mass of the sample is monitored during the experiment. (Perkin Elmer, 2010)

Figure 21-1 TA instrument "The New Discovery TGA", with TRIOS software version 3.3.0.4055

Researchers use TGA to evaluate the mass changes caused by these thermal events:

- Volatilization of moisture
- Volatilization of additives
- Decomposition of polymer or additives
- Decomposition of organic pigments
- Decomposition of some mineral fillers(i.e. calcium carbonate) (Naranjo,2008)

The technique is particularly useful for the following types of measurements:

• Compositional analysis of multi-component materials or blends
• Thermal stabilities
• Oxidative stabilities
• Estimation of product lifetimes
• Decomposition kinetics
• Effects of reactive atmospheres on materials
• Filler content of materials
• Moisture and volatiles content (Perkin Elmer, 2011).

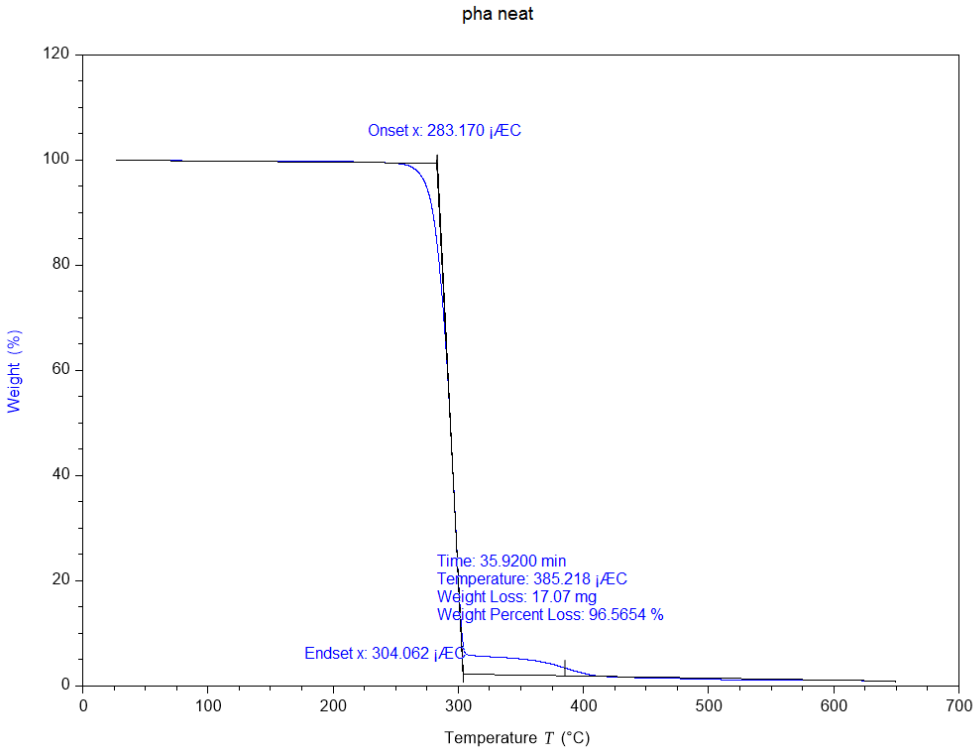

Figure 22-1 The TGA graphs of the neat PHBV, onset and endset temperature and weight loss on those points were shown by TRIOS software

Figure 22-1 shows the TGA curve of the neat PHBV. The onset temperature, Endset temperature, maximum weight loss and residue at any temperatures can be obtained from

machine with software (the new TA machine works with TRIOS software version 3.3.0.4055).

1.5 Thermomechanical analysis: DMA (Dynamic Mechanical analysis)

1.5.1 Theory

Polymers exhibit a viscoelastic property which means they have the mechanical behaviour of both solids and liquids. Basically, the mechanical properties of a polymer are linear dependent. A polymer appears hard under a fluctuating force at high frequency but in contrast it appears soft when the force applied slowly.

Applying a force to a sample, results in the deformation of the sample. The ratio of the applied force to the deformation is defined as the stiffness.

Stiffness=$F/\Delta L$

The Modulus is defined by:

Equation 2-1) $M=\sigma/\epsilon=F/\Delta L * L_0/A$ **(Figure 23-1)**

So the Modulus can be calculated from force (F) and displacement amplitudes (L)
Dynamical mechanical analysis (DMA) works by imposing a small cyclic strain on a sample and measures the outcome stress response, or equivalently, imposing a cyclic stress on a sample and measuring the resultant strain in reply (Chartoff, Menczel and Dillman, 2014).

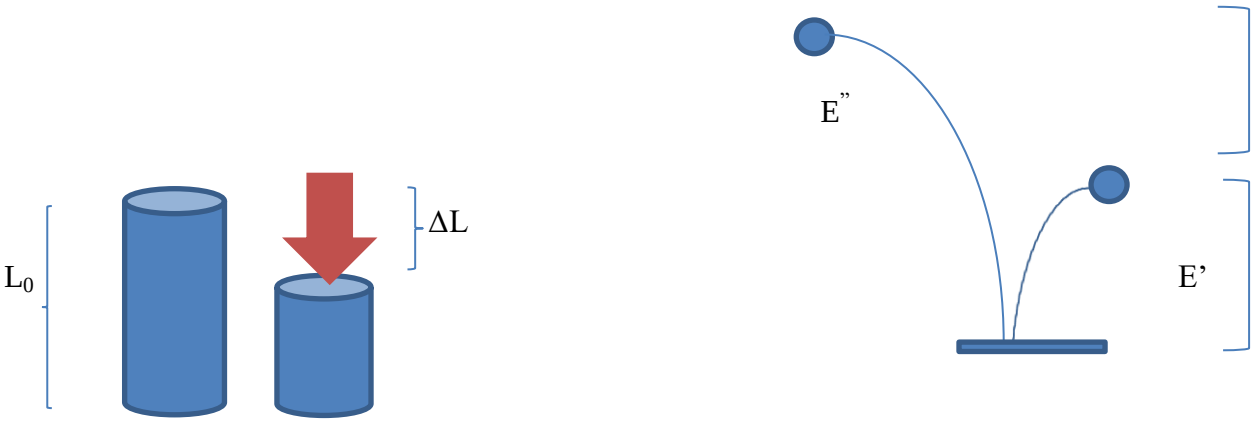

Figure 23-1 dimension changes by applied forces, E” and E’

DMA, measures the viscoelastic properties as well as, Storage and loss modulus, damping properties, and tan delta:

M*=complex modulus
Storage Modulus: $E' = M^* \cos \delta$
Loss Modulus: $E'' = M^* \sin \delta$
Loss factor (tan δ) or damping:
$\tan \delta = E'' / E'$

E’ represents the elastic or fully recoverable energy during deformation while E’’ represents the viscous or net energy loss. Tanδ is the ratio of loss to storage modulus, which combines the viscous and elastic components into a single term and can exhibit the curing behaviour of the polymer.

Although there are several accurate techniques for finding the glass transition of a polymer, like DSC, the most sensitive technique reported by researchers is DMA.

According to Hill, definitions of the dynamic properties of a material depend on the concept of resolving the stress wave into two waves (Figure 24-1), one which is in phase with the strain and the other which is 90 ° out-of-phase with the strain. The in phase resolved plot represents elastic response, and the 90" out-of-phase resolved plot represents viscous

response. The term "storage" is associated with the elastic part of the response, E', because mechanical energy input to elastic materials is "stored" in the sense of being completely recoverable. The term "loss" is associated with the viscous part of the response, E", because mechanical energy input to ideal liquids is totally lost through viscous heating (Hill, 2001).

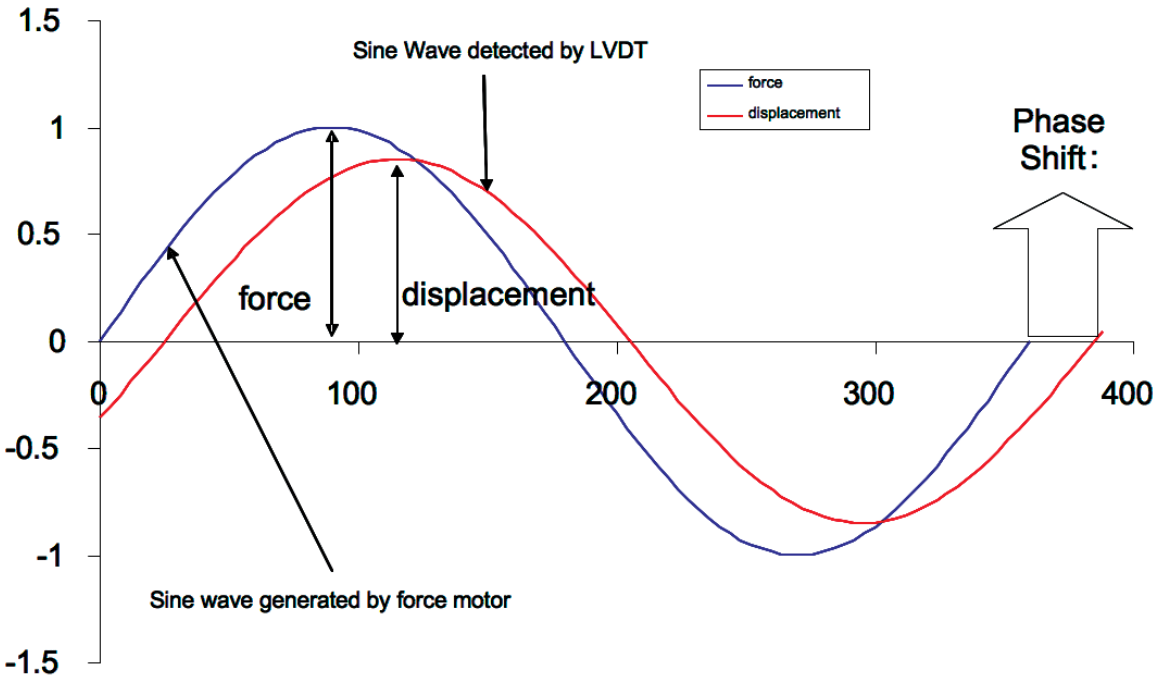

Figure 24-1 The relationship of the applied sinusoidal stress to strain is shown, with the resultant phase lag and deformation (Perkin Elmer, 2016)

According to Turi, T_g of a material can be labelled using the following parameter which illustrated in Figure 25-1.

- E' Onset: Occurs at the lowest temperature and relates to mechanical failure or plastic deformation.
- E" Peak: Occurs at the middle temperature and is more closely related to the physical property changes attributed to the glass transition in plastics. It reflects molecular processes and agrees with the idea that Tg is the temperature at the onset of segmental motion.
- Tan Delta Peak: Occurs at the highest temperature and is used historically in literature. It is a good measure of the midpoint between the glassy and rubbery states of a polymer. The height and shape of the tan delta peak can change and it depends on the amorphous content of polymer (Turi, 1997)

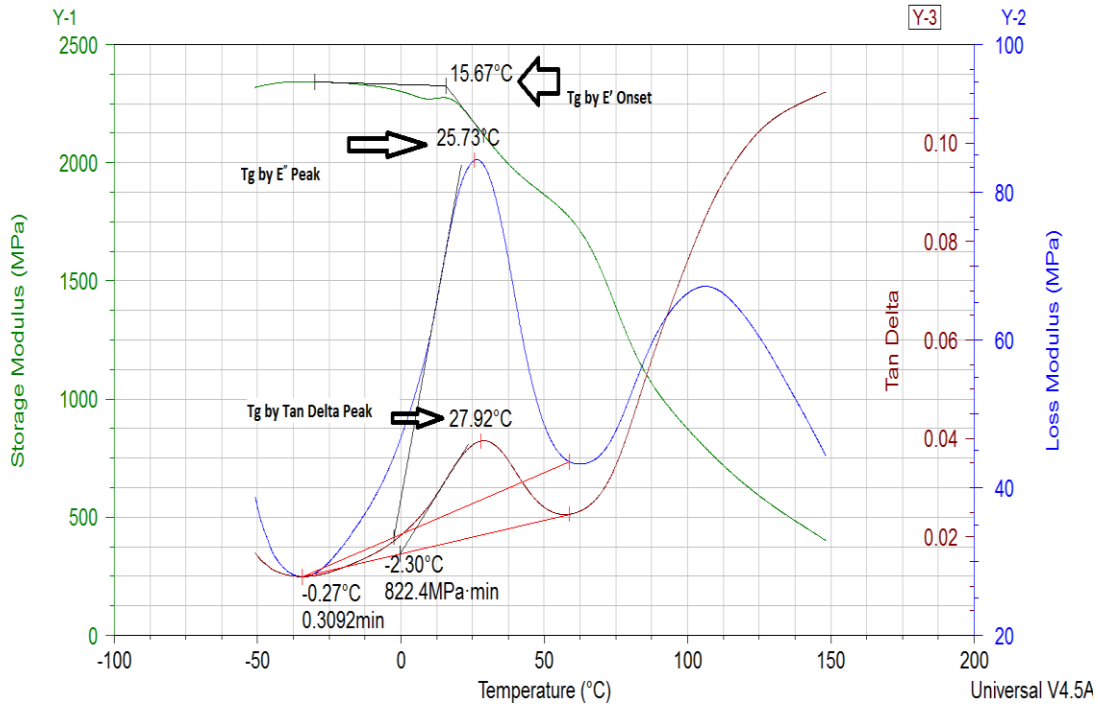

Figure 25-1 DMA and different Tg for extruded PHBV (from results of this study)

There are therefore three types of calculated the glass transition temperature. The first is from the onset of the drop in the storage modulus (E′) curve. This indicates the point where viscous motions begin to occur. The second is at the peak of the loss modulus (E″) curve. This shows the maximum chain slippage in a cross-linked system. Finally, the peak of the tan δ curve can be used to determine T_g. This indicates the point where the ratio of viscous response to elastic response is greatest (Epotek, 2016).

1.6 Crystallinity study

1.6.1 XRD X-ray powder diffraction

X-ray diffraction is mainly used to gain information about crystallinity, crystalline size, orientation of the crystallites, and phase composition in semi-crystalline polymers (Murthy and Reidinger, 1996).

Polymers are never 100% crystalline. XRD technique is used to determine the degree of crystallinity in polymers and also is a primary tool to determine the crystalline orientation.

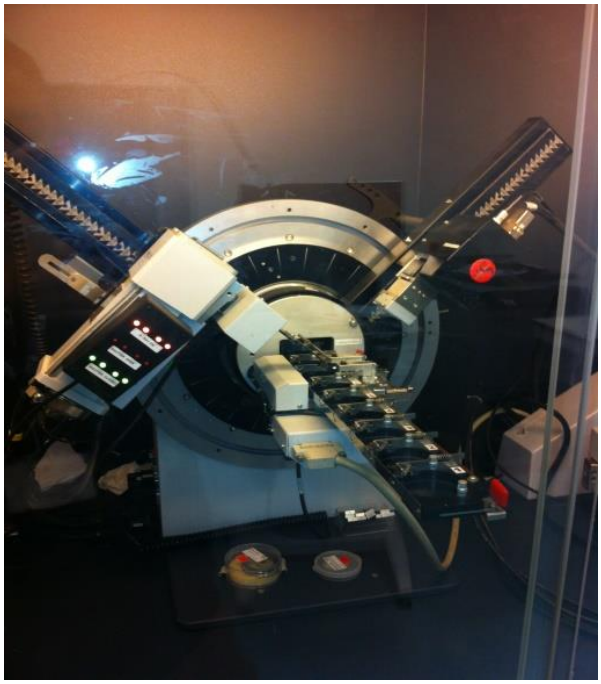

Figure 26-1 XRD with Buker D8 advanced copper-tube diffractometer equipped with a Linx Eye detector/ PSD (position sensitive) detector

1.6.1.1 Bragg's Law

"An X-ray which reflects from the surface of a substance has travelled less distance than an X-ray which reflects from a plane of atoms inside the crystal. The penetrating X-ray travels

down to the internal layer, reflects, and travels back over the same distance before being back at the surface. The distance travelled depends on the separation of the layers and the angle at which the X-ray entered the material. For this wave to be in phase with the wave which reflected from the surface it needs to have travelled a whole number of wavelengths while inside the material. Bragg expressed this in an equation now known as Bragg's Law (Cambridge Physics, 2016).

Equation 3-1) $$n\lambda = 2d\sin\theta$$

Where n is a positive integer and λ is the wavelength of incident wave.

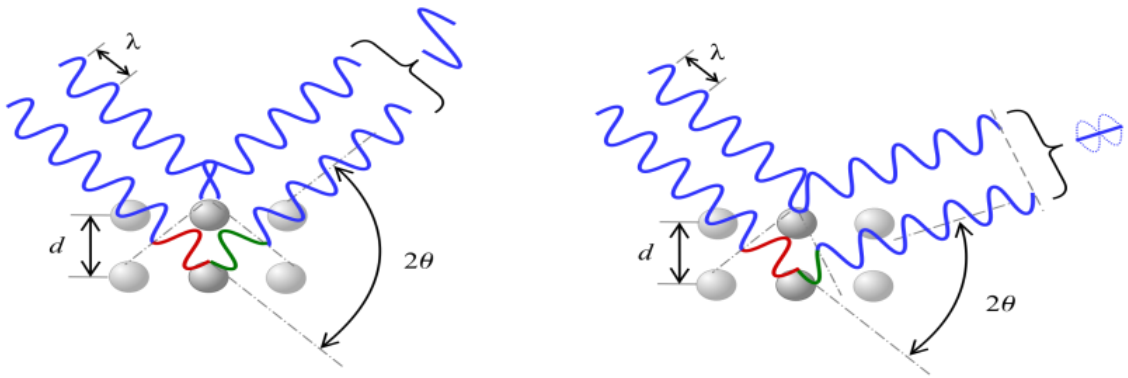

Figure 27-1 Bragg's law illustration (La Mecanica Cuantica, 2009)

According to Murthy and Reidinger the XRD pattern of a theoretically 100% crystalline polymer would be in forms of a series of sharp peaks, each corresponding to diffraction (reflection) from crystallographic planes. On the other hand, the XRD pattern of completely amorphous polymer would be a broad hump that shows the average separation of polymer chains. As a matter of fact, the XRD pattern of a semi-crystalline polymer would be then a superposition of crystalline reflections on an amorphous hump (Murthy and Reidinger, 1996).

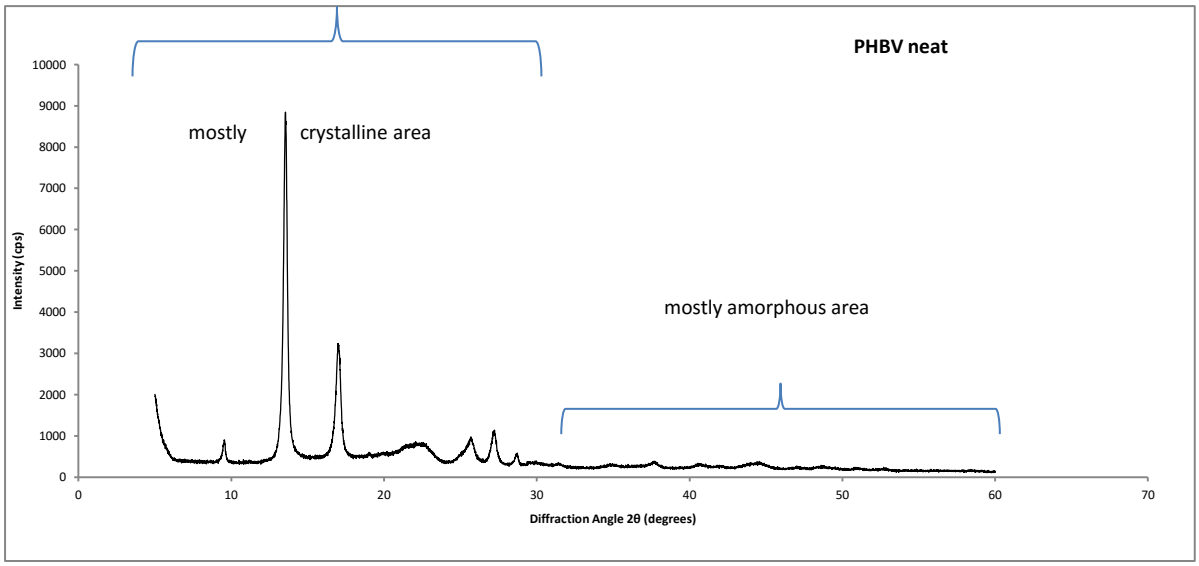

Figure 28-1 The XRD pattern of the PHBV neat, the mostly crystalline and amorphous areas are shown in the graph

When a semi-crystalline polymer crystallizes, part of the material remains amorphous. Therefore, a semi-crystalline structure can be described as a two phase model, consisting an amorphous and crystalline phase. The fraction of the crystalline phase in the material can be determined by analysing an XRD scan.

1.7 Chemical structure study

1.7.1 Fourier transforms infrared spectroscopy (FTIR)

Fourier transform infrared spectroscopy (FTIR) is one of the most important techniques used to identify polymeric materials. In infrared spectroscopy, IR radiation is applied to a sample. A part of the infrared radiation is absorbed by the sample and some of it is passed through (transmitted). The resulting spectrum represents the molecular absorption and transmission, creating a molecular fingerprint of the sample (Thermonocolet, 2001).

The advantages of FTIR are:

- Very fast
- Easy quantitative and qualitative analysis
- Low instrument cost

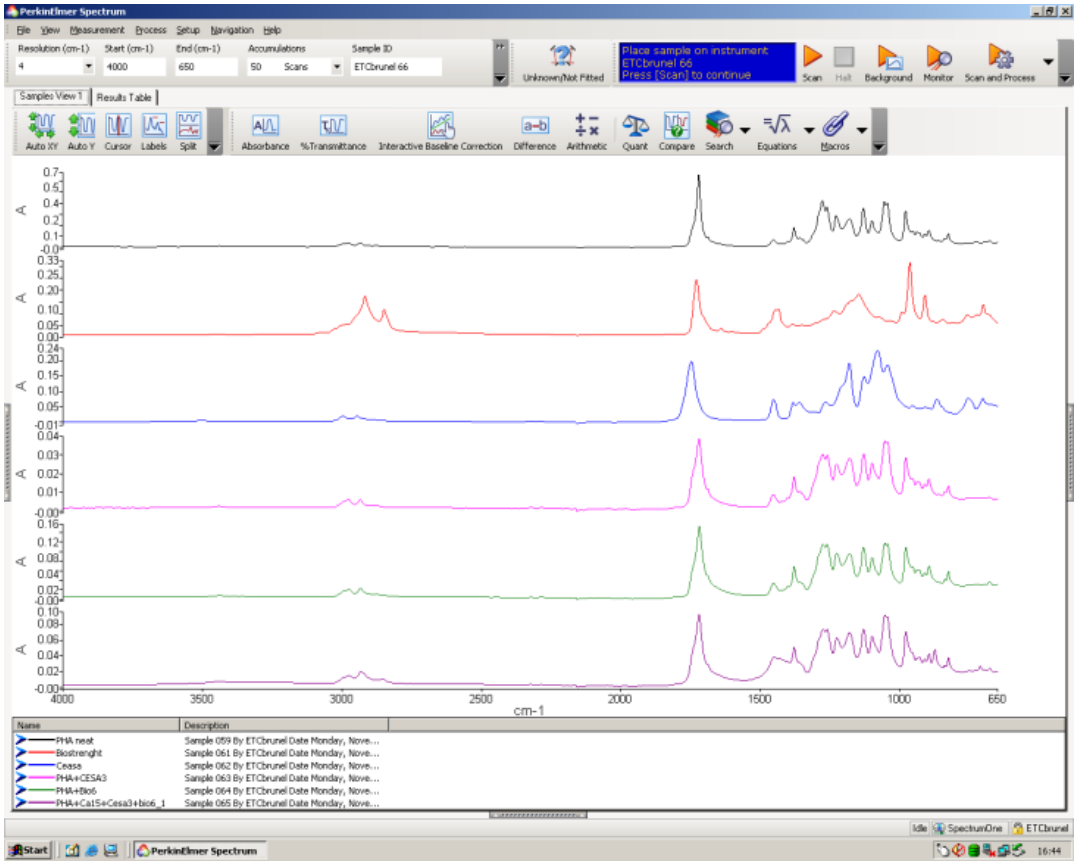

Figure 29-1 FTIR spectrum of the neat PHBV, impact modifier, chain extender, PHBV+CE, PHBV+IM, PHBV/CE/IM

For interpreting of FTIR data, the existence of a database is vital. Therefore, it is important when IR spectroscopy is used to identify structure of material, particularly functional groups which have characteristic bands in terms of intensity and frequency. The correlation of the chemical structure with IR absorption bands could help to assign the characteristic band in a material (Naranjo, 2008).

1.8 Mechanical properties study

1.8.1 Tensile test

Tensile test is one of the most fundamental types of mechanical test for polymers. Stress-strain curve is obtainable from a tensile test results.

Figure 30-1 Tensile tests with an Instron testing machine (model 3366), with 10 KN load cell and a crosshead speed of 5 mm/min

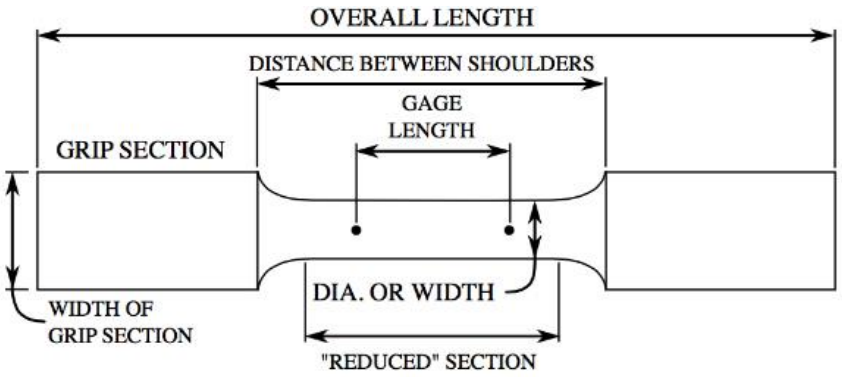

Figure 31-1 Schematic illustration of dumbbell tensile bar specimens

Specimens are based on ISO 527-1:93 & 527-2:93 with above dimensions:

Table 2-1 Table of dimensions comply with ISO 527-1:93 & 527-2:93

Overall length	190 mm
Distance between shoulders	110 mm
Gage length	80 mm
Width	10 mm
Width of grip section	20 mm
Thickness	4 mm

Figure 32-1 The example of 5 randomly chosen tensile bar to conduct tensile

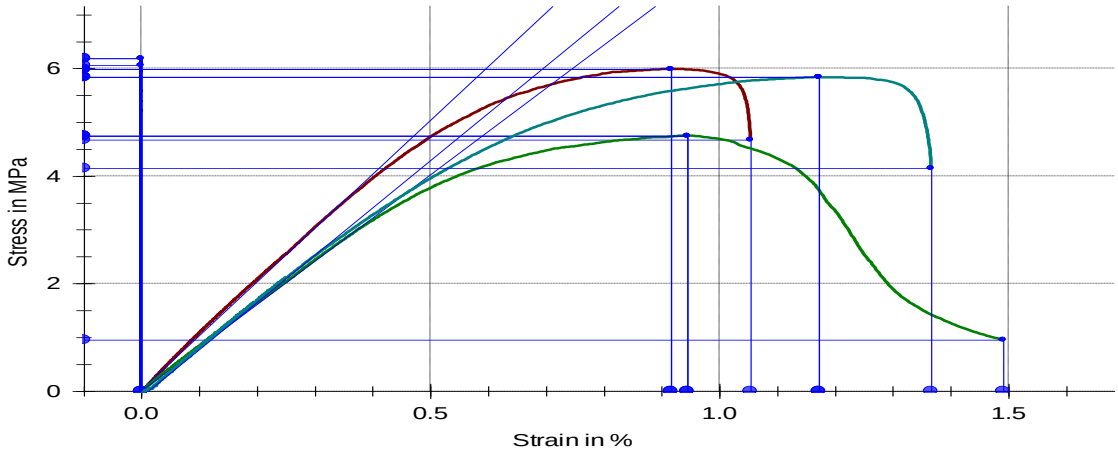

Figure 33-1 A typical stress-strain curve from PHA results (for 3 different PHA specimens tested here), Stress at the break (MPa), Elongation at the break (%), and Tensile strength (MPa) is pointed on axis

1.8.1.1 Hooke's law

The law of elasticity discovered in 1660 by the English scientist Robert Hooke. According to the Hooke's law, for relatively small deformations of an object, the displacement is directly proportional to the deforming force or load or for instances, within certain limits, the force required to stretch an elastic object such as a metal spring is directly proportional to the extension of the spring. . Therefore, the stress vs strain curve for many materials has a linear region. Hooke's law for a metal spring mathematically describes as:

Equation 4-1) $$F=kx$$

Where x is the extension of the spring (m), k is a constant called the rate or spring constant, F is the force applied (N)

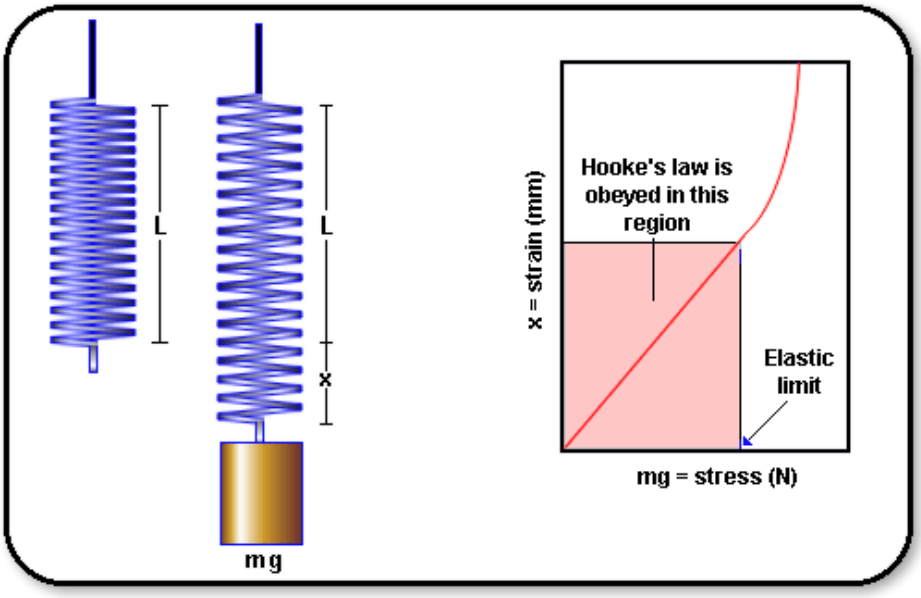

Figure 34-1 Hook's law illustrated, showing the displacement is directly proportional to the deforming force or load (Tutorpace, 2015)

The module of elasticity or Young's modulus is calculated according to Hooke's law from the slope of the stress-strain curves.

1.8.2 Flexural test

The flexural strength of a material is its ability to resist deformation under the load. The flexural modulus is the ratio of stress on strain in 3-point bending test and is determined from the slope of a stress-strain curve obtained from the flexural test.

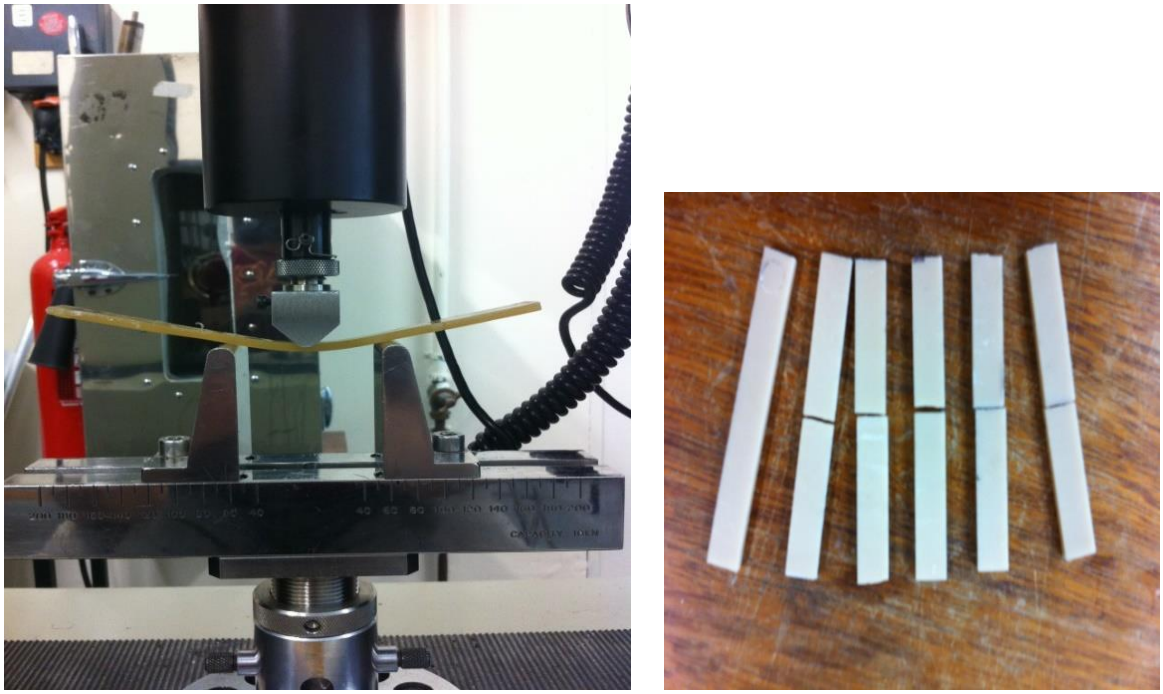

Figure 35-1 Flexural tests with an Instron testing machine (model 3366) and tested specimens

The test is based on ISO 178, and specimen's dimension is a cut with 80mmX10mmX4mm from an ISO 3167 type a specimen (Naranjo, 2008)

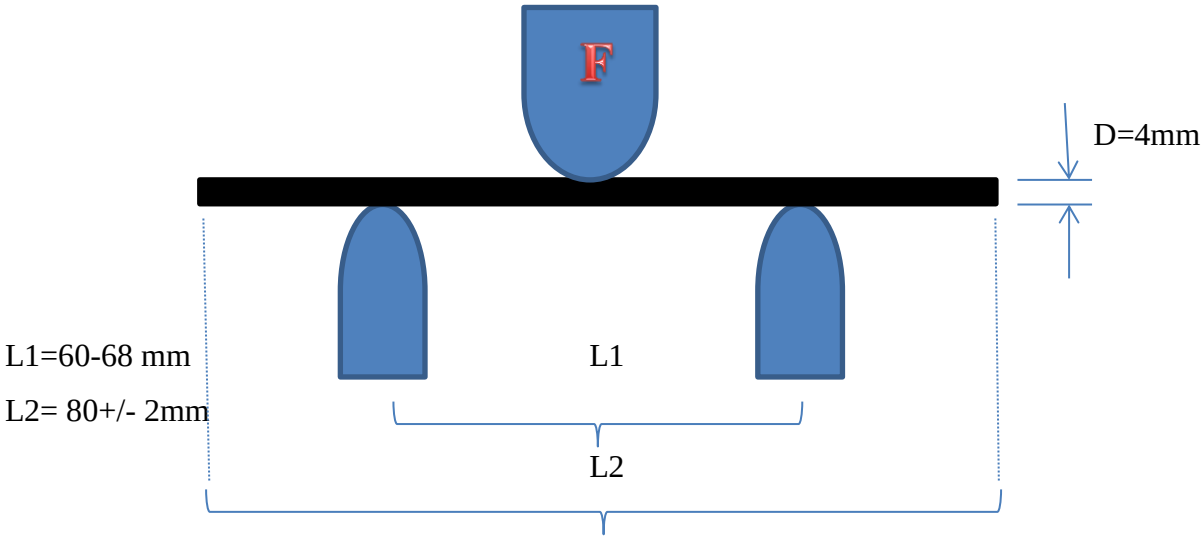

Figure 36-1 Schematic illustration of flexural test and required dimensions based on ISO 178

1.8.3 Impact properties

Drop weight impact test is one of the most common tests for composite materials. Drop weight impact test gives detailed information about failure mechanisms and behaviour of materials under impact. It basically works by the drop of a weight in a vertical direction, with a tube or rails to guide it during the "free fall" with the height and weight known, impact energy can be calculated (Instron, 2016).

The test has several advantages over other methods:

- It is applicable for moulded samples, moulded parts with complicated shapes
- It is unidirectional with no preferential direction of failure. Failures originate at the weakest point in the sample and propagate from there
- Failure can be defined by deformation, crack initiation, or complete fracture, depending on the requirements (Instron, 2016).
- The test is very simple but interpreting of data's is difficult

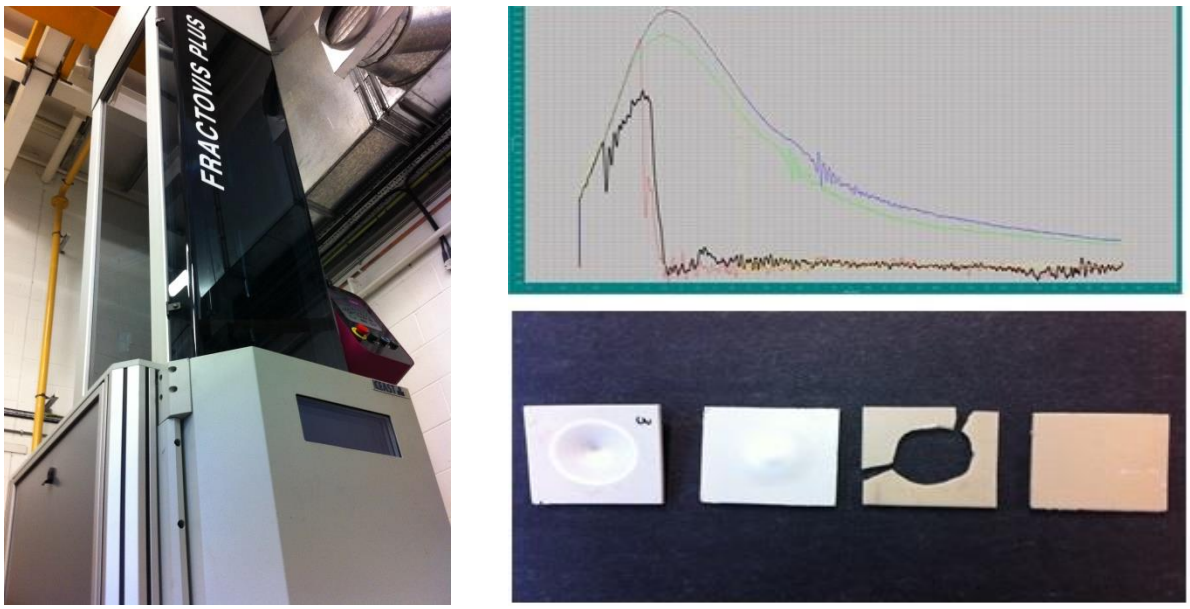

Figure 37-1 left) CEAST Fractovis Plus impact tester Model 7520 right top) impact graph, the y axis is Force (N) and the x axis is time(ms), right down) specimens of PHA plate with the different frailer behaviour

The specimens used for the drop weight testing are the injection moulded 150x150x4 mm plates according to BS EN ISO 6603 which cut into 60x60 mm squares. The data is plotted as force, energy, or displacement vs. time (Figure 37-1).

Bibliography Chapter 1

- Anonymous, (2016),” Dynamic Mechanical Analysis (DMA) A Beginner's Guide”,by Perkin Elmer, online at : http://www.perkinelmer.com/CH/CMSResources/Images/44-74546GDE_IntroductionToDMA.pdf (Accessed 17 Aug 2016)

- Azapagic, A., Emsley, A. and Hamerton, I. (2003), “Polymers, the environment and sustainable development”, John Wiley & sons Inc, West Sussex England, pp. 2-9

- Barnes, D. K. A., Galgani, F., Thompson, R. C. and Barlaz, M. (2009), “Accumulation and fragmentation of plastic debris in global environments”, Philosophical Transactions of the Royal Society B, Vol 364, issue 1526, pp.1985-1998.

- Browne, M.A., Crump, P., Niven, S.J., Teuten, E.L., Tonkin, A., Galloway & T., Thompson, R.C. (2011),”Accumulations of microplastic on shorelines worldwide: sources and sinks”. Environmental Science and Technology, Vol 45, Issue 21, pp. 9175-9179

- CalRecycle – California Department of Resources Recycling and Recovery (2012): PLA and PHA Biodegradation in the Marine Environment. State of California, Department of Resources Recycling and Recovery, Sacramento, California

- Cambridge physics, (2016), “X-Ray Diffraction”, [online] Available at : http://www-outreach.phy.cam.ac.uk/camphy/xraydiffraction/xraydiffraction7_1.htm (Accessed 14 Aug 2016)

- Chartoff, R. P., Menczel, J. D. and Dillman, S. H. (2014), “Dynamic Mechanical Analysis (DMA)”, in book: Thermal Analysis of Polymers: Fundamentals and Applications edited by Menczel and Prime,John Wiley & son Inc., page 387-497

- Daniels, N. (2016), “Plant-based biodegradable water bottle fights plastic”, Material world magazine, [online] Available at: http://www.iom3.org/materials-world-magazine/news/2016/may/01/plantbased-biodegradable-water-bottle-fights-plastic-waste (Accessed at: 12 Aug 2016)

- Ecobiomaterial, (2016), [online] Available at: http://www.ecobiomaterial.com/who-i-am/physiology-of-pha-metabolism/ (Accessed at: 13 Aug 2016)

- El-Kadi, S. (2010), “Bioplastic Production from Inexpensive Sources”, VDM Verlag Dr. Müller, pp. 45-60

- Epotek, (2016), [online] available at: http://www.epotek.com/site/files/brochures/pdfs/adhesive_application_guide.pdf (Accessed 17 Aug 2016)

- Eurostat, (2016), [online] Available at: http://ec.europa.eu/eurostat/statistics-explained/index.php/Waste_statistics , (Accessed at 13 Aug 2016)

- Harding, K., G., Dennis J.S., Von Blottnitz, H. and Harrison S.T. (2007) “Environmental analysis of plastic production processes: Comparing petroleum-based polypropylene and polyethylene with biologically-based poly--hydroxybutyric acid using life cycle analysis”, Journal of Biotechnology, Vol 130, pp. 57–66

- Hill, L. W. (2001), “Dynamic Mechanical Analysis of Property Development during Film Formation”, in book titled: “Film Formation in Coatings” edited by: Provder & Urban, Chapter 6, pp. 104–123

- InnovativeIndustry, (2011), “BioSuccinic Acid: Rising Bioplastic and Feedstock for Green Chemicals”, [online] Available at: http://www.innovativeindustry.net/biosuccinic-acid-rising-bioplastic-and-feedstock-for-green-chemicals , (Accessed at : 13 Aug 2016)

- Instron, (2016), “Impact test types”, [online] Available at: http://www.instron.co.uk/en-gb/our-company/library/test-types/impact-testing/test-types (Accessed 15 Aug 2016)

- IPCS, (2016), POLYMER, [online] available at: http://training.itcilo.it/actrav_cdrom2/en/osh/kemi/ctm9.htm (Accessed at: 12 Aug 2016)

- Kim, S. and Dale, B., E. (2005), “Life Cycle Assessment Study of Biopolymers (Polyhydroxyalkanoates) - Derived from No Tilled Corn”, The International Journal of Life Cycle Assessment, Vol 10, Issue 3, pp. 200-210

- Kosior, E., Braganca, R., M. and Fowler, P. (2006) ”Lightweight compostable packaging: literature review”, The Waste & Resource Action Program, INN003/26 (2006), pp. 1–48

- La Mecanica Cuantica, (2016), [online] Available at : http://la-mecanica-cuantica.blogspot.co.uk/2009/08/la-espectroscopia-de-rayos-x.html (Accessed 14 Aug 2016)

- Li, M., Li, Z. and Xu, J. (2010),” Viscoelastic Properties of a Modified Bio-polymers Prepared by Blending Poly (3-hydrobutyrate-co-4- hydrobutyrate) with Chain extenders”, 2010 3rd International Conference on Biomedical Engineering and Informatics (BMEI 2010), pp. 1739-1742

- Li, H. and Huneault, M. A. (2011), “Effect of Chain Extension on the Properties of PLA/TPS Blends”, Journal of Applied Polymer Science, Vol. 122, Issue 1, pp.134–141

- Longmold technology (2009), “injection moulding of thermoplastics”, [online] available at : http://www.longmold.com/viewnews.php?id=87 (Accessed 14 Aug 2016)

- MarketsandMarkets, 2013,”Polyhydroxyalkanoate (PHA) Market, By Application (Packaging, Food Services, Bio-medical, Agriculture) & Raw Material — Global Trends & Forecasts to 2018”, available online at: http://www.marketsandmarkets.com/Market-Reports/pha-market-395.html access (Accessed 14 Aug 2016)

- Murthy, N. S. and Reidinger, F. (1996), “X-ray diffraction-polymers”, in book of “A Guide to Materials Characterization and Chemical Analysis 2nd Edition” edited by Sibilia, J, P, Wiley-VCH Inc, pp.148-149

- Naranjo, A., Noriega, M., Roldan-Alzate, A., Sierra, J. and Oswald, T. (2008), “Plastic testing and characterization-industrial application”, Hanser Verlag, München,
    - pp. 70-220

- Nova (2012), [online] Available at: www.nova-institut.de/download/Meta-LCA%20Publication (Accessed at: 13 Aug 2016)

- Nyquist (2015),”Lower oil prices but more renewables: What’s going on?”, [online] Available at: http://www.mckinsey.com/industries/oil-and-gas/our-insights/lower-oil-prices-but-more-renewables-whats-going-on (Accessed at: 11 Aug 2015)

- Parvin, N., Ullah, S., Mina, F. and Gafur, A. (2013), “Structure and mechanical properties of talc and carbon black reinforced high density polyethylene composites: effect of organic and inorganic fillers”, Journal of Bangladesh Academy of Sciences, Vol. 37, No. 1, pp.11-20

- PerkinElmer, (2010), “TGA: a beginner’s guide”, [online] Available at: http://www.perkinelmer.co.uk/CMSResources/Images/44-74556GDE_TGABeginnersGuide.pdf (Accessed 14 Aug 2016)

- PerkinElmer, (2010), “Characterization of Polymers Using TGA”, [online] Available at: http://www.perkinelmer.co.uk/CMSResources/Images/44-132088APP_CharacterizationofPolymersUsingTGA.pdf (Accessed at 14 Aug 2016)

- Pfaendner, R., (2013)“polymer additives”, in book : “Handbook of Polymer Synthesis, Characterization, and Processing” edited By Enrique Saldivar-Guerra, Eduardo Vivaldo-Lima, [online] Access at : https://books.google.co.uk/books?id=4WHvBFnJ-g4C&printsec=frontcover#v=onepage&q&f=false (Accessed at : 13 Aug 2016)

- Pilla, S., Kramschuster, A., Yang, L., Lee, J., Gong, S. and Turng, L. S. (2008), “Microcellular injection-molding of polylactide with chain-extender”, Journal Materials Science and Engineering;C, Volume 29, Issue 4,pp.1258–1265

- Psarras, G. C., Manolakaki, E. and Tsangaris G.M. (2003),”Electrical relaxations in polymeric particulate composites of epoxy resin and metal particles”, Composites Part A: Applied Science and Manufacturing, Vol 33, Issue 3, pp. 375-384.

- Potsch, G. and Michaeli, W., 1995, “Injection moulding: an introduction”, first edition, Hanser/Gardner publications Inc, Cincinnati, page 2-7

- Posch, W.(2005), “shaping the future with filled plastics-innovative products made of polypropylene compounds”, conference paper at High Performance Fillers 2005: Cologne, Germany, 8-9 March 2005,page 4 from paper 10, [online] available at: https://books.google.co.uk/books?id=LwWLwj-fJrQC&pg=PA89&lpg=PA89&dq=talc+as+filler+and+nucleating&source=bl&ots=mQ2z9-xI7T&sig=yJURMc5d7_4frppucywqorFtdeI&hl=en&sa=X&ved=0ahUKEwiG_LTTkp_JAhXDbxQKHUPLDOg4ChDoAQgnMAE#v=onepage&q=talc%20as%20filler%20and%20nucleating&f=false (Accessed 13 Aug 2016)

- Philip, S., Keshavarz, T., Roy, I. (2007), “ Polyhydroxyalkanoates: biodegradable polymers with a range of applications”, Journal of Chemical Technology and Biotechnology, Vol 82,pp.233–247

- Rai, R. and Ray, I. (2011), “Polyhydroxyalkanoates: The emerging new green polymers of choise”,in book titled “Handbook of Applied Biopolymer Technology” edited by Sharma, S., Mudhoo, A., Royal Society of Chemistry, pp. 80-81

- Rauwendaal, C. (2010), “Understanding Extrusion”, second edition, Hanser Cincinati, page 8-15

- Reddy, M.M., Vivekanandhan, S., Misra, M., Bhatia, S.K. and Mohanty, A.K. (2013),” Biobased plastics and bionanocomposites: Current status and future opportunities”, Progress in Polymer Science, Vol 38, Issues 10–11, pp. 1653–1689

- Reddy, M.,M., Misra M. and Mohanty, A, K, 2012, “Bio-Based Materials in the New Bio-Economy”, Chemical Engineering Progress, Vol.108 ,issue 5, pp. 37–42

- Reference,(2016),[online] Available at: https://www.reference.com/science/biopolymer-fa6fe613ab1a0f8d# (Accessed at : 13 Aug 2016)

- Rosato, D. (2015), “Rapidly expanding bioplastics production capacity trends”, published [online] at: http://exclusive.multibriefs.com/content/rapidly-expanding-bioplastics-production-capacity-trends/engineering (Accessed at 11, Aug 2016)

- Sharma , P.K., Fu J., Cicek, N., Sparling, R. and Levin D.B. (2012), “Kinetics of medium-chain-length polyhydroxyalkanoate production by a novel isolate of Pseudomonas putida LS46”, Canadian Journal of Microbiology, Vol 58,issue 8, pp. 982-989

- Song, J., Kay, M. and Coles, R., (20110 ,“Bioplastics”, in book titled: “Food and Beverage Packaging Technology” edited by : Coles, R, Kirwan, J, M, John Willey & Son, page 307

- SPC, (2011), Sustainable Packaging, [online] available at: http://spcdesignlibrary.org/ (accessed at: 11 Aug 2016)

- Subramanian, M., N., (2013), “Plastics Additives and Testing”, Scrivener, New Jercy

- TED talk, (2010),” Are mushrooms the new plastic?” [online] available at : https://www.ted.com/talks/eben_bayer_are_mushrooms_the_new_plastic/transcript?language=en (Accessed at 12 Aug 2016)

- The guardian,(2015),” UK plastic bag use up for fifth year”, [online] Available at: https://www.theguardian.com/environment/2015/jul/24/uk-plastic-bag-use-up-for-fifth-year (Accessed at : 12 Aug 2015)

- Thermonicolet, (2001), “Introduction to Fourier Transform Infrared Spectrometry”, [online] available at: http://mmrc.caltech.edu/FTIR/FTIRintro.pdf (Accessed 15 Aug 2016

Chapter 2

Literature Review

2.1 Improvement of the polymer properties by blending

Polymer blending is a cheap, simple and time saving method to produce a new polymer alloy with specific properties. In fact, blending is a convenient method a cost-effective upgrading of resins and for tailoring these resins to suit the specific performance profiles for the desired application (Scobbo and Goettler, 2003).

The development and commercialization of a new polymer usually requires many years and is also extremely costly. However, by employing a polymer blending process – which is also very cheap to operate – it is often possible to reduce the time to commercialization of a new material to perhaps two to three years.

Polymer blends can be categorized in five main types:

- Thermoplastic–thermoplastic blends
- Thermoplastic–rubber blends
- Thermoplastic–thermosetting blends
- Rubber– thermosetting blends
- Polymer–filler blends

Since 1970, polymer blending has attracted a lot of attention as a cost-effective, simple method of developing polymeric materials with broad and versatile properties for commercial applications (Paul, 1989, Parameswaranpillai, Thomas and Grohens, 2015).

2.2 How to Design criteria for the polymer blending?

There are several reasons for the blending of two polymers:

- It could reduce the high-cost of a polymer with a low cost component
- Improve or develop the desired properties
- Create the new application for the material by changing the properties
- Change recyclability / compostability or renewability of the final composite
- Form a high performance compound from synergistically interacting polymers

In order to design the criteria, several steps should be considered:

- Define the objectives of blending: -The physical/chemical properties requirements
- Select the best choice of resins with properties that could satisfy the objectives
- The possible advantages/disadvantages which could occur by blending with the new component
- Design the experimental area for the blend
- The miscibility and or the method of compatibilizing
- Evaluate the cost feasibility (cost of components, compatibilizer, additives, compounding)and other manufacturing costs
- Define the requirement in the morphology of the composite
- Select rheological properties (molecular weights, compounding parameters, concentration of ingredients, amount of compatibilizer, type of deformation and intensity)
- Select the optimum fabrication method to yield the desired morphology (Brown, 2003).

Based on the Flory-Higgins theory, the entropy of mixing for the polymers is often very low, so the polymer mixtures mostly look phase separated into two components, just like oil and water. Generally, the majority of polymers are immiscible with each other. When these immiscible polymers are melt blended, different phases are formed from the different components, these different phases eventually separate in the final product, mostly because of the high surface tension between the immiscible polymer components in the interfacial region.

2.3 Thermodynamics of polymer blends

Thermodynamics science can determine the condition of the equilibrium state of the polymer blend and it can explain the phase diagram and the nature of the interface between the phases. Phase behaviour probably is the most important characteristic of the process of the blending of two or more polymers. There are several factors which influencing the miscibility of the polymer in a compound. Robeson stated that the combinatorial entropy contribution is very large in low molecular weight materials compared to long chain polymers. This contribution is the reason that solvent-solvent mixtures offer a much broader range of miscibility than polymer-solvent combinations. The range of miscible combinations involving polymer-polymer mixtures is much smaller (Robeson, 2007)

The main thermodynamic theory for describing the interaction between two polymers in a blend is the free-energy of Gibbs equation.

If the two polymers are mixed, the most frequent result is a system that exhibits a complete phase separation due to the repulsive interaction between the components (i.e. the chemical Incompatibility between the polymers).Complete miscibility in a mixture of two Polymers requires that the following condition is fulfilled:

Equation 1-2) $$\Delta G_m = \Delta H_m - T\Delta S_m < 0$$

Where ΔG_m= the Gibb's free energy, ΔH_m= the enthalpy of mixing and ΔS_m = the entropy of mixing at temperature T. According to Lipatov and Nesterov , "at constant temperature and pressure, the dissolution is a spontaneous process proceeding in the direction of diminishing Gibbs free energy of mixing"

For a system based on a thermodynamic process, by definition:

1. The free energy adopts a minimum value at equilibrium.

2. The free energy change is negative for spontaneous processes (Lipatov and Nesterov , 1997).

For the last 50 years, the Flory-Huggins Theory, supported by experimental data, has been a major theory for blending the polymers, in fact, this theory tells us that immiscibility of two polymers is a rule and miscibility is a rare phenomenon.

For non-polar polymer blends, the blend miscibility can be obtained by Flory-Huggins equation:

Equation 2-2) $$\frac{\Delta Gm}{RT} = \left(\frac{\phi 1}{N1} \ln \phi_1 + \frac{\phi 2}{N2} \ln \phi_1 \phi_2 * \chi_{12}\right)$$

Where ΔG_m is the Gibb's free energy due to nonpolar interactions, ϕ is the volume fraction; N the number of chain segments, and χ is the Flory-Huggins interaction parameter. The first two terms of right side in Flory-Huggins equation, are associated to entropy of mixing while the third part is associated with the enthalpy of mixing. For a polymer with a massive molar mass, the amount of entropy is very small, therefore the miscibility or immiscibility of the blend is strongly dependent on the value of the heat that is taken up or released upon the mixing of the two polymers; "the enthalpy of mixing".

Dependency on temperature as an indication of miscibility for two polymers helps to characterise the blend parameter by an interaction parameter. It acts like a pair of miscible polymers, in which each polymer has an advantage in properties but it can be characterized by a single transition temperature (T_g) taking place between T_g s of two individual polymers (Yu, 2014).

Lu and Weiss in a publication in Macromolecules journal in 1992 provided an equation which has perfectly proven the relationship between the glass transition temperature, T_g, and a binary interaction parameter χ, for miscible binary polymer blends. The equation including no adjustable parameters was based on a thermodynamic mixing formalism using enthalpy as the thermodynamic parameter. The enthalpy of mixing was written as a van Laar expression, and the T_g , was formally treated as a second-order Ehrenfest transition. The equation

satisfactorily predicts T_g-composition curves for miscible binary polymer blends that exhibit either positive or negative deviation from a linear mixing rule, depending on the strength of the interaction"(Lu and Weiss , 1992).

Therefore, as a matter of fact, the most common method used for the determination of the thermodynamic miscibility is to measure the glass transition temperature, T_g. However, it should be considered that according to Shultz and Young (1980) in many cases T_g is not sensitive to the thermodynamic miscibility of the components, but rather to the degree of dispersion. For instance, PMMA/PS solvent-mixed which didn't allow phase separation showed a single T_g, but the specimens revealed two T_g s when they were annealed (Shultz and Young, 1980).

When a system is miscible, a single T_g is obtainable from experimental tests, but a single T_g will also be demonstrated for immiscible systems having finely dispersed phases.

2.4 The glass transition in polymer blends

The glass transition behaviour of solid polymer blends has been shown in research to be an indication of the phase miscibility. Each component in the blend if it is immiscible with the other components shows a distinct T_g. This indicated a distinct segmental relaxation environment over the length scale intrinsic to the segmental motions. Olabisi, Robeson and Shaw stated that in general, the appearance of a single, distinct sharp glass transition at a temperature intermediate to the T_g s of the pure phases is characteristic of molecular homogeneity. Multiple T_g s however reflect the presence of micro phase separation or even partial miscibility of the blends components (Olabisi, Robeson and Shaw, 1979).According to Brostow et al, the T_g values are a function of composition for binary polymer blends, they indicate the miscibility, the compatibility and the immiscibility of the components in blends. Full miscibility could be identified by a single glass transition temperature for all the blends while in compatible systems there are two T_g values which depend on composition percentage and in immiscible polymers – not an infrequent case – T_g values for the pure components do not change with the composition. Figure 1-2 illustrates a schematic T_g appearance based on the composition of the components in a blend (Brostow, 2008).

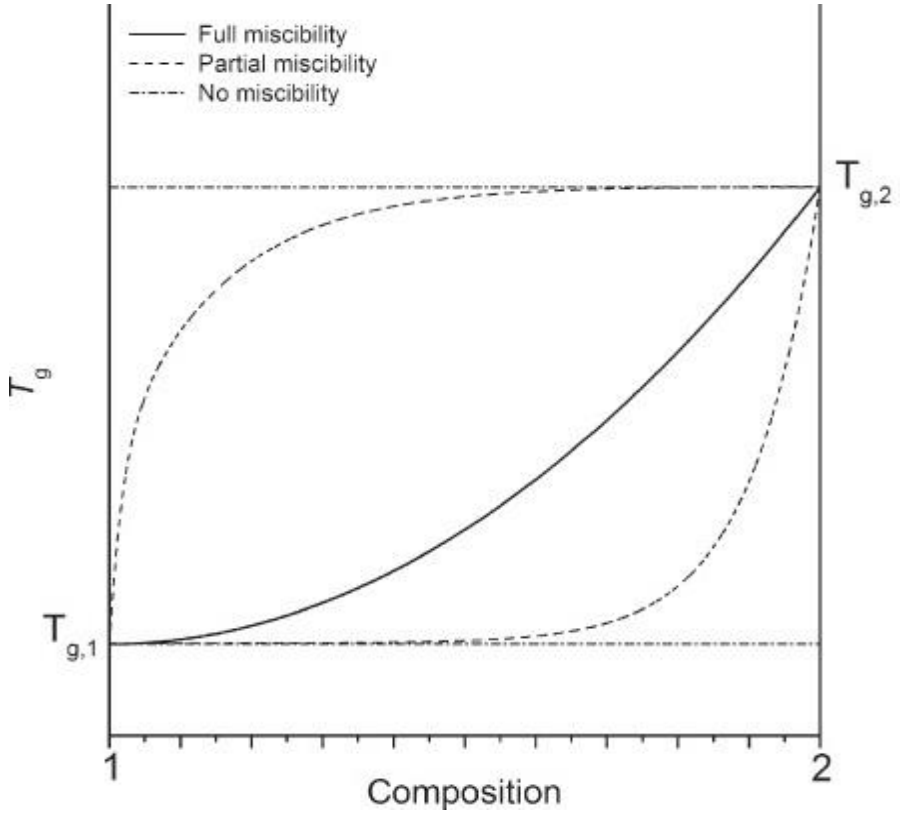

Figur1-2 A schematic representation of the dependence of T_g on composition in binary polymer blends: — fully miscible system;——compatible system; – ·– ·–immiscible system (Brostow, 2008)

Study shows that there have been several attempts to propose an equation which shows the relation between T_g and composition in binary blends. Fox equation (1965) applies to a binary blend system 1+2:

Equation 3-2) $$\frac{1}{Tg} = \frac{x1}{Tg1} + \frac{1-x1}{Tg2}$$

T_g =glass transition temperature of the blend, T_{gi} = T_g of component i, and xi is the mass (weight) fraction of component i. Fox equation is symmetric with respect to the components and only works based on prediction from properties of pure components (Fox, 1956).There are more other elaborated equation like Gordon and Taylor (GT) (1952) and Kwei (1984) equations for a more precise relation between T_g and composition:

Equation 4-2) $$T_g = [x_1 T_{g1} + k_{GT}(1-x_1)T_{g2}]/[x_1 + k_{GT}(1-x_1)]$$

Equation 5-2) $$T_g = [x_1 T_{g1} + k_{KW}(1-x_1)T_{g2}]/[x_1 + k_{KW}(1-x_1)] + q x_1(1-x_1)$$

k_{GT} & k_{KW} has to be evaluated from experimental data and represents unequal contributions of components to the blend. The index 2 in equations (3-2, 4-2, and 5-2) refers to the higher T_g component (Gordon and Taylor, 1952, Kwei, 1984).

Brostow et al proposed another equation based on experimental data for the PVA/PE blend. In the complete miscible systems the Fox Eq. (3-2) might be sufficient. With an increasing system immiscibility, the one-parameter Gordon–Taylor equation(4-2), the two-parameter Kwei equation(5-2), and finally for complicated systems the Brostow equation can effectively apply (Brostow, 2008).

However, homo polymer blend pairs having absolute thermodynamic miscibility in the entire volume are quite rare. Most polymers are immiscible from the thermodynamic standpoint since the entropic contribution to the free energy of mixing is negligible (Scobbo, 2000). According to Scobbo, "partially miscible blend pairs present two distinct glass transition temperatures. However, the two T_gs could be moved towards each other, the shift being dictated by the amount of each phase that is dissolved in the other or by the partitioning of oligomers or additives. In fact, with respect to modulus and temperature, several possibilities exist (Scobbo, 2000).

It should always be considered that there is not an exact temperature called the glass transition temperature T_g; there is a glass temperature region because the process of changing from the glassy state into either a liquid or a rubbery phase is a gradual process. The glass transition phenomenon consists of a broad temperature range. In spite of this fact researchers usually report a unique value for the so-called glass transition temperature (T_g), in the presence of the melting point T_m (Kalogeras and Brostow, 2008). While T_m values are often not dependent on the heating or the cooling process (freezing a liquid, melting a solid) or on the change rate (there are exeptions), the location of the glass transition region depends on both factors (Brostow et al, 2008).

There are two important limitations which could affect the assessment of T_g, these are mentioned in the work of Karasz:

- In order to be ensured that proper resolution exists between possibly overlapping relaxation in immiscible or partially-immiscible blends, the T_g of the individual components must differ by at least 20 ℃.
- The quantity of both components should be sufficient for detection, with the minor component at a minimum of 10 or 20 %. (Karasz, 1985)

A study of the crystallinity and changes in the glass transition of the phases of an immiscible blend of two highly crystalline polymers is often complex. The complexity happens due to the chance of crystallization of one or both components in different conditions .This difficulty also applies to a blend of PHBV with PBS in DSC tests, making it difficult to distinguish T_gs. Kim argued that the transitional behaviour in the blends of two crystalline polymers is difficult to assess by DSC due to the breadth and relative low intensity of the glass transitions (Kim and Park, 1998). It could be explained that the PHBV α phase crystal spherulites always form prior to the PBS and PBS spherulites must progress past the existed PHBV spherulites because it was developed after an induction period that has been long enough to allow the PHBV spherulites to grow to their full extent. Therefore it is difficult to investigate PBS crystallization kinetics from the melt for PHBV/PBS blends. In this study we could only report the data with respect to PHBV crystallization kinetics.

The similar phenomenon has been reported by Chiu et al about miscible blends of Poly (vinylidene fluoride) with PHB, although the PVDF and PHB crystallized over essentially the same temperature region. Due to the proximity of melting point but their crystallization rates were very different in that the crystallization of PVDF always occurred prior to PHB. The scenario is not completely the same for PHBV/PBS as PBS starts its crystallization after PHBV is crystallized completely (Chiu, Huang and Don, 2008)

2.5 Compatibilization of the polymer blends

Researchers often define chemical compatibility as a complete molecular mixing. However, the macromolecules don't fit on this definition due to their large molecular size. In fact, many heterogeneous systems would be seen as a homogeneous system, despite of the phase separation witnessed in the electron microscopy or two distinguishable T_g's observed by the thermomechanical techniques. Thus, in the study of macromolecular systems, mixing of the polymer segments chains is not effective unless the miscibility conditions are evaluated persuasively.

According to Majumdar & Paul, immiscible blends exhibit poor mechanical properties and phase morphology due to an undesirable interaction between the molecular segments of the components. That undesirable interaction would lead to:

1- A large interfacial tension during melting process make it difficult for component's particles to disperse uniformly in melt and rearrangement (e.g. coalescene) afterwards

a. Lack of interfacial adhesion in the solid state, the main reason for the mechanical failure due to the poor phase interaction.

Generally, compatibilization can cure these defects by the production of graft or block co-polymers which present an interfacial or coupling agent (Majumdar and Paul, 2000).
Kim and White stated that although, the immiscible blend's mechanical, thermal and rheological performance mostly depends on the characteristics of each individual component, it also depends on the morphology of the blend and the interfacial tension between different phases. In order to control the morphology and reduce the interfacial tension, it requires the process of compatibilization. In fact, compatibilization of a blend doesn't change the phase separation completely but the minor phase is stabilised and better dispersed in the base matrix (Kim and White, 2011)

Utraki defined compatibilization as "a process of modification of interfacial properties of an immiscible polymer blend, leading to creation of a polymer alloy". And a polymer alloy is

defined as “An immiscible polymer blend having a modified interface and/or morphology” (Utraki, 1998).

Fink stated that the principle requirements for a compatibilizer in a reactive process ought to be:

- An optimizer of the interfacial tension
- Provide effective mixing in order to lead to an acceptable morphological texture
- The polymer molecules must contain chemical functional groups which can react and form primary bonds during reactive processing and also the functional groups must be reactive for the reaction which is expected to occur across the melt phase boundaries.
- The speed of the reaction must be quick enough in order to occur within the extruder or mixer.
- The bond formed as a result of the compatibilization must remain stable through secondary processing such as injection moulding.
- The adhesion between the phases in the solid condition should be enhanced (Fink, 2005).

The architecture of the compatibilizer at the interface is dependent on the structure of the reactive chains. Brown announced that the reaction systems for compatibilization could occurr in terms of topology in different categories:

- Chain cleavage and recombination
- Graft copolymer formation
- Block copolymer formation
- Covalent cross-linking (Brown 1992).

Brown argued that “The formation of an optimum dispersed phase particle size and the long-term stabilization of the blend morphology are critical if the blend is going to have optimum properties and in particular good mechanical properties. If this morphology is not stabilized, then the dispersed phase may coalesce during any subsequent heating and high stress treatment such as injection moulding” (Brown, 2003)

2.6 Nonreactive blends

The majority of the immiscible polymers form a rough combination with a sharp interface consists of the large lump of material caused by the interfacial tension which consequences to the weak interfacial adhesion (Chang, 1997).

The effects of a block copolymer on the miscibility of the polymer blends have been investigated by researchers in many studies. The block copolymer basically resides at the interface and reduces the molecular tension by separating the homopolymers from the interfacial region. The effect has been discussed in several case studies by Fayt, Jérôme and Teyssié using SEM and TEM (Fayt, Jérôme and Teyssié, 1987). In fact, the exact location of the components in such a system strongly depends on the molecular weight of the di-block copolymer. If it is low the segment of the copolymer is stretched and the homopolymers are excluded from the interfacial region known as dry brush phenomena, while on the contrast, the homopolymers can penetrate into the interfacial region known as wet brush phenomena (Fayt, Jérôme and Teyssié, 1987, Lindsey, Paul and Barlow, 1981).

Leibler developed a theoretical prediction with the help of a microscopic statistical theory of phase equilibria in non-crystalline block copolymers. The results revealed the presence of a suitable block or graft copolymers leads to a reduction in the interfacial tension in phases of an immiscible blend (Lieber, 1979).

If blend of polymers (A/B) is being compatibilized by a block copolymer(C-b-D), it is important to identify the location and distribution of C-b-D in A/B, which could determine the interfacial tension, interfacial thickness, interfacial adhesion, phase dispersion, phase coalescence, and mechanical properties of the final blend. The block copolymer can be located in various places:

- Located at the interface
- Within A and/or B as micelles
- Randomly dispersed in both polymer matrix
- Existing at the free surface

Moreover, there are some factors which can alter the location and the distribution of the block copolymer C-b-D in the A/B blend:

1- Interaction parameters from the Flory-Huggins equation(χ_{AB} , χ_{AC}, χ_{AD}, χ_{BC}, χ_{BD}, χ_{CD})
2- Volume fractions ϕ_A, ϕ_B, ϕ_{CD}
3- Molecular weights of polymers M_A, M_B, M_C, M_D
4- Process Temperature
5- Processing condition (Chang, 1997).

Lieber mentioned that in the condition of high immiscibility when interaction parameters are such that: $\chi_{AD} >> \chi_{AC}$ and $\chi_{BC} >> \chi_{BD}$ and the molecular weights of the two polymers in the copolymer are equal ($M_C = M_D$), a thermodynamic driving force exist to orient the copolymer at the interface (Lieber, 1982).

In Many cases, surprisingly, the block copolymers are more efficacious compatibilizers than graft copolymers. The later one hinders the accessibility to the backbone of the copolymer due to a high amount of the branches (Markham, 1990). The relation between the interfacial tension and the miscibility of a blend is well established in researches. The immiscibility generally declined linearly with an increase in the amount of compatibilizer molecules up to the critical micelle concentration(CMC) [the concentration of surfactants above which micelles form and all additional surfactants added to the system go to micelles]. Any additional copolymer beyond the CMC doesn't show any effects on interfacial tension in polymer blends (Fayt, Jérôme and Teyssié, 1987; Markham, 1990).

2.7 Reactive blends

Reactive polymer compounding provides a sophisticated method for the production of polymer blends and alloys. There are several advantages for reactive compatibilization over simple mechanical blending. Tsukahara, Ismail and Shonaike stated that the first advantage could be the connectivity between the phases of components which can be improved by the formation of stronger chemical bonds such as a covalent bond. The second advantage was

that the phase morphology can be assessed and optimized when a chemical reaction such as grafting, cross-linking and polymerization occurs.

The third advantage is that the morphology of the component phases by the generation of a covalent bond can be assessed by a stabilization of the phase-separated domain morphology in the blend. Furthermore, a simultaneous progression of the chemical reactions with processing is an advantage in the economical production of polymer blends and alloys (Tsukahara, Ismail and Shonaike, 1999).

Table 2.1 Example of reactive blending and alloys (Tsukahara, Ismail and Shonaike, 1999)

Type	Reaction	Polymers
Reactive and nonreactive compatibilization (improvement of interface)	Coupling reaction	HIPS, ABS
	Polymerization reaction	PP/Nylon
	In-situ formation of block and graft copolymer	
Self-curing or self-vulcanization	Cross-linking reaction Random site type and telechelic type	CP/PAA, ENR/XPCL
Reactive filler	Polymerization	PMMA/PBA
Dynamic vulcanization	Cross-linking reaction	EPDM/PP
Interpenetrating polymer network (IPN)	Polymerization reaction	

Table 2.1 shows some examples of reactive blending and alloys produced by different reactive blending methods.

One important aspect of reactive compatibilization according to Majumdar and Paul is that more surface area is generated by breaking down the dispersed phase through the interfacial reaction. The probability becomes higher for functional groups to find each other and react to form more copolymer, which could result in a finer dispersed particle size (Majumdar and Paul, 2000).

Utraki stated that the ideal conditions for reactive processing are:

- An effective dispersive and distributive blending method to achieve a desirable renewal of interface
- The compatibilizer should have a reactive functionality group, with strong tendency to react with at least one of the polymers
- A sufficient reaction rate to ensure that there is enough time for the in situ reaction

The chemical reaction often leads to the formation of a covalent or an ionic bond (Utraki, 1998).

Polyester blends are commonly compatibilized by reactive blending methods. The reactive process is applicable to most polyesters containing nucleophilic end groups, such as carboxylic acid/or hydroxyl groups that tend to react with the many functional groups of compatibilizers such as amine, epoxy and oxazoline (Olabisi, Robeson and Shaw, 1979). However, the forming of a true covalent reaction between the majority of polyester compatibilizers has not been reported in the literature with a solid evidences especially for the maleic anhydride based compatibilizers (Olabisi, Robeson and Shaw, 1979) . The epoxy-functional compatibilizer apparently showed a better performance than the MAH (maleic anhydride) because the end epoxy group could react with the terminal carboxyl and/or hydroxyl groups of polyesters by a common melt processing method. The only problem that might occur during the process was identified as the lack of enough time for a complete effective reaction, which could be curable by the addition of a suitable catalyst.

2.8 Different methods for study of polymer-polymer miscibility

According to Olabisi, Robeson and Shaw (1979), there are several methods for determining polymer-polymer miscibility.

2.8.1 Glass Transition Temperature

2.8.1.1 Mechanical Methods

The mechanical methods are the most common techniques among researchers for studying miscibility. Basically, by applying the small-amplitude cyclic deformation to the polymers, the elastic and viscoelastic properties can give vital information about the transitions that occur on the molecular scale over a broad temperature range. For the immiscible polymer-polymer systems, there is no change to the transition temperature of each individual component of the blends, while on the other hand, for miscible systems, a single and unique transition temperature is observable by dynamic mechanical test.

2.8.1.2 Dielectric Methods

There are analogue relations between the electrical properties and the mechanical properties of a polymer. The dielectric constant, ε', the dielectric loss factor, ε", and the dielectric strength are similar to compliance, mechanical loss and tensile strength, respectively. The dissipation factor, tan δ (ε"/ ε') could be an indication of the polymer transition which can support the glass transition temperature determined by the other methods.

2.8.1.3 Calorimetric methods

Generally, in differential scanning calorimetry (DSC), the specific heat of the polymer shows a change when it in in the glass transition region. However, for highly crystalline polymers since only the amorphous side of the polymer contributes to the transition from the glassy state to the rubbery state, the glass transition temperature is very weak and it is difficult to detect by DSC.

There are also other methods bases on the transition detection such as dialotermic methods, thermo-optical analysis, and radioluminescence spectroscopy.

2.8.2 Microscopy

2.8.2.1 Visible, Including Phase Contrast

Detecting differences in the refractive index of phases and the contrast between opacity and colour of two distinctive phases could be studied by transmitted-light and phase contrast microscopy.

2.8.1.2 Electron microscopy

Transmission electron microscopy (TEM) and scanning electron microscopy (SEM) has been widely used for observing the miscibility of a polymer blend system.

SEM reveals more information on the morphology. A domain size of 10 nm can be determined by SEM.

Although TEM requires a complicated sample preparation, the resolution of TEM is better than optical microscopy and SEM (Gedde, 1999).

Basically the morphology of the blend could provide vital information about the final pattern of the drop breakup, the fabrication process and the coalescence rates at the end of blending. With melt blending by extrusion, the minor component phase is broken up to form the dispersed phase. The size and shape of the dispersed phase are controlled by the interfacial tension, rheological properties, and the complex strain field of the extruder (Wu, 1987).

It should be noted that if the phase size increases with an increase of the dispersed-phase concentration, the probability of impingement of particles also increases. Reactive compatibilization alters the balance between the drop break up and coalescence by a reduction in the interfacial tension and stabilizes by after a steric effect. These phenomena produce much smaller dispersed-phase particles (Majumdar and Paul, 2000).

Kaplan used the SEM and claimed that the compatibility of a macromolecular system can be defined by a compatibility number:

Equation 6-2) $$\mathbf{N_c} = {\boldsymbol{exprimental\ probe\ size}}/{\boldsymbol{domain\ size}}$$

The experimental probe size in a mechanical test, for example, would be the segmental length associated with the T_g phenomenon. The domain size is the average length in which only one component exists:

- when $N_c \rightarrow 0$, incompatible system: two transition are observable by dynamic mechanical testing, corresponding to the T_g s of the each of the polymers. A change in the volume fraction of the polymers, only changes the peak's height and does not shift them along the temperature axis.
- when $N_c \rightarrow 1$, partially compatible system: shows a broadened modulus curve. The two glass transition temperatures are shifted inward due to an increase in the phase interaction between the polymers.
- when $N_c \rightarrow \infty$, compatible system: only one main transition is observable by dynamic mechanical testing because , the composition fluctuations are small enough to average out over the probe distance. A change in volume fraction of the components results in a shift along the temperature axis (Figure 2-2).

The symbol (→) in above, is a conditional in Eulerian logic. (Kaplan, 1976).

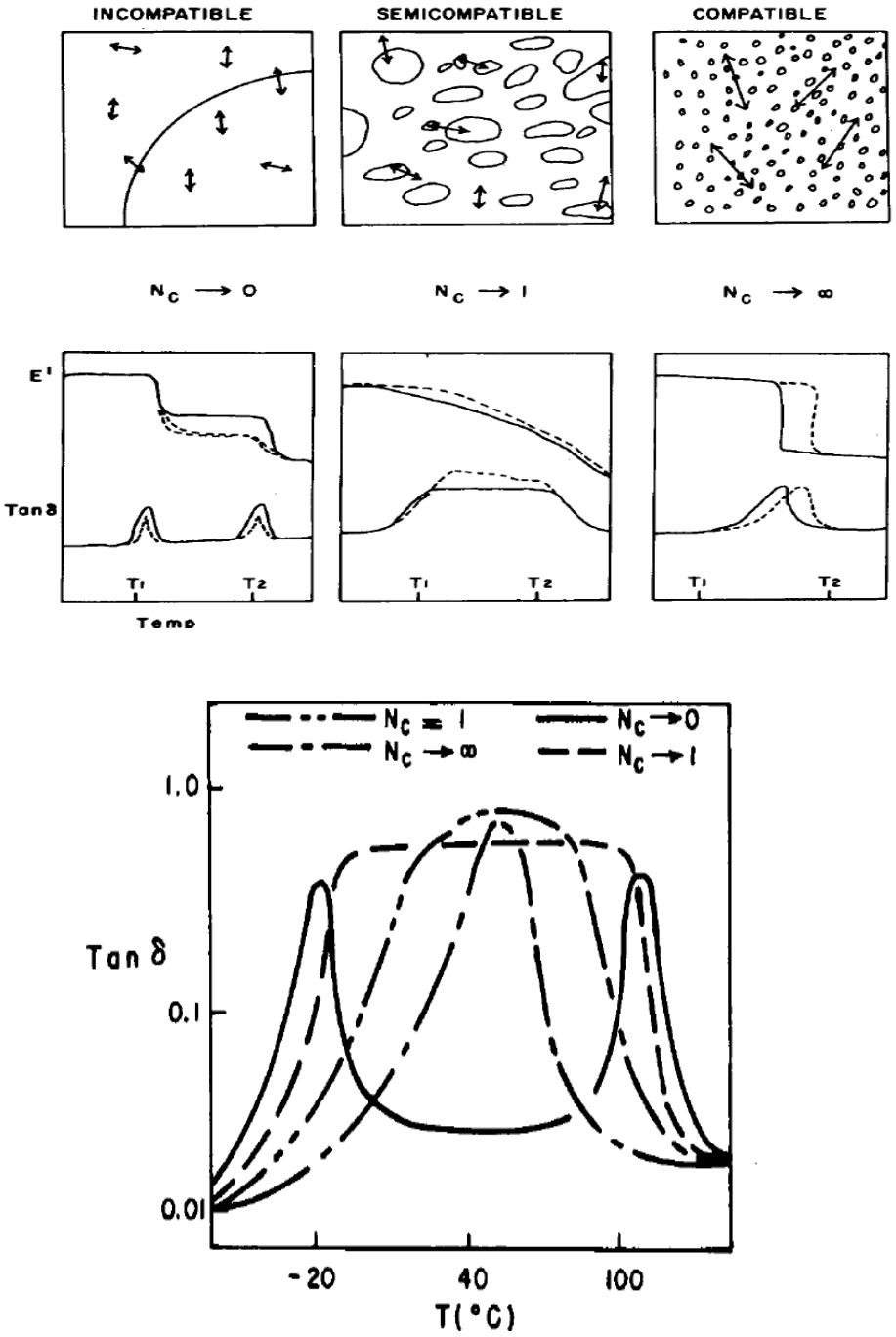

Figure 2-2 Schematic representation of incompatible, partially compatible, and compatible systems, probe size and domain size in Electron Microscope and corresponding Dynamic Mechanical behaviour at below and in right, tan δ vs temperature for different systems (Kaplan, 1976)

Kaplan presented a schematic representation of incompatible, partially compatible, and compatible systems (top-left). The probe size is represented by the arrows and the domain size by circles in electron microscope and at the down left the corresponding dynamic mechanical behaviour is illustrated (Figure 2). In right picture the tan δ vs temperature for different systems is shown (Kaplan, 1976).

There are other methods for determining polymer-polymer miscibility such as scattering methods (cloud-point method, conventional light scattering method, pulse-induced critical scattering, neutron scattering and X-ray scattering), or Ternary-solution method (Olabisi, Robeson and Shaw, 1979).

DMA were used to obtain the T_g of the samples in this study because they are more sensitive than the thermal analysis technique (DSC). DMA is one of the most sensitive techniques available for characterizing the mechanical behaviour of materials. However, as it was mentioned T_g is a region of phase change. There are three different values for the T_g from DMA, one value from the storage modulus E′, another one from the loss modulus E″, or as popular to report by researchers, from the tan $\delta = E''/E'$.

2.9 Reinforcement of the polymer composite

The definition of the reinforcement in polymers depends on different perspectives but in general it is a process which the polymer matrix is combined with different solid, liquid, a gases substance that is heterogeneously distributed and presents a distinguishable phase boundary with polymer matrix.

Thermoplastic are the most widely produced polymers in the world. The reinforcement of thermoplastic composites with different fillers and fibre has been around for many years. Composites are also defined as materials with two or more discrete phases with an interface between the phases. Karger-Kocsis, however mentioned that this definition is generally applied to the materials containing reinforcing ingredients identified by a high aspect ratio, such as fibres, platelets, flakes. In fact, these materials could improve the mechanical and

thermal properties of the polymer matrix (Karger-Kocsis, 1995). Fillers with low aspect ratio are mostly used to reduce the price of the composite and often their incorporation consequences on sacrificing some mechanical properties. Although, according to the researchers the variation between these two definitions are arbitrary.

Polymer composites are mixtures of polymers with inorganic or organic additives having certain geometries (fibres, flakes, spheres, and particulates). Bio-composites are composites consisting of a matrix (resin) and a reinforcement of natural fibres, fillers or particulates. Bio-composites can be classified on the basis of the intended application:

- Bio-composites for ecological applications
- Bio-composites for biomedical applications

Bio-composites for ecological applications are combinations of natural fibres or fillers with polymer matrices from both non-renewable and renewable resources and are characterized by environmental degradability.

Bio-composites for biomedical applications are combinations of bio-stable or degradable polymers with inert or bioactive fillers intended for use in orthopaedics, bone regeneration, or tissue engineering applications (Xantos, 2010).

Additives for polymer composites are categorized as:

- Reinforcements
- Fillers
- Reinforcing fillers

Reinforcements usually increase the polymer modulus and its strength. Basically, the modification of the mechanical properties of a polymer is often considered as the primary function of the added reinforcing fillers. However, the incorporation of these additives might affect the crystallinity, the transparency and the thermal stability of the polymer matrix as well.

Composites could be classified in:

- Continuous composites; the resin, mostly thermosets, are reinforced with long fibres. They are usually prearranged in certain geometric patterns. They may become the major component of the composite (they can constitute as much as 70% by volume in oriented composites).
- Discontinuous composites; when the composites are reinforced with the anisotropic reinforcing additives (short fibres or flakes). They are arranged in the composite in different orientations and multiple geometric patterns. The arrangement is dictated by the selected processing and shaping methods, most often extrusion and injection moulding. In this case, the content of the additive does not usually exceed 30–40% by volume.(Xantos,2010; Raghupathi, 1990)

Xanthos defined the parameters that affecting the properties of composites as:

- The properties of the additives (inherent properties, size, and shape)
- The composition
- The interaction of components at the phase boundaries, or condition in interphase, compatibilization state
- The method of fabrication (Xantos, 2010).

Scientists use the term “reinforcing filler” to describe discontinuous additives. They could modify the mechanical properties of the polymer, particularly strength. In fact, inorganic reinforcing fillers are stiffer than the matrix and deform less, causing an overall reduction in the matrix strain, especially in the vicinity of the particle as a result of the particle–matrix interface.

Different type of fillers with their function and chemical formula are illustrated in Tables 3-2 & 4-2:

Table 2-2 Chemical families of fillers for plastics (Xantos, 2010)

Chemical family	Examples
	Inorganics
Oxides	Glass (fibers, spheres, hollow spheres, and flakes), MgO, SiO2, Sb2O3, Al2O3, and ZnO
Hydroxides	Al(OH)3 and Mg(OH)2
Salts	CaCO3, BaSO4, CaSO4, phosphates, and hydrotalcite
Silicates	Talc, mica, kaolin, wollastonite, montmorillonite, feldspar, and asbestos
Metals	Boron and steel
	Organics
Carbon, graphite	Carbon fibers, graphite fibers and flakes, carbon nanotubes, and carbon black
Natural polymers	Cellulose fibers, wood flour and fibers, flax, cotton, sisal, and starch
Synthetic polymers	Polyamide, polyester, aramid, and polyvinyl alcohol fibers

Table 3-2 Different type of Fillers and their functions (Xantos, 2010)

Primary function	Examples of fillers	Additional functions	Examples of fillers
Modification of mechanical properties	High aspect ratio: glass fibers, mica, nanoclays, carbon nanotubes, carbon/graphite fibers, and aramid/synthetic/natural fibers	Control of permeability	Reduced permeability: impermeable plate-like fillers: mica, talc, nanoclays, glass flakes
	Low aspect ratio: talc, CaCO3, kaolin, wood flour, wollastonite, and glass spheres		Enhanced permeability: stress concentrators for inducing porosity: CaCO3 and dispersed polymers
Enhancement of fire retardancy	Hydrated fillers: Al(OH)3 and Mg(OH)2	Bioactivity	Bone regeneration: hydroxyapatite, tricalcium phosphate, and silicate glasses
Modification of electrical and magnetic properties	Conductive, nonconductive, and ferromagnetic: metals, carbon fiber, carbon black, and mica	Degradability	Organic fillers: starch and cellulosic fibers
Modification of surface properties	Antiblock, lubricating: silica, CaCO3, PTFE, MoS2, and graphite	Radiation absorption	Metal particles, lead oxide, and leaded glass
Enhancement of processability	Thixotropic, antisag, thickeners, and acid scavengers: colloidal silica, bentonite, and hydrotalcite	Improved dimensional stability	Isotropic shrinkage and reduced warpage: particulate fillers, glass
		Modification of optical properties	beads, and mica Nucleators, clarifiers, and iridescent pigments: fine particulates and mica/pigment hybrids
		Control of damping	Flake fillers, glass, and BaSO4

Nowadays, the new technologies provide a broad range of applications for fillers with the development and improvement of their properties. These additional or improved functionalities make the fillers not only an additive for cost reduction but an additive with multi-functional effects. The optimization of the effect of multi-functional fillers on the properties of polymers will be an important field for researchers and composite producers.

2.10 Core-shell Impact modifier

PHAs are a family of environmentally degradable polymers (biopolymer) which can be a possible substitute for some petroleum based polymers. Mechanical properties of PHBV, a copolymer of PHA's family make them suitable replacements for petrochemically produced bulk plastics (polyethylene, polypropylene etc.). However, some serious drawbacks associated with PHBV have hindered its widespread usage. Issues such as a narrow processing window, low impact resistance and brittleness coupled with a sluggish crystallinity and a rapid thermal degradation that provide challenges for using the material in conventional processing machinery. There have been several attempts by researches to overcome the low impact resistance of PHBV and also the brittleness. Blending with biopolymers or conventional petroleum based polymers, compounding with the rubbery polymers or impact modifier additives have been reported in researches (Corre, Bruzaud and Grohens, 2013; Javadi et al, 2010; Avella, 1995)

According to Corre, Bruzaud and Grohens, the low-impact strength of pure PHBV can be improved through the blending with PPC. PPC is a biodegradable aliphatic polycarbonate, with a low Young's modulus and elongation at break of 400%, While PHBV exhibits a high modulus close to 4 GPa and elongation at break less than 1% (see figure 9-5c & 9-5d). The blending of the 40% PPC to the 60% PHBV is doubled the compound's elongation at break % (Corre, Bruzaud and Grohens, 2013).

Javadi et al. stated that blending PHBV with PBAT can improve the mechanical properties of PHBV such as specific toughness (MPa/kg.m^3) up to two orders of magnitude compare to the neat PHBV and elongation at breaks (%) to more than 500%. However, that is also accompanied with a dramatic reduction in the tensile strength and modulus compare to the neat PHBV (Javadi et al., 2010).

Avella et al. examined altering in the mechanical properties of PHBV (4% HV) after blending with PBA (acrylate elastomer, polybutylacrylate). The existence of the rubbery PBA particles in PHBV matrix changed the impact properties due to the toughening effect of robber phase (stress absorbers). However, similar to PHBV/PBAT blend, a decrease of Young's modulus and tensile strength was also observed (Avella et al., 1995).

The core-shell structure particles which comprise of rubbery and glassy layers were commercially introduced for toughened PVC many years ago (Paul and Bucknall, 2000). The effect of micro-encapsulated core-shell grafted Polymethylmethacrylate-cross linked Acrylate/ Butadiene rubber impact modifier under trade name of Biostrength has been promising for the improvement of the impact property of PLA (biodegradable polyester). In this study, the effect of Biostrength additive on thermal and mechanical properties and crystallinity and morphology of PHBV is investigated.

2.10.1 Principles

According to Cruz-Ramos, the great advantage of using core-shell particles over other impact modifiers is that their size remains the same during processing and is dispersed with their primary size inside the polymer matrix (Cruz-Ramos, 2000).

Figure 3-2 shows schematically the typical architecture of a core-shell polymer, which consists of a soft core, made up of a crosslinked rubber phase to absorb impact energy, encapsulated in a hard compatibilizing phase, a “shell” of rigid polymer that is grafted to the core.

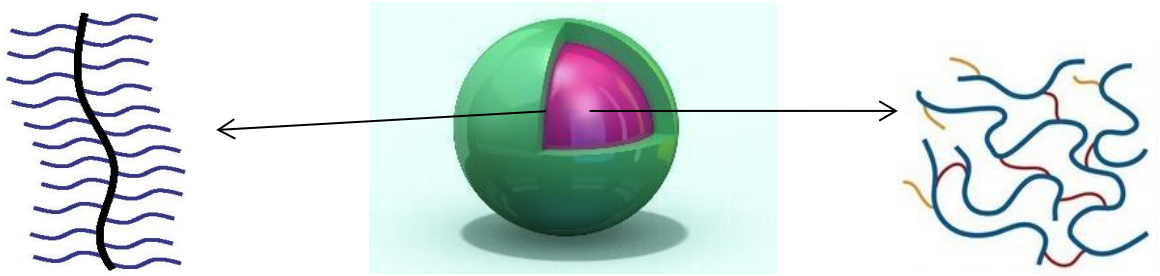

Graft-linking phase | Core-shell structure | Crosslinked rubber

Figure 3-2 The schematic structure of the core-shell impact modifier

Basically in commercial forms, the inner phase is often made of a cross-linked rubber based on either Polybutadiene/copolymer (MBS family) or poly butyl acrylate (PBA)/copolymer (AIM family).

It is mostly copolymerized with styrene. The glass transition temperature T_g of the core is often very low at about -50 to -80 ℃ while the hard shell, mostly made of PMMA/copolymer or SAN (styrene-acrylonitrile copolymer) exhibits a much higher T_g than that of the core.
The hard shell of the core-shell structure has three primary functions:

1- It must allow isolation of the particles from the emulsion as a hard coating around rubbery cores, preventing them from adhering to each other during the drying process.
2- Similarly when the particles are dispersed inside the matrix it should prevent the rubber particles from aggregating and the sticking to each other
3- After dispersion in the matrix, the shell will act as a compatibilizer that binds the rubbery phase to the matrix.

Cruz-Ramos stated that a key factor in the performance of core-shell particles as an impact modifier is the miscibility condition between shell polymer and the host matrix. However, it should be considered that “solubilisation or interaction of the matrix polymer into the grafted layer must occur for the proper interfacial adhesion to develop. This solubilisation process is far more complex than the mere miscibility between the same two polymers when none of

them are grafted, because the shell polymer is immobilized on one end by being grafted onto the core" (Cruz-Ramos, 2000).

Major factors in core-shell toughening of polymer matrices are:

1- Particle size: the effectiveness of the particle dimensions on the toughening of a polymeric material are strongly depends on the inherent fracture mechanism of the matrix. Therefore, generally for brittle glassy polymers with a tendency to craze, large particles in excess of 1μm are more effective than smaller particles. On the other hand, matrices that can absorb fracture energy via shear yielding are effectively toughened with particles smaller than 0.5 μm or less.
2- Glass transition temperature: Maintaining a consistent glass transition temperature in the core as well as shell is a key factor to determine the quality of an impact modifier. A consistency which doesn't effect by weatherability.
3- Adhesion: as it will be mentioned later, the miscibility conditions between the shell and the host matrix is an important factor for the effectiveness of the impact modifier. The lack of miscibility sometimes requires an alternative strategy to enhance the compatibilization between the shell of impact modifier and the matrix of the host polymer.
4- Microstructural variants: for instance multilayer particles that provide an optimum balance of stiffness and impact resistance or a more sophisticated morphology inside the rubber cores (Cruz-Ramos, 2000).

Bibliography Chapter 2

- Avella, M., Calandrelli, L., Immirzi, B., Malinconico, M., Martuscelli, E., Pascucci, B. and Sadocco, P. (1995), "Novel synthesis blends between bacterial polyesters and acrylic rubber: a study on enzymatic biodegradation", Journal of Environmental Polymer Degradation, Vol. 3, No. I, pp. 49-60

- Brostow,W. , Chiua, R. , Kalogerasb, I. , M. and Vassilikou-Dovab, A. (2008), "Prediction of glass transition temperatures: Binary blends and copolymers", Materials Letters Vol: 62, pp. 3152–3155

- Brown, S. , B. (1992), "In Survey of Chemical Reactions of Monomers and Polymers during Extrusion Processing in Reactive Extrusion, Principles and Practice" Edited by Xanthos, M, Hanser Publisher, Munich,

- Brown, S., B., (2003),"Reactive compatibilization of polymer blends",in polymer blend handbook , Ed by Utraki, Kluwer Academic Publishers, pp. 339-415

- Chang, F., C. (1997), "Compatibilized Thermoplastic Blends", in e-book , handbook of thermoplastic by Olabisi , O, 1997, page 493,online available at: https://books.google.co.uk/books?id=h2mcx1Xsfs0C&pg=PA497&lpg=PA497&dq=non+reactive+compatibilization&source=bl&ots=Zw5Je1r6UD&sig=Xwp5h51KqncSchDdDBR75j2zkxY&hl=en&sa=X&ved=0ahUKEwjXg9O7irHLAhWBqXIKHZYFA9kQ6AEIPjAF#v=onepage&q=non%20reactive%20compatibilization&f=false (Accessed 16 Aug 2016)

- Chiu, J., H., Huang, M., J. and Don, M., T. (2008)," Spherulitic Morphology and Crystallization Kinetics of Melt-Miscible Blends of Poly (vinylidene fluoride) with Poly(3-hydroxybutyrate)", Tamkang Journal of Science and Engineering, Vol. 11, No. 2, pp. 201-209

- Corre, Y., M., Bruzaud, S. and Grohens, Y., (2013), "Poly (3-hydroxybutyrate-co-3-hydroxyvalerate) and Poly (propylene carbonate) Blends: an Efficient Method to Finely Adjust Properties of Functional Materials" , Macromolecular Materials and Engineering, Volume 298, Issue 11, PP. 1176–1183

- Cruz-Ramos, C. A. (2000), “Core-shell impact modifier”, in book “Polymer Blends, vol2: performance, edited by Paul and Bucknal, 2000 John Willey & sons,Inc

- Fayt, R., Jérôme, R. and Teyssié, P. H. (1987), “Characterization and Control of Interfaces in Emulsified Incompatible Polymer Blends”, Journal of Polymer Engineering and Science, , Vol. 27, No. 5

- Fink, J. K. (2005),”Reactive polymers: fundamental and applications: a concise guide to industrial polymers”, William Andrew Publishing, NY, page 513, [online] available at: http://books.google.co.uk/books?id=fJNIjIwUNpMC&printsec=frontcover#v=onepage&q&f=false (Access 16 Aug 2016)

- Fox, T. G. (1956) “Influence of diluent and of copolymer composition on the glass temperature of a polymer system”, Journal of Bulletin American Physics Society. Vol 1, pp 123-125

- Gedde, U. W. (1999), “Polymer Solution” in book of “Polymer Physics, Springer science+business media Dordrecht, page 71

- Gordon, M., Taylor, J. S. (1952),” Ideal copolymers and the second-order transitions of synthetic rubbers. i. non-crystalline copolymers”, J. Appl. Chem. Vol 2, Issue 9 ,pp. 493–500

- Javadi, A. , Kramschuster, A. J., Pilla, S., Lee, J., Gong, S. and Turng L. S. (2010), “Processing and characterization of microcellular PHBV/PBAT blends”, Polymer Engineering & Science, Vol 50, Issue 7, pp. 1440–1448

- Kalogeras, M. I. and Brostow, W, (2008),” Glass transition temperatures in binary polymer blends”, Journal of Polymer Science: Part B: Polymer Physics, Vol. 47, Issue 1, pp. 80–95

- Kaplan, D. S. (1976), “Structure-Property Relationships in Copolymers to Composites: Molecular Interpretation of the Glass Transition Phenomenon”, Journal of Polymer Science, Vol. 20, pp. 2615-2629

- Karasz, F., E., (1985),"Glass transition and compatibility; phase behaviour in copolymer containing blends", in polymer blends and mixtures, Edited by: Walsh, Higgins and Maconnachie, Martinus Nijhoff Publishers,Boston

- Karger-Kocsis, J., Harmia, T. and Czigany, T, (1995) "Comparison of the fracture and failure behaviour of polypropylene composites reinforced by long glass fibers and by glass mats", Compos. Sci. Technol. Vol 54, pp. 287–298

- Kim, E., K. and White L.,J. (2011) "manufacturing of polymer blends using polymeric and low molecular weight reactive compatibilizers", in "encyclopedia of polymer blends : volume 2 :processing by Avraam I. Isayev,first edition , Wiley_Vch Verlag GmbH

- Kim, J., Y. and Park, O. O. (1998)," Miscibility's and Rheological Properties of Poly (butylene succinate)–Poly (butylene terephthalate) Blends", Journal of Applied Polymer Science, Vol. 72, Issue 7, pp. 945–951

- Kwei, T. K. (1984) "The effect of hydrogen bonding on the glass transition temperatures of polymer mixtures", J. Polym. Sci. Lett. Vol 22, Issue 6, pp. 307–313

- Leibler, L., (1979), "Theory of Microphase Separation in Block Copolymers", Macromol, Vol. 13, No. 6, November-December 1980

- Lieber, L., (1982),"theory of phase equilibria in mixtures of copolymers and homopolymers , Macromolecules, Vol. 15, issue 5, pp. 1283-1290

- Lindsey, C., R., Paul, D. R. and Barlow, J. W., (1981), Mechanical properties of HDPE–PS–SEBS blends, Journal of applied polymer science, Vol 26, Issue 1,January 1981 ,Pages 1–8

- Markham, R., L. (1990), "introduction to compatibilization of polymer blends", Jouranl of advanced polymer technology, Vol 10,issue 3, pp. 231-236

- Mujumdar, B. and Paul, D. (2000)," Reactive compatibilization", in book "Polymer Blends: Formulation and Performance, Volume1", Edited by: Paul and Bucknall, John Wiley & sons, Inc., pp. 540

- Olabisi, O., Robeson L., M., and Shaw, M., T., (1979),"Polymer-Polymer Miscibility"Academic press, New York, pp, 325-326

- Parameswaranpillai, J., Thomas, S. and Grohens, Y, (2015), "Polymer Blends: State of the Art, New Challenges, and Opportunities" in book titled : "Characterization of Polymer Blends: Miscibility, Morphology, and Interfaces", First Edition, Edited by Thomas, Grohens and Jyotishkumar, Wiley-VCH Verlag GmbH & Co. KGaA

- Paul, D., R. (1989) Control of phase structure in polymer blends, in Functional Polymers (eds D.E. Bergbreiter and C.R. Martin), Plenum Press, New York, pp. 1–18.

- Robeson, L., (2007), "Polymer Blends: A Comprehensive Review", [online] available at: http://content.schweitzer-online.de/static/catalog_manager/live/media_files/representation/zd_std_orig__zd_schw_orig/017/624/104/9783446225695_content_pdf_1.pdf (Accessed 15 Aug 2015)

- Scobbo, J.J., Jr and Goettler, L., A., (2003), "Applications of polymer alloys and blends", in Polymer Blends Handbook, edited by Utracki, Kluwer Academic Publishers, pp. 951–976.

- Scobbo, JR., J., J. (2000),"Thermomechanical performance of polymer blends, in book "polymer blends", volume 2, edited by Paul and Bucknall, 2000, John Wiley & Sons, pp.341

- Shultz, A, R and Young, A, L, (1980), "DSC on Freeze-Dried Poly (methyl methacrylate)-Polystyrene Blends", Journal of Macromolecules, vol 13, issue (3), pp 663–668

- Thomas, S., Sinturel, C. and Thomas, R. (2014) "Micro and Nanostructured Epoxy / Rubber Blends", page 228-235 [online] Available at : https://books.google.co.uk/books?id=4PtwBAAAQBAJ&printsec=frontcover&dq=Thomas+S+2014+glass+transition+miscibility&hl=en&sa=X&ved=0ahUKEwjoyZH6yqfNAhUjDsAKHUsRDMoQ6AEILTAD#v=onepage&q&f=false (Accessed 15 Aug 2015)

- Tsukahara, Y., Ismail, S. and Shonaike, G, O, (1999),"Development in reactive blending", in book "Polymer blends and alloys" edited by Shonaike and Simon, 1999, Marcel Dekker Inc, pp. 622

- Utraki, L, A, (1998), "Commercial Polymer Blends", First edition, Chapman & Hall INC, pp. 82

- Wu, (1987), "Formation of Dispersed Phase in Incompatible Polymer Interfacial and Rheological Effects", Polymer Engineering and Science, Vol 27, No. 5, pp. 335-343

- Yu, Y, (2014) "Viscoelastic Measurements and Properties of Rubber-Modified Epoxies", in e-book titled: Micro and Nanostructured Epoxy/Rubber Blends, edited by Thomas, S., Sinturel, C., Thomas, R. , Wiley-VCH Verlag GmbH & Co., pp. 219-234

- Xanthos, M, (2010),"Functional Fillers for Plastics", Wiley-VCH Verlag GmbH & co, pp. 8

Chapter 3

Talc as a nucleating agent and reinforcing filler for PHBV

3.1 Introduction

Global consumption of conventional plastics has increased noticeably in recent years. However, the depletion and price fluctuation of petroleum resources and the escalated rising environmental awareness about the effects of synthetically produced materials has produced lot of attention in biologically derived polymers. Poly (3-hydroxybutyrate-co-3-hydroxyvalerate), PHBV belongs to the family of biodegradable bacterial bio-polyesters which have gained lot of interest with researchers due to their ability to be a substitute for many conventional petroleum-based polymers. Basically, the biggest issue among PHBV has been identified as their inherent brittleness. There have been several studies about PHB and PHBV and their issues like brittleness, its narrow window of processability and the slow rate of crystallinity which hindered their commercial usage (Vidhate, Innocentini-Mei, D'Souza, 2012, Bugnicourt et al, 2014). Because of the slow crystallization rate, a film made from PHBV will stick to itself even after cooling. The reason for this is that a substantial fraction of the PHBV remains amorphous and tacky for long periods of time (Liu, et al, 2002). According to Kai, He and Inoue, there are several possible causes for brittleness. The bacterially synthesized PHB or its copolymer PHBV is completely known as isotactic stereo regular polyester, with a high tendency to crystallize. However, the nucleation density of bacterial PHBV is too low to initiate efficient crystallization. Consequently, the crystal spherulite's size is exceptionally large size and thus the possibility of brittle failure by cracks is high among PHB and PHBV copolymer (Kai, He and Inoue, 2005). They hardly flow and the behaviour of necking is limited and they also have at low impact resistance.

Nucleating agents are widely used to modify the properties of various polymers. The rate of crystallization and the size of the crystals have a strong impact on the mechanical and optical properties after processing. The addition of nucleating agents to semi-crystalline polymers

provides a surface on which the crystal growth can start. As a consequence, fast crystal formation will result in many small crystal domains. Cycle times in injection moulding are reduced and physical properties such as flexural modulus, strength, heat distortion temperature and hardness will increase (Kucerova, 2008). Subsequently, the clarity and transmittance will improve. Nucleating agents used for optimizing the optical properties are called clarifying agents. Nucleating agents decrease the average size of spherulites and prevent the formation of large, inter-spherulitic cracks upon embrittlement.

Shanks and Tiganis stated that homogenous nucleation does not guarantee consistent properties, due to the appearance of nucleation phenomena within crystallization. Therefore as a matter of fact the crystallization will be controlled too much by processing times and consist of wide range of distributed sizes. In contrast, heterogeneous nucleation gives crystals the uniform size, and it controls crystallization for its initial stage of the phenomena (Shanks and Tiganis, 1998).

In summary, the nucleation agents are small crystalline particles that are dispersed in the melt and remain solid in the process; a large number of tiny crystals form from the melt on them at the start of the crystallization process. The size and number of the crystalline structures will alter the impact strength. The size of the spherulites can be affected by the crystallization condition and nucleating agents. Basically large spherulites with a similar percentage of crystallinity show more brittle failure than fine spherulites and thus the strain is in contrast to average size of the spherulites (El-Hadi, 2002).

3.2 Material

ENMAT^{TM} Y1000 is PHBV with 3 *mol%* of hydroxyvalerate (HV) content without any additive substances and supplied in white powder form manufactured by Tianan Biologic Material Co. (Ningbo, P. R.China). The talc was kindly provided by Imery's under trade name of Crys-talc^{R} 7, a fine white powder with median particle diameter: d50 1.9 μm and d95 7.6 μm. Four batches of PHBV/talc with weight ratios (w/w) of 100/0, 90/10, 85/15, 80/20 were prepared.

3.3 Sample preparation

3.3.1 Preparation of the Blend

Before processing through an extruder, PHBV in powder form was first dried in a vacuum oven at a temperature of 60 ℃ for 24 hours to remove moisture. Drying of this polymer is vital as moisture in this polymer induces hydrolytic chain scission during the processing at high temperature. The talcum powder was used as received. All the components were premixed in a plastic bag by manually tumbling for 5 mins and were fed by a calibrated powder twin screw feeder into the extruder. The extruder used was a Betol co-rotating intermeshing twin-screw extruder (40 mm diameter, L/D =21/1, Amp=5-10) at 200 rpm, The extruder consisted of five barrel sections and each section was equipped with independently controllable electric heating and water cooling system. All of the extrusion variables, including barrel and die temperatures, and the temperature distribution are shown in Table 1-3:

Table 1-3 Temperature profile of the extrusion process

Section	Zone6(Die)	Zone 5	Zone 4	Zone3	Zone2	Zone1
Temperature	164	169	165	170	160	155

Using a single strand die, the extrudate was cooled through a water bath and then pelletized for subsequent processing. A few of the batches were not possible to strand because of their high viscosity. These batches were collected from the die and then granulated by a S.U.I-Cumberland granulator.

3.3.2 Injection moulding

The specimens for mechanical properties were obtained by injection moulding in a Demag NC III, 150 Tone, injection moulding machine. Table 2-3 shows the processing parameters used:

Table 2-3 injection molding parameters of PHBV and its talc composites

Conditions	first heating zone ℃	second heating zone ℃	third heating zone ℃	Fourth heating zone ℃	Nozzle heating ℃	Injection pressure bar	Injection time sec	Cooling time sec	Cycle time sec	Mould temperature ℃	Injection speed
Tensile bar	160	160	160	160	160	160	4	40	62.5	30	low
Plate	150	150	155	155	155	160	4	60	82.5	30	Medium

All the processing parameters were modified during several trial mouldings in order to obtain the optimum conditions. The biggest issue for the processing of the specimens occurred when material stayed slightly more than previous ones in barrel, thus approximately the first 15 numbered specimens (the tensile bars and for the plates the first 5 approximately) where uniform and then they start to shrink inside the mould which many times it ends up with damaged at edges specimens or stuck in mould and didn't release immediately after mould unclamped. The reason behind that was not clear but it might be through thermal degradation or narrow windows process ability of PHBV. Therefore the smallest injection moulders (shorter barrel's length) could reduce the residence time inside heating zones.

3.3 Experimental

3.3.1 Differential Scanning Calorimetry (DSC)

The melting temperature T_m of specimens was measured by a TA Instruments DSC/Q2000 with a Universal Analysis 2000. The external block measurements were carried out under a nitrogen atmosphere to minimize oxidative degradation. The specimens were encapsulated in

DSC aluminium zero pans and then introduced into the closed calorimeter cell. The instrument was calibrated with indium prior to starting the test.

3.3.1.1 Non-isothermal crystallization

The samples were first heated to 200 ℃ at a heating rate of 10 ℃/min and isothermally held for 5 min to eliminate any thermal history. The samples were then cooled at the same heating rate of 10 ℃/min to -20 ℃ and then again heated to 200 ℃ with same heating rate for obtaining the second heating cycle.

3.3.1.2 Isothermal crystallization

PHBV neat and PHBV/talc samples with weight fractions of 90/10, 85/15, 80/20 were heated up to approximately 30 ℃ above the melting point(about 200 ℃), and held isothermally for 5 minutes to eliminate any thermal history. The sample was then rapidly cooled down at the heating rate of 80 ℃/min to the pre-determined isothermal temperatures and kept until crystallization was completed. The procedure were repeated for the three pre-determined temperature of 110 °, 120 °, 130 °C for each of the compounds. The curves of heat flow (W/g) vs time (min) shown in (Figure 2-3).

3.3.2 Thermogravimetric Analysis (TGA)

The thermal stability of the PHBV and the process of thermal decomposition were investigated by Thermogravimetric analysis (TGA) using a TA instrument “The New Discovery TGA”, with TRIOS software version 3.3.0.4055 under nitrogen atmosphere. The temperature range was from room temperature to 650◦C with a heating rate of 10°C/min.

3.3.3 Dynamic Mechanical Analysis (DMA)

Dynamic Mechanical analysis (DMA) was performed using a DMA Q800, TA, USA. The accurately measured rectangular samples 127x12x4 mm were cooled to -50 ℃ and then

heated up to 150℃, with heating rate of 2℃/min, under a maximum force of 1 N, a frequency of 1 Hz and an amplitude of 5 μm using the single cantilever system.

3.3.4 X-Ray Diffraction

X-ray diffraction analyses of Neat PHBV and its composite with talc was carried out with A Buker D8 advanced Copper-tube diffractometer equipped with a Linx Eye Detector PSD (position sensitive) detector. Diffraction Data were acquired at ambient temperature in the angular region (2θ) of 5-60°, with a time of 3.5 second per step and with an increment of 0.01 °/step.

3.3.5 Morphology with SEM

The morphologies of PHBV, talc, and PHBV/talc (90/10, 85/15, 80/20) composites were analysed using a scanning electron microscope. A SUPRA ZEISS 35VP with 20KV accelerating voltages and SE detector was used. The scanning electron microscopy of fractured samples of Charpy impact testing was conducted at room temperature. The specimens were dried for two hours prior to gold coating.

3.3.6 Mechanical properties

Tensile tests were performed with an Instron testing machine (model 3366) according to ASTM D 638 standard for tensile testing. A 10 KN load cell was used with a crosshead speed was of 5 mm/min. At least five samples were tested for each reported value.

3.3.7 Three-point bending DMA

The heat distortion temperature (HDT), deflection temperature under load (DTUL) of the extruded PHBV and PHBV/Talc composite were measured by TA/DMA Q800 3-point bending clamp. Rectangular specimens with length, width and thickness of approximately 50x13x4 mm were used. These were first measured accurately and then fixed between instrument’s clamps.

Based on HDT testing procedure instruction by TA instrument, a calculation had to be carried out prior to the test. The reason for this was that the largest three-point bending clamp available on the Q800 held a sample of maximum length, width and thickness of 50 mm 15 mm and 7 mm, respectively. These dimensions are very small and don't meet the standard ASTM D 648 requirement for the test specimen. The calculation for the correction was as follows:

1. Calculate the force (F) required to achieve the desired stress.

Force could be obtained by the three-point bending equation (reference):

$F = 2/3\ (\sigma\ (T_{DMA}^2\ W_{DMA} / L_{DMA}))$

Where σ = Stress on the ASTM and DMA sample = 455 kPa = 455,000 Pa = 455, 000 N/m2 = 0.455 N/mm^2

- F = Force (Newton)
- T_{DMA} = Thickness of the DMA sample,
- W_{DMA} = Width of the DMA sample
- L_{DMA} = Length of the DMA sample = 50 mm

2. Calculate the strain (ε) in the ASTM sample at the deflection of 0.25 mm

$\epsilon = 6\ d_{ASTM}\ T_{ASTM} / L_{ASTM}^2$

where ϵ = Strain on the ASTM and DMA sample

- d_{ASTM} = Deflection in the ASTM sample = 0.25 mm
- T_{ASTM} = Thickness of the ASTM sample = 13 mm
- L_{ASTM} = Length of the ASTM sample = 127 mm

3. Calculate the required deflection (d) in the DMA sample so that there is an induced strain equivalent to ϵ.

$d_{DMA} = \epsilon\ L_{DMA}^2 / (6\ T_{DMA})$

where d_{DMA} = Deflection at ϵ stain

Similar calculations may be performed for samples of any width and thickness.

The next step was to program a test to heat the sample from 20 ℃ to 180 ℃ at the heating rate of 2 ℃/min under the conditions of the calculated applied load (Wadud and Ulldrich, 2016).

3.3.8 Impact properties

There are several methods for measuring the impact behaviour of polymers, such as Charpy and Izod impact test (notched and un-notched) and Gardner drop-ball or drop-weight test. In order to investigate the impact properties with the energy rate higher than the maximum pendulum performance, and more accurate results, the drop weight instrument was used. The PHBV and PHBV/talc blends were injection moulded into the rectangular 150x150x4 mm plates according to BS EN ISO 6603 using the conditions given in table 2. The injection moulded plates were then cut into 60x60 mm squares and labelled for impact testing. The impact conditions of the test were set according to the BS EN, ISO 6603 drop weight method. A CEAST Fractovis Plus impact tester Model 7520 was used.

3.4 Thermal properties

3.4.1 Non isothermal crystallization

Figure 1-3 shows the non-isothermal DSC curves of PHBV and PHBV/talc composites with concentrations of 90/10 and 80/20. All the non-isothermal DSC measurement of PHBV/talc composites produced two melting point peaks (second heating cycle). These were shifted slightly by the different concentrations of talc in the composites. The phenomena of two endothermic peaks in the DSC curve could be caused by the reorganization of crystals during the low rate of heating rate of 10 ℃/min. Reorganization is a process when improvements or perfections of the initial metastable crystallites occur while recrystallization is a similar process, when a distinguishable exothermic peak is witnessed between the two endothermic peaks in the melting area of DSC curve (Wunderlich, 2005).

The melting of polyvinylidene fluride PVDF presented two endothermic peaks with a clear exothermic peak in between, the lower melting point was associated with the original metastable crystals and formed at the crystallization temperature from the amorphous phase

and the second peak represent the melting of perfected crystals, recrystallized and perfected during the heating process of the DSC (Wunderlich, 2005; Elzayat et al, 2012). Menczel & Prime announced that polyethylene also shows the same behaviour in the DSC curve because the crystal partially melted and reorganized into thicker crystals during heating at the rate of 10 ℃/min. He also stated that a faster heating rate could decrease the recrystallization but not eliminate the double melting point peaks (Menczel & Prime, 2009).

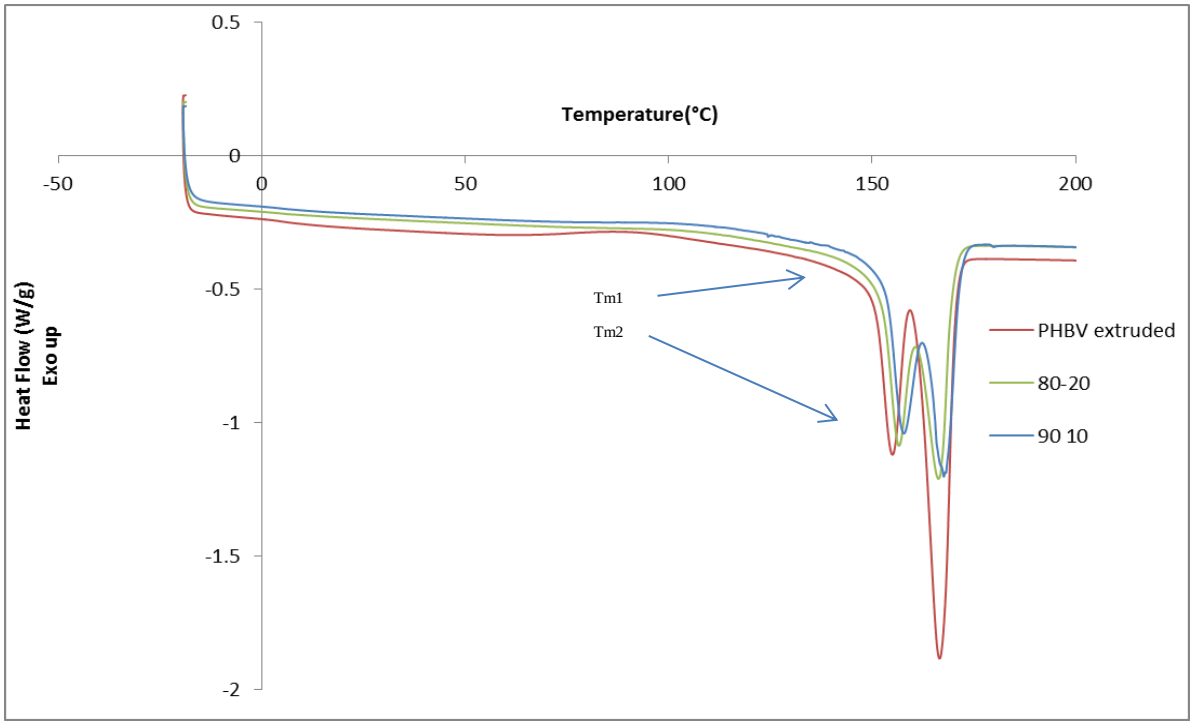

Figure 1-3 Non-isothermal DSC of PHBV/talc composites

Liu and Gunaratne & Shanks and Wang et al also stated that the double melting peaks of PHBV were caused by melting, recrystallization and re-melting during heating (Liu, 2002, Gunaratne, Shanks, 2005, and Wang, Yamamoto, Cakmak, 1996).

It has been mentioned that, the extruded PHBV exhibited the lowest T_{m1} and T_{m2} (two melting peaks), Liu argued that it indicated that the worst crystal perfection with the lowest lamella thickness existed in the neat PHBV compared to the filled composite. With the increasing nucleation effect of the filler, the melting point T_{m1} becomes higher. The melting temperature T_{m2} is independent of the nucleating agent, perhaps because it resulted from the

melting of reorganized crystals during the heating of the sample. The nucleating agents forced the peak of T_{m1} to shift and depressed the T_{m2} peak (Liu, 2002), although it might be caused by change in concentration of polymer in composites.

These results indicate that the talc cause an increase in the crystallization rate and improves the perfection of the crystals of PHBV.

3.4.2 Isothermal crystallization

There are plenty of researches about analysing of polymer crystallization kinetics with DSC. The use of differential scanning calorimetry to study polymer crystallization kinetics is studied by Hay, Fitzgerald, and Wiles in order to determine accurate crystallization parameter and find out the limitation of DSC and the choice of operating conditions. (Hay, Fitzgerald, and Wiles, 1976)

The well-known Avrami equation (Equation 2-3) is used widely by researchers to analyse the isothermal crystallization of polymers. The equation is also known as the Johnson-Mehl-Avrami-Kolmogorov equation, or JMAK equation. The equation was popularized by Melvin Avrami in the series of papers published in the Journal of Chemical Physics from 1939 through 1941, so very often it is simply called Avrami equation.

The isothermal crystallization behaviour of PHBV and different concentration of PHBV/Talc can be described by the Avrami equation. The relative degree of crystallinity X_{rel} at time t is given by the following:

Equation 1-3) $$\boldsymbol{X_{rel}}=\frac{\boldsymbol{Xc(t)}}{\boldsymbol{Xc(\infty)}}=\int_0^t \frac{\mathbf{d}\boldsymbol{H(t)}}{\mathbf{d}\boldsymbol{t}}\,\mathbf{dt}\,/\int_0^\infty \frac{\mathbf{d}\boldsymbol{H(t)}}{\mathbf{d}\boldsymbol{t}}$$

where $X_C(t)$ and $X_C(\infty)$ are the degrees of crystallinity at time t and that at the end of crystallization, respectively, and $dH(t)/dt$ is the rate of heat flow during the crystallization process at time t. The latter was measured from the moment when the sample was cooled to the appropriate crystallization temperature. X_{rel} can be obtained from the following expression:

Equation 2-3) $$\mathbf{1 - X_{rel} = \exp(kt^n)}$$

Here, *n* is the Avrami exponent, which is determined by the mode of crystal nucleation and the crystal growth geometry under the actual conditions. The parameter *k* is an isothermal crystallization rate constant. Taking a 'double logarithm' of Equation (2-3) gives the following:

Equation 3-3) $$\mathbf{\log[-\ln(1 - X_{rel})] = n \log t + \log k}$$

The plot of $\log(-\ln(1 - X_{rel}))$ against $\log t$ gives a straight line, whose slope is *n* and its intercept on the ordinate is $\log k$. In the investigations of isothermal crystallization at time *t*, $dH(t)/dt$ was recorded and then integrated against the time *t* to give the values of $X_C(t)$ and $X_C(\infty)$.

When $X_{rel} = 0.5$ in Equation (3), the half crystallization time, $t_{0.5}$, which is the time taken for 50 % of 'total-volume' of crystallization is given by the following:

Equation 4-3) $$\mathbf{t_{0.5} = \left(\frac{ln2}{K}\right)^{1/n}}$$

The isothermal crystallization of neat PHBV at the set temperatures of 130 ℃, 120 ℃, 110 ℃, is illustrated in figures 2-3 a, b, c, and d.

Figure 2-3 illustrates the isothermal crystallization behaviour of PHBV neat and PHBV/talc compounds with different concentrations using DSC.

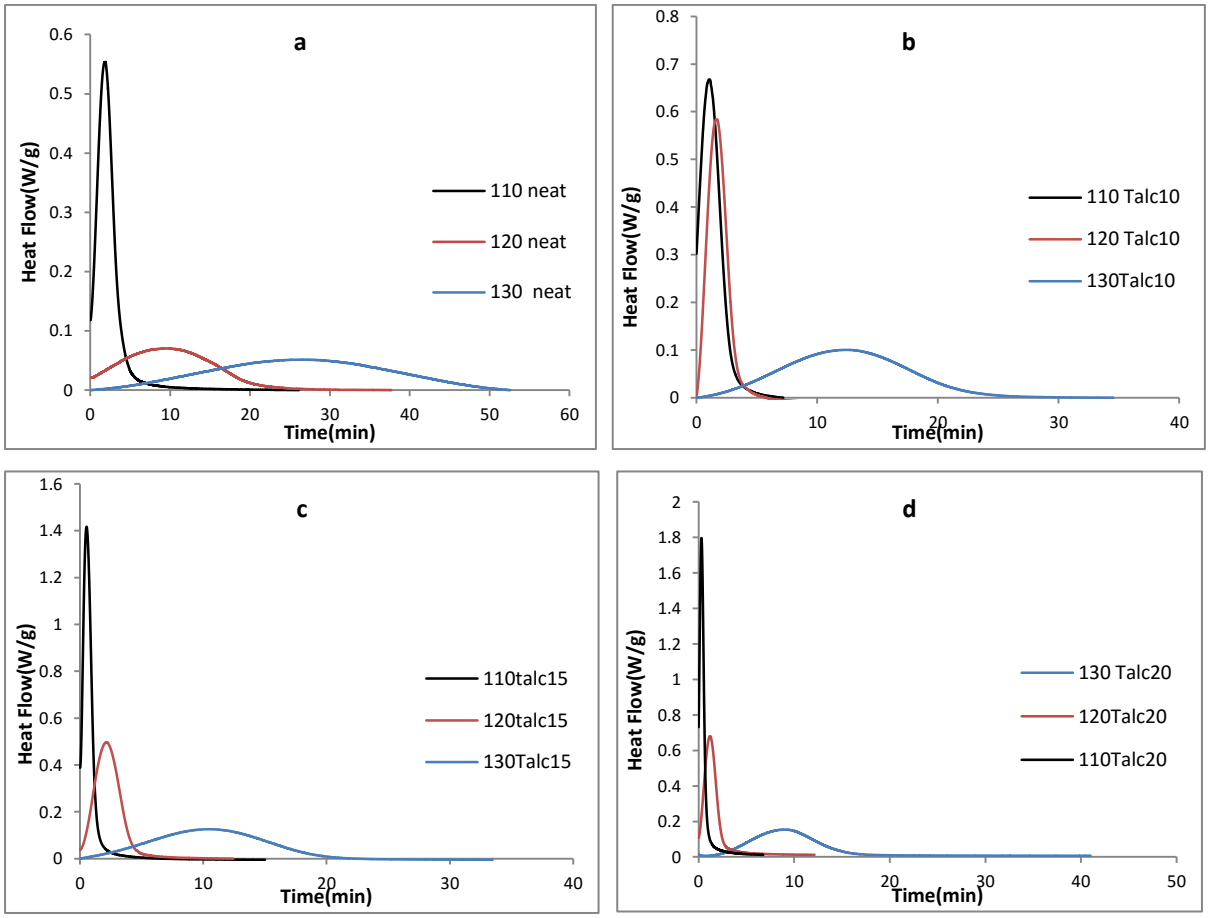

Figure 2-3 The DSC heating curves of PHBV/talc composites at different concentration a) 100/0, b) 90/10, c) 85/15, and d) 80/20, isothermally crystallized at the three different crystallization temperatures, 110,120 and 130 °C

The results clearly show that the process is temperature dependent and the rate of crystallization decreases at higher temperature. Moreover, the rate of crystallization is increasing isothermally with increasing of talc concentration (Figure 4-3 shows the comparison between PHBV and its composites at 130 °C)

The area under the curve of each crystallization graph shows the relative crystallinity and it is plotted versus time in Figure 3-3.

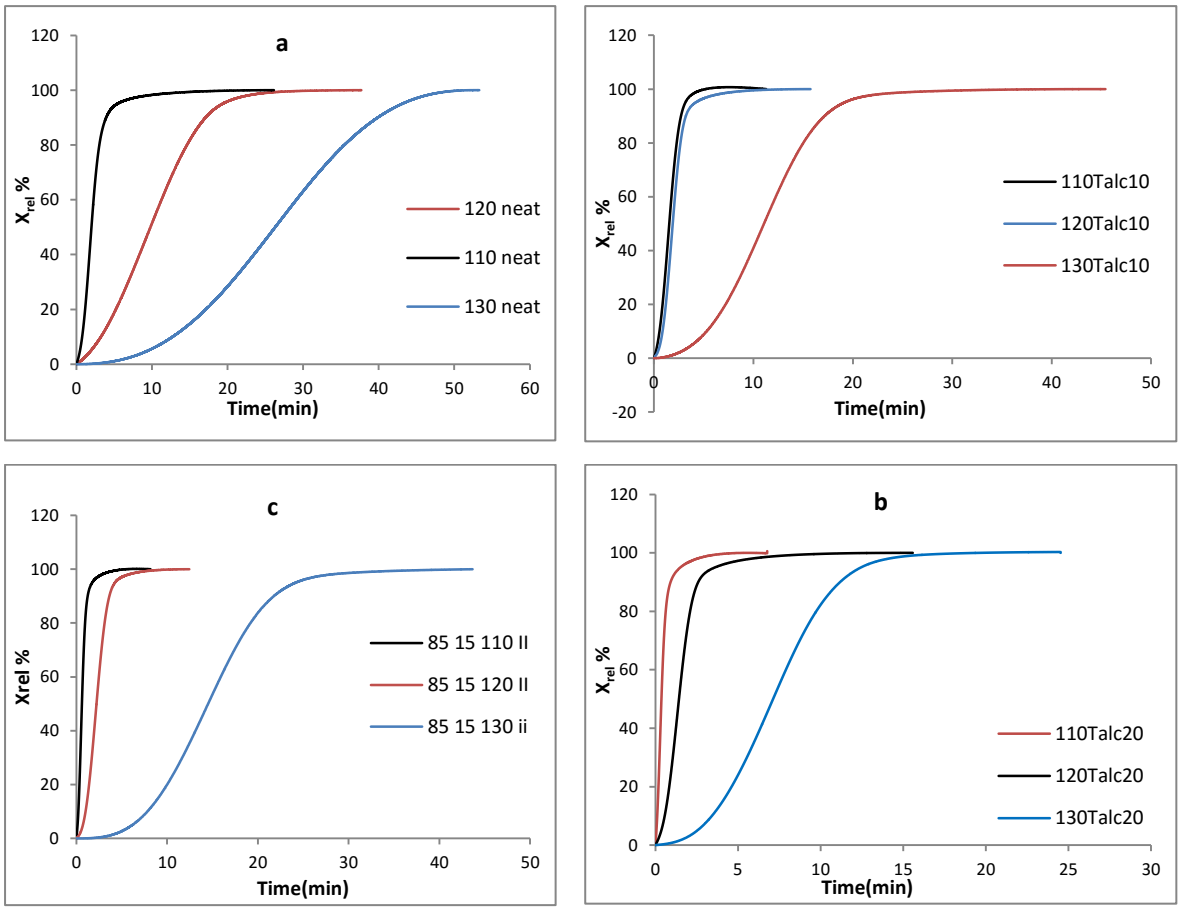

Figure 3-3 The relative crystallinity (X_{rel} %) versus time for the neat PHBV and PHBV/talc composite with concentrations of 90/10, 85/15 and 80/20 at isothermal temperatures of 110, 120 and 130 ℃.

Figure 3-3 shows the relative crystallinity of PHBV neat and its blends with talc at the three different concentrations and the three set crystallization temperatures vs time. It is clear that the time to 100% crystallization is temperature dependent (the time varies in different isothermal temperatures) for all specimens although for 90/10, the process is pretty close at temperature of 110 and 120 ℃.

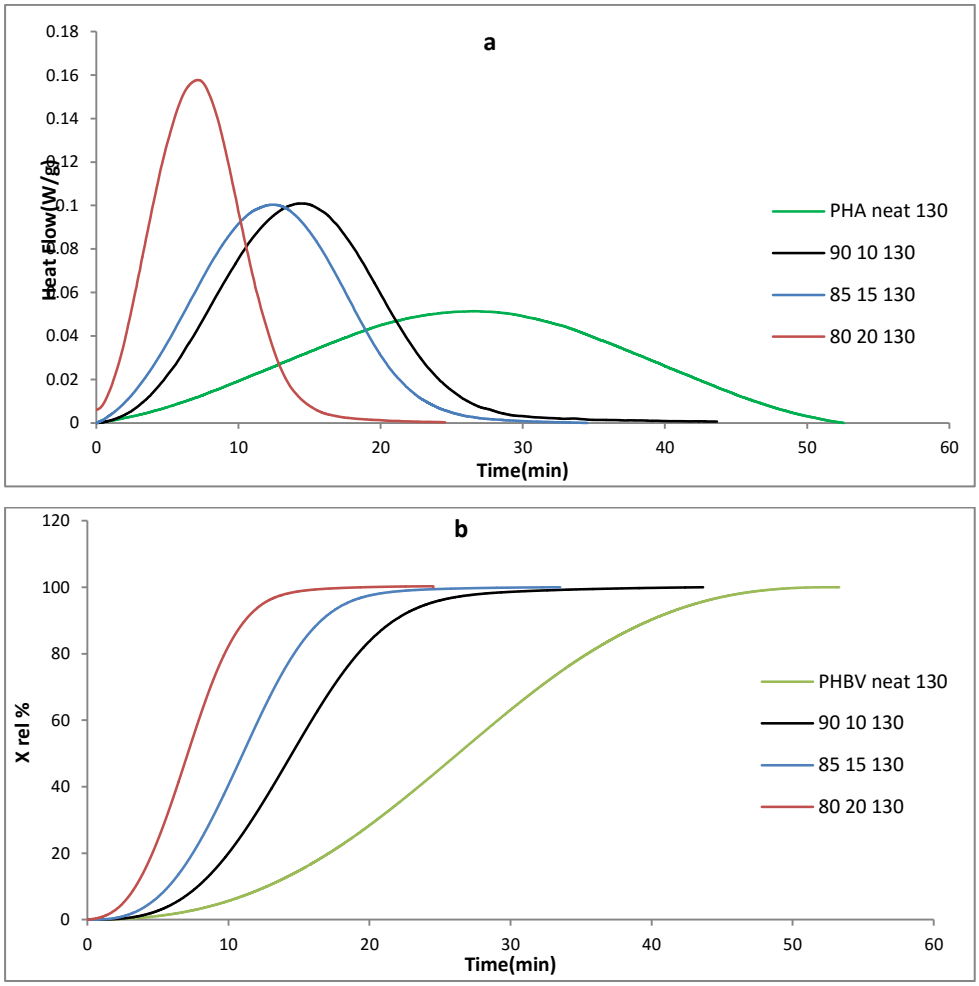

Figure 4-3 a) Comparison between the isothermal crystallization of PHBV and PHBV/talc composites at 130 ℃ and b) A comparison between the relative crystallinity of PHBV and PHBV/talc composites at 130 ℃

Figure 4-3 presents the effect of the talc concentration on the relative crystallinity of the PHBV/talc composites. While it takes about 50 min for the neat PHBV to completely crystalize at 130 ℃, The crystallization time decreases to less than 20 min for the composite with 20% talc.

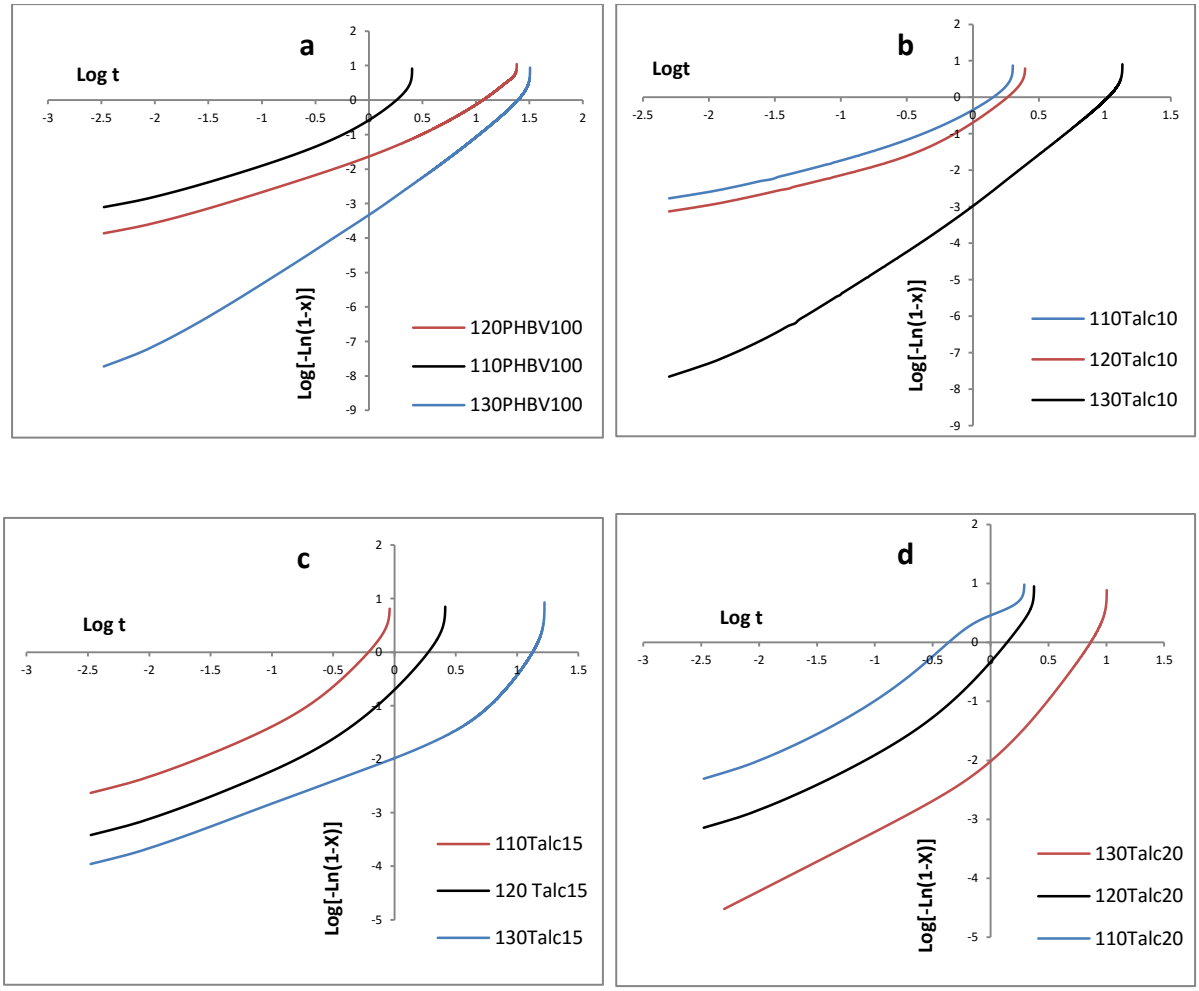

Figure 5-3 The Avrami's plots for PHBV and PHBV/talc

Figure 5-3 illustrate the log [-ln (1-X_{rel})] vs log (t), and from the slope and the intercept of the graphs in Figure 5-3 the Avrami's components, *n* and *k* were calculated (Table 3-3). Time of half crystallinity ($t_{0.5}$) has been calculated from the Equation (4-3).

However, it should be considered that the Avrami equation is only applicable to the linear part of the graph because it is based on many assumptions such as linear crystal growth, primary nucleation, constant volume, and so forth. It is usually valid at low conversions. Therefore, in this study the *n* and *k* were calculated from the initial linear segment of the Avrami's plots.

Avrami's parameter:

Table 3-3 The Avrami's parameter from the slope and the intercept of the graphs

Sample PHBV/Talc	Tc (℃)	*n*	*k* (min-1)	$t_{0.5}$ (min)
100-0	110	1.59	0.34	1.85
	120	1.65	0.02	8.49
	130	2.43	0.000382	21.71
90-10	110	1.58	0.55	1.14
	120	1.78	0.18	1.92
	130	2.82	0.0012	14.5
85-15	110	1.56	2.19	0.48
	120	1.85	0.20	1.85
	130	2.92	0.002	12.45
80-20	110	1.58	2.68	0.4243
	120	1.74	0.50	1.21
	130	2.96	0.00297	6.30

From Table 3-3 it can be seen in that at a specific temperature the value of *n* for PHBV/talc compounds with different concentration hasn't shown a dramatic change which indicates that the mechanism of crystallization after adding talc was not affected by different concentration of talc.

Generally, with using the Avrami's formula for analysing the crystallization of polymers, It has been proven that the *n* value is dependent on crystal geometry (rod, disk or sphere), nucleation mode (athermal, thermal or simultaneous, Sporadic) and rate determination (nucleation controlled or diffusion controlled) (Wunderlich, 2005). Furthermore, the value of Avrami exponent *n* was found to vary between 1 and 4, corresponding to the various growth forms from the rod-like to the sphere-like. The exponent *n* had values lower than 2 for the extruded PHBV, which corresponds to a rod-like morphology formed by heterogeneous

nucleation. It can be seen that by the incorporation of the talc inside polymer matrix, the *n* value increases to lower than 3. Thus the mechanism of nucleation and growth of the crystal is more similar to a two dimensional growth on a lamellar structure as it can be expected from an epitaxial growth mechanism. It is broadly accepted that the spherulite growth in polymer belongs to three-dimensional growth, and *n* values should be 3 or 4. However, it still could be a spherulite growth which is not three dimensional. Bian, Ye and Feng argued that various polymers, such as PET and nylon, have different *n* values in similar crystallization conditions, although they have the same spherulite crystal morphology. For the same polymer, such as PET, the *n* values can vary regularly with the change of isothermal crystallization temperature from the melt (Bian, Ye and Feng, 2003). Similar behaviour is also witnessed here in the crystallization of PHBV and its compounds with talc. Furthermore, Neat PHBV and its composite with talc in temperatures which set in crystallization's temperature range or with a large degree of supercooling showed a crystallization mechanism of spherical growth on diffusion from athermal (simultaneous) nucleation. In an ideal situation, the theoretical *n* value would be 1.5 for such a case (Wunderlich, 2005).

For each sample, the amount of *k* reduces with increasing the crystallization temperature, while the crystallization half time ($t_{0.5}$) value increases with temperature. It could be justified that with increasing temperature the crystallization rate decreases due to the fact that the melt crystallization is temperature dependent. This is a characteristic of nucleation controlled crystallization associated with the nearness of the crystallization temperature to the melting temperature T_m. Moreover, the *k* value for the PHBV/talc composites is increased by an increase of the talc concentration in the composite at a particular temperature.

The value of $t_{0.5}$ reduces with the increasing of the talc amount. The above results indicate that with the addition of the talc, the crystallization rate of the PHBV increases in the composites. The possible reason could be proposed to explain the slow-down of the crystallization rate of PHBV after introducing of talc. Talc therefore apparently enhances the nucleation of the PHBV in the composites. In other words, the presence of talc has a positive effect on the primary nucleation of PHBV. Therefore, the increasing the amount of talc in the PHBV/talc composites did not change the crystallization mechanism of PHBV, but increased the crystallization rate of PHBV in the composites compared with neat PHBV when they crystallized isothermally at any pre-determined temperatures.

3.4.3 Thermogravimetric analysis (TGA)

Thermogravimetric analysis (TGA) was used to determine the thermal stability and decomposition of the PHBV, and its talc filled composites. The thermal stability of the investigated samples was determined by the value of T_i, the initial decomposition temperature and T_e, the temperature of the maximum rate of decomposition. The residue of specimens at 600 °was also recorded. Derivative weight loss curve has been used to tell the point at which weight loss is most apparent and also the thermal range which decomposition actually occurs. Figure 6 shows the TG curves and DTG curves of the PHBV and PHBV/talc and the results are given in Table 4.

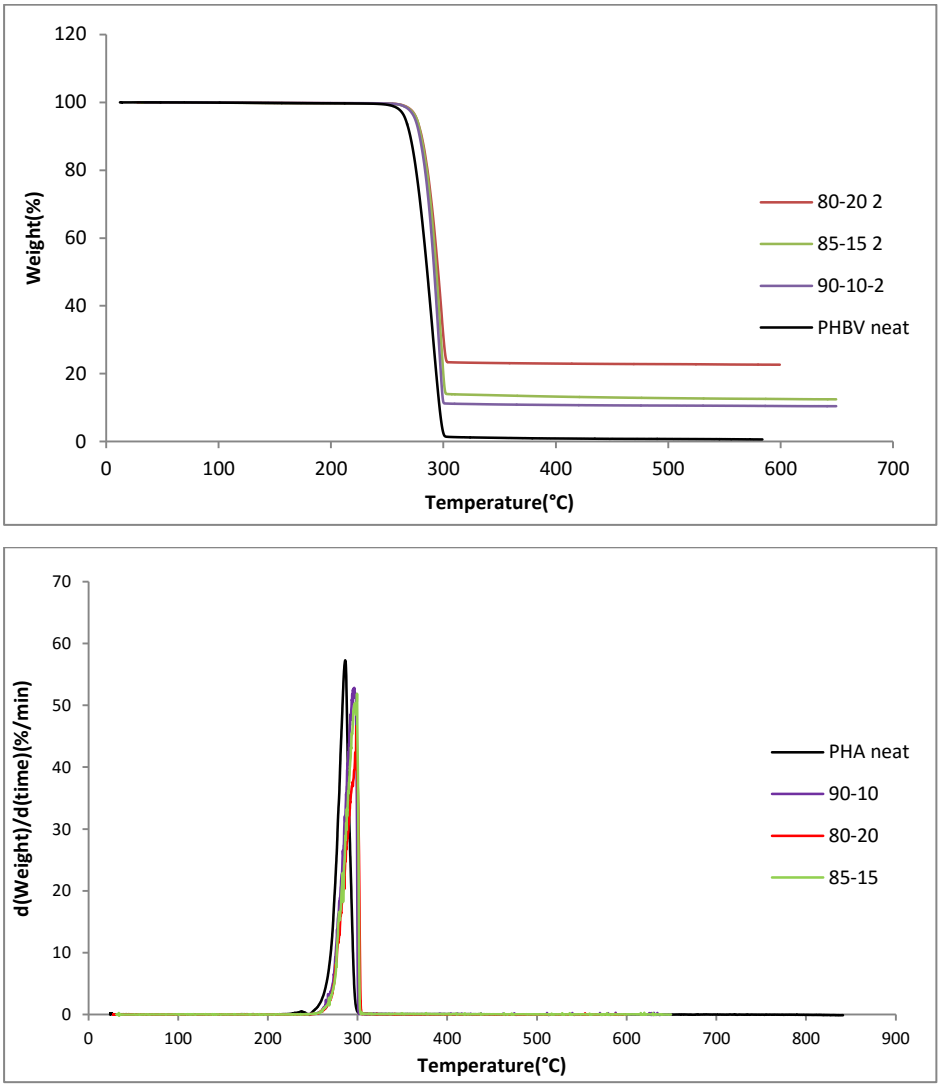

Figure 6-3 TGA & DTG graph of PHBV and PHBV/Talc composite

Table 4-3 The values of characteristic temperatures of TGA and DTG graphs, T_i = the initial decomposition temperature and T_{end} = the end decomposition temperature, Δm_i =Mass loss in T_i(%) , and residue at 600 ℃ (%)

Specimens PHA/Talc	T_i (℃)	Δ_{mi} (%) (Mass loss)	T_e (℃)	Residue at 600 ℃ (%)
100/0	253	98.45	294	0.64
90/10	263	88.720	300	10.47
85/15	262	85.804	303	13.54
80/20	263	77.823	303	22.11

As it shows in Table 4-3, the thermal decomposition of PHBV started at 253 ℃ and then accelerated rapidly to a peak rate at 285 ℃ (Figure 6-3). The thermal stability of the composites didn't enhance significantly with increasing the amount of talc. However, with 20% talc in the compound, T_i became 263 ℃ and thermal degradation has been retarded by almost 10 ℃ compare to the neat PHBV. As it shown in DTG graph in Figure 6-3, the weight loss of PHBV and PHBV/talc was happened in a one-step process between 240 and 305 ℃ and the maximum rate of mass loss is distinguishable by a single peak in DTG. The residue at 600 ℃ (%) could be referenced as amount of talc concentration in composites. It should be considered at 600 ℃ just 0.64 % weight fraction of the PHBV residue existed in the compounds and differences at residue percentage would be all the talc weight fraction in the composites. The obtained exact weight fraction of talc by TGA might justify some irregular results for the 85/15 compound.

Fast thermal degradation of PHA in the conventional plastic processing machinery is considered to be one of the main issues that make the processing of these biopolymers challenging (Xantos, 2010). There have been various studies to use different approaches for improving the thermal stability of the PHBV. The effect of nano-additives and nano-clay has been reported as an effective method to improve the thermal stability of PHA. The layered silicates known as sheet silicates or phyllosilicates are a large group consists of mica, chlorite, clays, talc and serpentine which are defined as fine, soft & low density minerals (Mondominerals, 2016). Bruzaud and Bourmaud declared that PHBV–organoclay

nanocomposite using Cloisite 15A as organoclay, degraded at a higher temperature than the pure PHBV. Based on TGA results they found that the thermal stability of the nanocomposites systematically increases with increasing clay, up to a loading of 5 wt% and the initial decomposing temperature is enhanced by 30 ℃ (Bruzaud and Bourmaud, 2007). The delay in the polymer decomposition can be explained by a decrease in the diffusion of oxygen throughout the composite material due to the homogeneous dispersion of the clay sheets. The silicate layers should also provide a heat barrier, which would enhance the overall thermal stability of the system (Plackett, 2012, Pandey, et al, 2005).

However, Lim et al stated that the thermal stabilization effect of the Organo- Montmorillonite (OMMT) occurred with a low concentration of OMMT that doesn't improve at higher concentrations. This has been explained by the presence of clay particle agglomerations which acts as sites for heat accumulation and even can reduces the enhancement effect (Lim et al, 2003). It thus can be postulated that the silicate layered in the talc will have similar thermal stabilization effect on PHBV copolymer. As it has been seen in table 4, the initial temperature of the thermal decomposition first increased and then stayed constant with increasing talc concentration in the PHBV/talc composites.

3.4 Thermomechanical Properties

3.5.1 Dynamic Mechanical Properties

The temperature dependence of the dynamic storage modulus (E_1) and tanδ (the ratio of the loss modulus to the storage modulus, E_2/E_1) of the PHBV composite with talc are given in Figure 7 and 8. The highest value in the peak of the tan (δ) curve often is used by researchers to determine T_g. Figure 7 shows the effect of temperature on the storage modulus (MPa). The graphs show that with increasing the amount of talc in the composite there is a substantial increase in the storage modulus. This is shown by the upward shift in the curves from 100/0 to 90/10 and 80/20 with approximately a linear response. The composite with 85/15 did not however, show the expected modulus increase based on the other specimens. This irregular trend could be possibly happened due to low accuracy of the exact concentration of the talc in

the compound, as it has been shown in table 3; the residue of material after decomposition of 85-15 PHBV composite was measured to be less than expected. The change in storage modulus with the increase in the talc content is evidence of the reinforcing effect of talc.

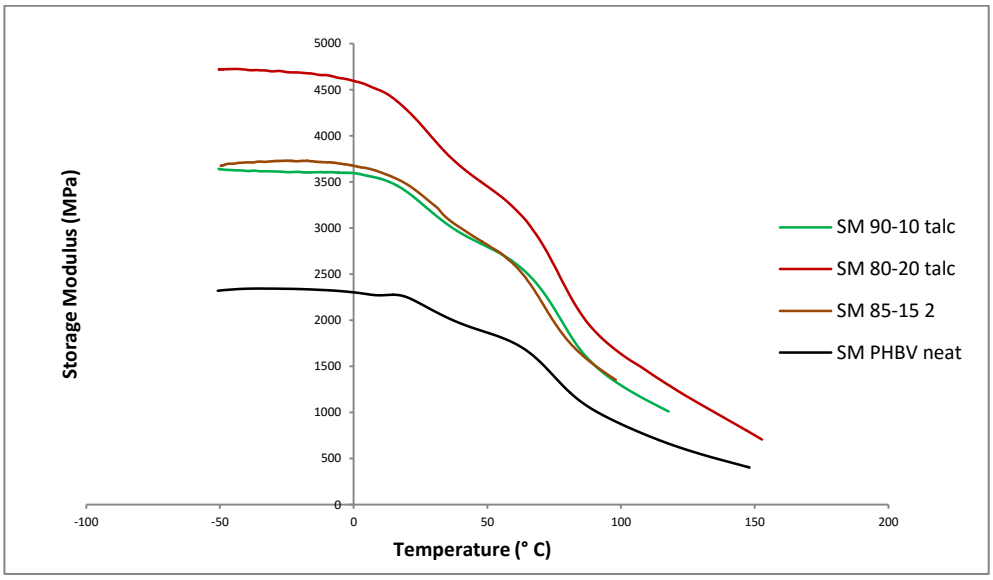

Figure 7-3 The storage modulus of PHBV/talc composites with the four concentrations of 100/0, 90/10, 85/15 and 80/20

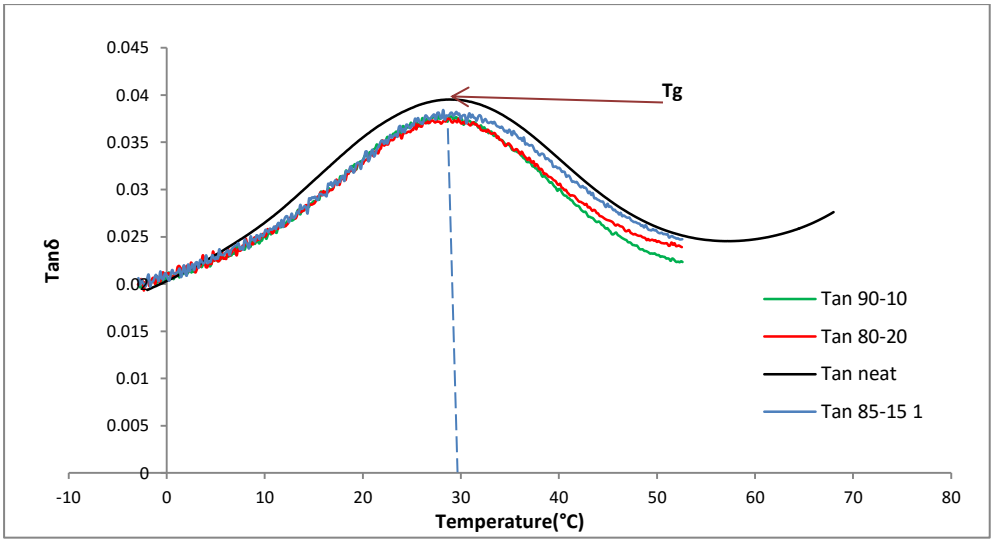

Figure 8-3 The Tan δ of PHBV/talc composites with the four concentrations of 100/0, 90/10, 85/15 and 80/20

Landel and Nielsen declared that fillers have a larger effect in increasing the storage modulus of polymers above T_g than that below T_g. The main reason for this could be the large modulus ratio E_2/E_1 of the polymer above the T_g in the rubbery phase compare to the rigid glassy state. A less important reason would be the larger Poisson's ratio above Tg and the presence of induced thermal stresses below T_g in glassy state (Landel and Nielsen, 1994).

Figure 8-3 shows that there is not a distinguishable change in the glass transition temperatures of the composites with an increasing amount of talc also compared to the neat polymer. However the value of tanδ decreases slightly by increasing the amount of talc. This could be caused by the storage modulus increasing according to the formula of tanδ= $\frac{E2}{E1}$ (E_2 is Loss modulus and E_1 is storage modulus) [Chapter 2].

3.5.2 The heat distortion temperature (HDT)

The heat distortion temperature (HDT), deflection temperature under load (DTUL) or softening temperature represent the maximum temperature that a thermoplastic polymer is considered to be rigid. In fact, polymer sample doesn't deform and able to support a load up to this temperature, for some appreciable time.

Different materials exhibit a tendency to have particles with a specific shape based on the crystal structure and processing conditions. A term for describing the shape of particles and fibres is called "the aspect ratio", which is the ratio of the longest dimension to the smallest. According to DeArmitt, the aspect ratio for a cubic or spherical crystal is one, for platy fillers it is in a range of ~5-50 and for nano-clay or fibres it could be ~100-1000. Generally, isotropic fillers those that roughly have a spherical shape induce the least increase in the HDT compared to anisotropic fillers such as talc, kaolin, mica, and wollastonite. High aspect ratio fillers such as glass fibre and nano-clay provide the maximum improvement in the HDT (De Armitt, 2011).

According to Nielsen and Landel filled polymers in general have a greater heat distortion temperature than pure polymers (Nielsen and Landel, 1994). The heat distortion (HDT) is the maximum temperature at which a polymer remains as a rigid material under the HDT test

conditions. It is a very important and practical property of the material. Researchers usually tend to report HDT temperature arbitrarily as a single point. It is in contrast with T_g which is a specific property of the polymer which settles in a temperature region where transition from glassy state to rubbery state occurs and have different value by the type of the chosen curves, whether from storage modulus or loss modulus or most popularly from Tan δ curve. However, according to De Armitt adding a high aspect ratio filler to amorphous polymers, the HDT temperature will approach the glass transition temperature of matrix (De Armitt, 2011). It has been determined that by increasing the amount of filler, the HDT cannot be further improved because the polymer phase is soft and deforms and fillers are not efficient to improve HDT in amorphous polymers. On the other hand, adding fillers especially anisotropic fillers like glass fibres are effectively improving the HDT and bring it close to the melting point of the polymer. It is well accepted the fillers are extending the limits of the operating temperature for semi-crystalline polymers (De Armitt, 2011). It has also been declared by Nielson that for the amorphous polymers, the HDT value is almost close to the glass transition temperature. For the semi-crystalline polymers it will be shifted to the melting point, depending in the level of crystallinity (Nielsen and Landel, 1994)

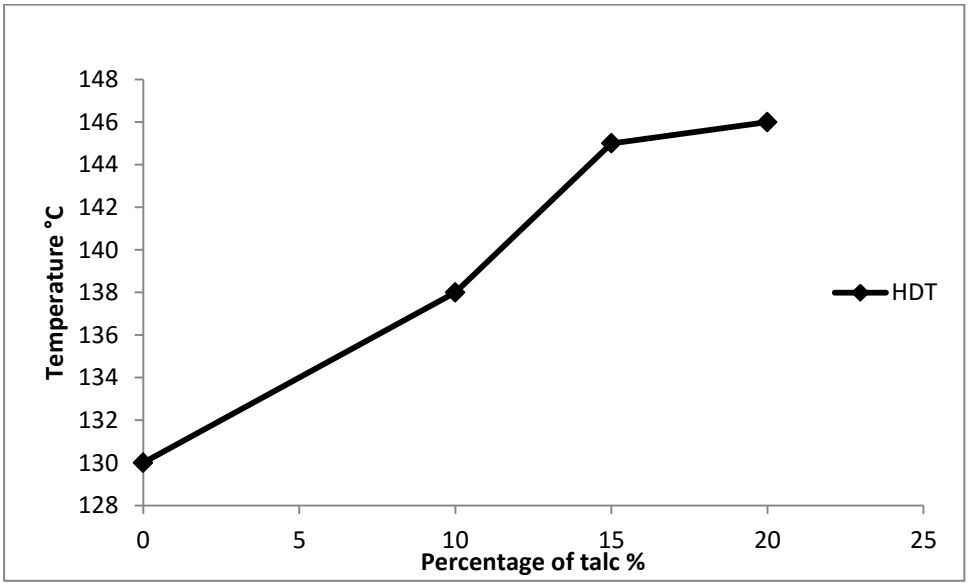

Figure 9-3 The heat deflection temperatures (HDTs) of neat PHBV and its talc-filled composites

The heat deflection temperatures (HDTs) of PHBV and its talc-filled composites are presented in Figure 9-3. The HDT value of PHBV was 130 ℃. The HDT value of the talc-filled PHBV is dramatically increased to 138 ℃ with the 10% weight fraction. This increased further to 145 ℃ with 15% weight fraction of the talc. Only a slight increase to 146 ℃ was recorded with a 20% weight fraction of added talc.

The increase of the modulus and the reduction of high temperature creep for filled polymers have been found to be the key factors for the improvement of the HDT value. According to Xanthos, however for directional fillers, the coefficient of thermal expansion (CTE) is mainly dependent on the orientation filler/particles, due to differences between the CTE of the filler and the matrix (Xantos, 2010). Whaling, Bhardwaj and Mohanty mention that the modulus-temperature dependency is also a critical factor in determining the HDT value of a material (Whaling, Bhardwaj and Mohanty, 2006). As it has been discussed in section 3.5.1, the DMA results clearly show that the talc-filled PHBV composites exhibited higher storage modulus values than the neat PHBV at low temperatures with them coming closer together at higher temperatures (see Figure7). This phenomenon has also been reported by researchers but with a lower value for the HDT (Whaling, Bhardwaj and Mohanty, 2006).

The DMA result could also be associated with the improvement in the HDT values for the talc-filled PHBV composites. In fact, the improving HDT properties of talc-filled PHBV is supported by the DSC and TGA (Figures 2-3, 3-3, 4-3, 9-3) results which indicate that talc plays an important role in enhancing the crystallization and also heat resistance of PHBV and its composites.

3.5 X-ray powder diffraction (XRD)

It has been reported by Chan, Kummerlowe and Kammer, that PHBV copolymers with less than 40 mol% HV units crystallize as the PHB crystalline lattice (Chan, Kummerlowe, and Kammer, 2004). Yokouchi et al first reported that “the unit cell in PHB chain is orthorhombic, with α=5.76 Å, *b*=13.20 Å, and *c* (fabric period) = 5.96 Å and two molecules pass through the unit cell” (Yokouchi et al, 1973). In this study the hydroxyvalerate content of the PHBV copolymer is 3% and therefore the crystal structure can be expected to be similar to the PHB,

an orthorhombic crystal system. Hocking and Marchessault mentioned that in the crystal line of PHB molecules, the orthorhombic unit cells in a helical form are repeated in with a two-fold screw axis along the chain propagation direction (Hocking and Marchessault, 1998).

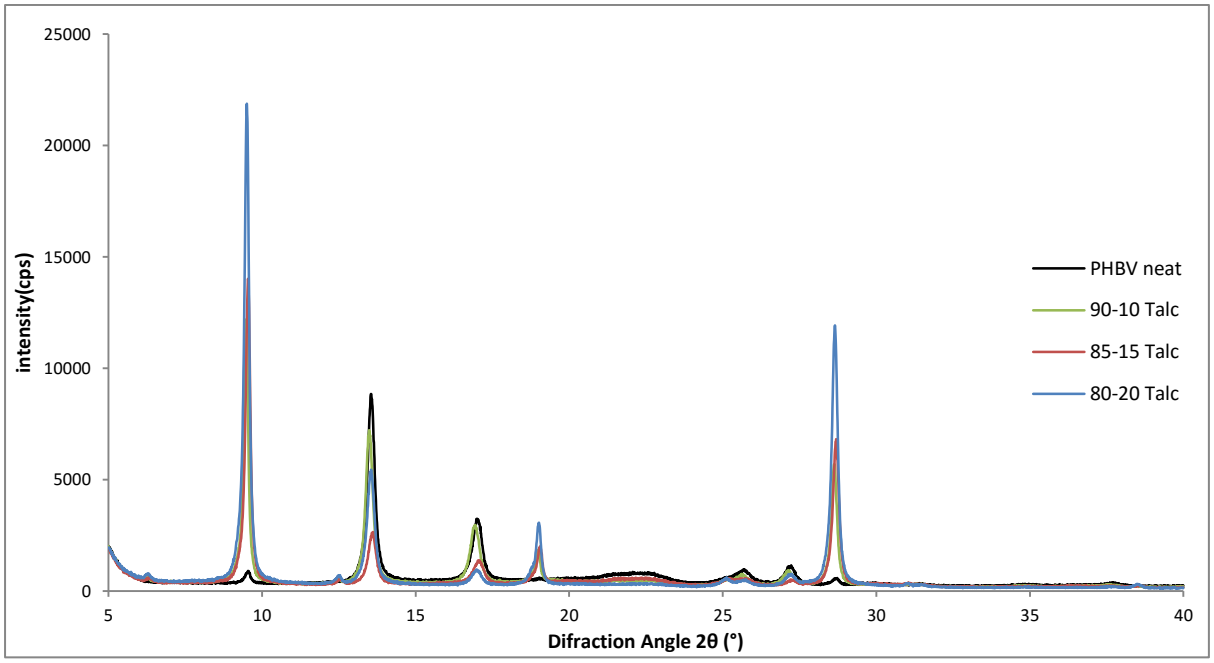

Figure 10-3 XRD graph of PHBV extruded and it's composite with talc in different concentrations

X-ray diffraction 1D patterns of the extruded PHBV and PHBV/talc composites are shown in Figure 10-3. This illustrates that the neat PHBV presents two strong diffraction peaks at around 13.54 ٩(Figure 12-3-c) and 17.00 °corresponding to {020} and {110} planes (Miller index), respectively of the orthorhombic crystal structure.

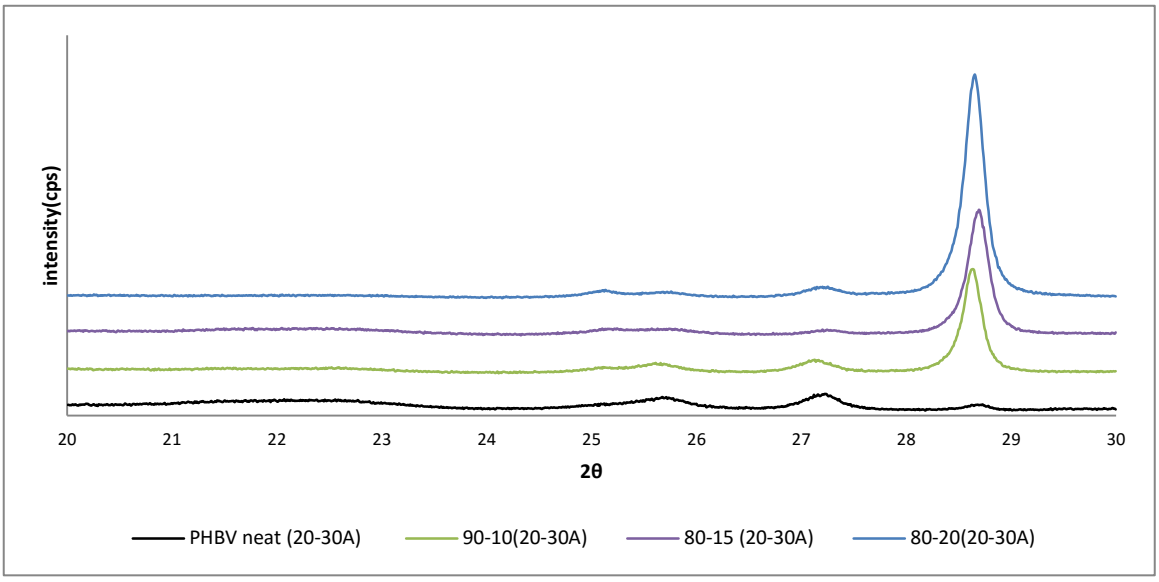

Figure 11-3 XRD graph of the amorphous region that decreased between 20-30 °and the nucleation occured in this region (these traces have been displaced).

Figure 11-3 shows the amorphous region decreases in region between 20-30 °(A crystalline phase exhibit sharp distinct peaks corresponding to fixed 2θ values. Conversely, amorphous phase being of short order shows a hump in XRD in a broad range)

Figure 12-3-a to 12-3-c illustrate that the peaks at 19°, 25°, 12.5° correspond to the nucleation of talc effect inside the compound. Wu, Wen and Hou (2004), Obata and Sumitomo (2001) reported that three sharp diffraction peaks assigned to the reflection of talc are at ca 2θ = 9.5◦, 19.0◦ and 28.7◦, and are attributed to the {002}, {020} and {006} reflections of the talc crystals (Wu, Wen and Hou 2004; Obata and Sumitomo, 2001). Therefore, the crystalline structure of the polymer matrix is not affected by the presence of talc: the PHBV/talc composites show the presence of the three talc peaks, 2θ = 9.5° (Figure 7-3-d), 2θ = 19 ◦ (Figure 12-3-a), 2θ = 28.7 (Figure 11-3). So, whether the PHBV is in the pure state or in the talc compounds, it shows the same diffraction patterns the pure PHBV are present. However, it has to be stated that the intensities of the three talc peaks are proportional to the talc content.

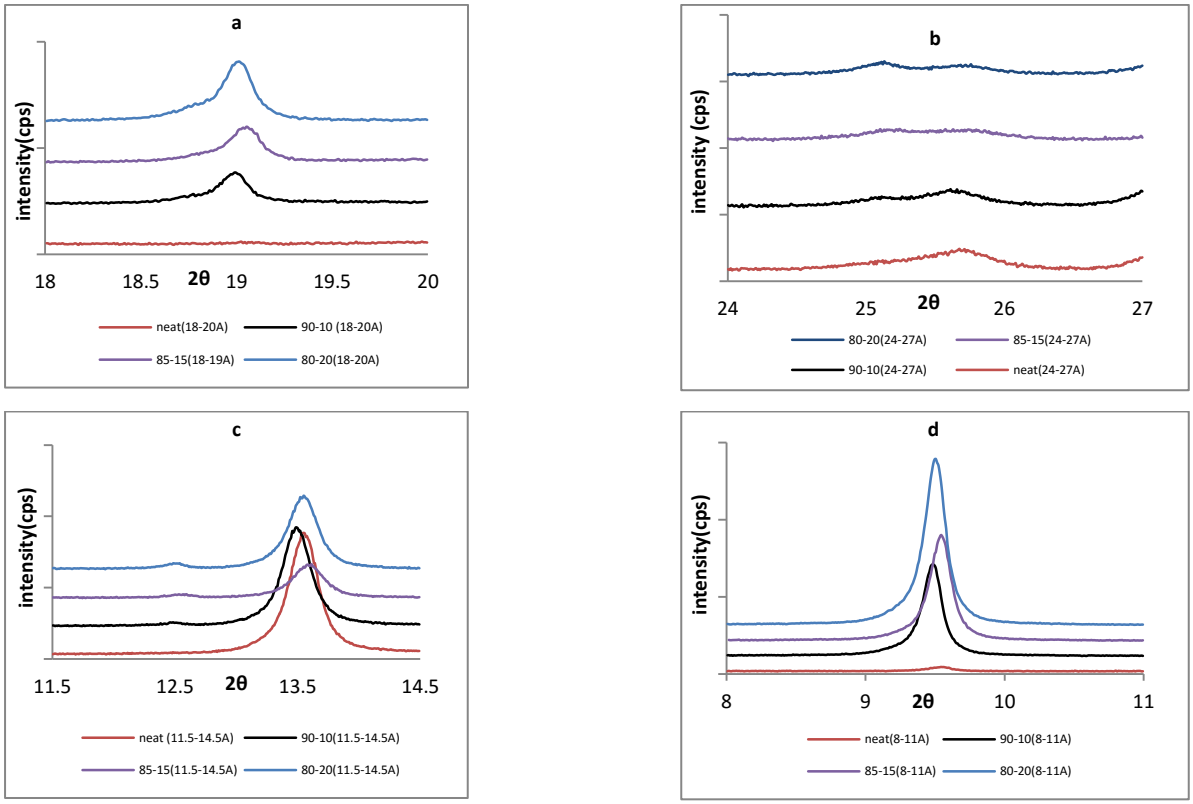

Figure 12-3 XRD peaks at 19 °, 25 °, 12.5 °and 9.5 °

Kunioka, Tamaki and Doi stated that PHBV with less than 40% 3HV crystallized in the P (3HB) lattice, while those with the 3HV composition more than 50% mol crystallized in the P (3HV) lattice.. This phenomenon is called isodimorphism (Kunioka, Tamaki and Doi, 1989). From XRD result the degree of crystallinity is shown in the Figure 13-3:

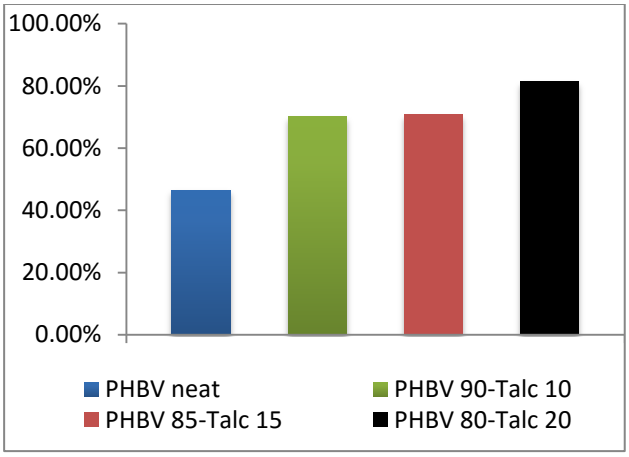

Figure 13-3 Degree of crystallinity of PHBV neat and PHBV/Talc composites

Figure 13-3 shows the degree of crystallinity of PHBV and its composites with talc. It clearly shows that neat PHBV is 46.5% crystalline, Incorporating 10% talc the degree of crystallinity incenses to 70%, for 85-15 talc it just slightly increases to 70.8%. It finally becomes 81.40% with 20% talc in the polymer matrix.

3.7 Mechanical properties

3.7.1 Tensile and Flexural Testing

The tensile and flexural properties of PHBV and PHBV/talc composites are illustrated in Table 5-3:

Table 5-3 The tensile and flexural properties of PHBV and PHBV/talc composite

PHBV/Talc %	Tensile strength MPa (SD)	elongation at break %	Elasticity Modulus GPa	Flexural Modulus GP
100/0	32.68(3.5)	1.2(0.18)	3.75(0.42)	3.9(0.69)
90/10	20.35(2.1)	0.9(0.13)	5.22(0.4)	4.77(0.57)
85/15	21.75(3.1)	0.7(0.45)	5.46(0.42)	5.07(0.69)
80/20	26.48(3.8)	0.8(0.15)	6.54(0.046)	5.94(0.33)

From Table 5-3, it can be seen that the tensile strength of PHBV and PHBV/talc composites decreases for the first added 10% talc and then increases for adding more content of talc. Similar phenomena was reported by Whaling, Bhardwaj and Mohanty, it has been declared that at the higher concentration of talc, the talc particles prevent the matrix from deformation and the composite resists at a higher stress but at a lower strain(Whaling, Bhardwaj and Mohanty, 2006).

However, the non-uniform size of the talc particles based on the morphology studies of specimens by SEM (Figure 16-3 & 17-3) could be another reason for that. Li et al stated that if the talc particles are not uniform and spread with different sizes, thus the amount of small particles rises with increasing the talc volume fraction. The result is that the composite has become more compacted because the smaller particles stand in the free spaces between the large particles. The density of particle distributed may account for the increase in the tensile strength of the composite at the higher talc concentrations (Li et al, 2001).

.

Table 5 shows that there is an increase in Young's modulus from a value of 3.75 GPa for the neat PHBV up to 6.54 GPa with the addition of 20% weight fraction of talc. This effect is due to the addition of the high modulus platy shape filler to a significantly lower modulus polymer matrix. De Armitt stated that platy shape fillers including mica generally increase the polymer modulus significantly more than isotropic fillers such as calcium carbonate, silica, dolomite, and fly ash. The improvement is strongly dependent on the aspect ratio of the filler. Fillers with a large aspect ratio have a greater effect and it is similar for both the Youngs and the flexural modulus. The tensile strength of the composites, however, is also affected by the level of adhesion between the filler and polymer. A coupling agent can enhance the effect of fillers. Moreover, the modification of the filler's surface area also may increase the adhesion with help of more contact area between filler and matrix of polymer (De Armitt, 2011).

The standard deviation of the modulus and the elongation at break is low (Table 5-3). This can be justified as the effect of good talc dispersion and distribution within the matrix. The homogeneous dispersion also will be discussed in morphology assessment by SEM images (Figure 17-3)

The increment of modulus of elasticity and flexural modulus could be explained by three different effects:

- Change in the crystallinity of the composite by nucleating effect of talc and more uniform and substantial size reduction of crystals
- The effect of the contribution of talc stiffness ($E_{talc} \approx 70$ GPa versus $E_{PHBV} \approx 3.75$ GPa)
- Talc particles orientation has an important role in increasing of the stiffness(29,30)

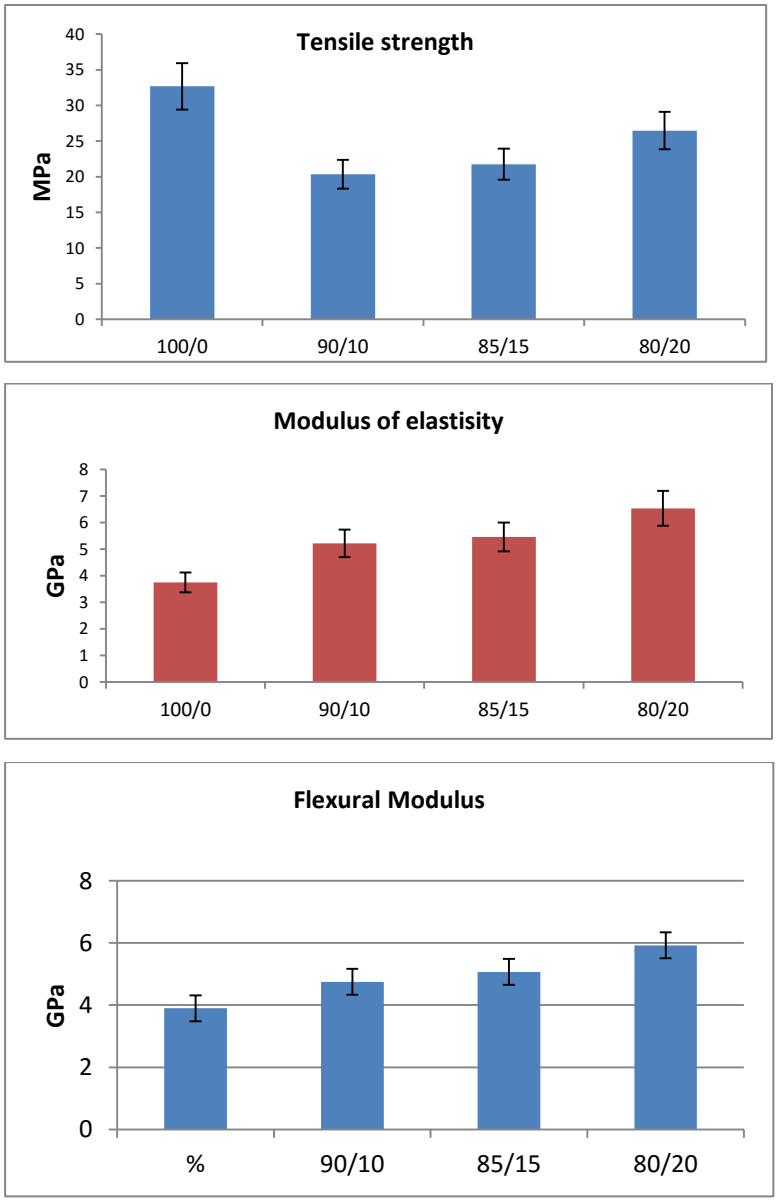

Figure 14-3 The Young's modulus, flexural modulus and tensile strength PHBV/Talc composite with different concentrations

The elongation at break (%) decreases by increasing the amount of talc in composites (table 5-3). This behaviour can be justified by the effect of fillers on matrix by restricting the chains mobility which reduces the level of plastic deformation before fraction resulting in matrix reinforcement (Castillo, Barbosa and Capiati, 2013; Echevarria, Eguiazabal and Nazabal, 1998)

The Halpin-Tsai equation (shown below) provides a mathematical model for predicting the elasticity of composite materials based on the geometry and orientation of the filler and the elastic properties of the filler and matrix. It is valid for high aspect ratio fillers; therefore it could be used for the talc particles platy structure.

Equation 5-3) $$\frac{Yc}{Ym} = \frac{(1+\zeta\eta Vf)}{(1-\eta Vf)}$$ (Halpin-Tsai equation)

where:

Equation 6-3) $$\eta = \frac{\frac{Yf}{Ym}-1}{\frac{Yf}{Ym}+\zeta}$$

Y_c=composite Young's modulus,

Y_m= corresponding matrix Young's modulus

Y_f= corresponding filer Young's modulus

ζ= a measure of the reinforcement that is equal to 2(L/D), depends on the boundary conditions (the geometries of inclusions and loading conditions) where (L/D) is the aspect ratio of the filler (L=length, D= thickness of the particles)

V_f = volume fraction of filler in composite this could be calculated from the following equation:

Equation 7-3) $$V_f = \frac{Wf}{Wf + (1-Wf)\frac{\rho f}{\rho m}}$$

where W_f is weight fraction of filler and ρ_f & ρ_m are the specific gravity of filler and matrix respectively (Halpin, 1969).

Y_m is 3.75 GPa as measured,

Y_f is taken as 70GPa which is the Young's modulus of other silicate fillers (such as glass)

ρ_f = 2.78 g/cm^3 , ρ_m= 1.24 g/cm^3

ζ is calculated from the aspect ratio of the average of 20 talcum powder particles observed in the SEM images (Figure 16-3,17-3) with Microsoft visio & excel software. The result was an aspect ratio of 10.

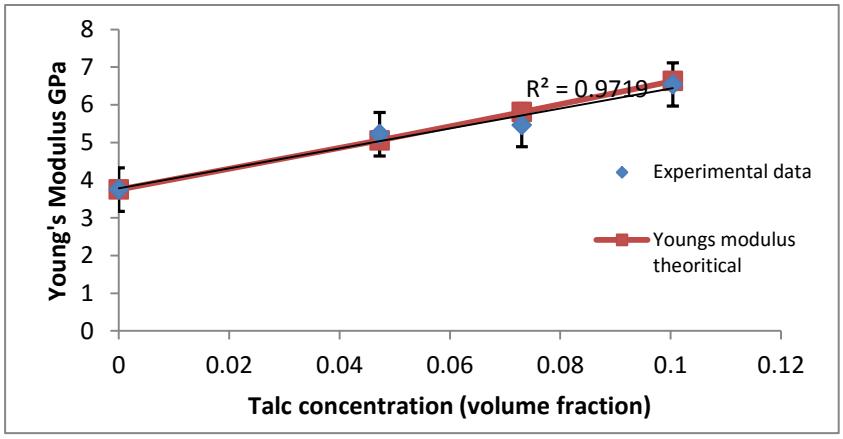

Figure 15-3 The experimental Young's Modulus and theoretical based on Halpin-Tsai equation

Table 6-3 The Young's Modulus of PHBV and PHBV/Talc composites based on the Halpin-Tsai prediction formula and experimental data

PHBV/Talc	W_f %	V_f %	Y_c GPa	Y_{cc} GPa
100/0	0	0	3.75	3.75
90/10	0.1	0.047	5.06	5.22
85/15	0.15	0.073	5.81	5.46
80/20	0.2	0.100	6.63	6.54

Table 6-3 shows the percentage weight fraction (W_f %) and the volume fraction (V_f %) of the filler, the theoretical Yong's modulus (Y_c) and the experimental Young's modulus (Y_{cc}). It can be seen in Table 6-3 and Figure 15-3, which the experimental data is very close to the theoretical data and the correlation factor is about 0.97 which indicates the accuracy of the results obtained from the tensile tests.

3.7.2 Impact resistance

The addition of mineral fillers does not generally increase the impact resistance. There are however, exceptions, such as the use of fine talc in polypropylene bumpers. In this case, 5 - 10% is added. Greater proportions result in a drop-off in impact resistance (Landel, Nielsen, 1994).

The addition of low volume fraction of talc filler has been reported to be effective in improving the impact toughness of polypropylene composites. Pukanszky et al indicated that the strain energy release rate of the talc-filled PP composites is dependent the talc concentration it up to a maximum at 10% talc after which it dropped with increasing talc content in the composites. It has been stated that an increase in the fracture toughness is associated with the filler or initiated plastic deformation of matrix or interaction between both of them. Since plastic deformation be of the matrix is considered to be the most important energy consumption process, the decrease of the effective cross section of the matrix with increasing filler content is main cause for the decrease in fracture toughness of the composites with high filler content (Pukanszky et al, 1994).

Similar phenomena have been witnessed by drop-weight impact test on plate form specimens with different talc concentrations summarized in Table 7-3. Table 7-3 shows change in different parameter including force and energy absorbed by the polymer.

Table 7-3 Dropped weight impact properties of PHBV and its composite with talc

Specimens	Peak Force [N]	Puncture Force [N]	Peak Energy [J]	Total Energy [J]	Puncture Energy [J]
PHA neat C3	1673 ± 280	798 ± 114	0.68 ± 0.2	4.87 ± 3.03	0.90 ± 0.34
PHA90+Talc10	2245 ± 135	1107 ± 67	3.29 ± 1.08	9.34 ± 2.06	4.17 ± 1.85
PHA80+Talc20	3129 ± 220	1544 ± 98	3.02 ± 1.65	12.51 ± 3.2	3.71 ± 1.35

It can be seen that the peak and puncture force increases with the amount of talc added. The total energy and peak energy increased by adding 10% talc but decreased for 20% talc and it is same for other properties as well.

3-8 Scanning Electron Microscopy

In general, two frequently used concepts for describing the structural character of polymeric composite materials are the composition and dispersion of the modified agent in the polymeric matrix (Wu, Wen and Hou, 2004). Apart from the widely studied isotactic polypropylene composites (Akinci, 2009; Mina et al, 2010), there are not many studies concerning the reinforcement fillers such as talc on conventional polymers like polyethylene and it is because the homogeneous by melt blending has been a challenging task for researchers (Parvin et al, 2013). Electron microscopy is an effective method to study dispersion of fillers in polymer matrix.

The morphology of pure talc is illustrated in Figure 16-3 (1-4) at different magnifications; it can be observed that the platy shape of talc particles dominates the whole morphology; however, spherical morphologies are also evident. The particles have a median diameter of d50=1.9 μm and d95=7.6 μm, and can be considered to be a very fine talc.

The images in Figures 17-3 (2&4) were taken from edge of specimens and images 17-3(3) from centre of the specimen in order to have a comparison of the orientation of the talc in the structure and centre of moulding. The images clearly show that the talc particles were randomly dispersed and oriented in the PHA matrix. Strong parallel orientation of particles align with the flow direction at the wall of the mould [Figure 17-3(2, 4)] and their random orientation with high tendency of parallel pattern with shear orientation in core of specimen is observable in images (Figure 17-3c).

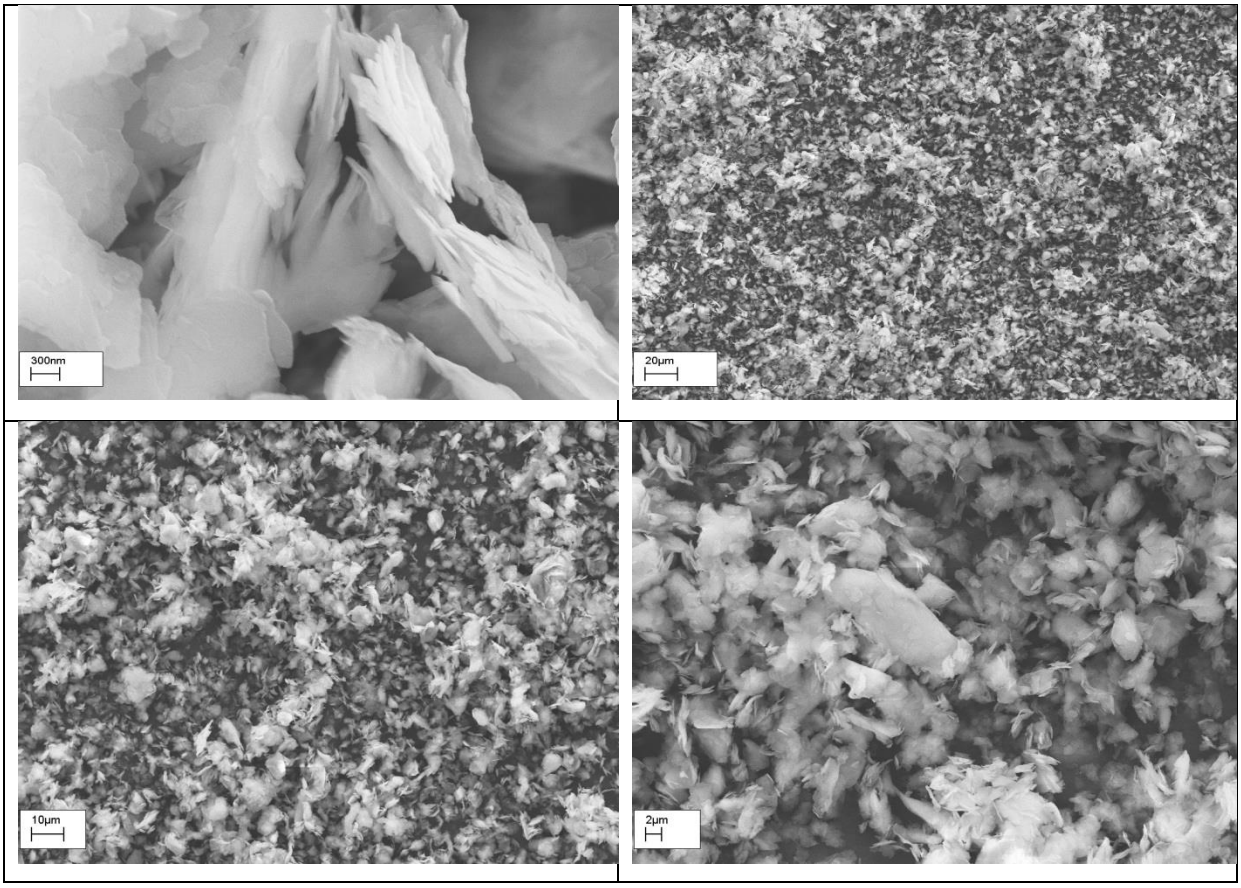

Figure 16-3 (1-4) - SEM images of talc particles at different magnifications

The lamellae of the talc particles and the polymer melt flow that are frozen close to the surface (skin) have an orientation favourable to the mechanical loading intension. This phenomena result from the fountain flow effect of the melt filling the mould (Figure 17-3). While in the core of specimens, particles show a more random orientation.

Similar Phenomena also has been reported by Whaling, Bhardwaj and Mohanty (2006) and in work of Pukanszky et al (2004) which indicates that talc particles tend to orient in the flow direction within processing in conventional plastic machinery due to their anisotropic structure when subjected to the shear stress and flow pattern during the processing (Whaling, Bhardwaj and Mohanty, 2006; Pukanszky et al, 2004).

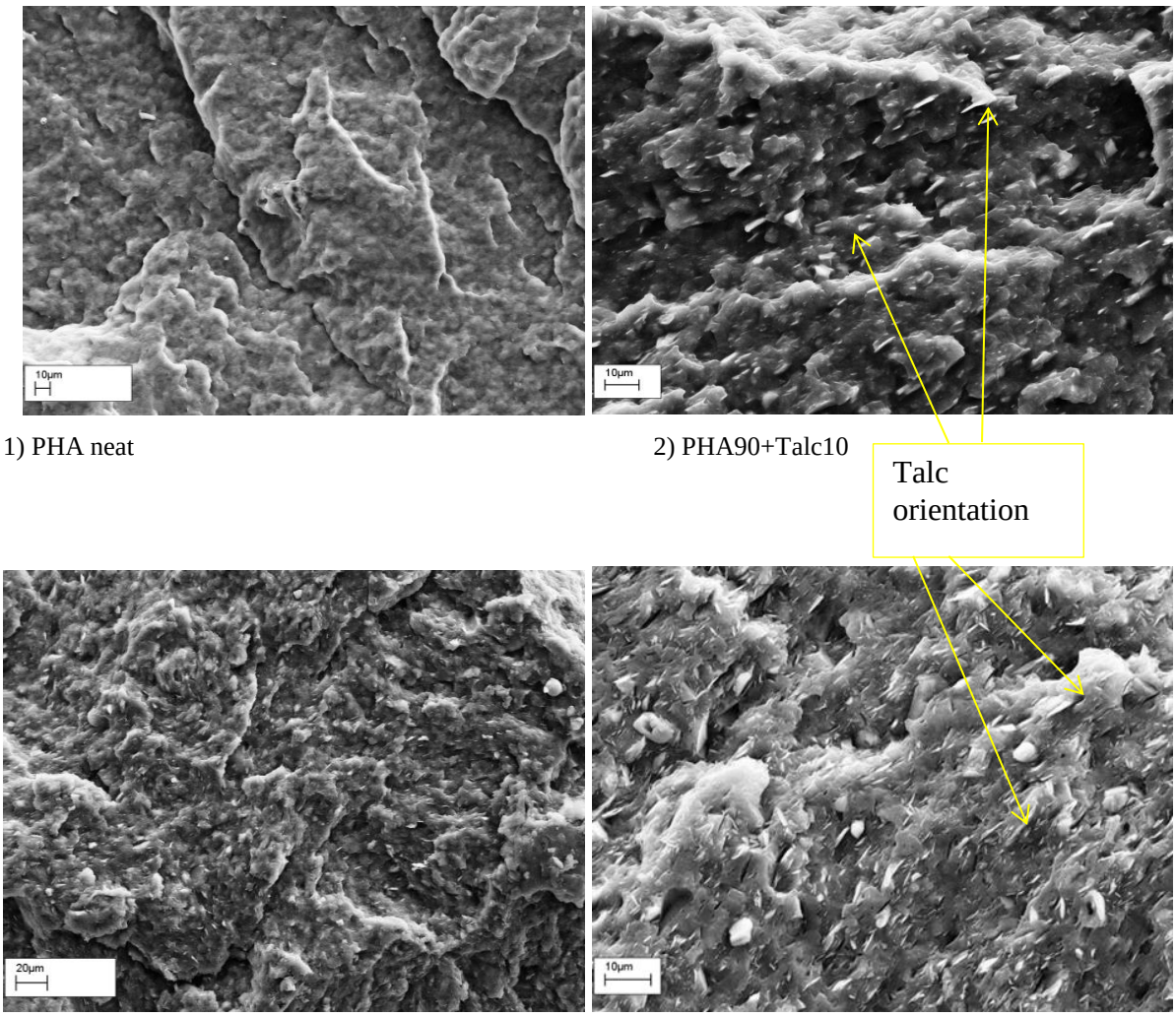

1) PHA neat

2) PHA90+Talc10

3) PHA85+Talc15

4) PHA80+Talc20

Figure 17-3 (1-4) SEM images of the fracture surfaces of the PHA/talc composites impact specimens with different talc concentrations.

According to Pukanszky et al the orientation and orientation distribution of particles in matrix is dependent of factors such as shear condition, flow pattern, mould filling rate and cooling condition (Pukanszky et al, 2004) while Whaling, Bhardwaj and Mohanty declared that the dispersion of particles in a polymer matrix also depends on shear stress developed to separate the particles within processing and the relative magnitudes of the adhesion and separating forces (Whaling, Bhardwaj and Mohanty, 2006).

Energy Dispersive X-Ray Analysis (EDX), referred to as EDS or EDAX, is an x-ray technique used to identify the elemental composition of materials. EDX systems are attachments to Electron Microscopy instruments (Scanning Electron Microscopy (SEM) or Transmission Electron Microscopy (TEM)) instruments where the imaging capability of the microscope identifies the specimen of interest. The data generated by EDX analysis consist of spectra showing peaks corresponding to the elements making up the true composition of the sample being analysed. Elemental mapping of a sample and image analysis are also possible.

The advantages of using Edax are:

- Ability to study dispersion in depth
- Use of large samples
- Minimum of difficulty in the preparation of test specimens
- Compositional information of individual agglomerates
- Facilitation to the automated image analysis techniques (

Edax results for the neat PHBV are shown in Figure 18-3 and Table 8-3.

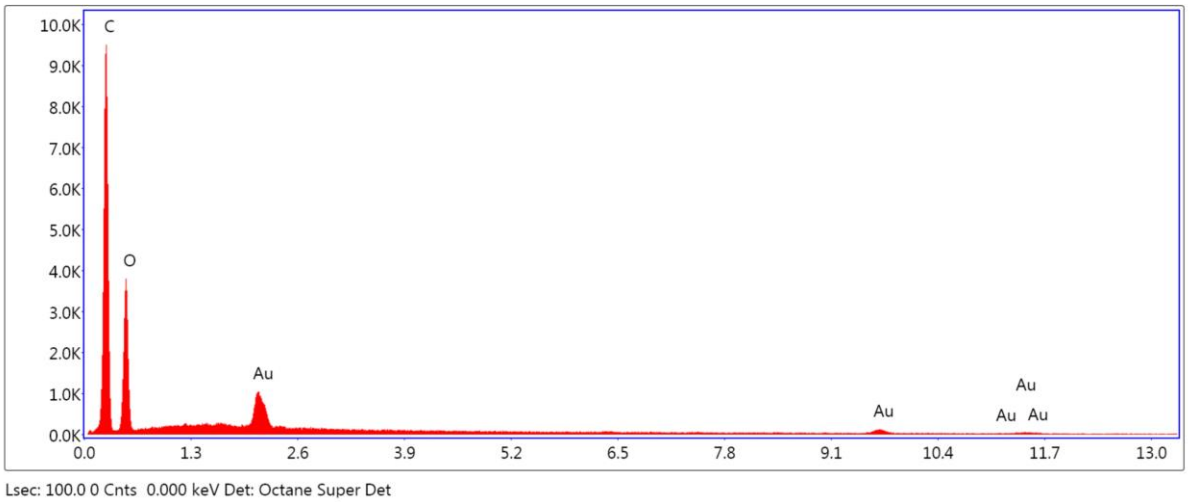

Figure 18-3 Edax spectra analysis of the neat PHBV of a random area on specimen

The three random areas (area1, area2 and area3) on each specimen of PHBV/talc 80/20 and 90/10 have been chosen and analysed by Edax. The results for the atomic percentage % of Mg and Si are shown in Figure 19-3.

Table 8-3 Edax results for the neat PHBV

Element	Weight %	Atomic %	Net Int.	Error %	K ratio
C K	57.9	68.1	613.6	5.4	0.3589
O K	35.5	31.4	240.2	10.0	0.0594
Au L	6.6	0.5	15.5	24.0	0.0431

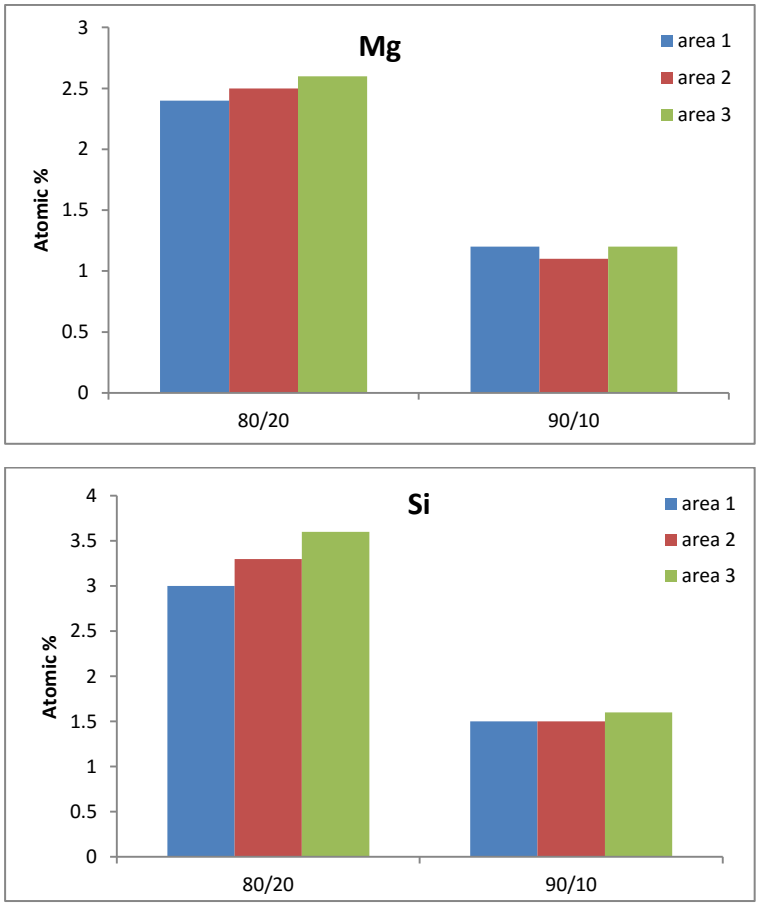

Figure 19-3 Mg and Si atomic percentage % of the PHBV/talc 80/20 and 90/10 specimens in the three random areas

Fig 19-3 depicts the EDS spectra of SEM photographs have been investigated for the distribution of talc particles in the PHBV matrix in three random areas (area1, area 2 and area 3). From these EDS spectra, it is verified that the talcum powder were distributed equally in polymer matrix and the concentration of silicon and magnesium presence increases with increasing the concentration of talc from 10% to 20%.

3.9 Conclusion

All non-isothermal DSC of the PHBV and PHBV/talc composites showed two peaks of melting point (second heating cycle)which is shifted slightly by different concentrations of talc in composites due to reorganisation and recrystallization of the polymer close and prior to the melting point.

Isothermal crystallization kinetics of the PHBV has been analysed using the JMAK equation and it showed how talc accelerated the crystallization of the PHBV and the Avramis component proved that the mechanism of crystallization is not changing with the different concentrations of talc.

The value of Avrami's component *n*, revealed the existence of a rod-like crystal structure at the lower temperatures shifting to disk and spherulite shapes in the higher isothermal crystallization temperatures. It also revealed that the value of *k* is reduced and $t_{0.5}$ is increased with an increase in temperature. The value of $t_{0.5}$ reduced with an increase in the amount of talc at a specific temperature. The above results indicate that the addition of talc increased the crystallization rate of PHBV in the composites. Therefore, talc enhances the nucleation of the PHBV in the composites which leads to a faster crystallization rate.

The XRD result showed the nucleating effect of talc with an increase in the crystallinity from 46.5% for pure PHBV to 81.40% for the composite containing 20% talc. It also revealed that the crystalline structure of the polymer matrix is not affected by the presence of talc which supported Avrami results with DSC (Table 3-3)

The TGA results indicated that the addition of talc could increase the temperature of degradation of PHBV/talc composite with 10% talc, but however, the thermal stability doesn't improve with increasing the amount of talc.

The DMA result revealed that the storage modulus of the composites increased with an increase in the content of talc, however the phenomena is not similar for 85/15 talc concentrations. It might be happened due to insufficient amount of talc inside the composite. This change in storage modulus demonstrated the reinforcing effect of talc.

There are no distinguishable changes in the glass transition temperatures with the addition of the talc to PHBV.

The heat distortion temperature of PHBV/talc composite increased significantly with an increase in the amount of talc.

The Young's Modulus and the Flexural Modulus increased with the addition of talc. The mathematical prediction of the modulus of elasticity of the composites using the Halpin-Tsai equation closely matched the experimental results presented.

The addition of mineral fillers does not generally increase the impact resistance. Drop-weight impact test, however, showed an enhancement in the energy absorbed by the composites. The results showed that the peak force and puncture force increased with the amount of talc added, but the total energy and the peak of energy first increased by adding 10% talc and then decreased for 20% talc.

Finally, SEM revealed the platy shape structure of the talc powder. The aspect ratio was calculated from the SEM images of the composites. The image also showed a good dispersion of the talc particles inside the polymer matrix. The orientation of the particles resulting from the shearing of the melt at the mould walls and the cold surface of mould was observed in the SEM images.

Bibliography Chapter 3

- Akinci, A. (2009), "Mechanical and structural properties of polypropylene composites filled with graphite flakes", Arch. Mat. Sci. Eng, Vol 35, Issue 2, pp. 91-94.

- Bian, J., Ye, S. R. and Feng, L. X. (2003),"Heterogeneous nucleation on the crystallization poly(ethylene terephthalate)", Journal of Polymer Science Part B: Polymer Physics ,Vol 41, Issue 18,15, September 2003 , pp. 2135–2144

- Bruzaud, S. and Bourmaud, A. (2007), "Thermal degradation and (nano) mechanical behaviour of layered silicate reinforced poly (3-hydroxybutyrateco-3-hydroxyvalerate) nanocomposites", Polymer Testing, Vol 26, pp. 652–659

- Bugnicourt, E., Cinelli, P., Lazzeri, A. and Alvarez, V. (2014), "Polyhydroxyalkanoate (PHA): Review of synthesis, characteristics, processing and potential applications in packaging", express Polymer Letters, Vol.8, No.11, 791–808 Available [online] at: www.expresspolymlett.com (Accessed 18 Aug 2016)

- Castillo, A., L., Barbosa, S., E., Capiati,N., J., (2013), "Influence of talc morphology on the mechanical propertiesof talc filled polypropylene", J Polym Res, Vol 20, Issue 5, pp. 2-9

- Chan, H., C., Kummerlowe, C., Kammer, H., W. (2004), "Crystallization and Melting Behaviour of Poly (3-hydroxybutyrate)-Based Blends", Macromolecular Chemistry and Physics, Vol 205, Issue 5, pp. 664–675

- De Armitt, C. (2011),"Functional Fillers for Plastics", in book Applied Plastics Engineering Handbook, by Kutz, Elsevier, page 458

- Echevarria G.G., Eguiazabal J.I. and Nazabal J. (1998), "influence of moulding conditions and talc content on the properties of polypropylene composites", Eur. Polym. J. Vol. 34, No. 8, pp 1213-1219

- El-Hadi, A., Schnabel, R., Straube,E., Müller, G. and Riemschneider, M. (2002), ”Effect of melt processing on crystallization behaviour and rheology of poly (3-hydroxybutyrate)(PHB) and its blends”, Macromolecular Materials and Engineering Journal,Vol 287, issue 5, pp.363-372

- Elzayat, M.Y.F., El-Sayed, S., Osman, H.M. and Amin, M. (2012),“X-ray diffraction and differential scanning calorimetry studies of a BaTi[O.sub.3]/polyvinylidene fluoride composites”, Polymer Engineering and Science Journal, Vol 52 ,Issue9, pp. 734-740

- Gunaratne, L.M.W.K. and Shanks, R.A., (2005), “Multiple melting behaviour of poly (3-hydroxybutyrate-co-hydroxyvalerate) using step-scan DSC”, European Polymer Journal, Vol 41, pp. 2980–2988

- Gupta, B. R. (1998), “Rubber Processing On A Two-Roll Mill”, Allied Publishers LTD, New Delhi, pp. 43-45

- Halpin, J. C., (1969), “Effect of Environmental Factors on Composite Materials”, US Air Force Material Laboratory, Technical Report AFML-TR-67-423

- Hay, J. N., Fitzgerald, P.A. and Wiles, M., (1976), “Use of differential scanning calorimetry to study polymer crystallization kinetics”, Journal of polymer, Vol 17, Issue 11, pp. 1015-1018

- Hocking, J. P. and Marchessault , R. H. (1998), “Polyhydroxyalkanoates” in book by Kaplan,D. L., “Biopolymers from Renewable Resources”, Springer-Verlag Berlin Heidelberg New York, pp. 230

- Kai,W. , He, Y. and Inoue, Y., (2005), “Fast crystallization of poly(3-hydroxybutyrate) and poly(3-hydroxybutyrate-co-3-hydroxyvalerate) with talc and boron nitride as nucleating agents”, journal of Polymer International, Volume 54, Issue 5, pp.780–789

- Kucerova, J. (2008),” Nucleating and clarifying agents for polymers”, [online] Available at: http://digilib.k.utb.cz/bitstream/handle/10563/7290/ku%C4%8Derov%C3%A1_2008_bp.pdf?sequence=1 (Accessed 17 Aug 2016)

- Kunioka, M., Tamaki, A. and Doi, Y., (1989), “Crystalline and thermal properties of bacterial copolyesters: poly (3-hydroxybutyrate-co-3-hydroxyvalerate) and poly (3-hydroxybutyrate-co-4-hydroxybutyrate)” , Macromolecules, Vol. 22, no. 2, pp. 694–7

- Landel, R. F., Nielsen, E. L. (1994),” Mechanical Properties of Polymers and Composites”, Second Edition”, Marcel Dekker Inc, New York, page 425

- Li, G., Helms, J. E., Pang, S. S. and Schulz, K. (2001), “Analytical Modeling of Tensile Strength of Particulate-Filled Composites”. Polym. Compos. Vol 22, pp. 593-603

- Lim, S. T., Hyun, Y. H., Lee, C. H. and Choi, H. J. (2003), “Preparation and characterization of microbial biodegradable poly (3-hydroxybutyrate)/organoclay nanocomposite”, Journal of Material Science letter, Vol 22, pp. 299 – 302

- Liu, W. J., Yang, H. L., Wang, Z., Dong, L. S., Liu, J. J. (2002), ”Effect of nucleating agents on the crystallization of Poly(3-Hydroxybutyrate-co-3-Hydroxyvalerate)”, Journal of Applied Polymer Science, Wiley Periodicals, Inc., Vol. 86, pp. 2145–2152

- Menczel, J. D., Prime, R. B. (2009), “Thermal Analysis of Polymers - fundamentals and applications”, [Online] John Wiley & Sons, Inc., Available at: https://books.google.co.uk/books?hl=en&lr=&id=p8MBBAAAQBAJ&oi=fnd&pg=PT8&dq=Thermal+Analysis+of+Polymers++fundamentals+and+applications&ots=Lg-nzvsxBO&sig=HHgstaDGMAflVdzq6A5KedjM_o#v=onepage&q=Thermal%20Analysis%20of%20Polymers%20-%20fundamentals%20and%20applications&f=false (Accessed 17 Aug 2016)

- Mina, F. M., M. A., Haque, M. K. H., Bhuiyan, M. A., Gafur, Y., Tamba and T. Asano. (2010), "Structural, Mechanical and Thermal Studies of Double-Molded Isotactic Polypropylene Nanocomposites with Multiwalled Carbon Nanotubes". J. App. Poly. Sci. Vol 118, pp. 312-319.

- Mondominerals, (2016),[online] Available at: http://www.mondominerals.com/uploads/media/mondo_bulletin_plastics.pdf (Accessed 18 Aug 2016)

- Obata, Y. and Sumitomo, T. (2001), "The effect of talc on the crystal orientation in polypropylene/ethylene-propylene rubber/talc polymer blends in injection molding" Polymer Engineering & Science, Vol 41, Issue 3, pp. 408–416

- Pandey, J. K., Reddy, K, R., Kumar, A. P. and Singh, R. P. (2005), "An overview on the degradability of polymer nanocomposites", Polymer Degradation and Stability, Vol 88, Issue 2, pp. 234-250

- Parvin, N., Ullah, S., Mina, F. and Gafur, A. (2013), "Structures and mechanical properties of talc and carbon black reinforced high density polyethylene composites: effects of organic and inorganic fillers", Journal of Bangladesh Academy of Sciences, Vol. 37, No. 1, pp.11-20

- Plackett,D. (2012), "PHA/Clay Nano-Biocomposite", in book of "Environmental Silicate Nano-Biocomposites" by Luc Av érous, Eric Pollet,London springer ,page 153

- Pukanszky, B., Belina, K., Rockenbauer, A. and Maurer, F. H. J. (1994), "Effect of nucleation, filler anisotropy and orientation on the properties of PP composites", Composites, Vol 25, Issue 3, Pages 205-214

- Shanks, R, A. and Tiganis, B. E. (1998), "Plastic additives: An A-Z reference", Edited by Pritchard, Chapman & Hall, London, Page 464

- Vidhate, S., Innocentini-Mei, L. and D'Souza, N. A. (2012), "Mechanical and electrical multifunctional poly (3-hydroxybutyrate-co-3-hydroxyvalerate)—multiwall carbon nanotube nanocomposites", Journal of Polymer Engineering & Science, Vol 52, issue 6, pp.1367-1374

- Wadud, S. E. B. and Ullbrich, R. R. (2016) "Using the DMA Q800 for ASTM International D 648 Deflection Temperature under Load", [online] Available at: http://www.tainstruments.com/pdf/literature/TA308.pdf (Accessed 17 Aug 2016)

- Wang, Y. D., Yamamoto, T. and Cakmak, M. (1996)," Processing characteristics and structure development in solid-state extrusion of bacterial copolyesters: Poly(3-hydroxybutyrate-co-3-hydroxyvalerate)", Journal of Applied Polymer Science, Vol 61, Issue 11, pp. 1957–1970

- Whaling, A., Bhardwaj, R. and Mohanty, A. (2006), "Novel Talc-Filled Biodegradable Bacterial Polyester Composite", Ind. Eng. Chem. Res.,Vol 45, Issue 22, pp. 7497–7503

- Wu, G., Wen, B. and Hou, S. (2004), "Preparation and structural study of polypropylene-talc gradient materials", Journal Polymer Int., Vol 53, pp. 749-755

- Wunderlich, B. (2005), "Thermal analysis. New York: Academic Press, pp. 400-402

- Xanthos, M. (2010),"Functional Fillers for Plastics",Wiley-VCH Verlag GmbH & co, page 35

- Yokouchi, M., Chatani, Y., Tadokoro, H., Teranishi, K. and Tani, H. (1973) "Structural studies of polyesters: 5. Molecular and crystal structures of optically active and racemic poly (β-hydroxybutyrate)", Journal of Polymer, Vol 14, Issue 6, Pp. 267–27

Chapter 4

Miscibility, crystallinity and mechanical properties of biodegradable blends of PHBV/PBS and its compatibilized blend by chain extender

4-1 Introduction

The evolution of polymer science has never been separated from experimenting with polymer blending. There has been a remarkable achievement in terms of developing significant new polymerization processes to manufacture both homopolymers and copolymers from the different monomers with variable and desirable properties. Since 1970, researchers have more tended to study a different approach by the modification of polymer properties by the blending of different polymers and additives. In fact, the process of copolymerization is very difficult for many pair of monomers. Therefore, the processing of the blending the polymer of these monomers has been considered by scientists in many researches.

Brown declared that polymer alloys are in fact, blends but not all the blends are alloy. Therefore a more precise definition for the polymer alloy would be, a blend of at least two immiscible polymers stabilized either by a chemical bond between the phases such as a covalent bond or ionic bond or by desirable intermolecular interaction, e.g., dipole-dipole, ion-dipole, charge-transfer, H-bonding, Van der waals forces, etc. (Brown, 2003)

4-2 Materials

The material chosen for the study was ENMAT^{TM} Y1000 is PHBV with 3 *mol%* of hydroxyvalerate (HV) content without any additive substances and supplied in white powder form manufactured by Tianan Biologic Material Co. (Ningbo, P. R.China). Bionolle™ 1020 series polybutylene succinate (PBS) -O-$(CH_2)_4$-O-CO-$(CH_2)_2$-CO, is purchased from Showa

Denko K.K. Japan with density of 1.26(g/cm^3) and melting point of 114 ℃ in pellet form. The Chain extenders are CESA®-extend an epoxy-functional styrene acrylic copolymers kindly provided by Clariant, Switzerland in masterbatch pellet form and Joncryl® ADR-4368 S, a styrene–acrylic multi-functional oligomeric chain extenders supplied by BASF Germany in powder form is an epoxy functionalized chain extender with high number average functionality (f_n >4) and epoxy equivalent rate = 285 g/mol.

PHBV

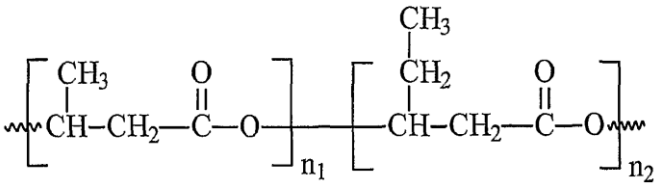

PBS

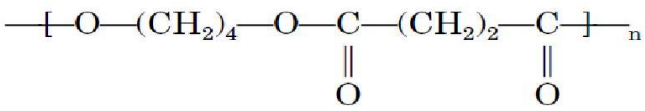

Chain Extender

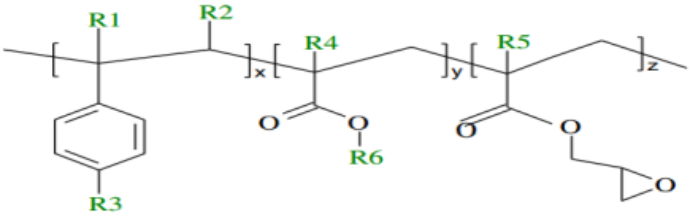

Figure 1-4 Chemical structure of PHBV, PBS and Chain Extender

(General structure of the Styrene–acrylic multi-functional oligomeric Chain extenders is shown at above. Where R1–R5 are H, CH3, a higher alkyl group, or combinations of them; R6 is an alkyl group, and x, y and z are each between 1 and 20).

4.2 Sample preparation

4.2.1 Preparation of the Blend

Before processing through an extruder, the PHBV in powder form and the pellets of PBS were first dried in a vacuum oven at a temperature of 60 ℃ for 24 hours to remove moisture. Drying of these polymers is vital as moisture in these polymers induces in hydrolytic chain

scission during the processing at high temperature. Chain extenders were used as they were received. All specimens of PHBV/PBS/Chain extender were prepared first by melt-compounding in a Betol co-rotating intermeshing twin-screw extruder (40 mm diameter, L/D =21/1, Amp=5-10) at 200 rpm. All the components were premixed in a plastic bag by manually tumbling for 5 mins and were fed simultaneously by a powder/pellet twin screw feeder with appropriate screw speed which was calibrated based on the screw speed and the actual material feed rate into the extruder to maintain the overall consistency. The extruder consisted of five barrel sections and each section was equipped with independently controllable electric heating and water cooling system. All extrusion variables, including barrel and die temperatures, and the extruder temperature profile is tabulated in Table 1-4:

Table 1-4 temperature profile of the extrusion process

Section	Zone6(Die)	Zone 5	Zone 4	Zone3	Zone2	Zone1
Temperature	164	169	165	170	160	155

Using a single strand die, the extrudate was cooled through a water bath and then pelletized for subsequent processing. A few of the batches were not possible to strand because of their high viscosity. These batches were collected from the die and then granulated using a S.U.I-Cumberland granulator. Four batches of PHBV/PBS with the weight ratios (w/w) of 100/0, 85/15, 70/30, 50/50 and six batches of PHBV/PBS/CE (two different chain extender, Joncryl and Cesa) with the weight ratios (w/w) of 85/15/2, 70/30/2 and 50/50/2 were prepared.

4.2.2 Injection moulding

The specimens for mechanical properties were obtained by injection moulding in a Demag NC III, 150 Tone, injection moulding machine. Table 2-4 shows the processing parameters used:

Table 2-4 injection molding parameters of PHBV and its talc composites

Conditions	first heating zone ℃	second heating zone ℃	third heating zone ℃	Fourth heating zone ℃	Nozzle heating ℃	Injection pressure bar	Injection time sec	Cooling time sec	Cycle time sec	Mould temperature ℃	Injection speed
dumbbell	160	160	160	160	160	160	4	40	62.5	30	low
Plate	150	150	155	155	155	160	4	60	82.5	30	Medium

All the processing parameters were modified during several trial mouldings in order to obtain the optimum conditions. It should be noted that there was an issue in the processing of the PHBV each time, when it remained slightly more than previous ones in barrel or in the middle of the processing time. For instance after around the first 15 numbered tensile bars and approximately after the first 8 plates, specimens were no longer uniform and they would start to shrink inside the mould after which many times it would end up with damaged specimens at the edges or would stick in the mould and wouldn't release immediately after the mould unclamped. The reason behind that was not clear but it might be through thermal degradation or narrow windows process ability of PHBV. Therefore the smallest injection moulders (shorter barrel's length) could reduce the residence time inside heating zones.

4.3 Experimental

4.3.1 Differential Scanning Colorimetry

The melting temperatures T_m of the specimens were measured by a TA Instruments DSC/Q2000 with a Universal Analysis 2000. The external block measurements were carried out under a nitrogen atmosphere to minimize oxidative degradation. The specimens were encapsulated in DSC aluminium zero pans and then introduced into the closed calorimeter cell. The instrument was calibrated with indium prior to starting the test.

4.3.1.1 Non-isothermal crystallization

The samples of PHBV/PBS and PHBV/PBS/CE were first heated to 200 ℃ at a heating rate of 10 ℃/min and isothermally held for 5 min to eliminate any thermal history. The samples were then cooled at the same heating rate of 10 ℃/min to -20 ℃ and then again heated to 200 ℃ with same heating rate for obtaining the second heating cycle.

4.3.1.2 Isothermal crystallization

PHBV/PBS samples with three different weight fractions of the 85/15, 70/30, 50/50 were heated up to about 200 ℃ approximately 30 ℃ above the melting point, and held isothermally for 5 minutes to eliminate any thermal history. The sample was then rapidly cooled down at the rate of 50 ℃/min to the pre-determined isothermal temperature and kept until crystallization was completed. The procedure were repeated for the three pre-determined temperatures of 100 °, 110 °and 120 °C for each of the compounds.

4.3.2 Thermogravimetric Analysis (TGA)

The thermal stability of the PHBV/PBS and PHBV/PBS/CE and the process of thermal decomposition were investigated by Thermogravimetric analysis (TGA) using a TA instrument “The New Discovery TGA”, with TRIOS software version 3.3.0.4055 under nitrogen atmosphere. The temperature range was from room temperature to 650 ℃ with a heating rate of 10 ℃/min.

4.3.3 Dynamic Mechanical Analysis (DMA)

Dynamic Mechanical analysis (DMA) was performed using a DMA Q800, TA, USA. The accurately prepared rectangular samples 127x12x4 mm were cooled to -50 ℃ and then heated up to 150 ℃, with heating rate of 2 ℃/min, under a maximum force of 1 N, a frequency of 1 Hz and an amplitude of 5 μm using the single cantilever system.
Multi frequency DMA tests were performed with samples having similar dimension and test conditions as above, but at five set frequency of 5Hz, 7.9 Hz, 12.6 Hz, 19.8 Hz and 20 Hz.

4.3.4 Fourier Transform Infrared Spectroscopy (FTIR)

The PHBV extruded pellet, the PBS pellet and Joncryl powder were first scanned with 1, 5, 10, 50 and 100 scans on a Shimadzu Fourier Transform Infrared (FTIR) spectrometer FTIR-8400S, using a Specac Quest Single Reflection ATR accessory, consisting on a Diamond crystal at a fixed angle of 45 °. The spectra were collected over the 4000 cm^{-1} to 400cm^{-1} wavenumber range, at a resolution of 4 cm^{-1}. As there were no significant differences in the spectrums of 10, 50 and 100 scans just big resolution, the number of accumulations for the FTIR experiment was set at 10 for rest of the sample analysis.

4.3.5 Mechanical properties

Tensile tests were performed with an Instron testing machine (model 3366) according to ASTM D 638 standard for tensile testing. A 10 KN load cell was used with a crosshead speed of 5 mm/min. At least five samples were tested for each reported value.

4.3.6 Impact properties

There are several methods for measuring the impact behaviour of polymers, such as Charpy and Izod impact test (notched and un-notched) and Gardner drop-ball or drop-weight test. In order to investigate the impact properties with the energy rate higher than the maximum pendulum performance, and more accurate results, the drop weight impact test was used.
The PHBV/PBS and PHBV/PBS/CE blends were injection moulded into rectangular 150x150x4 mm plates according to BS EN ISO 6603 (The British Standard for determination of puncture impact behaviour of rigid plastic) using the conditions given in table 2. The injection moulded plates were then cut into 60x60 mm squares and labelled for impact testing. The impact conditions of the test were set according to the BS EN, ISO 6603 drop weight method. A CEAST Fractovis Plus impact tester Model 7520 was used.

4.3.7 Morphology with SEM

The morphologies of PHBV/PBS and PHBV/PBS/CE were analysed using a scanning electron microscope. A SUPRA ZEISS 35VP with 20KV accelerating voltages and SE detector was used. The scanning electron microscopy of fractured samples of tensile test was conducted at room temperature. The specimens were fixed in epoxy resin and several times polished to get the best smooth surfaces. The specimens were then gold coated.

Result and discussion

4.4 Thermal properties

4.4.1 Non-isothermal crystallization

Non-isothermal second heating cycles of DSC results for PHBV and PBS and their non-reactive and reactive blends in different concentration are illustrated in Figure 2-4

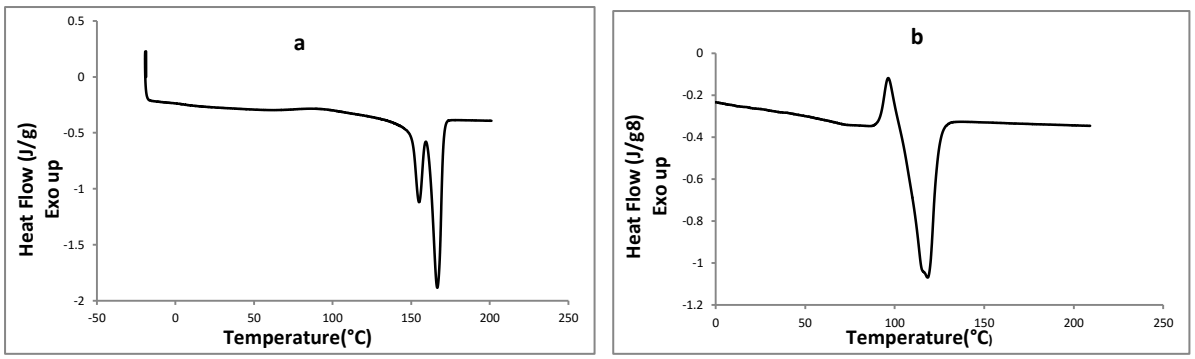

Figure 2-4 The second heating scan of non-isothermal DSC graphs for the neat PHBV (a) & PBS (b)

Figure 2-4a shows the double melting point of PHBV at about 154 and 166 ℃ and Figure 2-4b shows a cold crystallization exothermic peak at 95 ℃ prior to the melting of the PBS at 115 ℃.

Belfiore stated that the strong interaction between uncompatible polymers in a semi-crystalline polymer blend are:

- Decrease in the Gibbs free energy change for crystal formation when hydrogen bond strength increases
- Appearance of the several sequential melting events prior to main transition temperature

When two semi-crystalline polymers exhibit miscibility, that requires exothermic energetic interaction in molten state for two big molecular chains. Melting point depression of the semi-crystalline polymer then will occur as an outcome of the compatibilization in molten state, because of specific interaction such as hydrogen bonding, ionic attarctions of charged functional groups, or metal complexation. If the energetic interaction in the molten state is endothermic and unfavorable, then the blend is immisible (Belfiore, 2010). However, Rim, Runt and Howe argued that the compatibilization might consequences on elevation of melting point for one of the components through increasing of lamellar thicknesses and thermodynamics effects (Rim, Runt and Howe, 1984).

Figure 3-4 shows for the PHBV/PBS blends, heat conversion of the PHBV double melting point is depressed by increasing the concentration of PBS from 15% to 50%, which could be caused by the reduction of the PHBV amount in the blends. Figure 3-4a shows the second heating of the three samples of PHBV/PBS with 85/15, 70/30, 50/50 weight fractions. All of the blends gave two melting points. The higher T_m corresponds to the PHBV, while the lower T_m corresponds to the PBS in the blends. On the other hand, figures 3-4 b, c, and d show that with the presence of the chain extenders, the PHBV melting point is elevated of approximately 6 degree centigrade.

The phenomena could be stated as an altering of the miscibility of the blend by the presence of a chain extender which is more significant in blend containing Joncryl Chain Extender (for Cesa was about 2 ℃ but for Joncryl was about around 6 ℃).

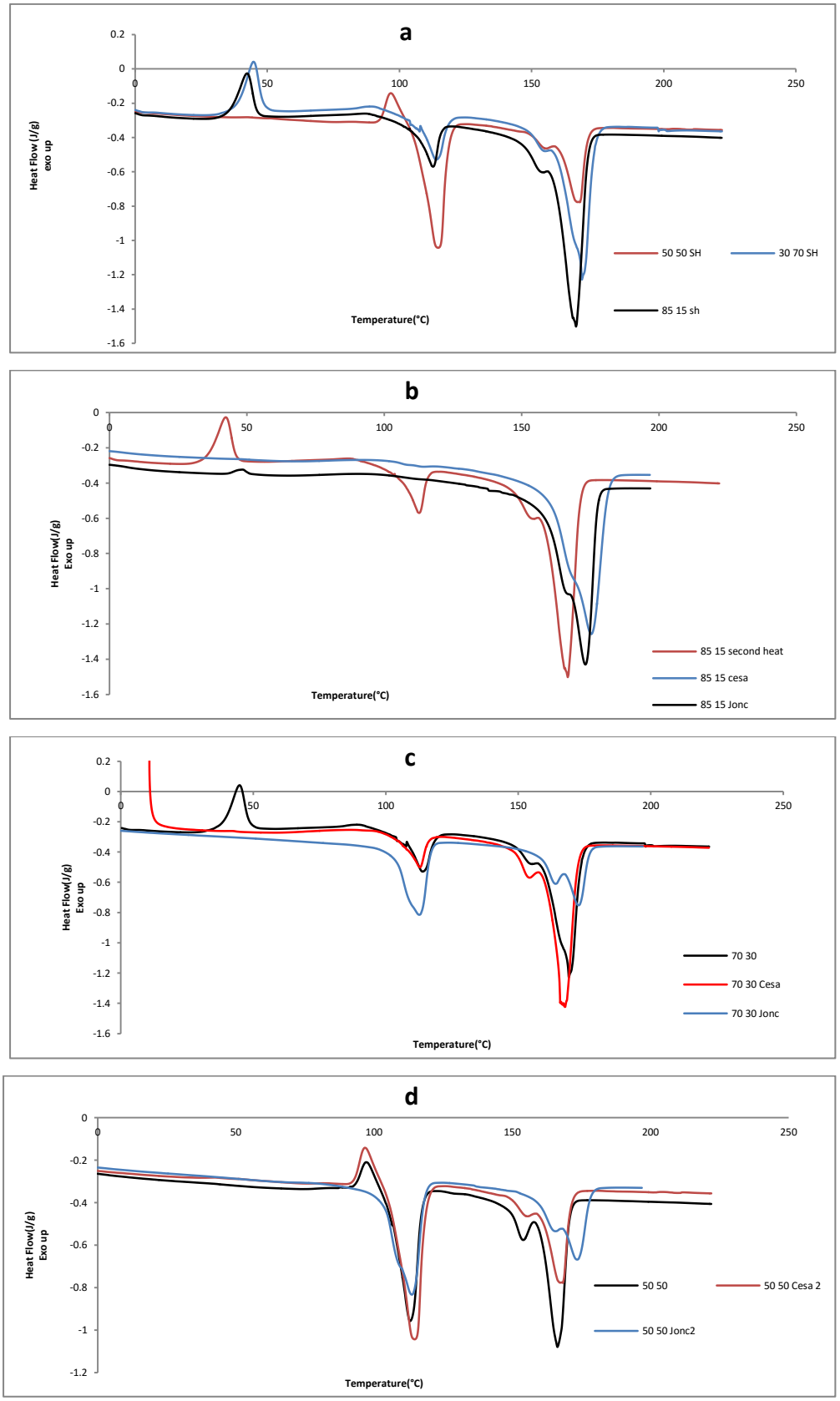

Figure 3-4 The second heating scan of non-isothermal DSC graphs for PHBV/PBS Blends in (a) three(85/15, 70/30 & 50/50) concentrations and (b, c, d)PHBV/PBS reactive blends with 2% Chain Extender (Joncryl) in powder from and Cesa-Extend in Masterbatch form)

The depression or elevation of the melting point in semi-crystalline polymer blends can be considered as enhancement of the miscibility between the two polymers. A completely immiscible blend usually does not show a depression or elevation of the melting point (T_m), while it could be significantly depressed for a miscible blend and slightly depressed or elevated for a partially miscible blend (Qui, Ikehara and Nishi, 2003).

In Figure 3-4b, the second heating scan for the blends with chain extenders show just an exothermic peak around the melting point of the neat PHBV in the blend. The cold crystallization peak disappeared, but for PHBV/PBS 70/30 and 50/50 samples (Figure 3-4c and 3-4d). The presence of the chain extender slightly elevated the melting point of PHBV for both compounds which is more significant for the blend of 50/50/Joncryl.

According to Shan, for the pure PHBV, the low homogeneous nucleation rate would prevent the polymer from crystalizing completely within the cooling process. The formed crystals with less perfection are prone to experience the melting and recrystallization process during the subsequent DSC heating to generate crystals with a higher thermodynamic stability. Thus, the low- and high-temperature melting peaks of pure PHBV shown in Fig 3-4 are probably ascribed to the melting of original crystals formed during melt moulding process and the formation of new crystals generated during DSC heating process. According to Verhoogt, Ramsay and Favis, the presence of two (or more) melting transitions for PHBV may be due to the crystal thickening and/or recrystallization, which occurred during the heating in the DSC (Verhoogt, Ramsay and Favis, 1994).

Rim and Runt also mentioned that the process of the reorganization of the chains was associated with some type of lamellar thickening mechanism. Therefore, if a polymer is subjected to reorganization upon heating, it is recommended to perform the thermal analysis at a variety of heating rates and observe the melting point. It also has been declared that for polymers that shows a single melting endotherm but whose behaviour is complicated by lamellar thickening, increasing the heating rate will decrease the observed T_m, because the chains haven't had enough time to recrystallize (Rim and Runt, 1982). The DSC curves of some polymers have been shown to exhibit multiple (usually dual) melting endotherms. Their melting point shows an exothermic peak in between which are often accepted to be the result

of melting, followed by recrystallization and again a final melting. However, if the higher melting endotherm peak is associated with the melting of reorganized material, one would expect the magnitude of this endotherm to decrease with increasing the heating rate (Rim and Runt, 1982).

The non-isothermal second cooling cycles of the DSC tests for PHBV and PBS and their non-reactive and reactive blends in different concentration are illustrated in Figures 4-4a to 4-4c:

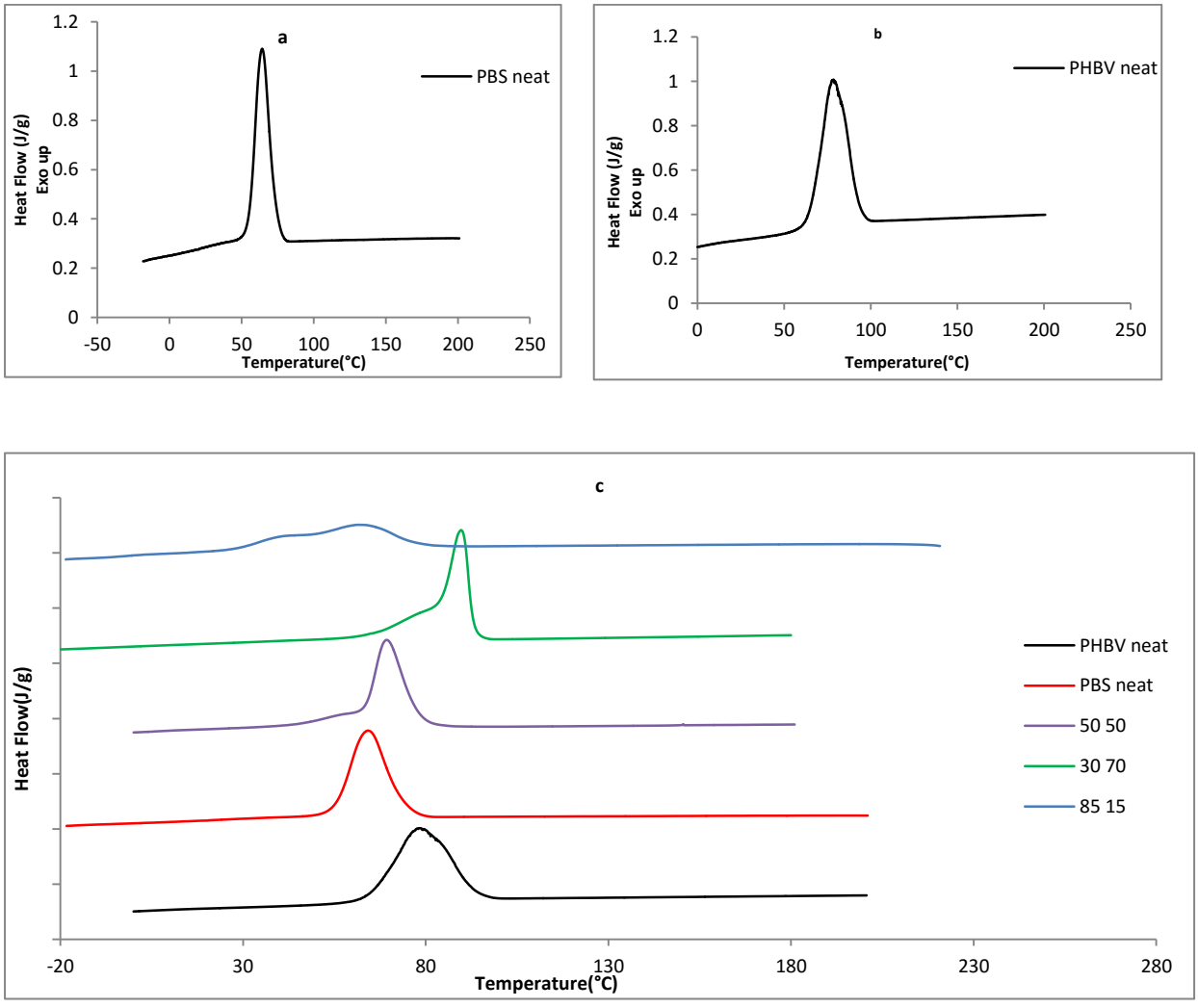

Figure 4-4 The first cooling cycle of DSC curve for PHBV & PBS neat and their blends with different concentrations

As shown in Figure 4-4, the crystalization of PHBV in the cooling scan occurred prior to the crystalization of PBS. For PHBV85-PBS15, the intensity of the peak is reduced and is moved to a

lower temperature than the neat PHBV. The initial crystalization temperature for the PHBV50/PBS50 is similar to the PHBV85-PBS15 compound. However, the PHBV70/PBS30 doesn't show any changes and initial crystalization temperature is same as the PHBV initial crystalization temperature.

Tables 3-4 & 4-4 show the following parameters of the melting points, T_m (℃); enthalpy of melting, ΔHm (J/g) ; crystallization and cold-crystallization temperatures T_c & T_{cc} ; enthalpy of crystallization and cold crystallization ΔH_c & ΔH_{cc} ; crystallinity percentage *X*(%):

Table 3-4 parameters of the melting points T_{m1} & T_{m2} (℃), enthalpy of the two melting point $\Delta H_{m1\&2}$ (J/g), and crystallization and cold-crystallization temperature T_c & T_{cc} and enthalpy of crystallization and cold crystallization ΔH_c & ΔH_{cc} as well as percentage of crystallinity X(%) for PHBV/PBS blends

Samples	Tm_1 ℃	Tm_2 ℃	ΔHm_1 J/g	ΔHm_2 J/g	T_c ℃	ΔH_c J/g	T_{cc} ℃	ΔH_{cc} J/g	X_{PBS} %	X_{PHBV} %
PHBV/PBS(100/0)		166		85	77	73				58.7
PHBV/PBS(85/15)	112	166	11	65	61	48	42	10	5.5	52.47
PHBV/PBS(70/30)	114	169	21	43	89	42	44	12	29.8	43.6
PHBV/PBS(50/50)	114	166	37	24	70	58	97	6	57.28	33.1
PHBV/PBS(0/100)	117		58		63	60	95	8	46.06	

X%=percentage of crystallinity is calculated from Equation 1-4:

Equation 1-4) $$\mathbf{X\% = \frac{(\Delta Hm - \Delta Hcc)}{Wm * \Delta Hm^{\circ}} \times 100}$$

where ΔH_m (J/g) = enthalpy of melting, W_m= weight fraction of the polymer in the compound, and ΔH_{cc} = cold crystallization

ΔH_m°; melting enthalpy of 100% crystalline=146.14 J/g for PHBV and 110.32 J/g for PBS. (Liu, Zhu, Chen, 2010, Correlo et al, 2009).

Table 4-4 parameters of the melting points T_{m1} & T_{m2} (℃), enthalpy of the two melting $\Delta H_{m1\&2}$ (J/g) and crystallization and cold-crystallization temperature T_c & T_{cc} and enthalpy of crystallization and cold crystallization ΔH_c & ΔH_{cc} as well as percentage of crystallinity X(%) for PHBV/PBS/Chain Extender blends

Samples	Tm_1 ℃	Tm_2 ℃	ΔHm_1 J/g	ΔHm_2 J/g	T_c ℃	ΔH_c J/g	T_{cc} ℃	ΔH_{cc} J/g	X_{PBS} %	X_{PHBV} %
PHBV/PBS/Cesa (85/15/2)		162		82	80	58				67.98
PHBV/PBS/Jonc (85/15/2)		163		82	79	54				67.33
PHBV/PBS/Cesa (69/29/2)	112	167	14	25	66	56			43.8	26.77
PHBV/PBS/Jonc (69/29/2)	113	172	21	29	89	58			62.24	29.6
PHBV/PBS/Cesa (49/49/2)	112	166	27	39	72	58	96	5	40.75	54.42
PHBV/PBS/Jonc (49/49/2)	114	174	35	26	90	61			64.6	36.3

Finding a distinguishable T_g for PHBV from the DSC graphs of the blends was difficult. A similar observation was also reported by Zhang, Xiong and Deng in a study of PHB, the attribute could be explained by very fast crystallization and also by the fact that the amorphous areas do not present enough mobility to characterize the T_g (Zhang, Xiong and Deng, 1995). All the melting data and enthalpy of fusion ΔH_f in Table 3-4 & 4-4 are chosen from the second heating run. It also may be mentioned that according to lannace et al for the first heating, the polymer chains were basically organized in a random form and they reached the crystallization temperature (T_c) quickly. However, in the second heating the crystallization enthalpy (ΔH_c) increased, due to some crystals forming during the cooling, which requests great energy for crystallization (Iannace et al, 1994).

Table 3-4 shows that the addition of PBS decreases the crystallinity of PHBV. The crystallinity of the PBS increases from 5.5% for the blend PHBV85/PBS15 to 29.8% for

PHBV70/PBS30 and to 57.28 % for PHBV50/PBS50, while the PBS100 is 46% crystalline. As expected, if the composition of one polymer in the blend was decreased, its crystallization and melting enthalpy decreased and almost disappeared when its composition was very small. However, the crystallinity of PBS increased from 46.06% to 57.28% with a decrease in the concentration from 100% to 50%.

Table 4-4 shows for PHBV/PBS 85/15 containing the chain extender, the lower melting point disappeared and the compounds showed a single melting point with a shoulder, and the percentage crystallinity is close to PHBV neat. In the 70/30/2 compounds, the presence of the chain extender didn't significantly change the two melting temperatures. However, the percentage crystallinity of the PBS changed in the blend with a chain extender, being more significant a blend with Joncryl. On the other hand, the PHBV crystallinity was reduced in the presence of the chain extenders. For the 50/50 compound, the PHBV crystallinity increased by almost 20 percent for the Cesa specimen but it changed slightly in the blend that contained Joncryl. In contrast, the PBS crystallinity decreased by almost 17% for Cesa specimen while it increased by approximately 7% for the Joncryl blend.

4.4.2 Isothermal crystallization

The isothermal crystallization behaviour of PHBV with different concentrations of PBS was studied by DSC and was analysed by the well-known Avrami equation. The study materials of PHBV and PBS were both semi-crystalline biodegradable polyesters, with the PHBV being the higher melting point component. The Avrami equation describing the development of the relative degree of crystallinity with the crystallization time t is:

Equation 2-4) $$\mathbf{1-X_{rel}= \exp\left(-kt^{n}\right)}$$

(Avrami, 1939, 1940, 1941)

The exponent n in formula 2 is considered by researchers to indicate the type of nucleation and dimensionality of crystal growth and *k* is a composite rate constant. In homogeneous

nucleation, n = 2 and theoretically means 1-dimensional (1D) growth, n =3 is 2D growth, and n = 4 is 3D growth. In heterogeneous nucleation, n = 1 means 1D growth, n =2 is 2D growth, and n= 3 is 3D growth.

In fact, nucleation and crystal growth are more complicated for the composites, because the filler can play the role of a nucleation agent or limit the normal crystal growth in certain areas. Thus, the Avrami exponents of composites should be thought of as complicated values in two component composites (Ohkita and Lee, 2004).

According to Kumar, in the Avrami equation the temperature dependence is incorporated in the rate constant of k. On the other hand, n is obtained by sum of $p+q$, where p would be 0 or 1 depending on the performing predetermined temperature or sporadic nucleation and q would be 1, 2 or 3 depending on the shape of the crystal growth. Therefore, for homogenous nucleation, n would equal 3 for disk like crystal growth but it would be 2 for heterogeneous nucleation (Kumar and Gupta, 1997, Exner, Perez and Kasteva, 2016).

4.4.2.1 Avrami results for the PBS/PHBV blend

Figure 5-4 shows DSC curves of the isothermal crystallization at the three pre-determined temperatures of 100, 110 and 120 ° C for the three different concentrations of PHBV/PBS (85/15, 70/30, 50/50).

The results clearly show that the process is temperature dependent and the rate of the crystallization is slower at the higher temperature. Blending PBS with PHBV also decreases the crystallization rate of PHBV in compound. Basically, when a semi-crystalline polymer crystalizes in a cooling process, the lamella organize from a primary nucleus to grow radially to form spherulites.

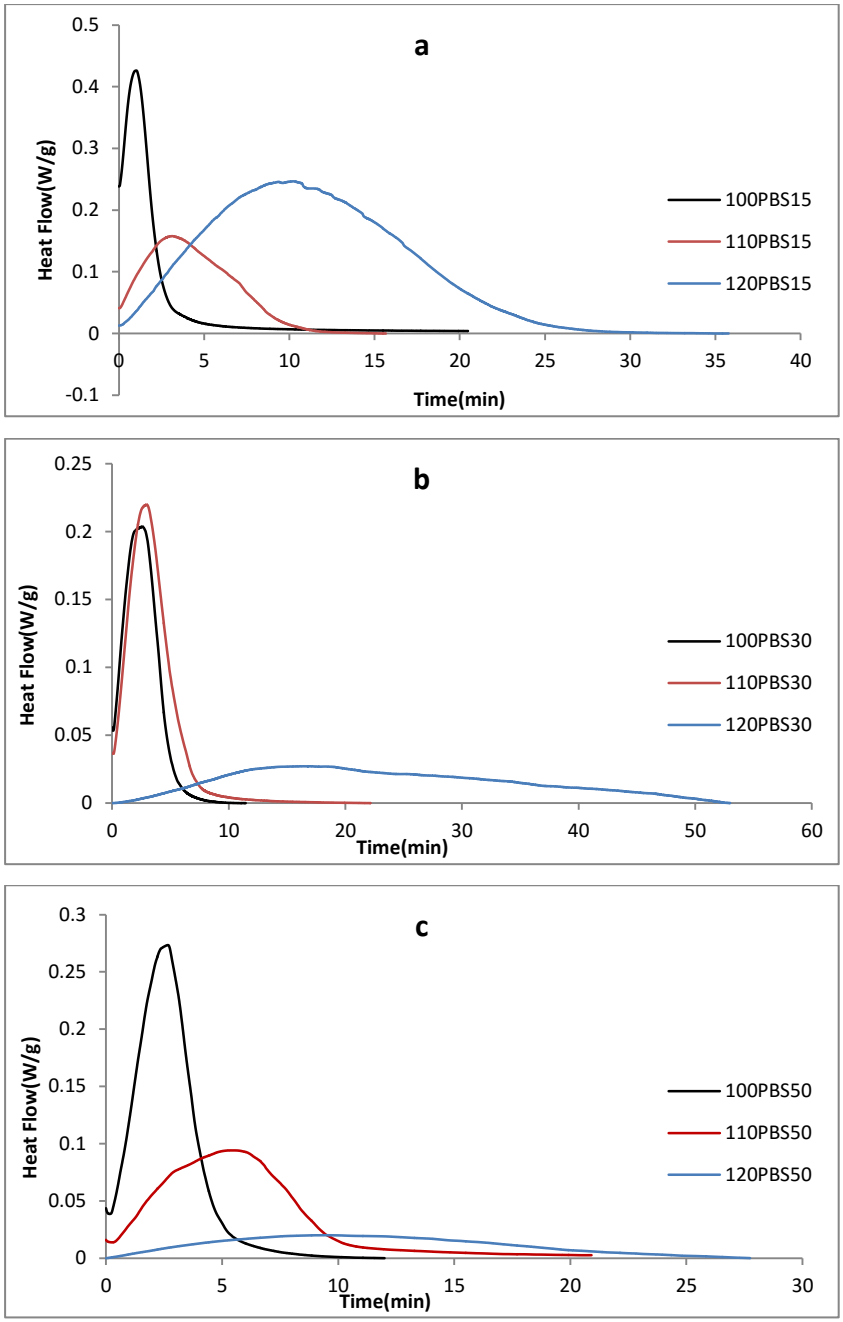

Figure 5-4 DSC curves of PHBV/PBS blends (a) 85/15,(b)70/30,(c) 50/50 respectively in pre-determined isothermal crystallization temperature at 100 °, 110 °, and 120 °C

The spherulites continue to grow until they impinge another spherulite which retards the growth and eventually stops it. The Avrami equation in fact is based on the impingement of crystals, which in nucleation process, the spherulites impinge and ultimately the

crystallization process stops (Wunderlich, 1973). Thus, the crystallization rate of PHBV could be reduced because they impinged with PBS crystals in compounds.
The area under the curve of each crystallization graph shows the relative crystallinity and it is plotted vs time in Figure 6-4.

Figure 6-4 shows the relative crystallinity of PHBV/PBS blends at the three different concentrations and the three set crystallization temperatures vs time. It is clear that the time to 100% crystallization (the 100% crystallization of crystalline part of PHBV) is temperature dependent for all specimens. In Figure 6-4a, $t_{0.5}$ (the half-crystallization time) at 100 ° C is smaller than t0.5 at 110 ° C but the crystallization time was shown to be longer at 100 ° C than 110 ° C. It could be explained that at the lower temperature, PBS also started to crystalize and it would be hindered the rate of PHBV crystallization in the compound due to PBS, PHBV crystal impingements.

The values of Avrami exponent n and crystallization rate constants k are obtained from the plots of log (-ln (1 –Xrel)) vs log (t) in Figure 7 and are listed in Table 5-4.

However, it should be considered that the Avrami equation is only applicable to the linear part of the graph because it is based on many assumptions such as linear crystal growth, primary nucleation, constant volume, and so forth. It is usually valid at low conversions. Therefore, in this study the n and k were calculated from the initial linear segment of the Avrami's plots.

Table 5-4 shows that the value of the Avrami exponent *n* for each specific isothermal crystallization temperature hasn't change significantly. It means the mechanism of crystallization didn't change with presence of PBS. The value of *n* at higher isothermal temperature is different than lower temperature. It indicates that *n* is temperature dependent.

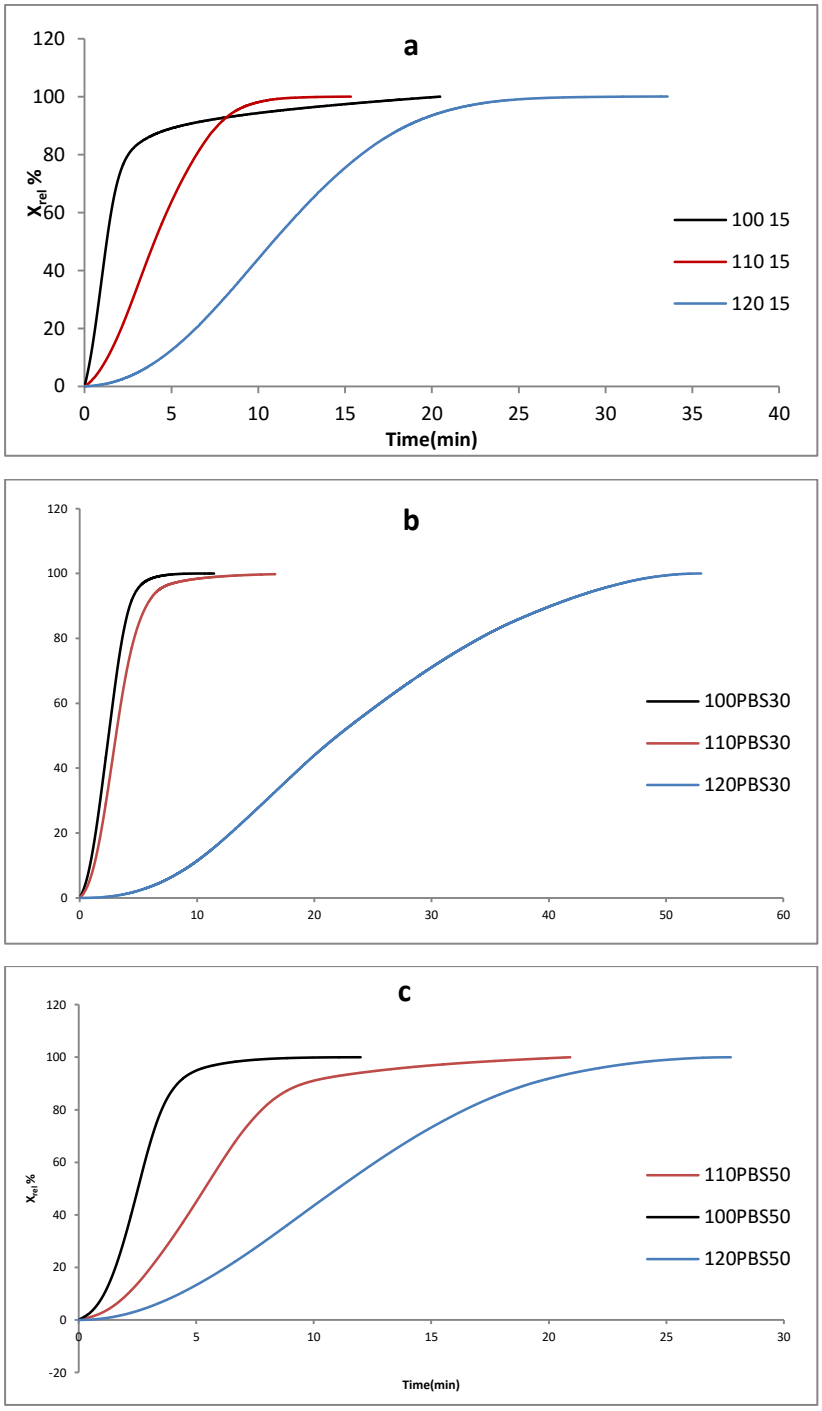

Figure 6-4 Development of relative crystallinity X_{rel} with the PHBV crystallization time (t) at the set isothermal crystallization temperature of 100 °, 110 °, and 120 ° C for a) 85/15,b) 70/30,c) 50/50 PHBV/PBS blends

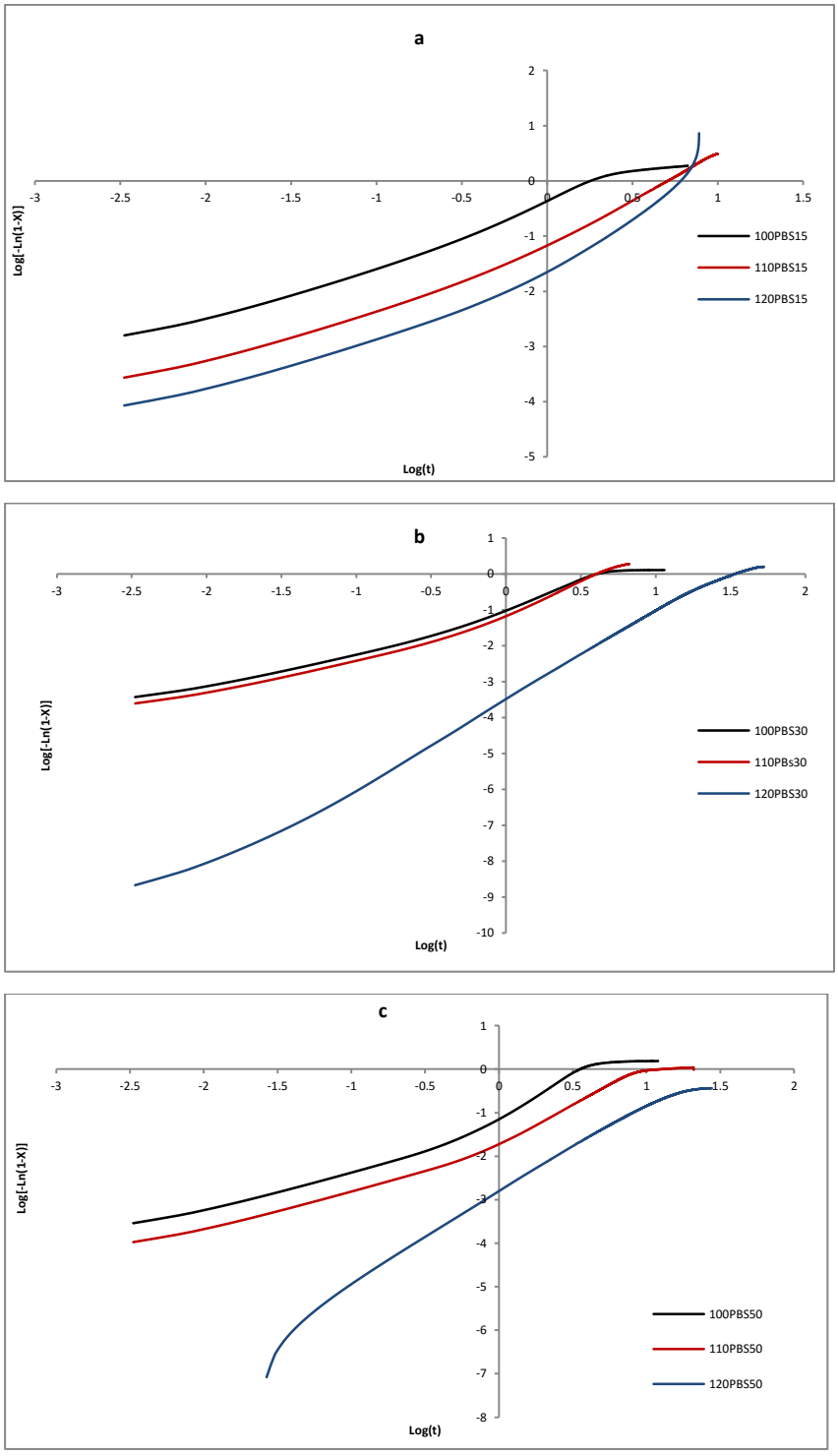

Figure 7-4 The related Avrami plots of PHBV crystallization

Table 5-4 The Avrami exponent (n), crystallization rate constant (*k*) and half-time crystallization ($t_{1/2}$), at different pre-determined crystallization temperature of 100, 110 and 120 °C

80/15	Temperature	*n*	*k* (min^{-1})	$t_{0.5}$ (min)
	100	1.2	0.39	1.6
	110	1.53	0.08	3.5
	120	2.06	0.009	6.6
70/30				
	100	1.32	0.11	3.43
	110	1.61	0.09	4.00
	120	2.14	0.005	28.5
50/50				
	100	1.41	0.11	3.50
	110	1.52	0.028	8.35
	120	2.09	0.002	29.4

When the PBS concentration increases the amount of *n* just slightly changes. However, it should be considered that, the nucleation and crystal growth are more complicated for blends, because the PBS in the molten form can limit the normal crystal growth at impinged spots. Table 5 shows that amount of *n* varies between $1<n<2$ and $2<n<3$ at different temperatures and it corresponds to the rod like shape and the disc like shape of crystal growth (Wunderlich, 2005).

It is widely accepted by researchers that the value of *n* is dependent on the nucleation mechanism and geometry of the crystal growth (Avrami, 1939. 1940, 1941). According to Peng et al, $n=3$ corresponds to two kinds of possible crystallization mechanisms. One is three-dimensional growth and instantaneous nucleation; the other is two-dimensional growth and homogeneous nucleation. It is widely accepted that PHBV exhibits a homogeneous nucleation. So, even for the obtained value of n=3 for PHBV, the crystallization mode of two-dimensional circular growth has been observed by polarized microscopy and the spherulite growth does not completely obey 3D the spherulitic propagation (Peng et al, 2003). Kumar mentioned that, for homogenous nucleation, *n* would equal to 3 for the disk like crystal growth but it would be 2 for heterogeneous nucleation (Kumar and Gupta, 1997).

Therefore, the crystallization of PHBV could have gone from a rod-like homogeneous nucleation to a complicated disk-like heterogeneous nucleation caused by crystal impingement in which PBS crystals act as a nucleation surface.

The value of the *k* in Avramis equation decreases in each compound with an increase in the crystallization temperature while the value of $t_{0.5}$ (half-time crystallization) increases with an increase of the crystallization temperature.

When the concentration of PBS increases in the compound, the value of $t_{0.5}$ also increases. This means that the presence of PBS retards the rate of crystallization of the PHBV inside the compounds.

4.4.3 Thermogravimetric Analysis (TGA)

Thermogravimetric analysis (TGA) was used to determine the thermal stability and decomposition of the PHBV/PBS compounds, with and without chain extender. The thermal stability of the investigated samples was determined by the value of T_{i1}, the initial decomposition temperature and T_1^{max}, the temperature of the maximum rate of decomposition. T_{i2} is the initial decomposition temperature of the more thermally stable polymer in the compounds and T_2^{max} is the temperature of the maximum rate of decomposition for the more thermally stable polymer in the compounds. The residue weight of specimens at 600 ℃ was also recorded. The derivative of the weight loss curve was used to determine the point at which the weight loss was the highest and also the thermal range at which the decomposition occurs.

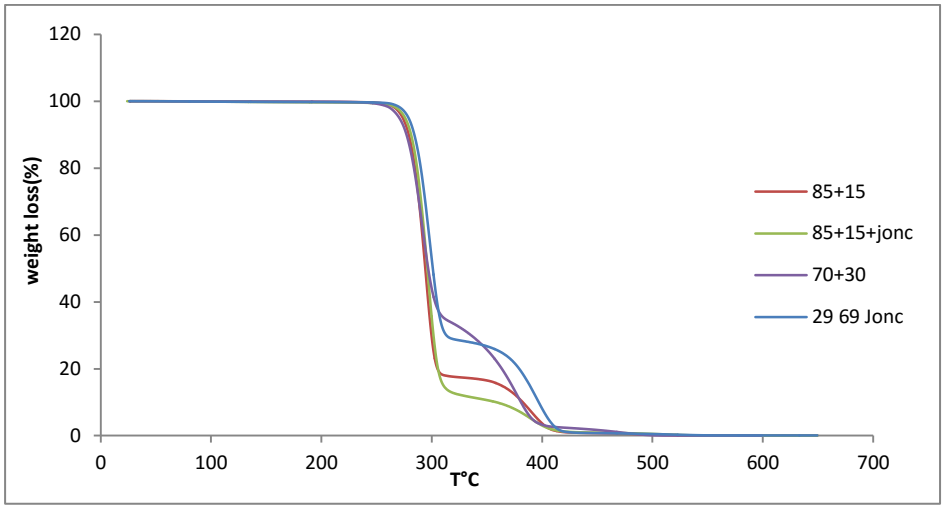

Figure 8-4 Thermal Gravimetric Analysis (TGA) for PHBV/PBS and PHBV/PBS/CE

The TGA curves of the PHBV and PBS blends in the two concentrations of 85/15 and 70/30 and in presence of the two chain extenders are given in Figure 8-4. The graphs show that the thermal degradation took place in two steps between 265-575 ℃, approximately. It can be seen the presence of the chain extender didn't increase the initial decomposition temperature, T_{i1} and T_{i2} significantly. However, the residue of the material at the end of each of the decomposition steps, T_1^{max} & T_2^{max} is different for both batches with more material decomposed at the first step of degradation in presence of a chain extender.

Figure 9-4 shows the effect of the chain extender on the thermal stability of the compounds at concentration of 50/50.

Figure 9-4a shows that the degradation of both polymers in the compound with joncryl is improved compared to the compound without the chain extender. It is clear that the thermogram curve shifted to a higher temperature with the presence of the CE.

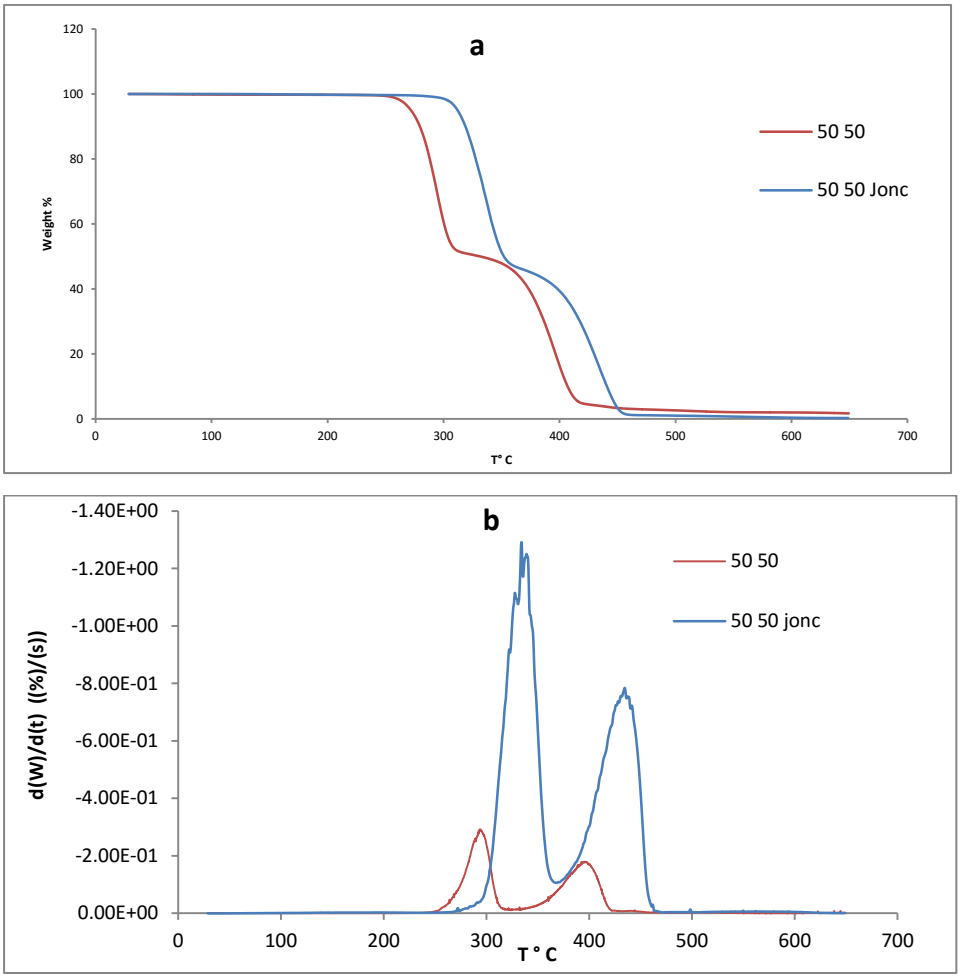

Figure 9-4 TGA & DTG graphs of PHBV/PBS 50/50 and PHBV/PBS/Chain Extenders 49/49/2

In Table 6-4, the values of thermal decomposition are shown with mass loss (%). It can be seen that, the presence of chain extender in 50/50 compounds, significantly improved the degradation temperatures by almost 40 ℃. The phenomena could be explained that the oligomer (Joncryl) acts as a chain extender and repairs the degraded chains by forming a branch copolymer. This is attributed to rebuilding the chains of degraded PHBV or PBS by introducing the CE.

In the DTG graph shown in Figure 9-4, the weight loss of PHBV50/PBS50 happened with a two-step process between 240 and 445 ℃ and the maximum rate of mass loss for each polymer is distinguishable by a single peak. The residue at 600 ℃ (%) could be taken as the amount of ash in the compounds. It should be considered at 600 ℃ just less than 0.3 % weight fraction of the PHBV residue existed in the compounds indicating that the addition of CE has

no effect on the thermal stability of PHBV/PBS at very high temperatures. It is clearly shows in table 6-4 that no obvious change of the weight residue at a high temperature was observed with the presence of CE in compounds.

A similar improvement has been reported by Pilla et al stating that the chain extender Cesa-extend increased the thermal stability of PLA (Pilla et al, 2009).

Table 6-4 The value of T_{i1}, the initial decomposition temperature and T_1^{max}, the temperature of the maximum rate of decomposition for the less thermally stable polymer in the compounds, T_{i2}, the initial decomposition temperature of the more thermally stable polymer in the compounds and T_2^{max}, the temperature of the maximum rate of decomposition for the more thermally stable polymer in the compounds, Δm_1 =Mass loss in T_{i1}(%), Δm_2 =Mass loss in T_{i2}(%) and the residue of specimens at 600 °for PHBV/PBS and PHBV/PBS/CE

Sample	T_{i1} ℃	T_1^{max} ℃	Δ_{m1}	T_{i2} ℃	T_2^{max} ℃	Δ_{m2}	Residue (%) at 600 ℃
PHBV/PBS 100/0	283.1	290.5	98.4	------	------	------	0.06237
PHBV/PBS 85/15	280.9	306.9	82.4	307	417.1	1.16	0.31
PHBV/PBS 70/30	283.1	310.1	61.6	311	419.3	98.67	0.27
PHBV/PBS 50/50	276.4	312.6	48.4	313	422.6	95.44	0.20
PHBV/PBS /Jonc 84/14/2	282.8	311.4	14.6	312	423.0	99.01	0.20
PHBV/PBS /Jonc 29/69/2	284.0	314.5	70.4	315	417.7	98.69	0.30
PHBV/PBS /Jonc 49/49/2	313.9	356.8	52.1	357	475.8	98.91	0.52

4.5 Thermomechanical Properties

4.5.1 Dynamic Mechanical Analysis (DMA)

Observing the Miscibility of the blends by changes in the T_g by single frequency DMA

The specimens of PHBV/PBS blends in different concentrations and their blends with chain extender were examined by the single cantilever DMA test. The storage modulus and the loss modulus of each specimen along with the graph of tan δ were obtained. The glass transition temperatures correspond to the highest point (peak) of the tan δ graph.

The glass transition temperatures of the neat PHBV and the PBS were obtained and are used as reference (Figure 10-4).

Figure 10-4 shows the DMA result of the PBS and PHBV neat at a frequency of 1 Hz. The glass transition temperatures can be obtained from the storage and loss moduli or from the tanδ curves. Researches widely tend to report the highest point (peak) of tanδ as a single temperature for the glass transition temperature. From Figure 10 the glass transition temperature of PHBV is 27.92 ℃ and PBS is -13.65 ℃.

The DMA results in Figure 11-4 show that all the PHBV/PBS specimens have two distinctive Tg s, which indicates the immiscibility of PHBV/PBS in blends. Qui, Ikehara and Nishi, also reported evaluating the miscibility of PHB/PBS blends with ratio from 80/20 to 20/80 by using DSC. It has been stated that “Experimental results indicated that PHB showed some limited miscibility with PBS for a PHB/PBS 20/80 blend as evidenced by a small change in the glass transition temperature and the depression of the equilibrium melting point of the higher melting point component PHB. However, PHB showed immiscibility with PBS for the other three blends as shown by the existence of an unchanged composition independent glass transition temperature and the biphasic melt” (Qui, Ikehara and Nishi, 2003)

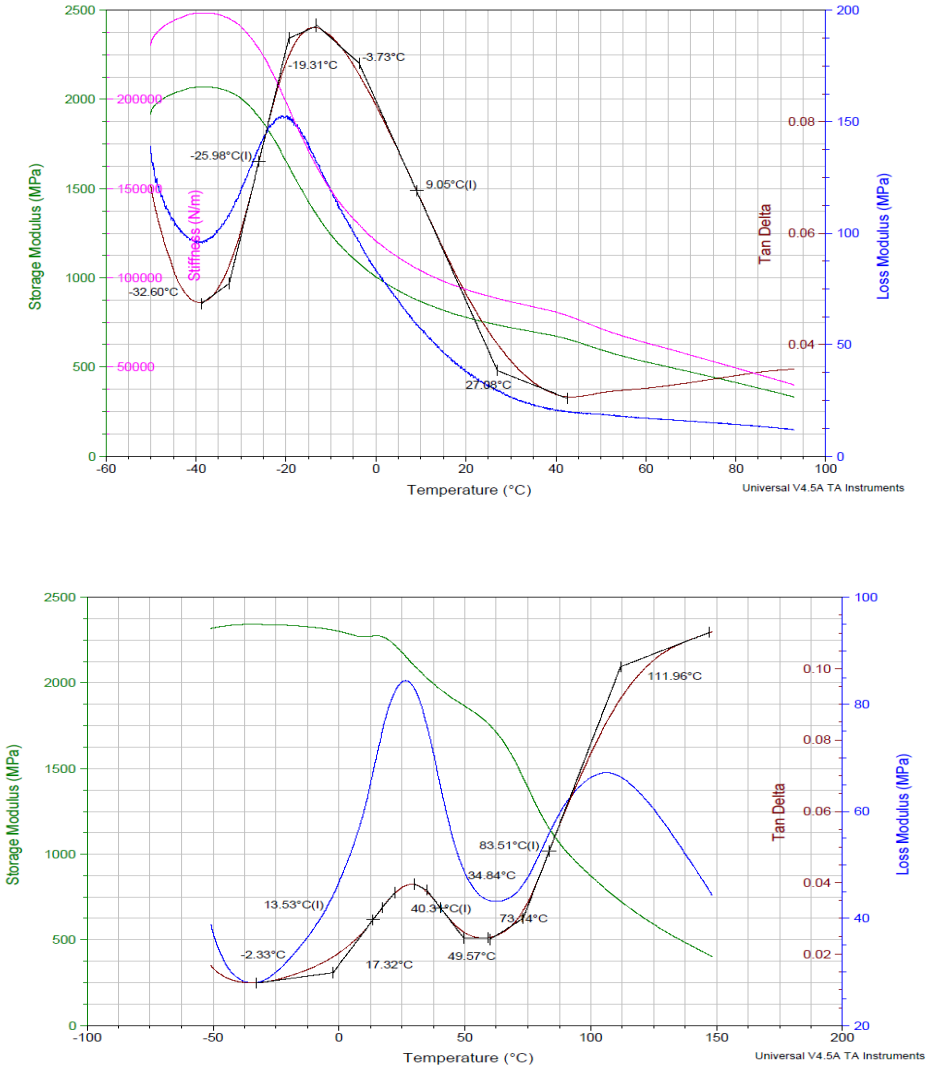

Figure 10-4 Storage and Loss Modulus with tanδ obtained by single cantilever DMA of the a) PBS and b) PHBV neat at frequency of 1 Hz

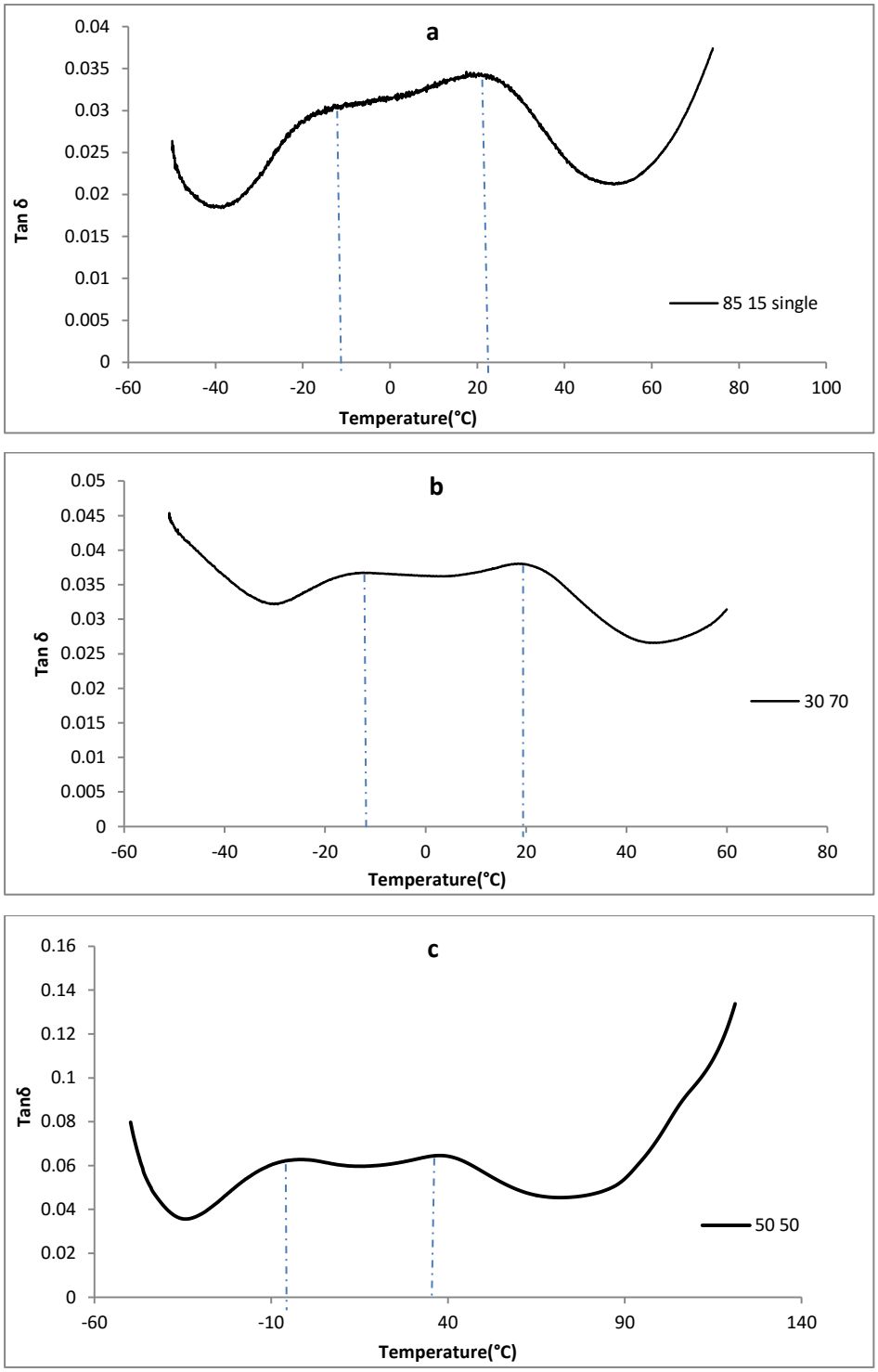

Figure 11-4 Tanδ graph of single cantilever DMA for PHBV/PBS blends with a) 85/15, b) 70/30, c) 50/50 concentrations (all dashed lines point T_g)

A similar process was examined by Qui, Ikehara and Nishi for a blend of PHBV/PBS in chloroform as the solvent in the cast mixture. They announced that the experimental results indicated that PHBV is immiscible with PBS as shown by the almost unchanged glass transition temperature and the biphasic melt (Qui, Ikehara and Nishi, 2003). Miao et al also declared the similar immiscibility behaviour from blending of PHBV with PES (polyethylene succinate) by observing the two composition independent glass transition temperatures corresponding to those of the neat components (Miao et al, 2008).

The DMA results of PHBV/PBS blends in presence of two chain extenders have been obtained and are illustrated in Figure 14-4:

It can be seen from the Figure 12-4 and Table 7-4 that the Tg for the PHBV is 27.92 ℃ (from the tan δ curve) and 25.73°C (from the loss modulus curve) and for PBS -13.56 ℃ and -13.65 ℃.

It clearly shows a difference of about 40 ℃ between the glass transition temperatures of PHBV and PBS. It has been reported by Karasz, that in order to get a distinctive peak and avoiding any misinterpretation, there should be at least 20 ℃ differences between glass transitions for an effective polymer blend. However, a definitive statement of the vital differentiation in the glass transitions is not possible. It strongly depends on the sharpness of the Tg s of the components, the proximity of the phase boundaries, on the instrumentational characteristics and a possible transitional smearing in the mixture (Karasz, 1985).

For 85/15 PHBV/PBS, two T_g s were observed which indicates the immiscibility of the two components. Although the glass transition temperature of PHBV decreased by about 7 degrees, partial miscibility was reported for the blend.

The 70/30 PHBV/PBS blend also showed similar behaviour, with the T_g varying slightly. The differences in the T_g s could be due to the differences in the component's concentration. However, for the 50/50 blend of PHBV/PBS, the smaller T_g was shifted upwards by 7 ℃, and the higher T_g also increased by about 3 ℃.

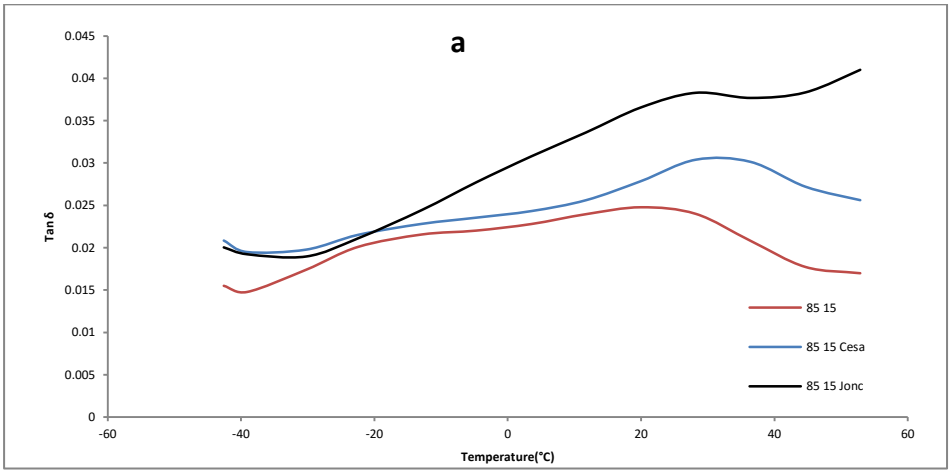

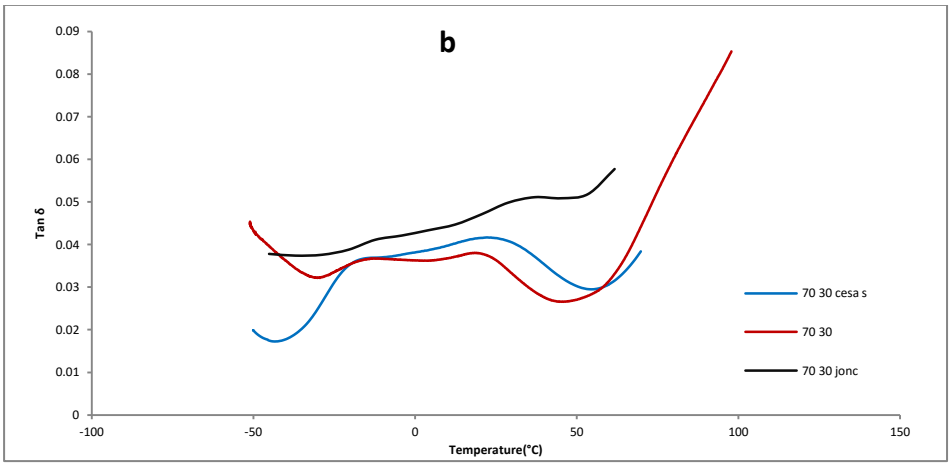

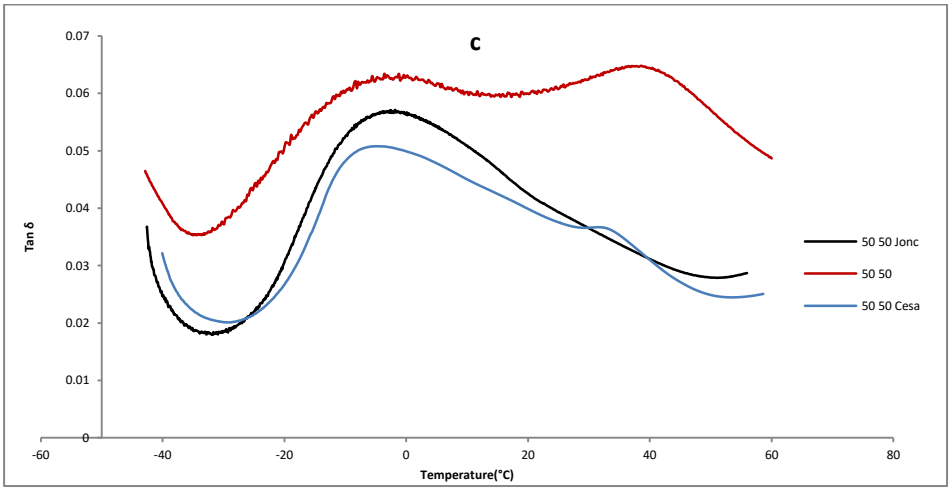

Figure 12-4 Tan δ graph of single cantilever DMA of PHBV/PBS bends in presence of two chain extender a)85/15 b) 70/30 c) 50/50

The tan δ of the PHBV/PBS (85/15) figure 14a shows two distinguishable T_g s at -13.87 & 20.27 ℃ respectively. For the 85/15/2 PHBV/PBS/CE, however, the presence of the chain extender shows a distinctive effect in the change of the T_g s. The blends with a chain extender exhibit only one T_g, at 29.98 & 36.42 °C (from the tan δ curve), close to the corresponding T_g of PHBV. The 50/50/2 PHBV/PBS/CE blend with Joncryl exhibited a single glass transition temperature at -1.8 ℃ (tan δ) and 2.45 ℃ (loss modulus) which could be placed in the middle of the temperature range corresponding to both polymers .

Table 7-4 The value of T_g from tan δ and loss modulus curves for PHBV/PBS and PHBV/PBS/Chain Extender

Samples	**Tan δ**		**Loss Modulus**	
PHBV/PBS/CE	T_g^{min}	T_g^{max}	T_g^{min}	T_g^{max}
100/0/0	27		25	
0/100/0	-13		-13	
85/15/0	-13	20	-14	18
70/30/0	-12	18	-15	19
50/50/0	-5	31	-8	28
85/15/2	30		28	
85/15/2$_m$	36		28	
70/30/2	-12	-29	-19	21
70/30/2$_m$	-17	24	-19	16
50/50/2	-2		2	
50/50/2$_m$	-5	23 (very small peak)	-10	21

4.5.2 Evaluating the Miscibility behaviour of components in blends by multi frequency DMA

The glass transition is technically a range of behaviour where scientists have agreed to report a single temperature as the indicator based on certain standards. Modulus values change with temperature and transitions in materials can be seen as changes in the storage/loss modulus or tan delta curves. The changes not only include the glass transition and melting, but also other transitions that occur in the glassy or rubbery plateau (Perkinelmer, 2016). Running a multi-frequency scan and calculating the activation energy of the transition is known as an effective method to determine that the result is really a T_g. The activation energy for a T_g is roughly 100-300 kJ/mol. In comparison a T_β has an activation energy of about 30-50 kJ/mol and at the melt, T_m, the frequency dependency collapses (Matsuka and Kwei, 1979).

Multi frequency DMA results for the blends of PHBV/PBS and PHBV/PBS/CE are illustrated at Figure 13-4 (a-f) and 13-4(g-i):

The graphs in Figure 13-4 & 14-4 (a-i) show multi frequency dynamical mechanical analyser (DMA) results with 5 random frequencies of 5, 7.9, 12.6, 19.8, 20 Hz for the PHBV/PBS and PHBV/PBS/CE compatibilized blends with the different concentrations. It is clear that the T_g is frequency dependent and that it changes to a higher temperature with increasing frequency.

The tan δ curves of the multi frequency DMA results also supported the single frequency (1 Hz) DMA results.

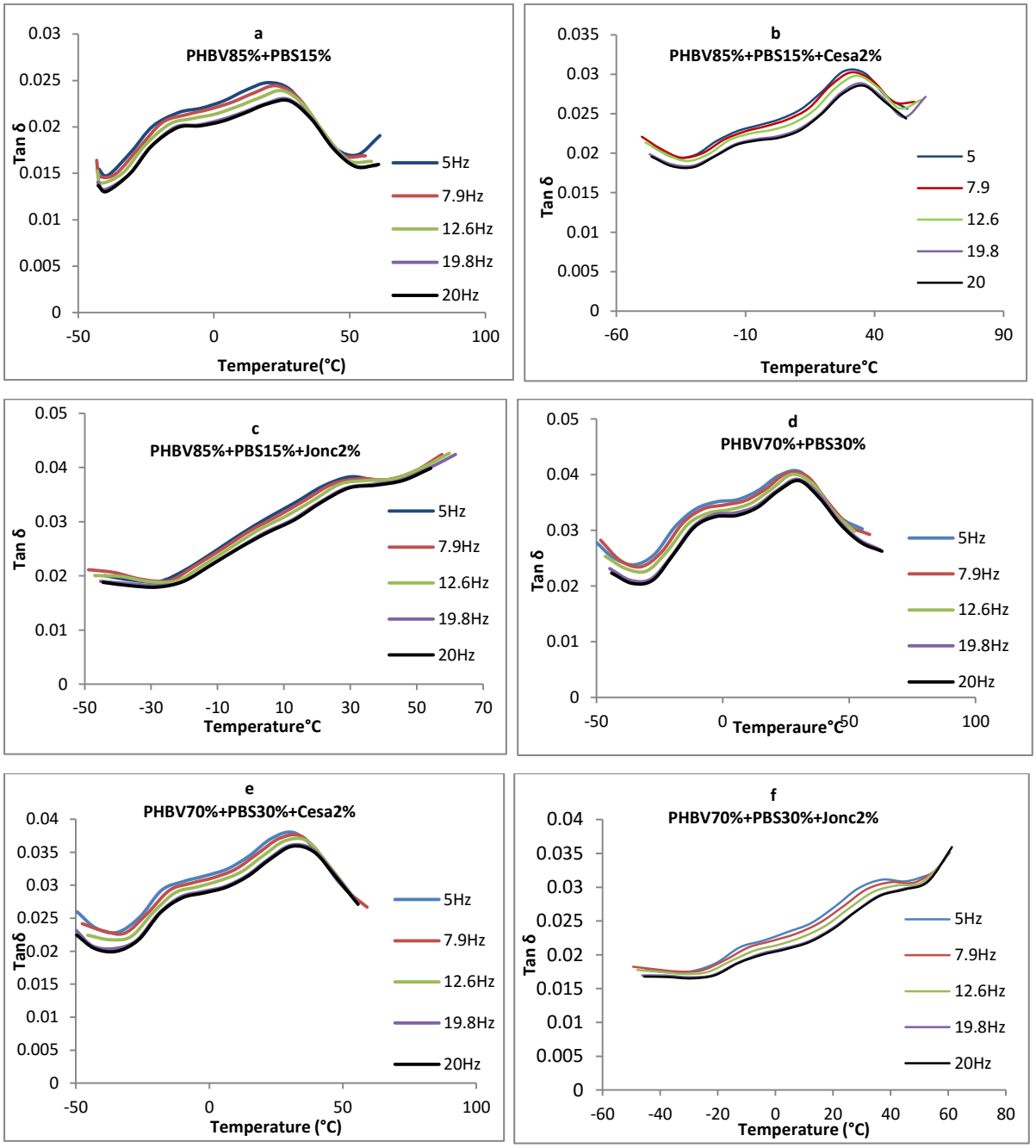

Figure 13-4 (a-f) Multi frequency DMA for PHBV/PBS and PHBV/PBS/CE

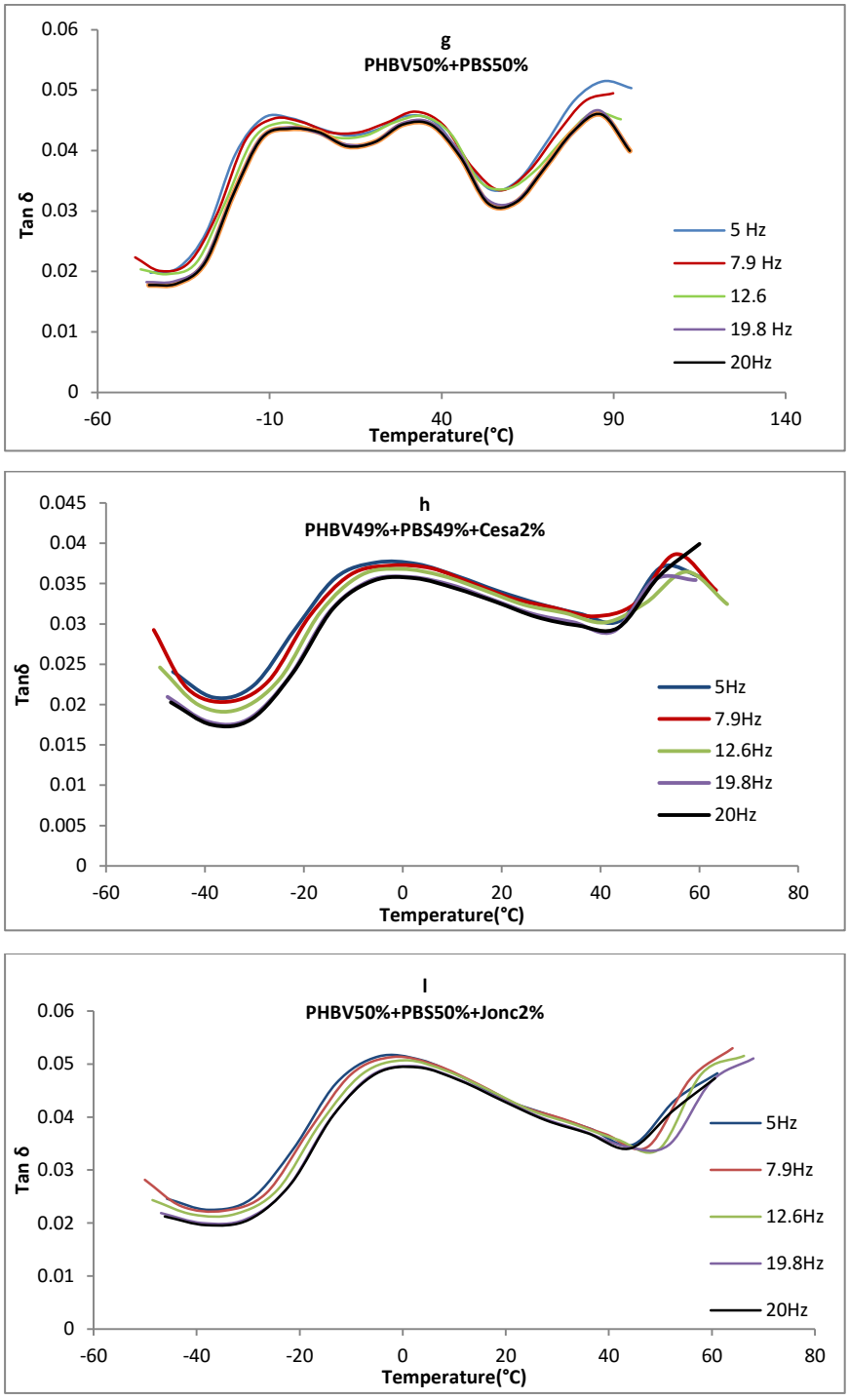

Figure 14-4 (g-i) Multi frequency DMA for PHBV/PBS and PHBV/PBS/CE

4.5.3 Measuring the activation energy of each blend based on the Arrhenius equation by multi frequency DMA

There are different phase transitions associated with polymers. Measuring the activation energy each transition temperature can approximately indicate the nature of the transition whether it is α, β or γ. Frequency-dependent effects such as glass transitions are distinguishable from a transition like the melting point which are not depend on frequency. The most important transition that occurs in the solid state is the so-called β relaxation in amorphous phase and the γ transitions in a semi crystalline solid. These transitions could be studied in-depth with DMA through measurements of mechanical loss maxima as a function either temperature or frequency. One of the characteristics that distinguish the β or γ transitions from a glass transition is that the temperature coefficient of those transitions are typically about 3, where the glass transition obeys the free volume formula and has a discernible activation energy more than 100 kJ/mol. In semi-crystalline polymers, the highest temperature transition, the α transition, is associated with the crystalline structure. The β transition for a semi-crystalline polymer corresponds to the glass transition in an amorphous polymer. The γ transitions in semi-crystalline polymers technically look like the β transition in the amorphous glass, with activation energy between 30-40 kJ/mol and temperature dependent loss intensity (Matsuka and Kwei, 1979).

The peaks in tan δ at very low temperature correspond to the ß and γ transitions in the polymer and are due to the motion of short lengths of the polymer backbone rather than the large scale increase in mobility that accompanies the glass-rubber transition. With the dynamic mechanical analyser (DMA), the T_g can be measured with high sensitivity by assessing the response of either the storage modulus (E_1), loss modulus (E_2), or loss tangent (tanδ) as a function of temperature. In dynamic mechanical analysis, T_g can either be defined as the temperature where the maximum loss tangent or the maximum loss modulus is observed, or as the inflexion point at which a significant drop of the storage modulus occurs. However, as mentioned in Chapter 2-5 there is no such exact temperature called the glass

transition temperature T_g; there is a glass temperature region because the process of changing from the glassy state into either a liquid or a rubbery phase is a gradual process (Chapter 2). In addition to the inherent resin chemical properties and the criterion used for estimating the T_g value, the factors related to instrument and test conditions, such as test frequency, heating rate, sample size and clamping effects can also influence the measured T_g value.

Multi-frequency DMA in all samples showed that increasing the test frequency leads to a shift of the T_g to a higher temperature. The purpose of this study was to determine the influence of the DMA test frequency on the evaluation of the activation energy related to the glass transition relaxation while the heating rate was kept constant. The glass transition temperature is a key transition in any material and is sometimes referred to as the α transition. Normally at a lower temperature, other relaxation events can be observed for polymeric materials. The β relaxation is normally attributed to polymer backbone conformation reorganization.

According to Smith and Bedrov, the main-chain β relaxation process involves local motions of the polymer chain backbone that do not require the cooperative motion of the surrounding chains and that the main-chain β relaxation process is a precursor for the primary α relaxation process.

However, the precise nature of these local motions, whether they are spatially and temporally homogeneous or heterogeneous, and how these motions ultimately lead to complete relaxation of the polymer, are not well understood (Smith and Bedrov, 2006). In order to determine if the observed T_g‘s of specimens are a genuine α transition, a multi-frequency scan was carried out and the activation energy of the transition was calculated. The activation energy for a T_g is approximately 100-400 $kJmol^{-1}$. It has been reported that the β relaxation has an activation energy of about 30-50 $kJmol^{-1}$ and at melting, the frequency dependency collapses (Matsuka and Kwei, 1979). The activation energy of these processes can be determined by applying an Arrhenius law (Ward, Hadley, 1993).

Dynamic mechanical studies usually indicate the presence of different transitions like the α transition or glass-rubber transition and the β transition.

In the glass transition region the damping is high because of the initiation of micro-Brownian motion in molecular chains (Barral et al, 1994).

In dynamic mechanical experiments, E_a can be estimated by using the time-temperature superposition principle, to superimpose the tan δ peaks determined by multi frequency DMA (Barral et al, 1994).

The tan δ peaks can be shifted for superposition along the logarithmic time axis. The temperature dependence of the test frequency may then be expressed in Equation 3-4:

Equation 3-4) $$\mathbf{F = A \exp\left(-\frac{Ea}{RT}\right)}$$

Where F is frequency, A is the pre-exponential factor, E_a is the activation energy, R is the gas constant and T is the temperature. As frequency is essentially a rate expression with units of s^{-1} the natural log of frequency can be plotted against 1 over temperature. The slope of this line is equal to the negative activation energy divided by the gas constant. The Arrhenius equation can be expressed:

Equation 4-4) $$\mathbf{Ln\,(F) = ln\,(A) - \frac{Ea}{RT}} \longrightarrow \quad \mathbf{E_a = -R\left[\frac{d(\ln F)}{d\left(\frac{1}{Tg}\right)}\right]}$$

A plot of ln frequency against 1/temperature is known as an Arrhenius plot (Equation 4-4). Arrhenius plots of PHBV/PBS and PHBV/PBS/CE are illustrated in Figure15-4. Table 8-4 shows the value of the activation energy of each compound.

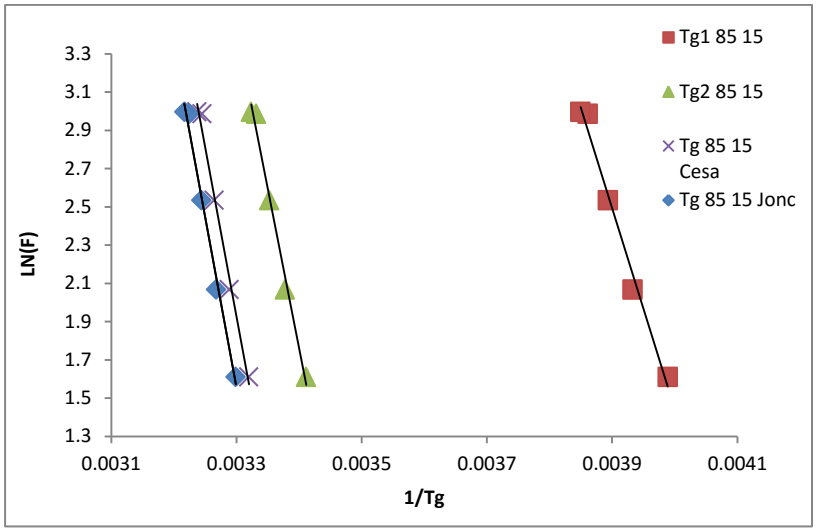

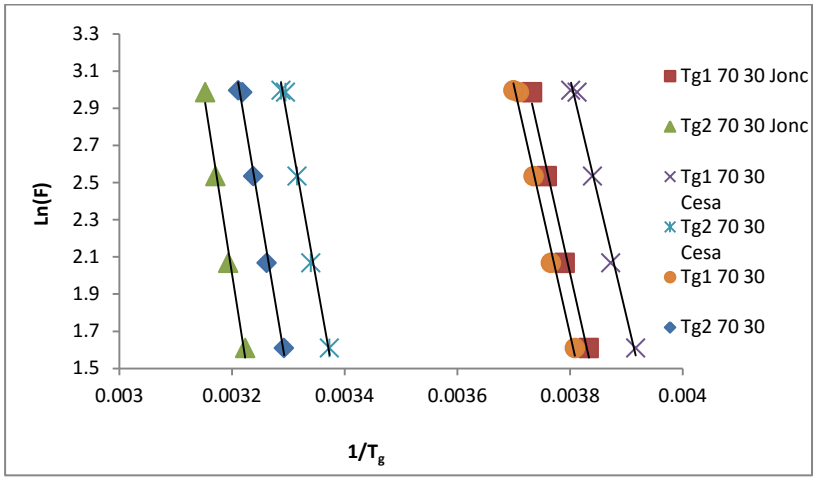

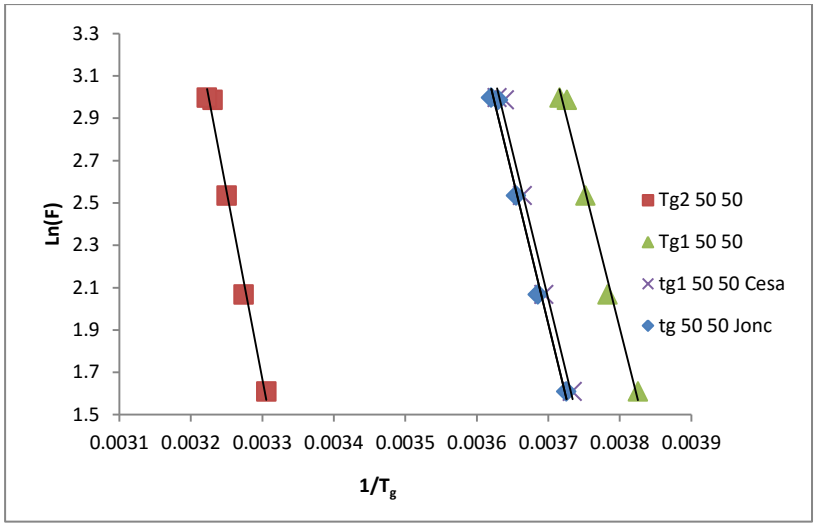

Figure 15-4 -The Arrhenius plots for PHBV/PBS compounds and PHBV/PBS with the chain extender (powder form and masterbach)

Table 8-4 The value of the activation energy for PHBV/PBS compounds and PHBV/PBS with chain extender (powder form and masterbach)

Samples	Activation Energy	
PHBV/PBS/CE	Ea_1 (kJ/mol)	Ea_2 (kJ/mol)
85/15/0	100	139
70/30/0	111	150
50/50/0	111	147
85/15/2	150	
85/15/2m	147	
70/30/2	113	160
70/30/2m	106	139
50/50/2	116	
50/50/2m	116	

As shown in Table 8-4, the value of the all E_a s are bigger than 100 kJ/mol and they clearly indicate an α transition and a true T_g for each components. For PHBV85/15, two T_g s and two activation energies are calculated. The 100.2 kJ/mol corresponds to the PBS activation energy and E_a =138.6 kJ/mol corresponds to the PHBV activation energy. The DMA results for the 85/15 blends shows that by adding a chain extender only one T_g has been observed from both the tan δ and the loss modulus graphs. The 85/15 blends T_g have an activation energy of about 150 kJ/mol which is closer to the corresponding activation energy of PHBV in an immiscible blend without the chain extender. For the 70/30 blends the presence of the chain extenders didn't change the activation energies of the two observed T_g s in the immiscible blends. For 50/50 blend, the activation energy is slightly more than activation energy corresponding to PBS in blend.

4.6 Mechanical properties

Polymer blending is an inexpensive, effective way to produce new polymeric materials. The properties of the product are influenced by the properties of the each component and also the degree of dispersion of the minor components in each polymer matrix. However, for the majority of the polymer blends, the improvement of the mechanical properties is difficult to achieve due to the poor dispersion of the minor component. Compatibilization can be used to improve the dispersion of minor component and enhance the mechanical properties. On the other hand, an increase of the elongation at break (%) of polymer blends traditionally indicates compatibility enhancement (Kum et al, 2007). The mechanical properties of PHBV/PBS in four concentrations of 85/15, 70/30, 50/50, 60/40 and three concentrations of 85/15, 70/30 and 50/50 with two chain extenders (Cesa-extend in masterbatch form and Joncryl-ADR in powder form) are illustrated in Figure 16-4 and 17-4 (a, b, c and d)

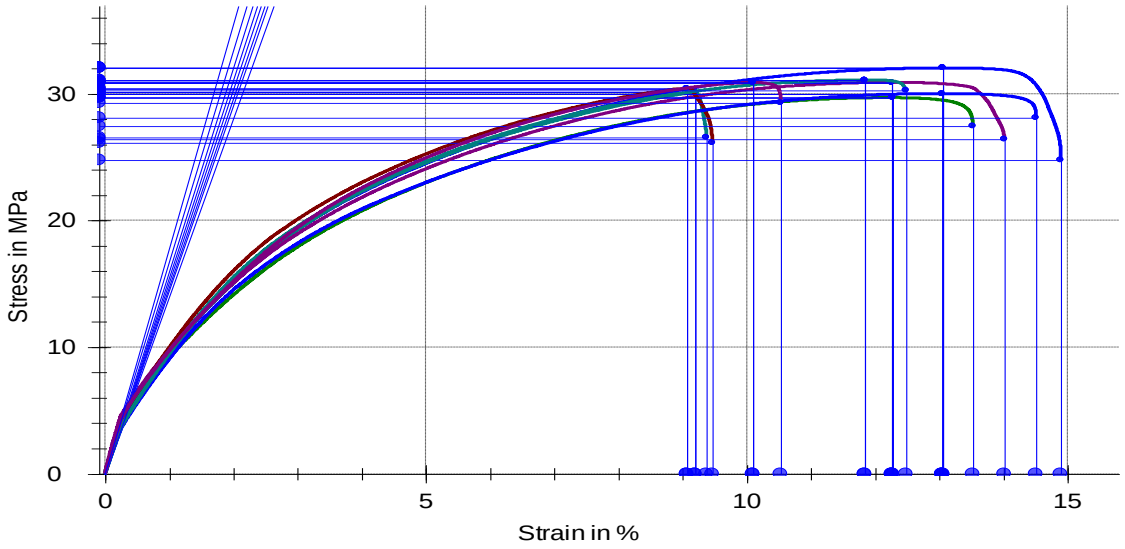

Figure 16-4 Typical stress-strain graph of PHBV/PBS/CE

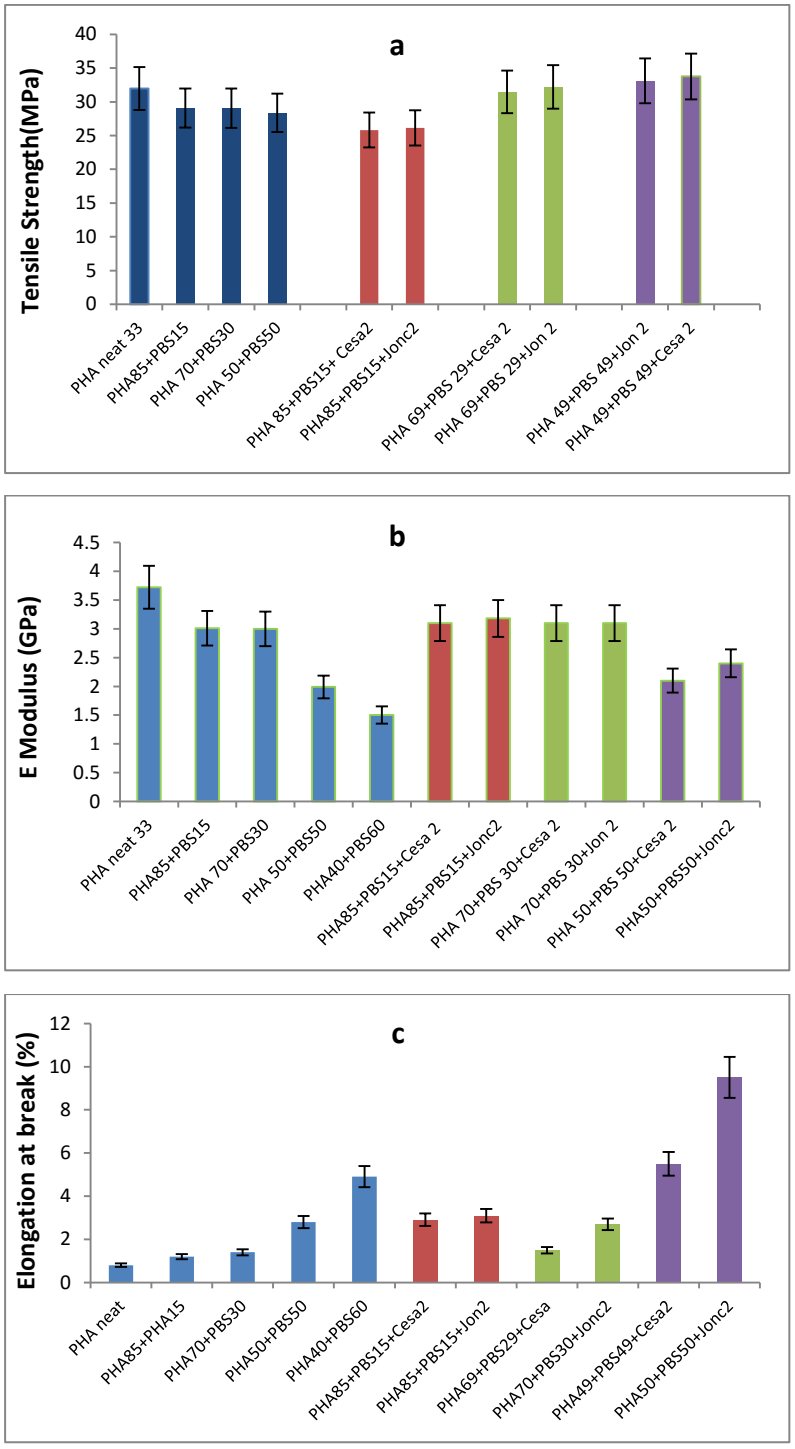

Figure 17-4 a) The Tensile Strength,-b) Young's Modulus and –c) Elongation at Break for PHBV/PBS and PHBV/PBS/Chain Extender

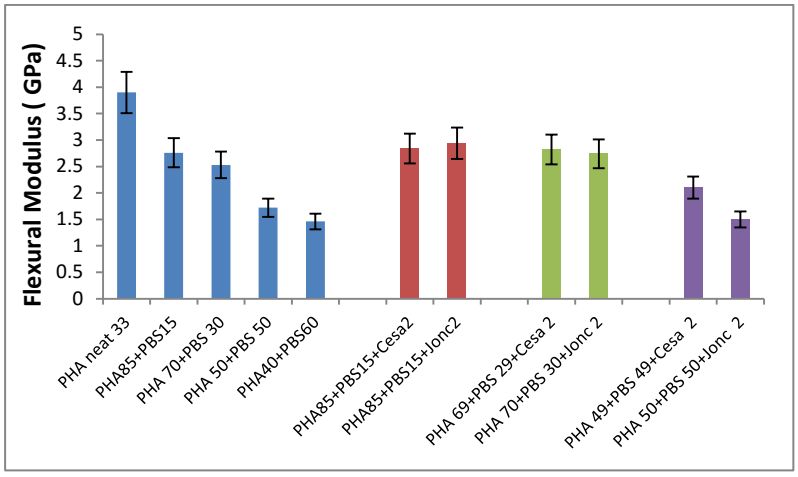

Figure 18-4 the flexural Modulus for PHBV/PBS and PHBV/PBS/Chain Extender

The values the modulus of elasticity for PHBV/PBS blends and their compound with chain extender were obtained from the slopes of the stress–strain curves (figure 16-4a for instance). Figure 17-4c shows that the E Modulus:

- Decreased with increasing the PBS content and droped from 3.72 GPa for the neat PHBV to 1.99 GPa for the PHBV/PBS 50/50 and even lower at 1.5 GPa for the PHBV/PBS 40/60 blend
- Addition of the chain extenders slightly increased the value of the E modulus and it decreased with increasing of the PBS content.

The values of tensile strength:

- Decreased with increasing of the PBS content in the blends
- Decreased for the 85/15 and then Increased for the 70/30 and 50/50 samples with the addition of the chain extender.

The tensile strength decreasing with an increase of the PBS content could be explained by the PBS acting as a plasticizer in the blends. While an increase in tensile strength of the compounds with chain extenders is probably because that the chain extender or its grafted copolymers only exist at the boundary of the PHBV and PBS and act as a connector to hold domains, and consequently results higher mechanical strength.

On the other hand, the elongation at break:

- increases with the increasing of the PBS content in the blends for all samples
- Significantly increased for the blends of PHBV/PBS/Joncryl 50/50/2

This later phenomenon could be explained by an increase in the miscibility of the compounds. It was expected that the low T_g and the higher mobility of PBS, would enhance the flexibility of its compound with PHBV and would consequently decrease the tensile strength of the material. Altering in the miscibility conditions of the compounds, particularly in 85/15 & 50/50 with chain extender, however increased the tensile strength of the compounds. This effect has been significant in improving of the elongation at break from 1.2% to 3.1% for 85/15 and 2.8% to 9.5% for 50/50 with chain extender, respectively.

It has been established over a time that an increase in the elongation at break indicates an improvement of the miscibility in the polymer blend. Wang et al. stated that in the miscible blend of PHBV and poly (3-hydroxybutyrate-co-4-hydroxybutyrate) (P3/4HB) (a single T_g in majority of the blend composition), the PHBV elastic modulus decreases and the PHBV elongation at break increases with addition of P3/4HB. While the trend of tensile strength is irregular which it first increases and then drops by increasing of the P3/4HB concentration in the blends (Wang et al, 2010). Therefore, it could be explained that similar phenomena occurred for PHBV/PBS blends when they become compatible.

Figure 18-4 shows the changes in the flexural Modulus of PHA neat and its blends with PBS with and without the presence of the chain extenders, Cesa and Joncryl.

The changes in the flexural properties are similar to that of the tensile properties. The flexural modulus decreases from 3.9 GPa to 1.46 GPa for 100/0 to 50/50 PHBV/PBS respectively. Increasing the amount of PBS in the blends, both the flexural modulus and flexural strength decrease which might be due to the plasticization effect of PBS and its low glass transition temperature.

Tang et al reported that compatibilized polyoxymethylene /thermoplastic polyurethane (POM/TPU) blends with Joncryl chain extender showed a significant improvement the tensile and flexural strengths (Tang et al, 2012).

Nevertheless, the practical application of PHBV is expected to improve, particularly where excellent mechanical properties are required.

4.7 Impact test

Polymer blending is a very common method to enhance impact properties of polymers. PHBV suffers from low impact resistance and there have been many attempts to improve the impact properties of the PHBV matrix. Reactive blending and compatibilization have also been examined to achieve the better toughness results particularly for the immiscible polymer blends. In principle, additives containing various functionality groups can react with the polyester carboxyl or hydroxyl end group in reactive blending process and by reducing the dispersed size phase.

Figure 19-4 shows the drop-weight impact test results for the specimens of PHBV/PBS and PHBV/PBS/Chain Extender. The results for different concentrations are summarized in Table 9-4.

Table 9-4 shows the energy absorbed by specimens increase with increasing the amount of the PBS content from 0 % (2,64J) to 50 % (7.59J). The energy peak increased with the amount of the PBS from 0 % (1.33J) to 30 % (4.21J) but it dropped to 2.79J for 50% PBS content (similar trends for force peak). For specimens with a chain extender, the peak energy and peak force increased with15 % PBS in the compound but they decreased for 30% and 50% PBS content. Compatibilisation reduced the absorbed energy and as it well established that the absorbed energy is directly related to deformation and mechanical resistance.

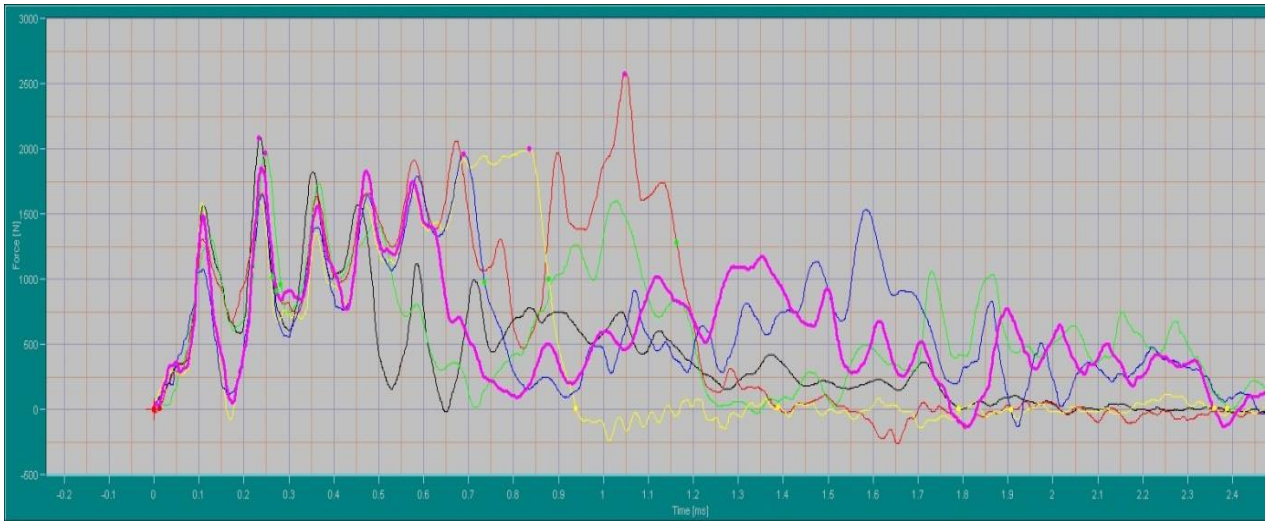

Figure 19-4 Typical drop- weight impact test for PHBV/PBS and PHBV/PBS/CE specimens [Y axis is Force (N) and X axis is time (sec)]

Table 9-4 Impact properties of PHBV/PBS and PHBV/PBS/CE by drop-weight impact test

PHBV/PBS/CE %	Peak Force (N)	Peak Energy (J)	Total Energy(J)
100/0/0	1482 ±123	1.33 ±0.27	2.64 ±0.32
85/15/0	1783 ±260	2.43 ±0.92	6.48 ±1.75
70/30/0	2106 ±445	4.21 ±1.4	6.89 ±1.9
50/50/0	1922 ±104	2.79 ±1.3	7.59 ±2.1
85/15/2	2030 ±277	4.18 ±1	5.44 ±1.3
70/30/2	2070 ±258	2.41±0.9	5.65 ±1.02
50/50/2	1883 ±631	1.84 ±2.1	4.25 ±2.2

4.8 FTIR analysis: reactive blend compatibilization and Vibrational assignment

Fourier transform infrared spectroscopy (FTIR) is a suitable technique for investigating specific intermolecular interaction in blends. FTIR can give a qualitative analysis of a polymer starting materials and finished products as well as analysing the components in the polymer mixtures. The chemical composition and the bonding arrangement of the constituents in a homo polymer, copolymer, and polymer composite can be obtained using Infrared (IR) spectroscopy (Bhargava, Wang and Koening, 2003). In order to study the possible interaction between the two bio-polyesters in the PHBV/PBS blend and their possible reaction with the compatibilizer through reactive compatibilization, the FTIR spectrum of each individual component and the blends are analysed separately.

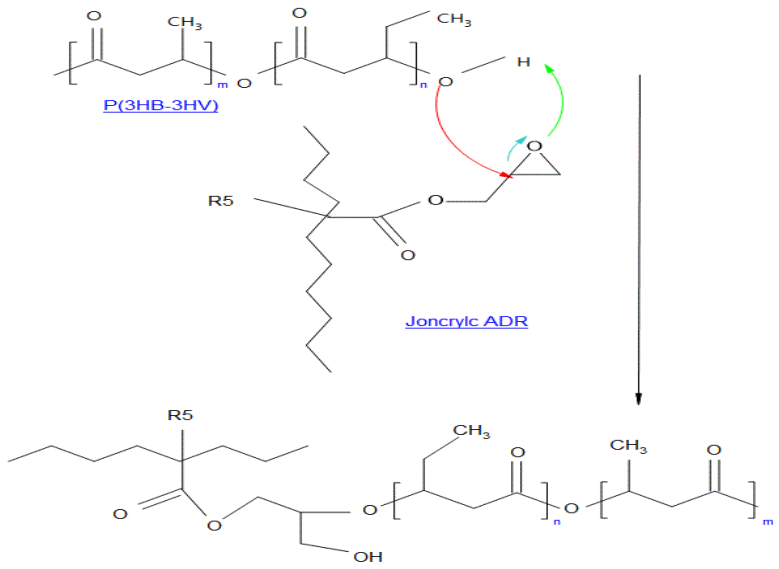

Figure 20-4 The possible predicted reaction between hydroxyl group of PHBV and oxirane ring (epoxide) in the epoxy functional oligomer (Joncryl ADR4368) leading to a branched graft copolymer

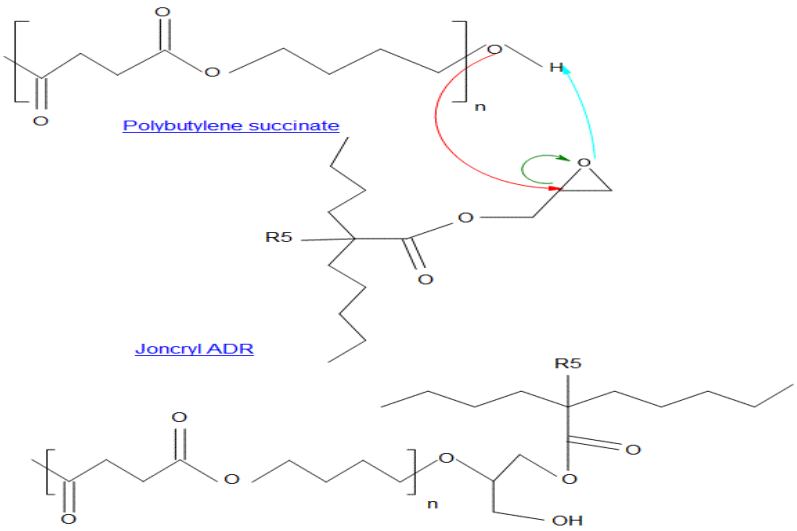

Figure 21-4 The possible predicted reaction between hydroxyl group of PBS and oxirane ring (epoxide) in the epoxy functional oligomer (Joncryl ADR4368) leading to a branched graft copolymer

Figure 20-4 and 21-4 show the proposed expected reaction between hydroxyl group of polyesters and epoxide functional group of the multi-functional styrene-acrylic oligomers (Joncryl ADR-4368). Villalobos stated that this oligomer is able to chain extend polycondensates in conventional plastic machinery such as for extrusion or injection moulding, without the use of a vacuum or catalysts, leading to long chain branching. For polyesters, glycidyl esterification of the carboxylic acid end groups takes place prior to the hydroxyl end group etherification. This latter reaction competes with etherification of the secondary hydroxyl groups and the main chain transesterification (Villalobos, 2006).

Figure 22-4 shows the proposed reaction between PHBV and PBS with Joncryl ADR. Theoretically the epoxy functional group could react with both the hydroxyl end group of polyester's chains and form a block co-polymer in the interfacial region thus reducing the interfacial tension and enhance the miscibility between the two immiscible polymers. The block copolymer accumulates at the interface between the two immiscible polymers, improving the interfacial adhesion and reducing the interfacial tension. When interfacial tension is reduced, the size of the dispersed particle reduces to a degree that is good for the mechanical performance.

On the other hand, the same low interfacial tension brings about a decrease in the tendency for the phase separated particles to coalesce and grow in size (Roe, 1993)

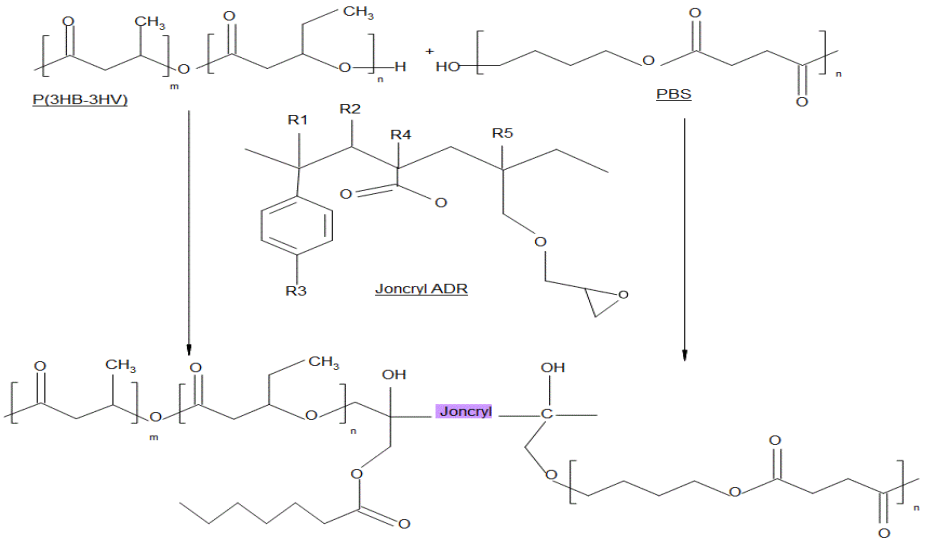

Figure 22-4 The possible reaction between PHBV and PBS in interfacial region by forming a block copolymer

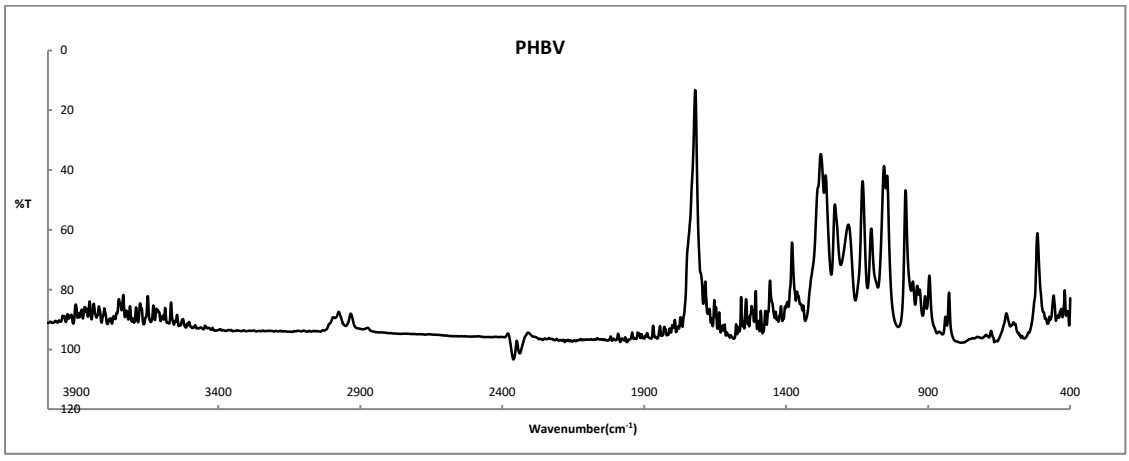

Figure 23-4 The FTIR spectroscopy of the neat poly-(3-hydroxybutyrate co-3-hydroxyvalerate) (PHBV)

Figure 23-4 shows that several bands have been observed in the FTIR spectrum of PHBV neat in the range of 4000-400cm^{-1} that could be identified with the groups' frequencies in database. They consist of the CH_3, CH_2, and the CO group wavenumbers.

Figure 24-4a shows that at 2977cm^{-1}, and 2875cm^{-1} two stretching modes (asymmetric and symmetric) assigned to CH_3 group is present. It also shows that the 2934cm^{-1} wavenumber belongs to the stretching mode of the asymmetric CH_2 group.

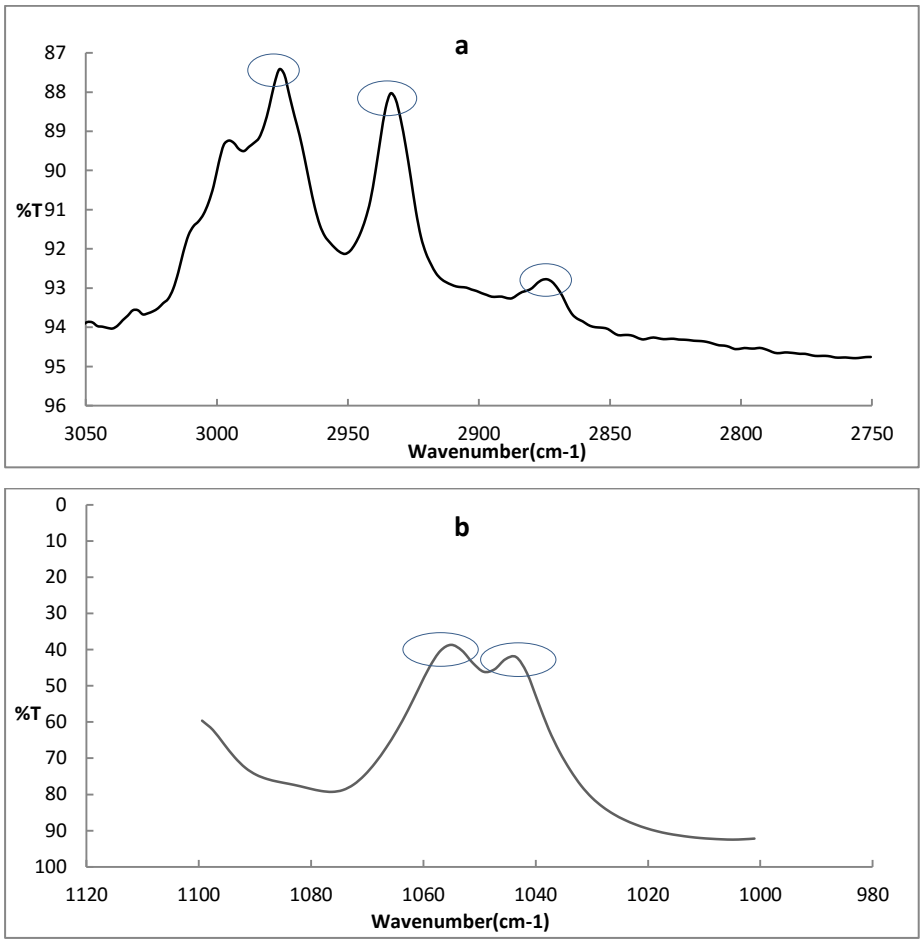

Figure 24-4 FTIR spectrum of PHBV in wavenumber range of 3050-2750 cm^{-1}(a), and 1120-980 cm^{-1} (b)

Figure 24-4b shows that there are two C-O stretching transition bands belonging to the carboxylic ester groups of the polymer at 1045 cm^{-1} and 1055cm^{-1} which could be identified as alkoxy C-O of ester group.

Usually, the most intense absorption in the IR spectrum belongs to the C=O stretching mode which in this case is an ester type peak and it can be observed at 1721cm^{-1} as an intense peak (Figure 23-4).

Figure 25-4 shows the FTIR spectrum of polybutylene succinate (PBS). The peaks at 1328cm^{-1} and 2945cm^{-1} are related to the symmetric and asymmetric vibrational bands of CH_2 in PBS chains respectively. Peaks in the range of 1143–1259 cm^{-1} resulted from the stretching of the –C–O–C– group in the ester linkages of the PBS. The intense peak at 1716cm^{-1} is related to C=O stretched band of the ester vibration groups of the PBS. The peak at 1045cm^{-1} is attributed to the stretching vibrations of –O-C-C- in PBS chains.

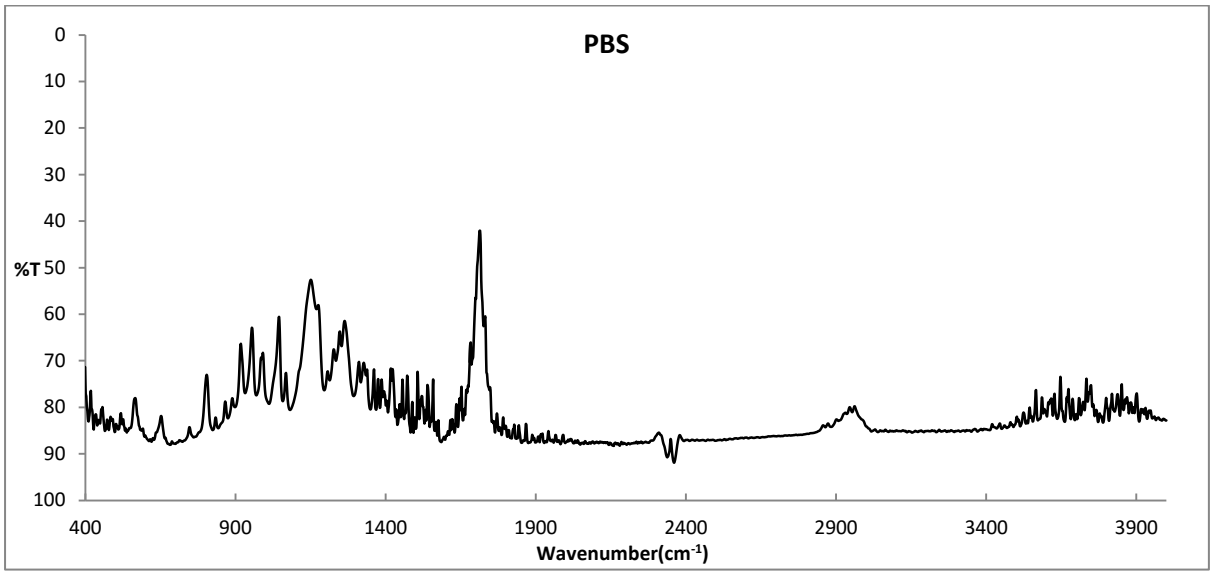

Figure 25-4 The FTIR spectroscopy of the neat poly-(butylene succinate) (PBS)

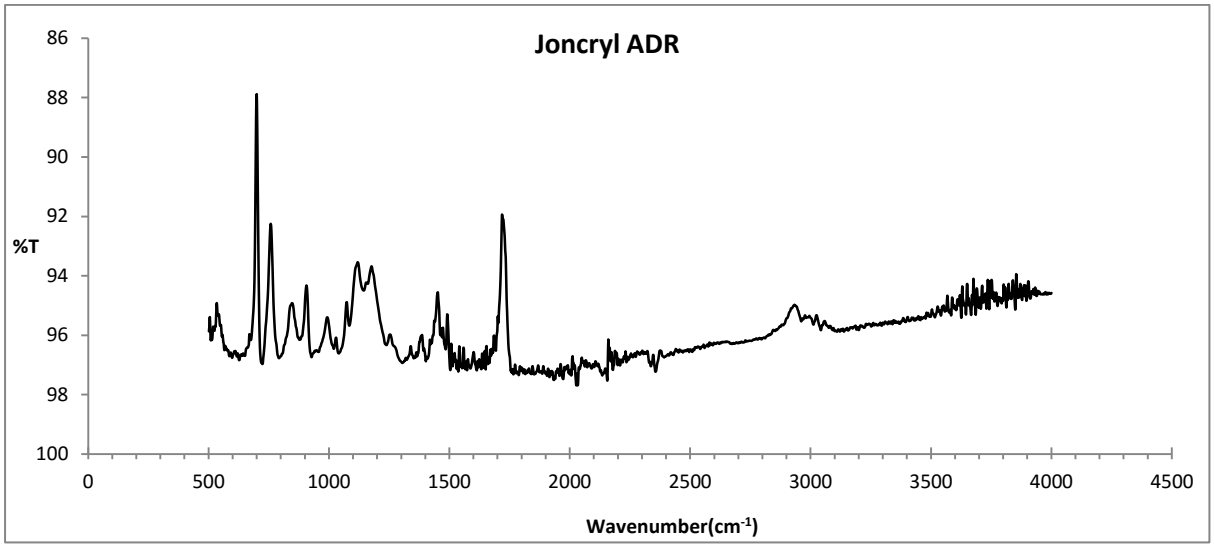

Figure 26-4 The FTIR spectroscopy of multi-epoxy functional styrene-acrylic oligomer chain extenders (Joncryl ADR)

The sharp peak marked at 1718 cm^{-1} fits a ketone carbonyl group. The FTIR spectra shows the C=C and C-H band of phenyl ring in molecules. The strong peak at 700 cm^{-1} can be attributed to mono-substituted phenyl C-H bending vibration.

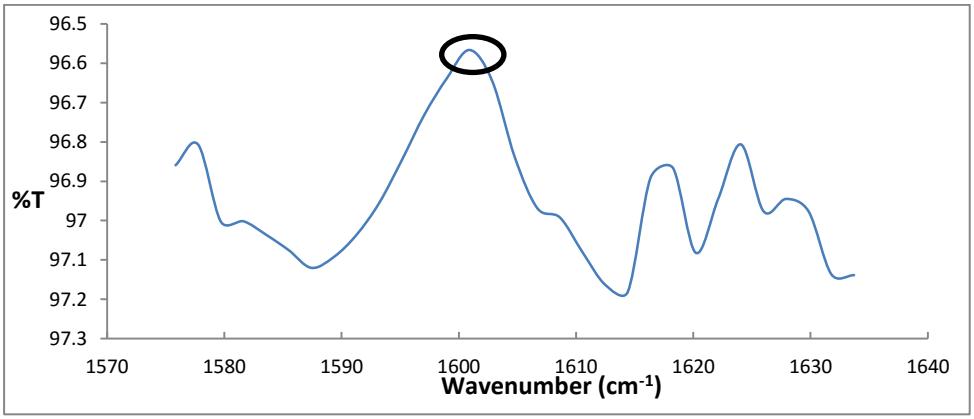

Figure 27-4 FTIR spectrum of Joncryl in wavenumber range of 1640-1570 cm^{-1}

Phenyl rings always have a strong, sharp peak in the region of 700 to 800 cm^{-1}. Phenyl rings generally show two very narrow peaks at 1450 and 1500 cm^{-1}. Also, phenyl rings almost always show weak craziness peak between 1650 and 2000 cm^{-1}. While the alkene spectrum showed a C=C peak between 1600 and 1700 cm^{-1} (FTIR spectrum of Joncryl in wavenumber range of 1640-1570 cm^{-1} in Figure 26), phenyl rings almost always show a weaker sharp peak right at 1600 cm^{-1} (Harvard, 2016).

According to Gonzalez, Cabanelas and Baselga, the characterization of epoxies involves much more than the location of the oxirane ring bands. There are many epoxy resins with different structures, different polymerization degrees...etc. IR spectroscopy can be used to characterize the nature of the epoxy (Gonzalez, Cabanelas and Baselga, 2012). C-H stretching of terminal oxirane group is observed in both cases at 3050 cm^{-1}. Two characteristic absorptions of the oxirane ring are observed in the range between 4000 cm^{-1} and 400 cm^{-1}. The first one, at 902 cm^{-1}, is attributed to the C-O deformation of the oxirane group. The second band is located at 3050 cm^{-1} approximately and is attributed to the C-H tension of the methylene group of the epoxy ring. This band is not very useful since its intensity is low and it is also very close to the strong O-H absorptions; but epoxy monomers produced at a low degree of polymerization, can be used as a qualitative indicative of the presence of epoxy groups.

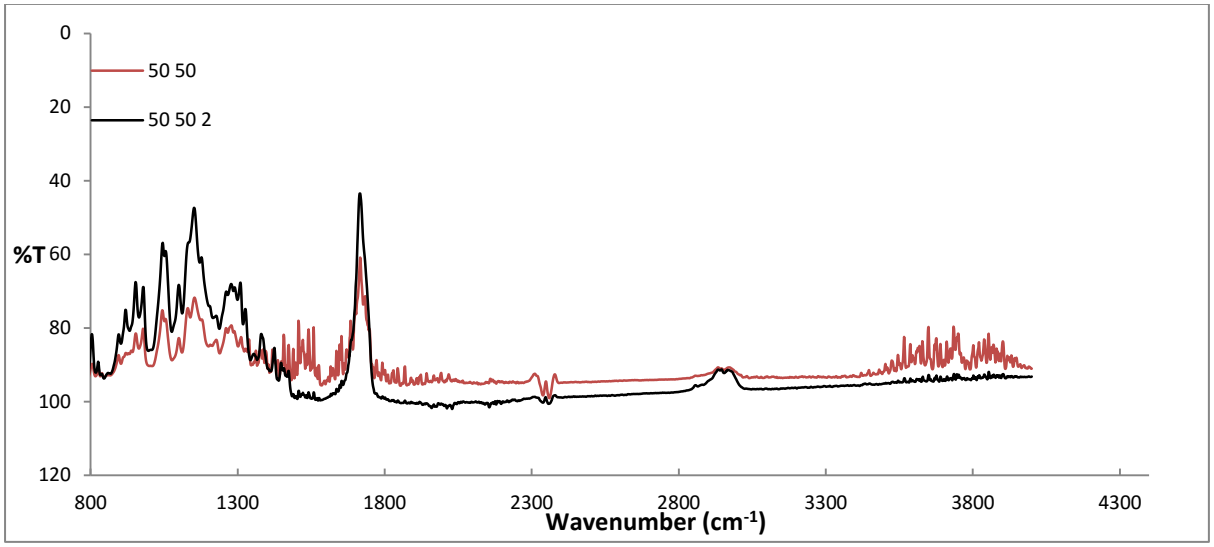

Figure 28-4 FTIR spectrum of PHBV/PBS and PHBV/PBS/CE, in the wavenumber range of 4000- 800 cm^{-1}

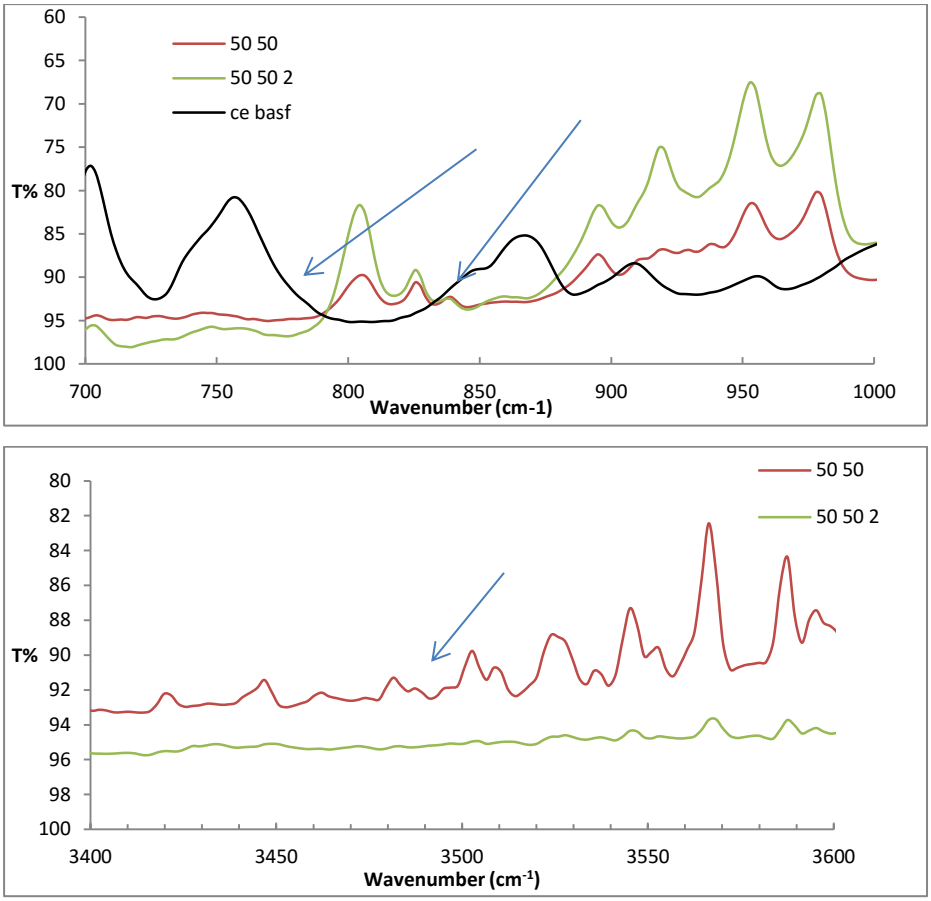

Figure 29-4 FTIR spectrum of PHBV/PBS and PHBV/PBS/CE, in the wavenumber range of 1000-700 cm^{-1} & 3600-3400 cm^{-1}

Two characteristic IR peaks can be seen in the spectra of Figure 28-4 compared to the Joncryl spectrum (Figure 26-4),

- A small peak at 846 cm^{-1} and very small peak 909 cm^{-1} is associated to stretching of C-O-C of oxirane group and C-O stretching of oxirane group. Those two peaks are not present in the compound of PHBV/PBS/CE.
- The peak at 3500 cm^{-1} was changed which is assigned to the O-H stretching (Gonzalez, Cabanelas and Baselga, 2012).

Those two IR peaks are only evidences to indicate that the proposed reaction might be happening in the compounds. The effective chain extension properties of the Joncryl as a chain extender & compatibilizer have been reported for a number of polymer blends by

researchers (Villalobos et al, 2006, Japon et al, 2001). In this study three chemical reactions were proposed by chemical formula in Figures 20-4, 21-4, 22-4 but however the supporting evidences from FTIR require more in-depth studies by other tools like microscopy FTIR. It is to be noted that in the several studies concerning the effect of Joncryl as a reactive chain extender, there is no reference to the use of the FTIR to analyse possible reactions between the polymers and the compatibilizer.

4.9 Morphology

SEM is an ideal technique for the assessment of samples with a high degree of surface relief to the large depth of field of the samples. The best result from a polymer blend is obtained when the two phases are immiscible, the internal phases are weakly bonded and the matrix is brittle. The surface of a brittle failure has an assortment of deboned particles and cavities. This morphology can be used for a basic evaluation of particles size distribution and adhesion between particles (Hobbs and Watkins, 2000).

Hobbs and Watkins stated that it is better to study polished or microtomed surfaces, because the surface is free from deformation and allows for a more random statistical sampling (58). It is well established that the types of morphology and the size of dispersed phases in the polymer blends can indicate the mechanical properties and rheological behaviour. In addition, the phase morphology can be studied to find the relationship between microstructure and the mechanical properties (Zhang, Mohanty and Misra, 2012).

Figure 30-4 shows the three possibilities of reactive blending at interfacial region. DeLeo and Velankar declared that the first possibility is for a linear mono-end-functional chains reacting to form a di-block copolymer, the second possibility is when an end-functional chain in one phase reacts with a multifunctional chain in the other to form a graft copolymer at the interface and the third possibility is that the two multifunctional reactive chains can lead to a crosslinked copolymer. The combination of these architectures is also reported in some studies (Deleo and Velankar, 2008).

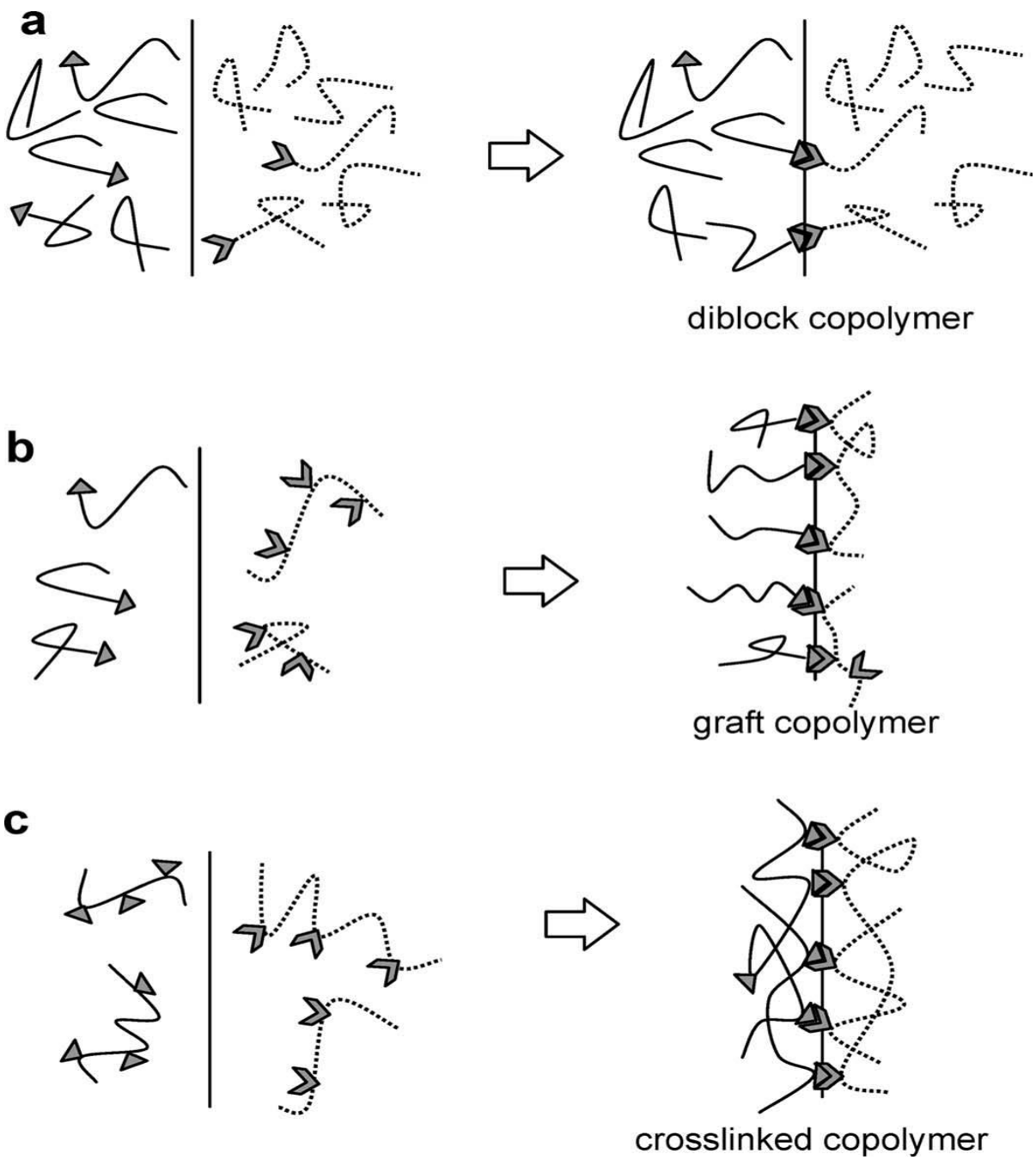

Figure 30-4 Reactive compatilization leading to various compatibilizer architectures at the interface forming a) a di-block copolymer b) a graft copolymer or c) a cross-linked copolymer(Deleo and Velankar, 2008)

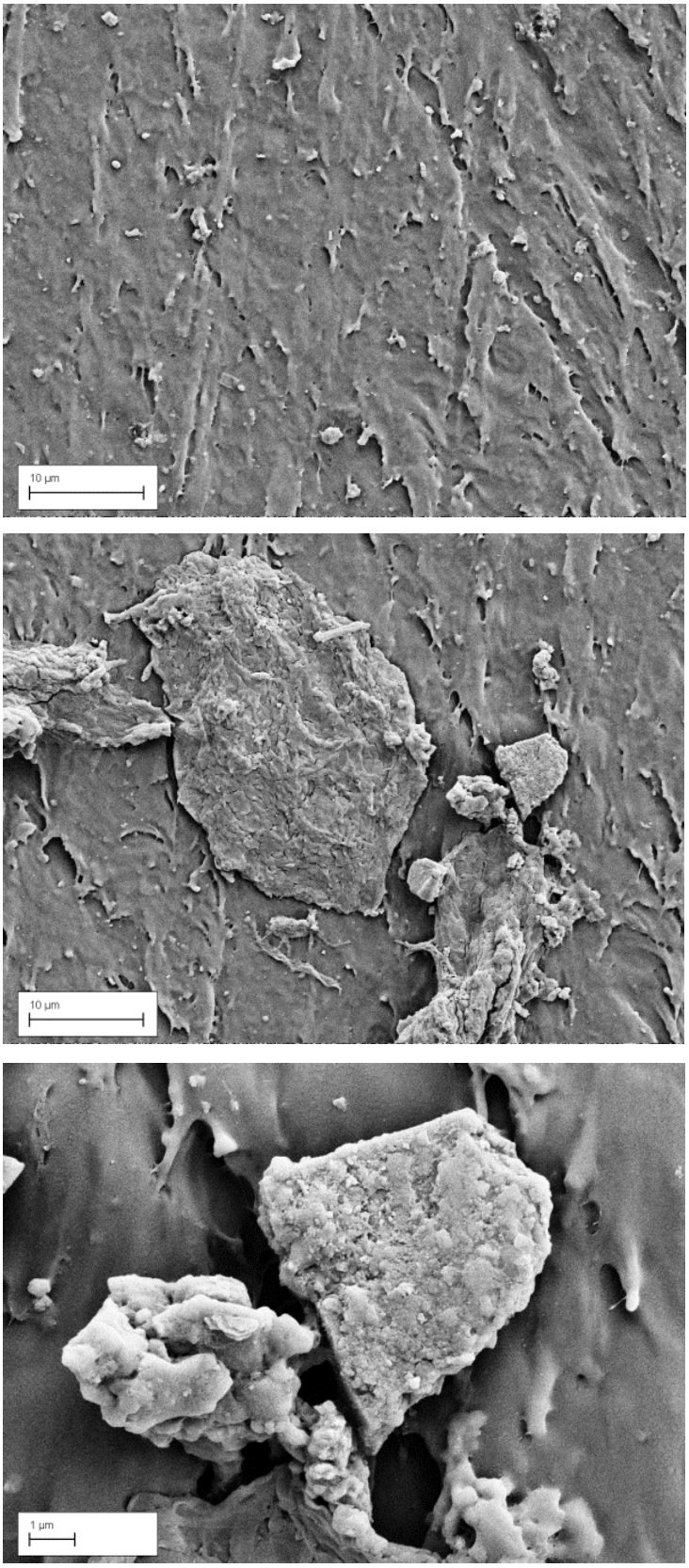

Figure 31-4 SEM images of polished tensile-fracture surfaces of PHBV/PBS 50/50 in two magnifications, 10 µm & 1 µm, the heterogeneous morphology of big lumps of PBS is observable

Figure 31-4 shows that a distinct two-phase morphology is discernible in all blends and also the heterogeneous morphology of PHBV/PBS blends is evident. The distribution of the big lump of dispersed phase (PBS with variation size from a few microns to more than 10 micron) in the matrix indicates the poor immiscibility between the two polymers. The typical isolated island morphology is also observable in the images. Some visual cavities can be observed in figure 31-4 and they reflect the weak interaction and the poor immiscibility between the two bio-polyesters.

Figure 31-4 & 32-4 show that the approximate diameters of the dispersed minor phases have changed from micrometre to the order of sub-micrometre in the blends. Figure 32-4 shows that the blend exhibits a typical drop matrix morphology composed of round drops of diameter of the order of several microns. There is not a significant amount of visible cavities in the images of the compatibilized reactive blends. Therefore, the big mass of aggregated PBS particles exhibited a poor adhesion between the matrix (PHBV) and PBS, while in the presence of the chain extender; fairly smooth fracture surface is evident, almost without the pull out of PBS particles.

This phenomena could be explained by a possible compatibilization with the formation of the di-block copolymer (A-CE-B) or graft copolymers (A-CE and/or B-CE) resulting in better dispersed phases and smaller particles. According to Ryan, the compatibilizer usually stabilizes micrometre- to sub micrometre-sized dispersions, and only in very special compositions do they show co-continuous morphology. In this study, observing a stable co-continuous morphology has been very difficult for all samples. However, forming a di-block or graft copolymer in the interfacial region of a compatibilized blend is more likely to result in a dispersed rather than a co-continuous phase morphology (Ryan, 2002).

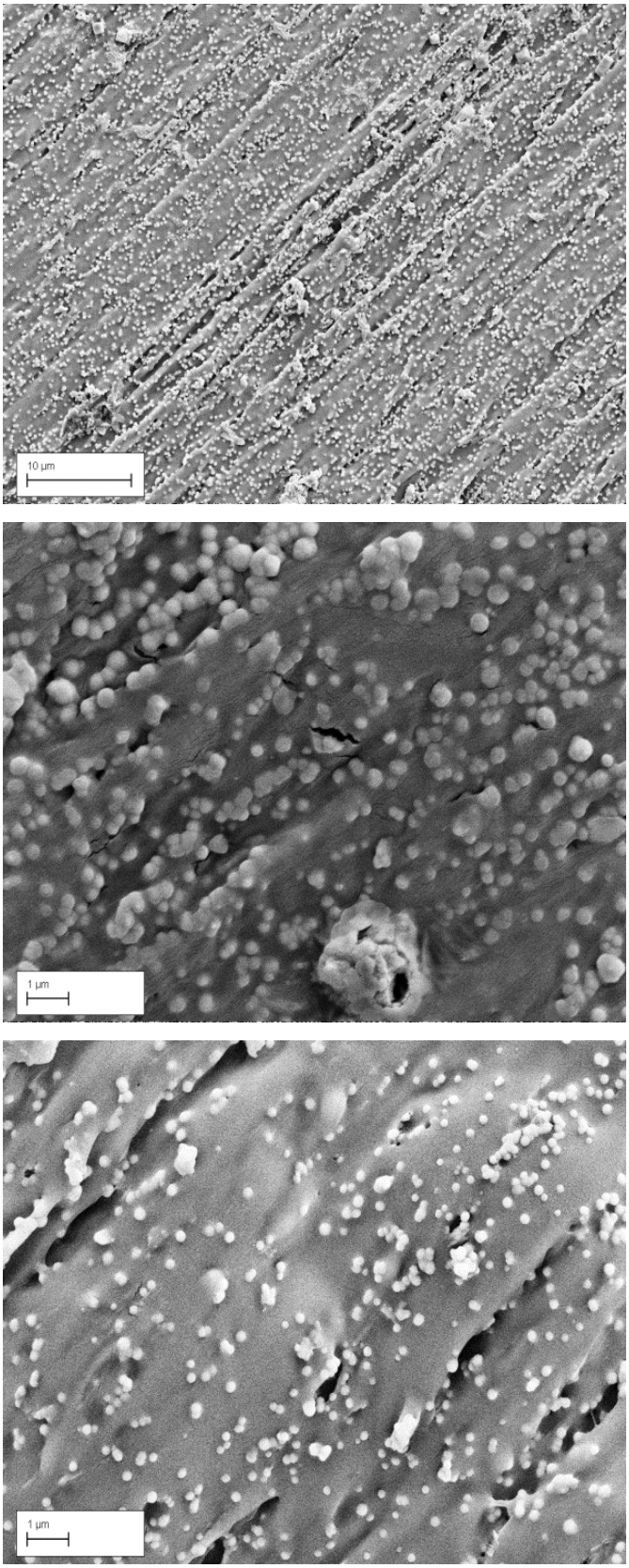

Figure 32-4 SEM images of polished tensile-fracture surfaces of PHBV/PBS/CE 50/50/2, the possible compatibilization by di-block copolymer consequences to better dispersed phases and smaller particles than particles size in blends without chain extenders

4.10 Conclusion

Non isothermal DSC analysis showed that the PHBV double melting point is depressed by increasing the PBS concentration in the PHBV/PBS blends. With the addition of the Joncryl and Cesa chain extenders to the blend the melting point of PHBV is elevated to a higher temperature due to increased miscibility of blends. The percentage of crystallinity of PHBV in the blend decreased with the addition of PBS.

Isothermal crystallization kinetics of the PHBV/PBS and PHBV/PBS/CE have been analysed using the JMAK equation and it showed that the time to 100% crystallization is temperature dependent. Blending PBS with PHBV also decreased the crystallization rate of PHBV in compound. The value of *k* in the Avramis equation decreased in each compound, with an increase in the crystallization temperature. The value of $t_{0.5}$ (half-time crystallization) increased with an increase of the crystallization temperature. When the concentration of PBS increased in the compound, the value of $t_{0.5}$ also increased due to decreased rate of crystallization of the PHBV in the presence of PBS.

The TGA results show that thermal degradation took place in two steps. For the PHBV/PBS 85/15 and 70/30, the presence of the chain extender didn't increase the initial decomposition temperature. However, the presence of chain extender in 50/50 compounds, significantly improved the degradation temperatures by almost 40 ℃.

The DMA results show that all the PHBV/PBS specimens have two distinctive T_g s, which indicates the immiscibility of PHBV/PBS in blends. The partial miscibility was also witnessed by shifting of T_g s to different temperatures. The presence of the chain extender in the blend of 85/15 showed one T_g to the corresponding T_g of PHBV and also the blend of 50/50 showed one T_g which be placed in the middle of the temperature range corresponding to both polymers. This indicates that the chain extender act as a compatibilizer in the blend of PHBV and PBS.

The DMA results were supported by the activation energy of T_g s. Each single and double Tgs were an α transition due to the Ea values obtained from Arrhenius plots.

The tensile strength decreased with increasing of the PBS content in blends. Addition of the chain extenders decreases the tensile strength in low concentration of PBS. In higher concentration of PBS, the tensile strength was increased in presence of the chain extenders.

The elongation at breaks increases with the increasing of the PBS content in the blends for all samples. It significantly increased for the blends of PHBV/PBS/Joncryl 50/50/2 which indicates the miscibility enhancement of the blend.

The Young's and flexural modulus are decreased with the addition of PBS. This may be due to the plasticization effect of PBS and its low glass transition temperature.
The amount of impact energy absorbed by the specimens increased with the increasing amount of PBS. The addition of the chain extender reduced the absorbed energy by the specimens.

The possible reaction between PHBV, PBS and the chain extenders was proposed and analysed by the FTIR results. The FTIR results showed that the peaks associated with the oxirane rings are disappeared in the compatibilized blends of PHBV/PBS.

The morphology study of the blends revealed that there was poor immiscibility between the two phases in the PHBV/PBS blends due to existence of a big lump of dispersed phase in the images. The large mass of aggregated PBS particles exhibited a poor adhesion between the matrix (PHBV) and PBS while in the presence of the chain extender; a fairly smooth fracture surface is evident, almost without the pull out of PBS particles.

Bibliography Chapter 4

- Avrami, M. (1941), "Kinetics of Phase Change: III.Granulation, Phase Change, and Microstructure". Journal of Chemical Physics, Vol 9, Issue 2, pp. 177–184.

- Avrami, M. (1940), "Kinetics of Phase Change: II.Transformation-Time Relations for Random Distribution of Nuclei". Journal of Chemical Physics, Vol 8, Issue2, pp. 212–224.

- Avrami, M. (1939), "Kinetics of Phase Change: I.General Theory". Journal of Chemical Physics, Vol 7, Issue12, pp. 1103–1112.

- Barral, L., Cano, J., López, A., Nogueira, P. and Ramírez, C. (1994), "Determination of the activation energies for α and β transitions of system containing a diglycidyl ether of bisphenol a (DGEBA) and 1,3-bisaminomethylcyclohexane (1,3-BAC)" J. Thermal Anal., Volume 41, Issue 6 ,pages 1463-1467

- Belfiore, L. A., (2010), "Physical Properties of Macromolecules", John Wiley & son Inc, New Jersey, pp. 320-322

- Bhargava, R., Wang, S. and Koening, J. L. (2003). FTIR micro spectroscopy of polymeric systems, Advances in Polymer Science, Vol.163, pp. 137-191, Springer, Verlag Berlin Heidelberg, Germany

- Brown, S. B. (2003),"Reactive Compatibilization of Polymer Blends", in Polymer Blend Handbook, Ed by Utraki, Kluwer Academic Publishers, Pages 339-415

- Correlo, V. M., Boesel, L. F., Pinho, E., Costa-Pintp, A. R., Alves da Silva, M. L., Bhattacharya, M., Mano, J. F., Neves, N. M. and Reis, R. L. (2009), "Melt-based compression-molded scaffolds from chitosan-polyester blends and composites: Morphology and mechanical properties". J. Biomed. Mater. Res., Vol 91A, pp. 489–504.

- DeLeo, C. L., Velankar, S. S. (2008), “Morphology and rheology of compatibilized polymer blends: Diblock compatibilizers vs crosslinked reactive compatibilizers”, J. Rheol. Vol 52, issue 6, pp. 1385-1404

- Exner, G., Perez, E. and Kasteva, M. (2016), in e-book: Liquid Crystalline Polymers: Volume 1–Structure and Chemistry, edited by: Thakur, V, G, Kessler, M, R, Springer Cham, New York, Pages 24-46

- Gonzalez, M. G., Cabanelas, J. C. and Baselga, J. (2012), “Applications of FTIR on Epoxy Resins –Identification, Monitoring the Curing, Process, Phase Separation and Water Uptake”, Infrared Spectroscopy - Materials Science, Engineering and Technology, Prof. Theophanides Theophile (Ed.), ISBN: 978-953-51-0537-4, InTech, [online] Available at: http://www.intechopen.com/books/infrared-spectroscopymaterials-science-engineering-and-technology/applications-of-ftir-on-epoxy-resins-identification-monitoringthe-curing-process-phase-separatio (Accessed 1 June 2016)

- Harvard, (2016), “Interpreting Infrared Spectra Painlessly, quickly, and correctly”, [online] available at: http://isites.harvard.edu/fs/docs/icb.topic26158.files/Interpreting%20IR.pdf (Accessed 21 Aug 2016)

- Hobbs, S. Y., Watkins, H. V. (2000), “Morphology Characterization by Microscopy Techniques”, in book of: Polymer Blends, Vol1, by Paul and Bucknall, , pp. 244-245

- Iannace, S., Ambrosio, L., Huang, S. J. and Nicolas, L. (1994), “Poly(3-hydroxybutyrate)-co-(3-hydroxyvalerate)/Poly-L-lactide blends: Thermal and mechanical properties”, , Journal of Applied Polymer Science, Vol 54, Issue 10, pp. 1525–1535

- Japon S., Luciani A., Nguyen Q. T., Leterrier Y. and Manson J. A. , (2001), “Molecular Characterization and Rheological Properties of Modified Poly(Ethy1ene

Terephthalate) Obtained by Reactive Extrusion ,Polym Eng Sci, Vol 41 , issue(8), pp1299-1309.

- Karasz, F. E. (1985)"glass transition and compatibility ;phase behaviour in copolymer containing blends", in polymer blends and mixtures Walsh , D, J, Higgins,J,S and A. Maconnachie(eds),Martinus Nijhoff Publishers,Boston

- Kum, K. C., Sung, Y. T., Kim, y. S., Lee, G. H., Kim, N. W., Lee, H. S., and Yoon, H. G. (2007), "Effects of compatibilizer on mechanical, morphological, and rheological properties of polypropylene/poly (acrylonitrile-butadiene-styrene) blends", Macromolecular Research, Vol 15, Issue 4, pp. 308-314

- Kumar, A. and Gupta, K. R. (1997), "Polymer Crystallization", in book of Fundamentals of Polymer Engineering, Marcel Dekker Inc., pp. 452

- Liu, Q. S., Zhu, M. F. and Chen, Y. M. (2010) "Synthesis and characterization of multi-block copolymers containing poly [(3-hydroxybutyrate)-co-(3-hydroxyvalerate)] and poly (ethylene glycol)", Polym Int, Vol 59, Issue 6, pp. 842–850

- Matsuka, S. and Kwei, K. T. (1979), "Physical behaviour of macromolecules", in book Macromolecules: An Introduction to Polymer Science edited by Bovey, F, A and Winslow,F, H , Academic Press inc, pp. 380-393

- Miao, L., Qiu, Z., Yang, W. and Ikehara, T. (2007), "Fully biodegradable poly (3-hydroxybutyrate-cohydroxyvalerate) /poly (ethylene succinate) blends: Phase behavior, crystallization and mechanical properties" , Journal of Reactive & Functional Polymers, vol 68 (2008),pp. 446–457

- Ohkita,T. and Lee, S. H. (2005), "Crystallization Behavior of Poly(butylene succinate)/Corn Starch Biodegradable Composite", Journal of Applied Polymer Science, Vol. 97, pp.1107–1114

- Peng, S., An, Y., Chen, C., Fei, B., Zhuang, Y. and Dong, L. (2003) Isothermal crystallization of poly (3-hydroxybutyrate-co-3-hydroxyvalerate). Eur Polym J Vol 39, pp. 1475–1480

- PerkinElmer, (2016), Available at: http://www.perkinelmer.co.uk/CMSResources/Images/44-74546GDE_IntroductionToDMA.pdf Accessed 19 Aug 2016

- Pilla, S., Kramschuster, A., Yang, L., Lee, J., Gong, S. and Tung, L. S. (2009), "Microcellular injection-molding of polylactide with chain-extender", Materials Science and Engineering C, Vol 29, Issue 4, pp. 1258–1265

- Qui, Z., Ikehara, T. and Nishi, T. (2003), "Poly (hydroxybutyrate)/poly (butylene succinate) blends: miscibility and non-isothermal crystallization", Polymer journal , Vol 44 , pp. 2503–2508

- Qui, Z., Ikehara, T. and Nishi, T. (2003), "Miscibility and crystallization behaviour of biodegradable blends of two aliphatic polyesters. Poly (3-hydroxybutyrate-co-hydroxyvalerate) and poly(butylene succinate) blends", Journal of Polymer ,Vol 44 (2003),pp 7519–7527

- Rim, P. B. and Runt, J. P. (1982), "Melting Point Depression in Crystalline/ Compatible Polymer Blends", Macromolecules Journal, Vol 17, pp. 1520-1526

- Roe, R. J. (1993), "Use of Block Copolymer as Polymer Blend Compatibilizer", available online at: http://www.dtic.mil/dtic/tr/fulltext/u2/a260435.pdf (Accessed 21 Aug 2016)

- Runt, J. P., Rim, P. B. and Howe, S. E. (1984) "Melting Point Elevation in Compatible Polymer Blends", Polymer Bulletin, Vol 11, pp. 517-521

- Ryan, A. J. (2002), "Polymer Science: Designer Polymer Blends", Journal of Nature Materials, Vol 1, pp. 8-10

- Smith, G. D., Bedrov, D. (2006), “Relationship Between the a- and b-Relaxation Processes in Amorphous Polymers: Insight From Atomistic Molecular Dynamics Simulations of 1,4-Polybutadiene Melts and Blends”, Journal of Polymer Science Part B: Polymer Physics, Volume 45, Issue 6, pp.627-643

- Tang, W., Wang, H., Tang, J., and Yuan, H. (2012) “Polyoxymethylene/Thermoplastic Polyurethane Blends Compatibilized with Multifunctional Chain Extender”, Journal of Apply Polymer Science, Vol 127: pp. 3033–3039

- Verhoogt, H., Ramsay, B. A. and Favis, B. D. (1994), “Polymer blends containing poly (3-hydroxyalkanoate) s”, journal of Polymer, Vol 35, Issue 24, pp. 5155-5169

- Villalobos, M., Awojulu, A., Greeley, T., Turco, G. and Deeter G. (2006), “Oligomeric chain extenders for economic reprocessing and recycling of condensation plastics”, Journal of Energy, Vol 31, pp. 3227–3234

- Wang, X., Chen, Z., Chen X. and Xu, K. (2010), “Miscibility, crystallization kinetics, and mechanical properties of poly(3-hydroxybutyrate-co-3-hydroxyvalerate)(PHBV)/poly(3-hydroxybutyrate-co-4-hydroxybutyrate)(P3/4HB) blends2, Journal of Polymer Science, Vol 117, Issue 2 , pp. 838–848

- Ward, I. M., Hadley, D. W. (1993), “An Introduction to the Mechanical Properties of Solid Polymers”, Wiley, New York.

- Wunderlich, B. (2005), “Thermal Analysis”, New York: Academic Press, pp. 400-402

- Zhang, L., Xiong, C. and Deng, X. (1995), “Biodegradable polyester blends for biomedical application”, Journal of Applied Polymer Science, Volume 56, Issue 1, pp. 103–112

Chapter 5

Effect of the core-shell structure impact modifier on mechanical, thermal, crystallization and morphology of PHBV

5.1 Introduction

PHAs are a family of environmentally degradable polymers (biopolymer) which can be a possible substitute for some petroleum based polymers. Mechanical properties of PHBV, a copolymer of PHA's family make them suitable replacements for petrochemically produced bulk plastics (polyethylene, polypropylene etc.). However, some serious drawbacks associated with PHBV have hindered its widespread usage. Issues such as a narrow processing window, low impact resistance and brittleness coupled with a sluggish crystallinity and a rapid thermal degradation that provide challenges for using the material in conventional processing machinery. There have been several attempts by researches to overcome the low impact resistance of PHBV and also the brittleness. Blending with biopolymers or conventional petroleum based polymers, compounding with the rubbery polymers or impact modifier additives have been reported in researches (Corre, Bruzaud and Grohens, 2013, Javadi et al, 2010, Avella, 1995)

5.2 Material

ENMAT^{TM} Y1000 is PHBV with 3 mol% of hydroxyvalerate (HV) content without any additive substances and supplied in white powder form manufactured by Tianan Biologic Material Co. (Ningbo, P. R.China). It has molecular weight of $4.5x10^5$, Purity=>98%, specific gravity 1, 25 g/cm^3. Core-Shell Acrylic impact modifier additive, Biostrength^R 280 was kindly supplied by Arkema, France in a white powder form, with a specific gravity of 1.0 and density of 0.45 g/cm^3, and a particle size of 2% max on 500 nm.

5.3 Sample preparation

5.3.1 Preparation of the blend

Before processing through an extruder, the PHBV in powder form was first dried in a vacuum oven at a temperature of 60◦C for 24 hours to remove moisture. Drying of this polymer is vital as moisture induces a hydrolytic chain scission at the high processing temperature. The Biostrenght Impact modifier powder is used as it was received. All the components were premixed in a plastic bag by manually tumbling for 5 mins and were fed by a calibrated powder twin screw feeder into the extruder. The extruder used was a Betol co-rotating intermeshing twin-screw extruder (40 mm diameter, L/D =21/1, Amp=5-10) running at 200 rpm, The extruder consisted of five barrel sections and each section was equipped with independently controllable electric heating and water cooling system. All of the extrusion variables, including barrel and die temperatures, are shown in table 1-5:

Table 1-4 Temperature profile of the extrusion process

Section	Zone6 (Die)	Zone 5	Zone 4	Zone 3	Zone 2	Zone 1
Temperature	170	175	180	170	170	160

Using a single strand die, the extrudate was cooled through a water bath and then palletized for subsequent processing. A few of the batches were not possible to strand because of their high viscosity. These batches were collected from the die and then granulated by a S.U.I-Cumberland granulator.

5.3.2 Injection moulding

The specimens for mechanical properties were obtained by injection moulding in a Demag NC III, 1.5 ton, injection moulding machine. Table 2-5 shows the processing parameters:

Table 2-5 Injection molding parameters of PHBV and PHBV/Impact modifier

Conditions	First heating zone ℃	Second heating zone ℃	Third heating zone ℃	Fourth heating zone ℃	Nozzle heating ℃	Injection pressure bar	Injection time sec	Cooling time sec	Cycle time sec	Mould temperature ℃	Injection speed
Tensile bar	140	155	170	170	170	160	4	60	82	30	**Medium**
Plate	140	150	165	165	165	160	4	60	82	30	**Medium**

All the processing parameters were modified during the several trial mouldings in order to obtain satisfactory specimens. The biggest issue for the processing of the specimens was the residence time for the material in the barrel of the injection moulding machine. The first 8 to 10 specimens looked fine and consistent but then for the next specimens, they start to shrink at the edges and deformation continues because probabely material would have remained more in the barrel. Therefore the smallest injection moulders can reduce the residence time inside heating zones.

5.4 Experimental

5.4.1 Differential Scanning Colorimetery (DSC)

The melting temperature T_m of the project materials was measured by a TA Instruments DSC/Q2000 with a Universal Analysis 2000. The measurements were carried out under a

nitrogen atmosphere to minimize oxidative degradation. The specimens were encapsulated in DSC aluminium Tzero pans and placed into the closed calorimeter cell. The instrument was calibrated with indium prior to starting the test.

5.4.1.1 Non-isothermal crystallization

The samples were first heated to 200 ℃ at a heating rate of 10 ℃/min. They were then held isothermally for 5 min to eliminate the effect of the previous thermal history. The samples were then cooled at the rate of 10 ℃/min to -20 ℃ and then again heated to 200 ℃ with same heating rate for obtaining the second heating cycle (10 ℃/min).

5.4.1.2 Isothermal crystallization

PHBV neat and PHBV/impact modifier samples with weight fractions of 97/3, 94/6, 90/10, 85/15, were heated up to approximately 30 ℃ above the melting point (about 200 ℃), and held isothermally for 5 minutes to eliminate the previous thermal history. The sample was then rapidly cooled down at the rate of 80 ℃/min to the required isothermal temperature and kept at that point until crystallization was completed. The procedure was repeated for three pre-determined temperatures of 100 °, 110 °, and 120 ° C for each of the compounds. The curves of heat flow (W/g) versus time (min) shown in (Figure3-5).

5.4.2 Thermogravimetric Analysis (TGA)

The thermal stability of the PHBV and the process of thermal decomposition were investigated by Thermogravimetric analysis (TGA) using a TA instrument “The New Discovery TGA”, with TRIOS software version 3.3.0.4055 under nitrogen atmosphere. The temperature range was from room temperature to 650 ℃ with a heating rate of 10 ℃/min.

5.4.3 Dynamic Mechanical Analysis (DMA)

Dynamic Mechanical analysis (DMA) was performed using a DMA Q800, TA, USA. The accurately measured rectangular samples 127x12x4 mm were cooled to -50 ℃ and then heated up to 150 ℃, with heating rate of 2 ℃/min, under a maximum force of 1 N, a frequency of 1 Hz and an amplitude of 5 μm using the single cantilever system.

5.4.4 Morphology with SEM

The morphologies of Biostrength , and PHBV/Biostrength compounds were analysed using a scanning electron microscope. A SUPRA ZEISS 35VP with 20KV accelerating voltages and SE detector was used. The scanning electron microscopy of fractured surfaces of Charpy impact test peaces was conducted at room temperature. The specimens were dried for two hours prior to gold coating.

5.4.5 Impact properties

There are several methods for measuring the impact behaviour of polymers, such as Charpy and Izod impact test (notched and un-notched) and Gardner drop-ball or drop-weight test. In order to investigate the impact properties with the energy rate higher than the maximum pendulum performance, and more accurate results, a drop weight instrument was used.
The PHBV and PHBV/IM blends were injection moulded into the rectangular 150x150x4 mm plates according to BS EN ISO 6603 using the conditions given in table 2. The injection moulded plates were then cut into 60x60 mm squares and labelled for impact testing. The impact conditions of the test were set according to the BS EN, ISO 6603 drop weight method. A CEAST Fractovis Plus instrumented impact tester Model 7520 was used.

5.5 Thermal properties

5.5.1 Non-isothermal crystallization

Non-isothermal second heating cycles of DSC results for PHBV neat and PHBV/impact modifier in different concentration are illustrated in Figure 1-5.

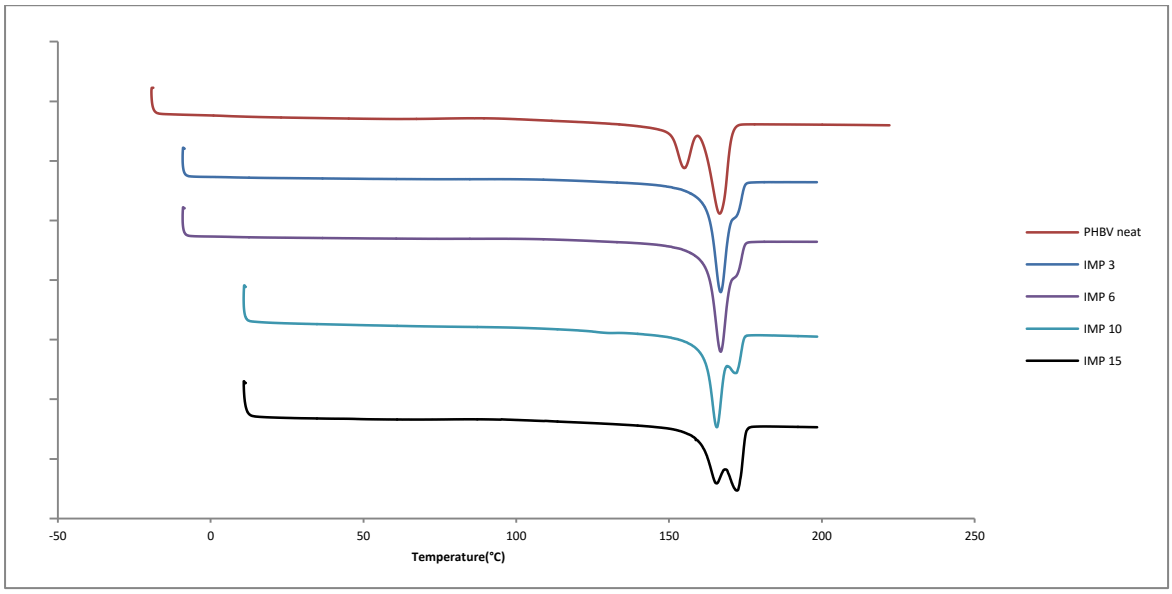

Figure 1-5 The second heating scan of non-isothermal DSC graphs for the neat PHBV(red) and PHBV/IM 97/3 (blue), 94/6(velvet), 90/10 (cyan), 85/15 (black)

As it is shown in Figure 1-5, the neat PHBV showed two melting points at 155 ℃ and 166.56 ℃ due to the recrystallization. The addition of the 3 *wt*% impact modifier removed the first melting point (155 ℃) and revealed a sharp peak at 167.05 ℃ with a small shoulder. The addition of the 6 *wt*% IM hadn't changed the melting point and its intensity. The addition of 10 *wt*%, a peak at 165.58 *wt*% is observable and the small shoulder has become more visible showing a second melting point at 171 ℃. Finally, with the addition of 15 *wt*% the first melting peak at 165.53 ℃ became less intense than the second one at 172 ℃. The second melting point at higher concentrations could be attributed to the melting point of the shell polymer in the impact modifier.

5.5.2 Isothermal crystallization

The effect of the Biostrength impact modifier on the isothermal crystallization of PHBV was studied using the Avrami's method described earlier (Chapter 3-4-2).

The comparison of the DSC graphs of the neat polymer and its compound with the impact modifier in the three concentrations of 3, 6, 10 *wt %*, and also the relative crystallinity, at the different temperatures are shown in Figures 2-5 and 3-5, respectively.

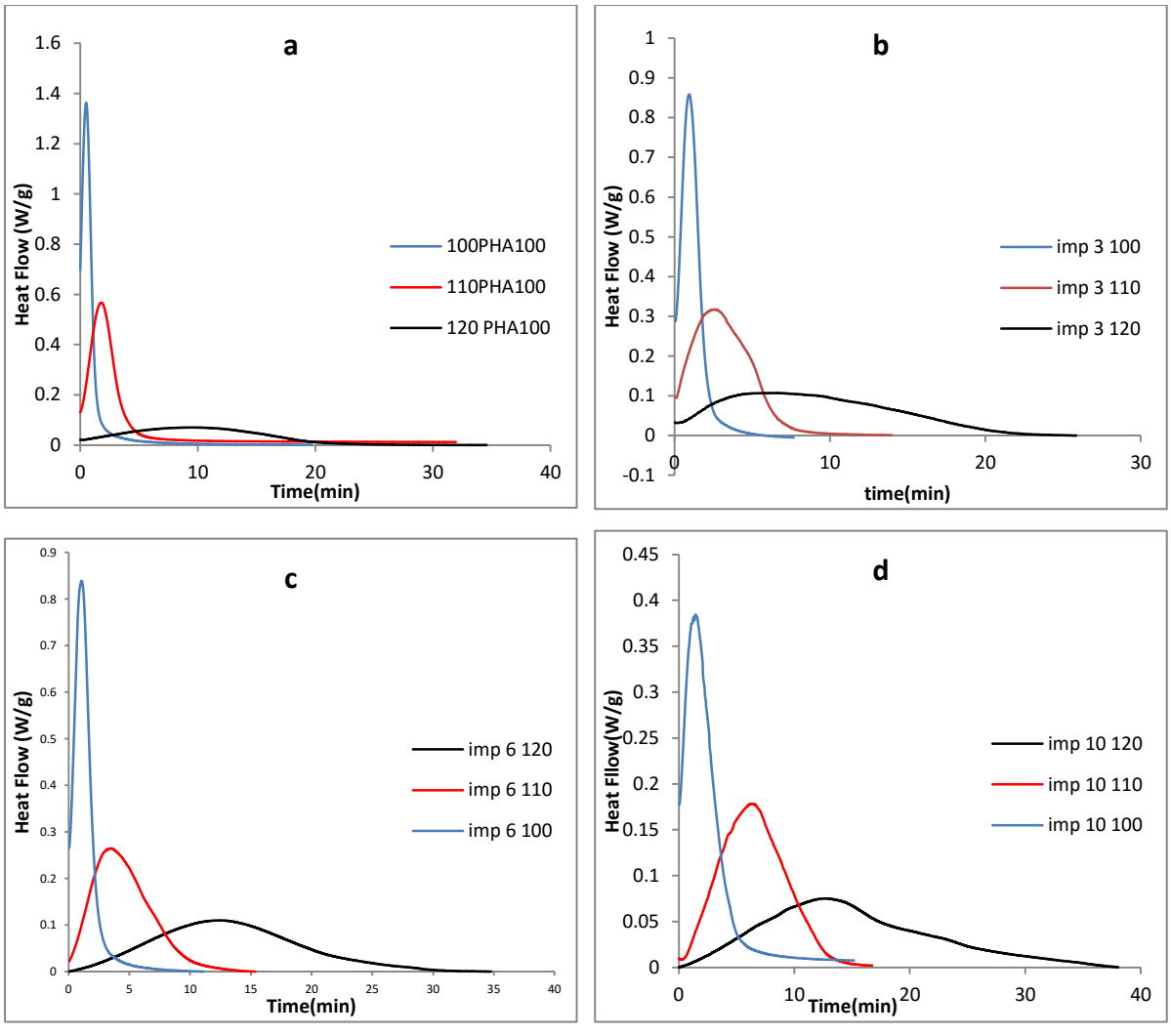

Figure 2-5 DSC isothermal crystallization graphs (Exo up) at 100,110,120 ℃ for a) neat PHBV 100/0 b) PHBV/IM 97/3 c) PHBV/IM 96/4 d) PHBV/IM 90/10

Figure 4-5 shows the relative crystallinity of PHBV neat and PHBV/impact modifier at the three different concentrations and the three set crystallization temperatures vs time. It is clear that the time to 100% crystallization (maximum level of crystallinity for the compound) is temperature dependent for all specimens.

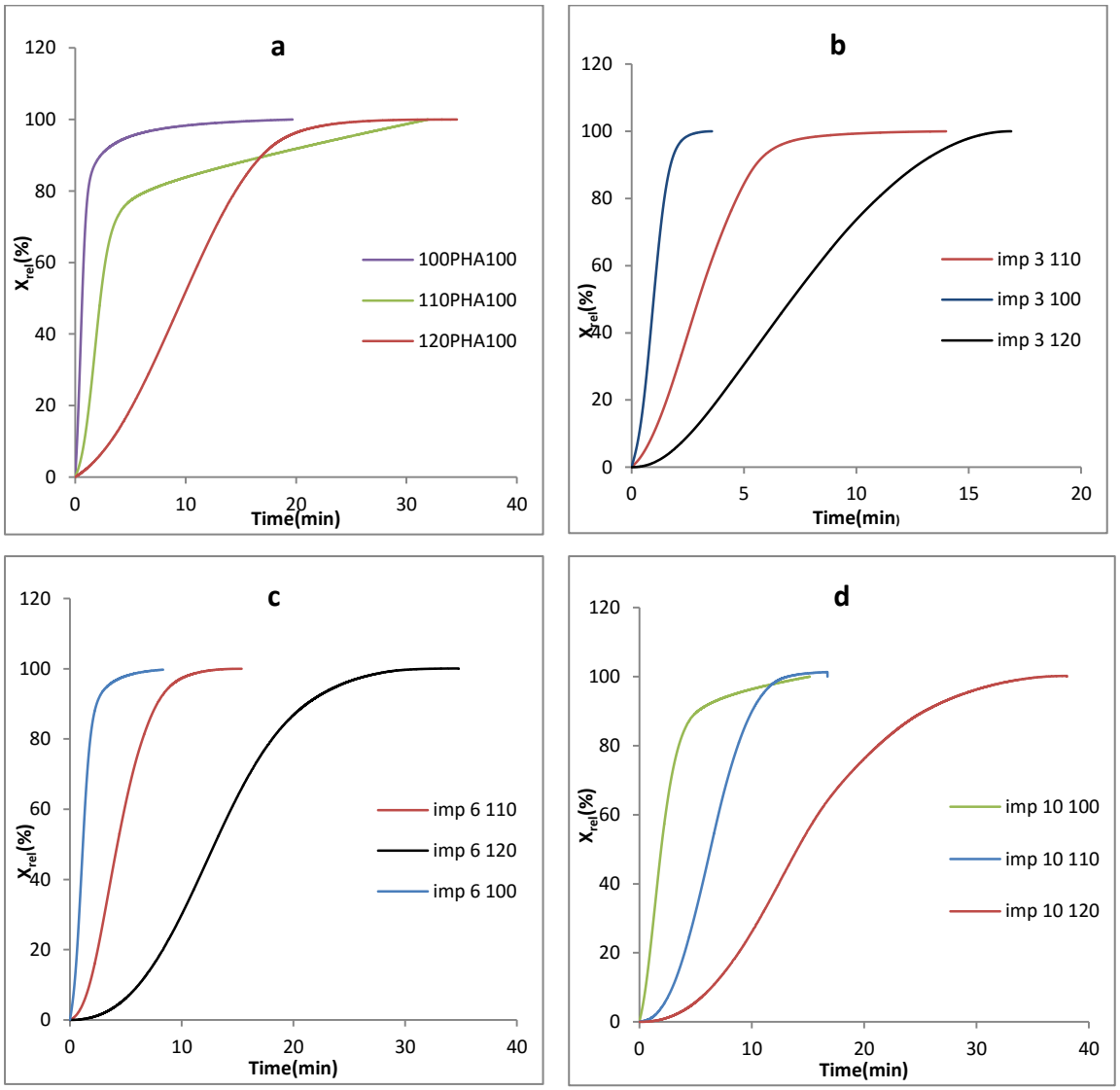

Figure 3-5 Development of relative crystallinity X_{rel} with the PHBV crystallization time (t) at the set isothermal crystallization temperature of 100 °, 110 °, and 120 °C for a) 100/0,b) 97/3,c) 94/6, d) 90/10 PHBV/IM blends

It can be clearly seen at Figure 2-5 b, c, d and Figure 3-5b, c, d that addition of the Biostrength impact modifier to the PHBV reduced the crystallization rate and prolonged the crystallization time.

Figure 4-5 illustrate the log [-ln (1-X_{rel})] vs log (t), and from the slope and the intercept of the graphs in figure 4-5 the Avrami's components, *n* and *k* were calculated (Table 3-5). The time to half crystallinity $t_{0.5}$ has been calculated from the equation (4-3).

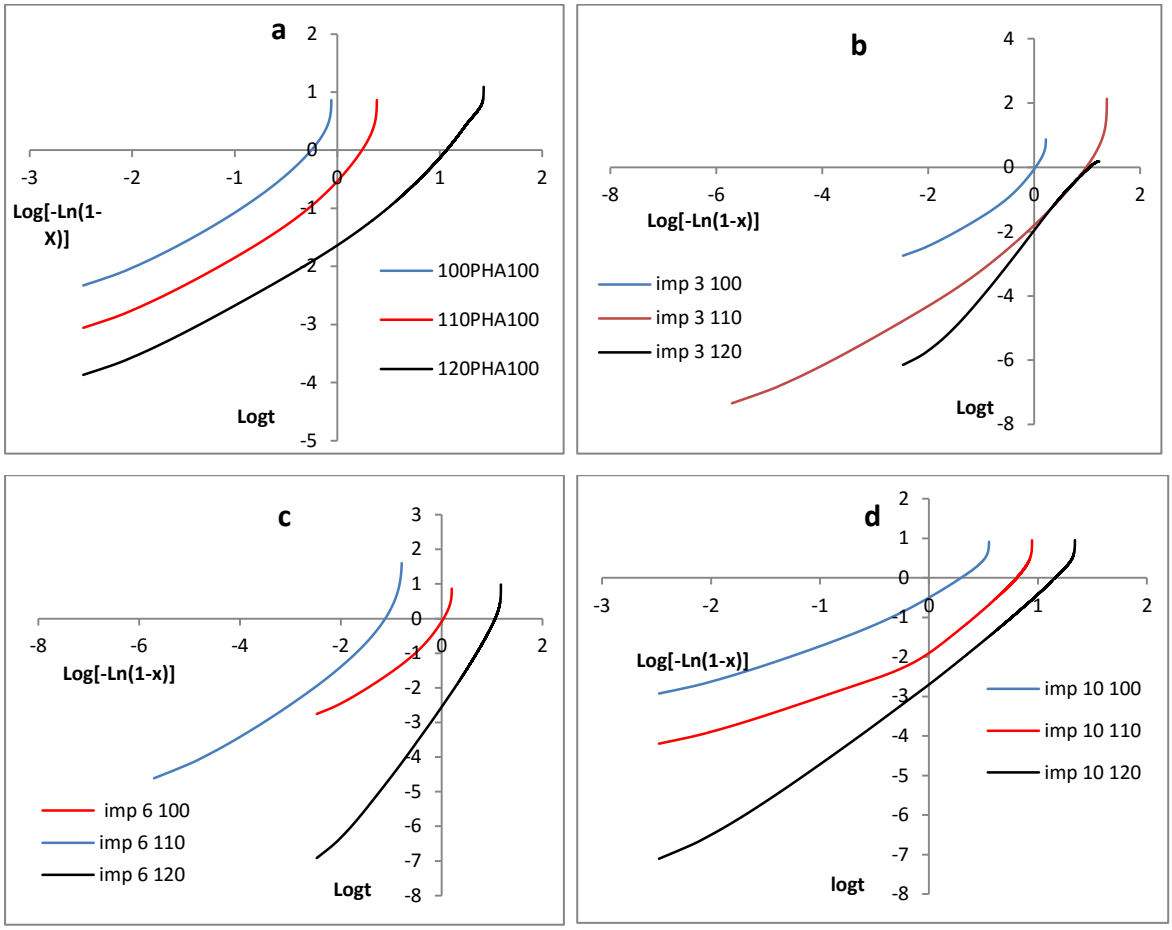

Figure 4-5 The related Avrami plots of PHBV crystallization and PHBV/IM blends

At a constant temperature, the Avrami's component, *n* for the PHBV with the different Biostrenght concentrations changed slightly. This could be explained by the crystallization mechanism not being affected by increasing the content of the impact modifier.

However, at 120 ℃, the value of *n* for the PHBV is lower than the PHBV/IM blends. This could be explained by the nucleation effect of the impurities in the neat polymer. Pan et al

stated that neat polymer usually contains some impurities that can induce the heterogeneous nucleation to some extent, which can surpass the ideal sporadic and homogenous nucleation in crystallization. This may cause a decrease of the *n* value of the neat polymer (Pan et al., 2013).

Table 3-5 Avrami exponent (n), crystallization rate constant (*k*) and half-time crystallization ($t_{1/2}$), at different pre-determined crystallization temperature of 100,110,120 °C

PHBV/Biostrength	T_c (℃)	*n*	*k* (min^{-1})	$t_{0.5}$ (min)
100-0	100	1.43	2.41	0.41
	110	1.59	0.34	1.85
	120	1.65	0.025	8.5
	100	1.56	2.19	0.48
97-3	110	1.98	0.20	1.85
	120	2.06	0.011	7.46
	100	1.51	0.87	0.86
94-6	110	2.02	0.042	3.41
	120	2.37	0.0028	10.12
	100	1.50	0.4	1.45
90-10	110	2.01	0.021	5.66
	120	2.28	0.00207	12.71

The value of *n* at the higher isothermal temperature is different from that at the lower temperature. It indicated that *n* is temperature dependent.

The value of *k* in the Avramis equation decreased in each compound with an increase in the crystallization temperature while the value of $t_{0.5}$ (half-time crystallization) increased with an increase of the crystallization temperature. The value of $t_{0.5}$ also increased with increasing the impact modifier concentration in compound. This meant that the presence of the impact modifier retarded the rate of crystallization of the PHBV inside the compounds.

5.5.3 Thermogravimetric analysis (TGA)

Thermogravimetric analysis (TGA) was used to determine the thermal stability and decomposition of the PHBV and PHBV/Impact modifier blends. The thermal stability of the investigated samples was determined by the value of T_i, the initial decomposition temperature and T_e, the temperature of the maximum rate of the PHBV decomposition. The residue of the specimens at 600 °was also recorded.

Figure 5-5 shows the TG curves of the PHBV and PHBV/IM and the results are given in Table 4-5.

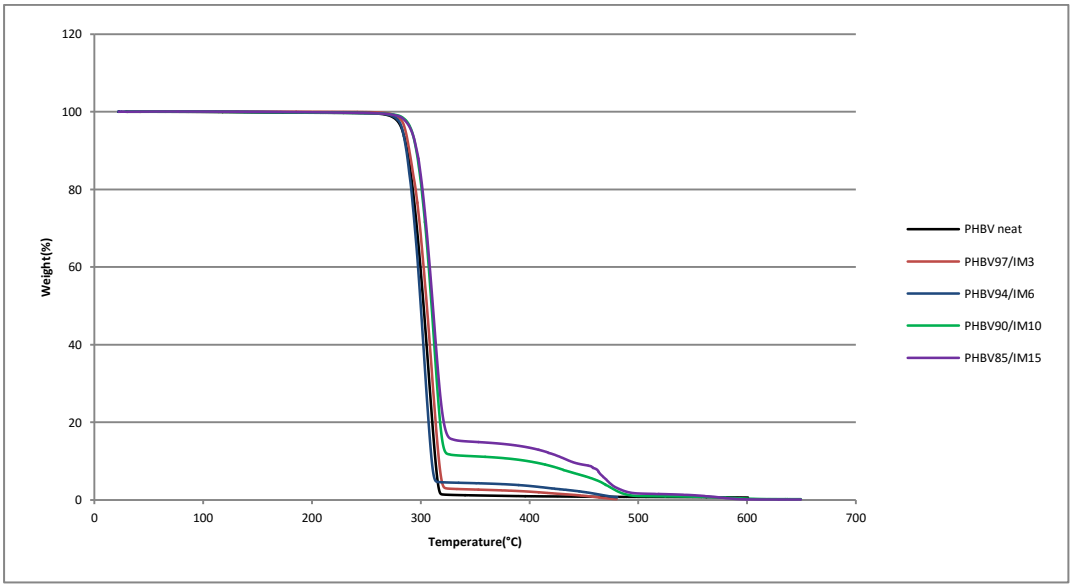

Figure 5-5 Thermal Gravimetric Analysis (TGA) for the neat PHBV and the PHBV/IM

Tabel 4-5 & Figure 5-5 shows that the thermal stability of PHBV is not significantly affected by the presence of the Biostrength impact modifier in the low concentrations of 3 *wt* % and 6 *wt* %. However, with addition of 10 and 15 *wt* % impact modifiers in the blends, the initiation temperature of the decomposition has shifted by about 5 and 6 degrees higher than that of the neat polymer.

Table 4-5 The value of T_i, the initial decomposition temperature, Δm_i =Mass loss in T_i (%), T_e, the temperature of the maximum rate of the PHBV decomposition and the residue of specimens at 600 °for the neat PHBV and the PHBV/IM

Specimens PHBV/IM	T_i (℃)	Δ_{mi} (%) (Mass loss)	T_e (℃)	Residue at 600 ℃ (%)
100/0	253	98	310	0.64
97/3	255	97	323	0.73
94/6	254	95	315	0.78
90/10	259	89	326	0.70
85/15	260	84	327	0.81

The weight loss of PHBV/IM happened in a two-step process. Δ_{mi} (%) is the mass loss at $T_{e,}$ and shows the remained mass at the maximum temperature of decomposition in blend. It is an important aspect that impact modifier is more or less thermally stable at the temperature up to 327.5 ℃.

The temperature of the maximum rate of decomposition, T_e , is retarded by almost 12 ℃ by the addition of 3 *wt*% impact modifier. With addition of 6 *wt*%, T_e is changed by 5 ℃. With the 10 % and 15% addition of the impact modifier, it shifted again to about 16 ℃ higher than that of the neat PHBV. As shown in the Table 4-5, the residue at 600 ℃ (%) is similar for the all samples.

5.6 Thermomechanical Properties

5.6.1 Dynamic Mechanical Analyser (DMA)

The storage modulus curves of PHBV/impact modifier blends are illustrated in Figure 6-5a. The graph shows a gradual decline in the storage modulus with increasing of the impact modifier concentration in blends. All of the graphs have a sharp drop between 0 and 50 ℃ which is associated with the glass transition region of the PHBV.

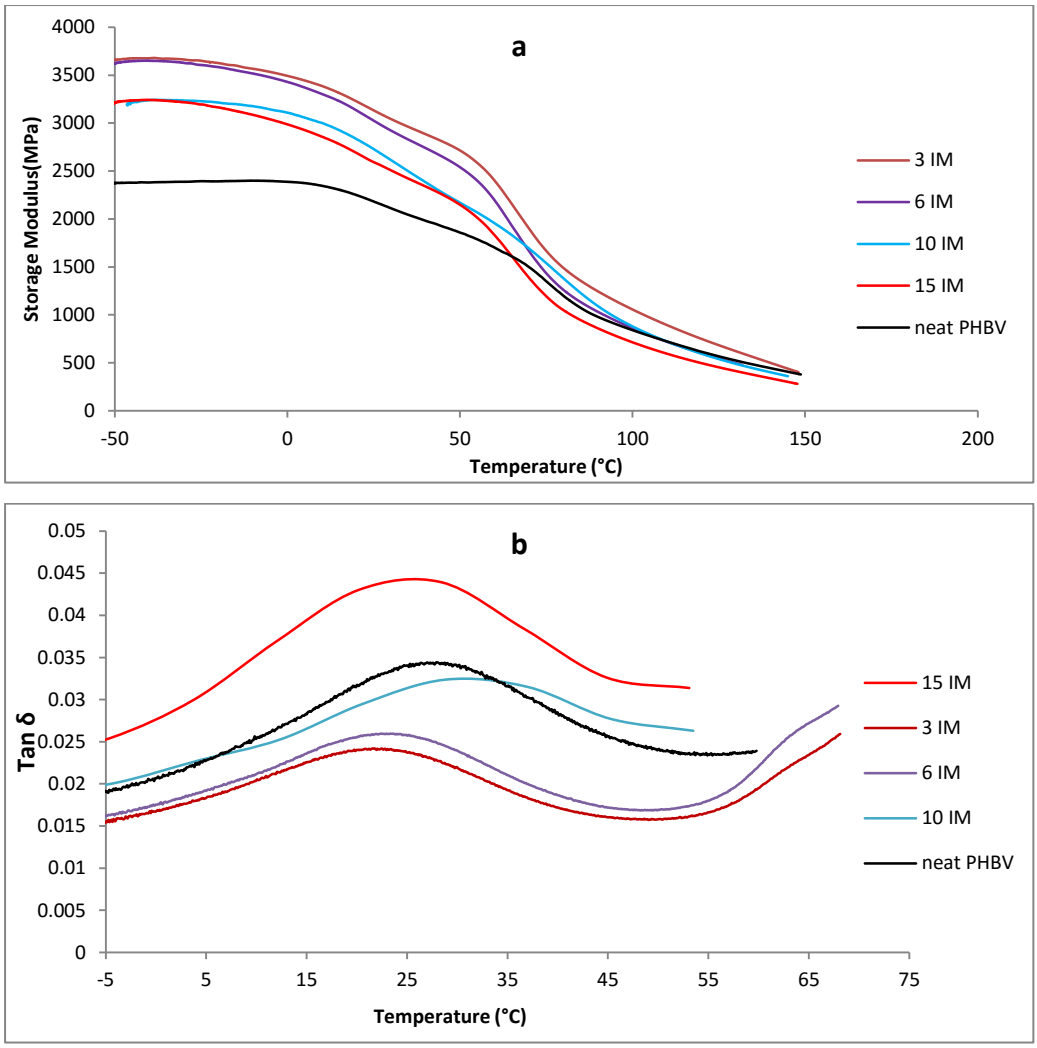

Figure 6-5 Dynamic mechanical Analysis for neat PHBV and PHBV/impact modifier (97/3, 94/6, 90/10, 85/15) .a) Storage modulus b) Tan δ

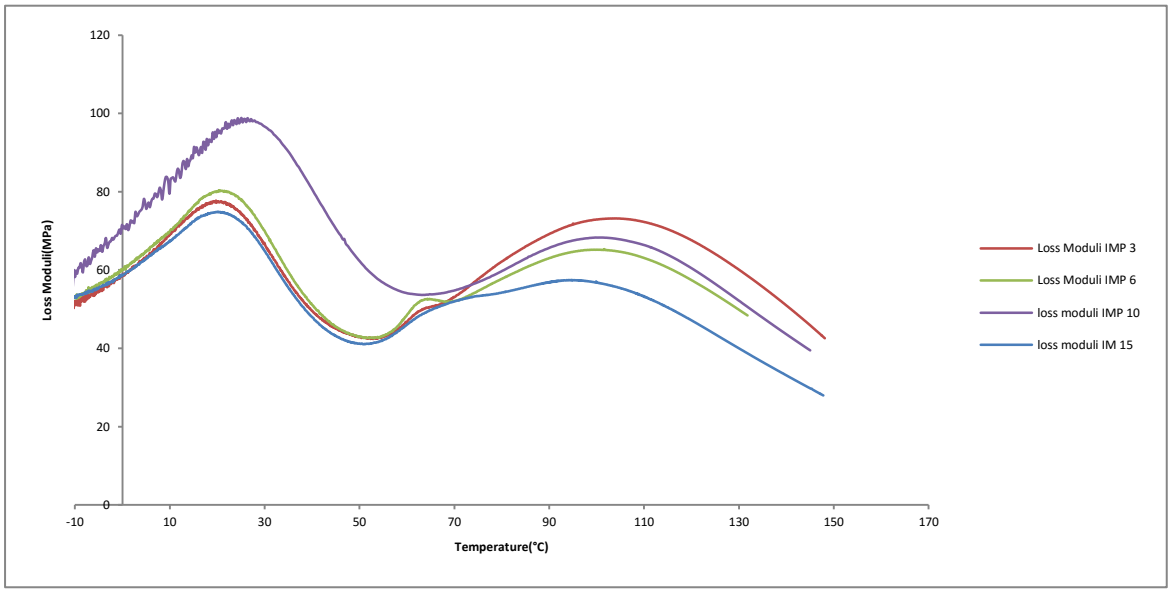

Figure 7-5 The loss modulus curves from DMA results for PHBV/IM 97/3, 94/6, 90/10, 85/15

The graphs in Figure 6-5 show that with incorporating of 3 *wt*% impact modifier in the PHBV, the storage modulus increased significantly in the low temperature range between 0 to 60 ℃. It indicates a decrease in the flexibility of the compounds. But however, as the concentration of the impact modifier increased in blends, the storage modulus dropped and became more sudden. It indicates that the rigidity of PHBV/impact modifier blends decreases as the impact modifier concentration is increasing. However at temperatures higher than 60 ℃, the storage modulus decreased and the values are become close to each other which indicate the enhancement of the rigidity of the samples.

The tan δ curves of PHBV neat and PHBV/impact modifier blends are shown in figure 6-5b. This shows clearly that in the temperature range between -50 to 70 °C only one peak is observable from the tan δ curves. This corresponds to the glass transition temperature of the PHBV. It changes slightly for the different concentrations of the impact modifier in the blends. However in all the curves the region behind the glass transition, the graph become noisy which could be an effect of the impact modifier in the blend.

In fact, a tan δ peak for the glass transition of PMMA was expected from the core of the Biostrength core-shell impact modifier. None of samples however, showed a distinguishable peak for the PMMA glass transition at temperatures up to 150 ℃.

However, from the loss modulus curves (Figure 7-5) there are a clear peaks which correspond to the PMMA glass transition temperature (T_g^{PMMA} = 100 °C). From the loss modulus curves, it is clear that there are two T_g s in the graph corresponding to PHBV and PMMA indicating the partially immiscibility of the blend of the two polymers.

The glass transition of the PHBV is slightly changed to a lower temperature for the samples with 3% IM (T_g=21 ℃) and6% IM (T_g=22 ℃) but it significantly increased for the compound with10% IM (T_g=31 ℃). However, it dropped for 15% IM to a value of T_g =26 ℃, which is quite close to the PHBV glass transition temperature (T_g=27 ℃). The PHBV/IM tan δ maxima as well as the corresponding glass transition temperatures were also observed in the temperature range between 20 to 30 °C. They increase slightly with an increase in the impact modifier concentration. These phenomena could be explained by an increase of the partial immiscibility of the PHBV with the impact modifier, but it is not a significant change.

5.7 Mechanical properties

5.7.1 Tensile and Flexural Testing

The effect of the core-shell impact modifier on the mechanical properties of PHBV was studied by the tensile and flexural test.

The typical stress-strain curve of PHBV/IM and Tensile Strength (MPa), Young's modulus (GPa), Elongation at break (%) and Flexural modulus (GPa) results are shown Figure 8-5 b, c, d and Figure 9-5.

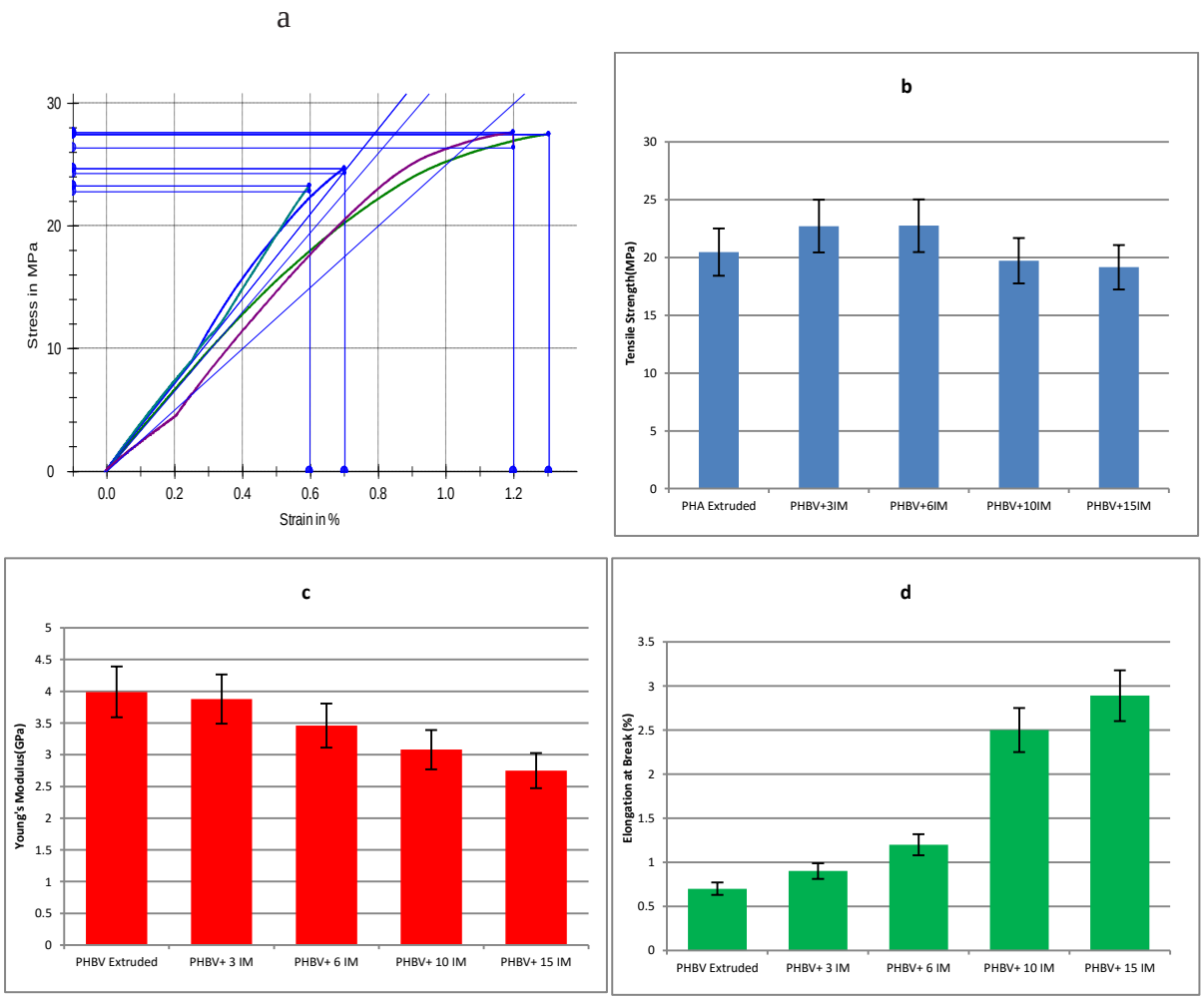

Figure 8-5 a) Typical stress strain graph for PHBV/IM –b) the Tensile Strength,-c) Young's Modulus and –d) Elongation at Break for the PHBV extruded and PHBV/Impact Modifier

It can be seen that the addition of 3% & 6 % impact modifier increases the tensile strength of the PHBV. The addition of 10% and 15% impact modifier, however, cause it to fall slightly. All samples showed brittle fracture similar to pure PHBV despite an increase in elongation at breaks.

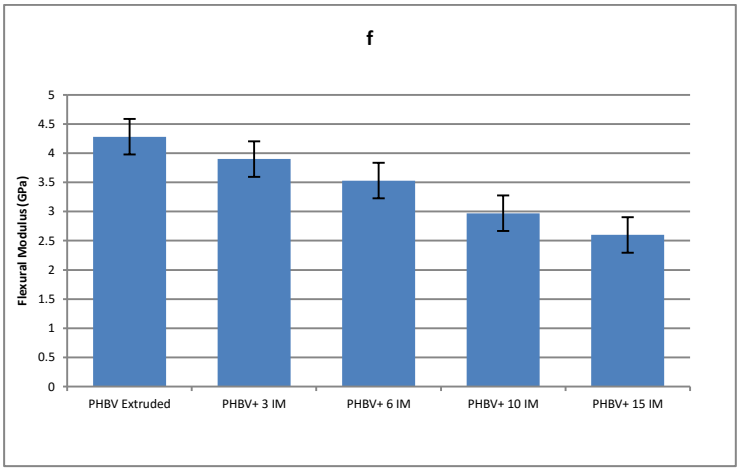

Figure 9-5 Flexural modulus for the PHBV extruded and PHBV/Impact Modifier

All samples didn't show any clear yielding behaviour upon stretching. Elongation at break % increases with an increase in the impact modifier content. On the other hand, the Young's modulus and the flexural modulus decreased with an increase in the impact modifier content. This could be explained by the effect of the lower modulus of the impact modifier on the overall modulus of the blends. Cruz-Ramos stated that as general rule, acrylic-type and MBS-type core-shell impact modifiers reduce the flexural modulus in various engineering resins and the modulus decreases by increasing the amount of additive in polymer. Epoxy systems toughened by about 15% impact modifier showed a 10 to 15 % reduction in the tensile and compressive yields (Cruz-Ramos, 2000).

A reduction in the modulus was to be expected by the presence of the impact modifier because the core is rubbery and soft. Moreover, another reason for the modulus reduction would be the poor dispersion of the core-shell particles in the polymer matrix due to a lack of immiscibility between shell polymer and matrix polymer. According to Kayano et al a large modulus reduction occurs when the dispersion is poor. They also stated that it is not just the size of the dispersed phase alone but the shape of these regions and the distribution of the modifiers in the matrix that could reduce the modulus. Moreover, a tendency towards co-continuity when the modifier is poorly dispersed will lead to a greater loss in stiffness (Kayano et al, 1996).

5.7.2 Impact properties

Dropped- weight impact tests on plate specimens are commonly used to study the practical fracture resistance of thermoplastic blends. The advantage of the drop-weight test is the simplicity, however, it is difficult to analyse the results mathematically. The impact properties of PHBV have been investigated by an instrumental drop-weight impact test. Figure 10-5 shows the appearance of plates subjected to the drop-weight impact test. Figure 11-5 shows the PHBV/impact modifier specimens at different concentrations.

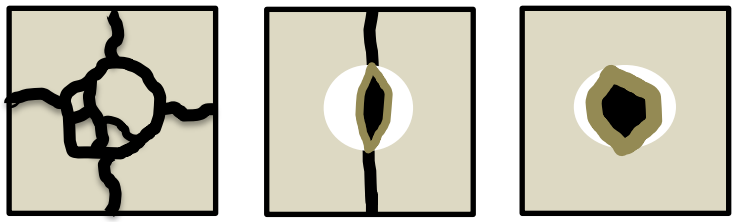

Brittle Semi-Brittle Ductile

Figure 10-5 Schematic diagram showing the appearance of plates subjected to falling – weight impact test and undergoing brittle, semi-brittle, and ductile failure (Bucknal, 2000)

a b

Figure 11-5 three different failure of PHBV/Impact modifier specimens a) 3% and 6% IM, b) 10% & 15 % IM

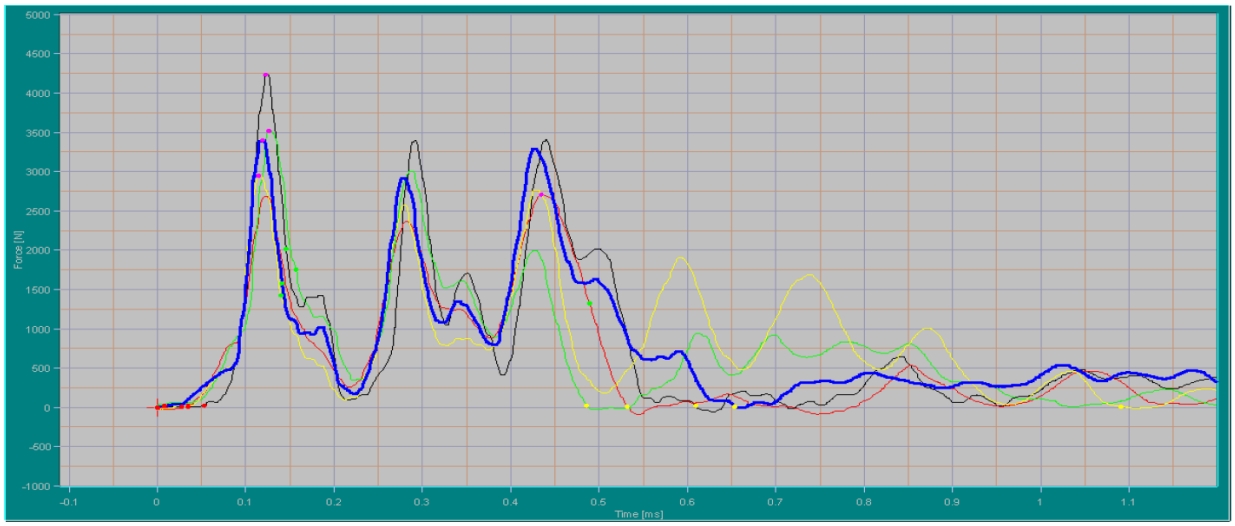

Figure12-5 Typical drop- weight impact test for PHBV/IM[Y axis is Force (N) and X axis is time (sec)]

Figure 12-5 shows a typical dropped-weight impact test for PHBV/IM specimens. The results are shown in table 5. Specimens with low concentrations of impact modifier showed brittle and semi brittle frailer behaviour. By increasing the amount of impact modifier to 10% and 15%, all specimens showed the semi-brittle behaviour.

Table 5-5 Dropped weight impact properties of PHBV and PHBV/impact modifier

Specimens	Peak Force[N]	Peak Energy [J]	Total Energy [J]
PHBV neat	1673	0.68	4.87
PHBV97+IM3	3326	1.33	4.95
PHBV94+IM6	3359	2.14	5.22
PHBV90+IM10	1667	3.48	7.59
PHBV85+IM15	1834	5.07	9.44

It can be seen from table 5-5 that the peak force is increased from 1673 N to 3326 N and 3359 N with addition of 3% and 6% impact modifier respectively. However, the peak force dropped to 1667 N and 1834N with addition of 10% and 15% impact modifier. A logical explanation for the phenomena was difficult to find. Both the peak energy (J) and total energy (J) increased with the addition of the Biostrength impact modifier as expected. The total

energy (J) which indicates the energy absorbs by specimens and relative impact resistance is increased from 4.87 J for neat polymer to 9.44 J for specimens with 15% additive. It should be noted that the Biostrength impact modifier is designed for the toughening of polylactide acid (bio polyester) PLA. According to the manufacture it can increase the Gardner impact strength of PLA by more than 5 times with addition of 10 to 15% impact modifier. Similar improvement was not observed for the PHBV.

5.8 Scanning Electron Microscopy (SEM)

Images in Figure 13-5 are SEM images of impact fracture surfaces of the neat PHBV. They show a relatively smooth surface which could indicate that little plastic deformation had taken place during the impact test.

The SEM images in Figure 14-5 shows that the impact modifier particles (average size = 0.1-0.5μm) are distributed with nano-size inside the matrix of PHBV even at the low concentration of additives. The cracks can be clearly seen in the images and they are mostly in the areas far from the impact modifier particles, and they appear to be stopped by the IM particles (see Figure 14-5).

It can be seen in Figure 15-5 that, there are lots of small cracks in the matrix of polymer in area close to impact modifier particles and that the crack propagation is stopped by the IM particles. The particles are distributed homogenously in the matrix of polymer. However, there are lot of aggregated particles visible in the images. The number of these aggregated particles increased with an increase in the IM content. Wu et al (2015) stated that it is clearly observable in SEM images of PLA toughened by core-shell impact modifier that a portion of the core– shell dispersed in the form of smaller particles or agglomerates having a diameter from two to five times that of the primary (non-agglomerated) single particles. Wu et al mentioned that the agglomerations may be due to van der waals or electrostatic forces, or other mechanisms. The hard shell of the impact modifier made it very difficult to break them up. As a result, the core–shell rubber particles tend to be dispersed as a mixture of single particles and larger agglomerates (Wu et al, 2015).

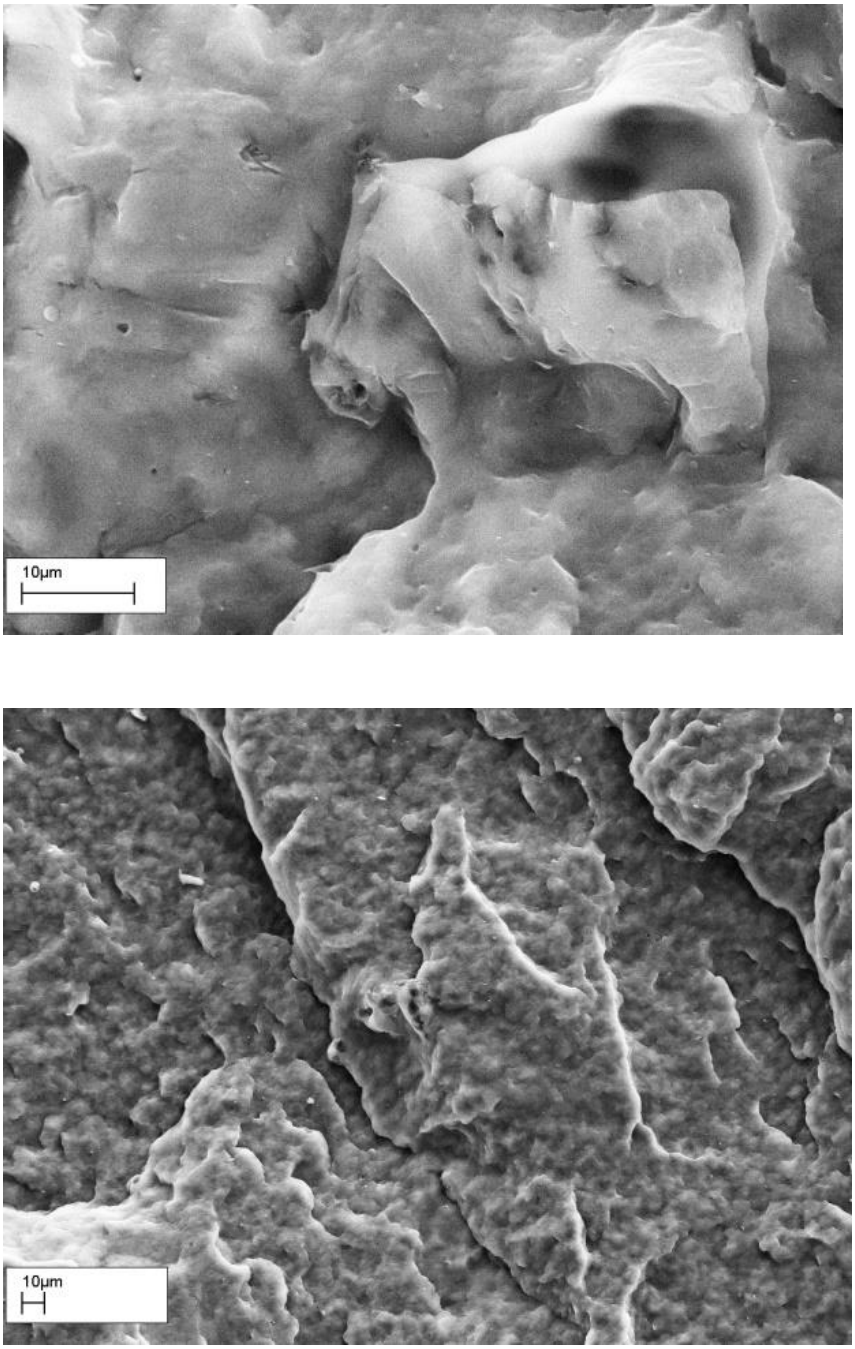

Figure 13-5 SEM images for PHBV neat with different magnifications

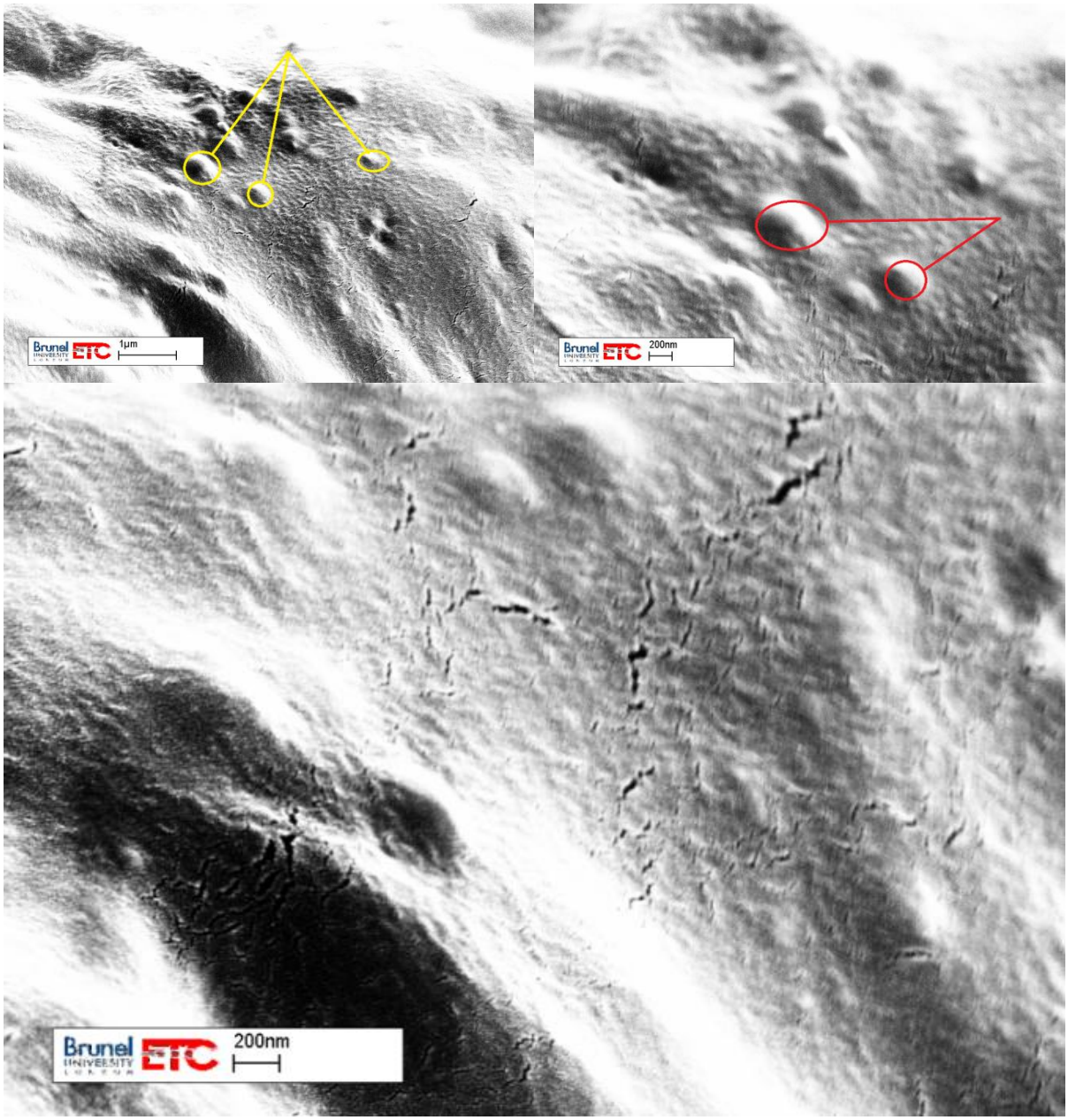

Figure 14-5 SEM images of PHBV97/IM3; the cracks are mostly in the areas far from the impact modifier particles

SEM images of PHBV90/IM10 with the different magnification are shown in figure15-5.

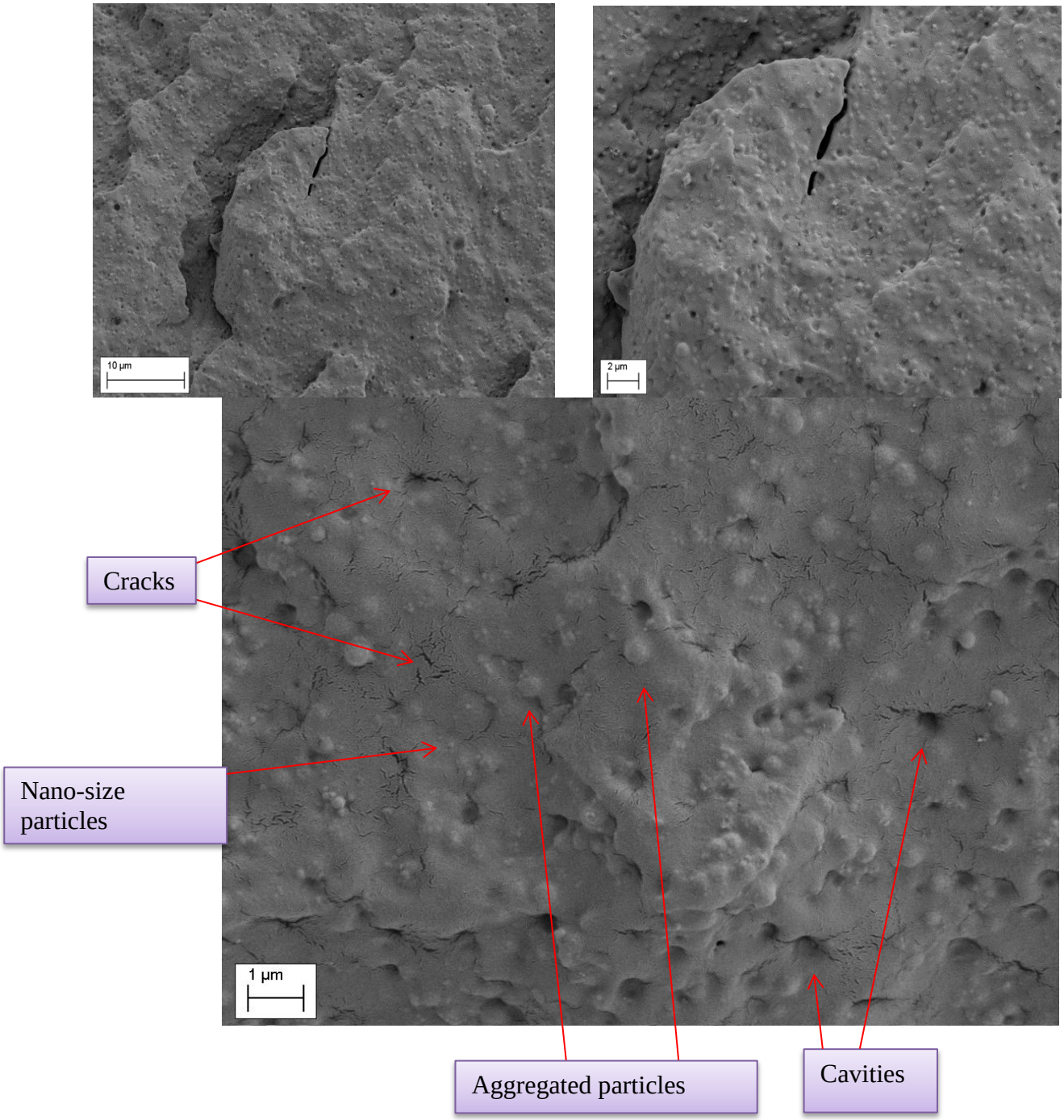

Figure 15-5 SEM images of PHBV90/IM10 fracture surfaces; the cavities and the aggregated particles and nano-size particles are shown on images. Prevention of cracks can be seen in areas close to cavities and particles.

This phenomenon is also observable in SEM images of PHBV/IM (Figure15-5). According to the additive data sheet, the Biostrength® 150 impact modifier has a primary particle size of

0.1 to 0.5 μm which was observed from all the SEM images. The aggregated particles size is not bigger than 0.5 μm (Arkema, 2013).

SEM images of PHBV85/IM15 with the different magnification are shown in figure16-5.

From images in Figure 15-5 and 16-5, many cavities can be observed in the SEM images of the PHBV/IM 90/10 and 85/15. The cavities indicate the lack of miscibility between the shell polymer (PMMA) and the matrix of PHBV. Moreover, the amount of agglomerated particles increased with an increase in the impact modifier from 10% to 15% *wt*. It is important therefore, to control an optimal ratio of additive considering that the mechanical properties might be dropped by increasing the IM amount while the impact resistance hadn't change significantly.

Generally, the effective performance of the core-shell particles depends on the adhesion to the matrix polymer or in another word, the miscibility and the interaction of the shell polymer with the matrix polymer. Cruz-Ramos stated that an inspection of the Flory-Huggins interaction parameter or the interaction energy density values is an effective method for assessing the performance of core-shell impact modifier on the toughening of a particular polymer. Therefore, a low value of the interaction parameter (or a negative interaction energy density) for the blend of the impact modifier and the polymer, indicative of miscibility, determines the effectiveness of the toughening.

According to Cruz-Ramos, the impact modifier's shell made of PMMA is very effective for toughening PVC, which is partially immiscible with PMMA. It is also effective with PC which is partially miscible with PMMA. On the other hand, the core-shell impact modifier with a PMMA as shell is less effective toughener for PBT. Moreover, no improvement in impact resistance could be seen in the case of PET and nylon due to their highly immiscibility of their blends with PMMA (Cruz-Ramos, 2000).

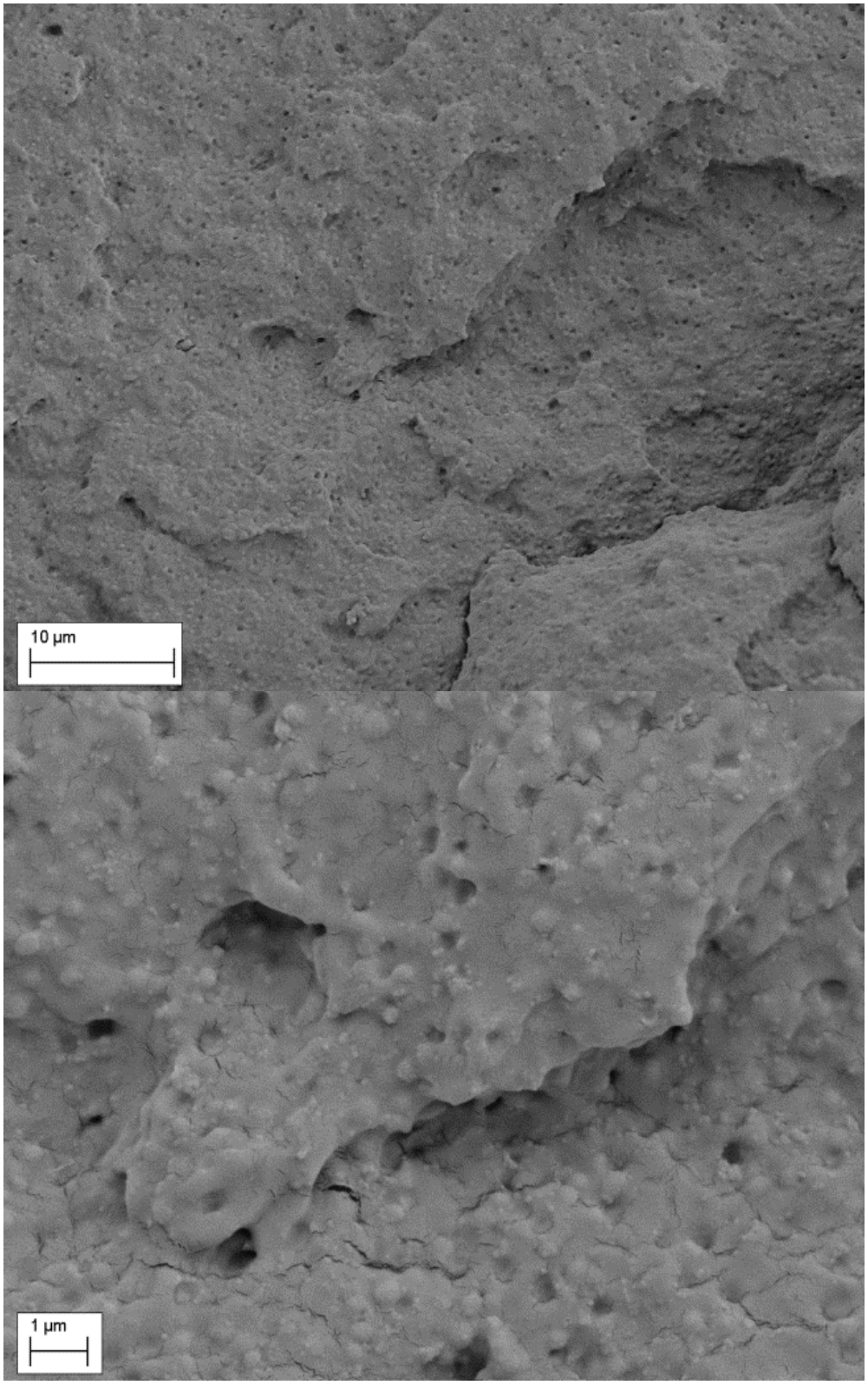

Figure 16-5 SEM images of PHBV85/IM15 fracture surfaces

5.9 Conclusion

Non-isothermal DSC results for PHBV and PHBV/IM showed a different type of melting peak at an approximately constant range of temperatures. The recrystallization peak of neat PHBV was changed with the addition of the IM and it moved to a higher temperature at the high concentrations of the impact modifier.

The isothermal Avrami results from the DSC measurement revealed that the time to maximum crystallization was temperature dependent. The addition of the impact modifier to the PHBV reduced the crystallization rate and prolonged the crystallization time.
The TGA results showed that the thermal stability of PHBV didn't significantly change in the presence of the impact modifier and the residue at 600 ℃ was similar for all the samples.
The DMA results showed a gradual decline in the storage modulus with an increase inthe impact modifier concentration. . All the tanδ's graphs showed one single peak which could correspond to the glass transition temperature of PHBV. These changed slightly with the different concentration of the impact modifier. Surprisingly, however the loss modulus results showed a clear peak which almost corresponded to the PMMA glass transition temperature (T_g^{PMMA} = 100 °C). From the loss modulus curves, it is clear that there are two T_g's in the graphs correspondent to PHBV and PMMA and they indicate the partial immiscibility between shell of impact modifier and the PHBV.

The mechanical properties revealed that the tensile strength of the blends increases first and then drops off at the higher concentrations of IM. The elongation at break increased with the addition of IM. On the other hand, a decrease was witnessed in the Young's modulus and flexural modulus with an increase of the amount of IM in the compounds.

The drop-weight impact modifier showed an improvement of the energy absorbed by the compounds, increasing with an increase in the amount of IM from 4.87 J for neat polymer to 9.44 J for specimens with 15% additive. However, the improvement was not as satisfactory as results for PLA.

Finally, the SEM images showed the average fine dispersion of different sized particles inside the matrix, from 0.1 to 0.5 μm, both single particles and aggregated particles were observed. The amount of aggregated particles increased with an increase in the impact modifier concentration in the compounds.

Bibliography Chapter 5

- Anonymous, (2013), “Biostrength® 150 and 280 impact modifier”, [online] available at: http://www.additives-arkema.com/export/sites/acrylicmodifiers/.content/medias/downloads/literature/biostrength-150-impact-modifier.pdf?_ga=1.148089271.1623741908.1488546459 (Accessed 21 Aug 2016)

- Avella, M., Calandrelli, L., Immirzi, B.,Malinconico, M., Martuscelli, E., Pascucci, B. and Sadocco, P. (1995), “Novel synthesis blends between bacterial polyesters and acrylic rubber: a study on enzymatic biodegradation”, Journal of Environmental Polymer Degradation, Vol. 3, No. I

- Bucknall, C. ,B. , (2000), “Characterizing Toughness Using Empirical Tests”, in book “Polymer Blends, vol2: performance, edited by Paul and Bucknall, 2000 John Willey & sons,Inc

- Corre, Y., M., Bruzaud, S. and Grohens, Y., (2013), “Poly(3-hydroxybutyrate-co-3-hydroxyvalerate) and Poly(propylene carbonate) Blends: an Efficient Method to Finely Adjust Properties of Functional Materials”, Macromolecular Materials and Engineering, Volume 298, Issue 11, pp. 1176–1183

- Cruz-Ramos, C., A., (2000), “Core-shell impact modifier”, in book “polymer blends, vol2: performance, edited by Paul and Bucknall, 2000 John Willey & sons,Inc

- Kayano, Y., Keskkula, H., & Paul, D. R. (1998). Fracture behaviour of polycarbonate blends with a core-shell impact modifier, Polymer, Vol 39, Issue 4, Pages 821-834

- Javadi, A., Kramschuster, A. J., Pilla, S., Lee, J., Gong, S. and Turng, L. S. (2010), "Processing and characterization of microcellular PHBV/PBAT blends", Polymer Engineering & Science, Volume 50, Issue 7, Pages 1440–1448

- Pan, P, Shan, G, Bao, Y and Weng, Z, (2012), "Crystallization kinetics of bacterial poly (3-hydroxylbutyrate) copolyesters with cyanuric acid as a nucleating agent", Applied polymer science, Volume 129, Issue 3, pp. 1374–1382

- Wu, L., Li, Z., Sun, S., Zhang, Y., Wu, D., Zhang, H., Dong, L., Deng, Y. and Zhang, H. (2015), "The Effect of Core–Shell Ratio of Acrylic Impact Modifier on Toughening PLA", Advances in Polymer Technology, 0, 21632, 10.1002/adv.21632

Chapter 6

The conclusion and future work

The work presented in this thesis gives some insight on the characterization behaviour of the PHBV reinforced by talcum powder as filler, blended with PBS in presence of a chain extender as compatibilizer and toughened by an impact modifier. In the future, this work can be extended and improved in the following areas:

- Improvement of the PHBV's processing window to avoid thermal degradation has been vital in this study. The issue arose when PHBV compounds were injection moulded and the compound stays slightly longer in machine's barrel. The issue was identified as the shrinkage or deformation of material at the edge of the dumbbell and plate specimens. The problem was dealt with by changing the processing temperature or injection speed parameters and making adjustments it in the injection moulding machine. It would be significant if systematic approaches are defined and conducted in the form of trial and error to obtain substantial experimental data from process.

- The results in this study showed that talcum powder acts as nucleating agent on PHBV by

    1. Altering significantly its sluggish crystallinity
    2. The reinforcing effect by improving its mechanical properties when talc is used as a filler (high concentrations).

    There are still not complete results for the measurment of the heat distortion temperature with DMA and crystalline structure study by XRD. Moreover, in the morphology study, analysis of the filler dispersion by using Edax in SEM, backscattered SEM and TEM could be suggested. Improved SEM machines also provided the better ability to measure the aspect ratio of filler. It would be

recommended to compare the experimental mechanical results with the other theoretical methods such as Kelly and Tyson's or the modified rule of mixture models.

- The results of this study showed that PHBV and PBS miscibility could be exponentially enhanced by the incorporation of a chain extender. It has been proposed that the chemical interaction of an additive functional group could be the reason of that enhancement, whether it happened by forming graft polymers or by forming a di-block copolymer at the interfacial phases. However, Raman spectroscopy and Microscopic FTIR could provide more information about the interaction. The next step could be examination using different substances containing reactive functionality groups rather than an expensive commercially chain extender. More elaborate study of crystal impingements at PHBV/PBS blends is also suggested to understand more deeply the crystallization kinetic in the blend of two bioplastics.

- During this study, the effect of an encapsulated core-shell impact modifier in different properties of PHBV has been studied extensively. The results have shown that the effectiveness of the impact modifier is strongly dependent on the miscibility condition between the matrix polymer and the impact modifier's shell polymer. Therefore, it will be suggested in order to improve the miscibility a coupling agent, different compatibilizers or even chain extenders could enhance the miscibility between two polymers (PHBV and PMMA) and consequently the impact performances of PHBV. Additionally, the FTIR and Raman technique could be used to analyse the qualitative interaction between substances in the compound. Furthermore, a deep analysis of the different impact test (Charpy, Izod and Drop-ball) and comparing of the results would help to understand the effect of this modifier more efficaciously.

- There are several possible applications for the resin of PHBV developed in this study. It can be mentioned from the thermoforming/injection moulding packaging containers to bone tissue scaffolds or drug delivery systems. Using new technologies and especially plastic additive manufacturing (AM) such as 3D printing, fused deposition modelling, selective laser sintering, stereolithography and 3D plotting are suggested for further study of these innovative materials.

Bioplastics are the material of the future. The widespread usage of this material is strongly dependent to its performances inside sustainability development components. The new technologies empower the bioplastic industry to find their applications and environmental awareness that helps the society embrace further concepts before the depletion of resources or environmental disasters (waste plastic in the world's seas has been recognised by the United Nations as a major environmental problem*) impose the transformation. However, an ideal alliance between plastics from non-renewable and renewable resources will bring a sustainable balance especially with the new developments in the recycling technology.

Errors and limitation

Experimental error is always with us; it is in the nature of scientific measurement that uncertainty is associated with every quantitative result. This may be due to inherent limitations in the measuring equipment, or of the measuring techniques, or perhaps the experience and skill of the experimenter.

The present author has considered his results for accuracy, precision, limit of detection, and selectivity. These have been discussed with the results obtained where necessary. However, a summary is given in Table 1-6 and 2-6.

Table 1-6 Instrumental errors and accuracies

Technique	Error/Accuracy/Limitation
Extrusion	Temperature zones: ± 10 ℃, Screw speed: ± 40 rpm
Injection moulding	Temperature zones: ± 10 ℃, Mould temperature: ± 5 ℃, Injection pressure: ± 15 bar, Cooling time: ± 10 sec
TGA	T_1: ± 1 ℃, Residue at 600 ℃: ± 2%
Mechanical properties	Tensile strength: ±3.5 MPa, elongation at break: ±4%, Elasticity Modulus: ± 0.3 GPa, Flexural modulus: ± 0.5 GPa
Impact properties	The errors varied in different aspects of the impact properties (peak force and etc.). All standard derivations are illustrated in the result and discussion sections.

Table 2-6 Instrumental errors and accuracies

Technique	Error/Accuracy/Limitation
DSC/Avrami's	The Avrami equation represents data at low degree of conversion. The fit at higher degree of conversion is poor. Therefore, the exponents are obtained from the slope of the very initial linear part of the curve. However, the amount of k and $t_{0.5}$ critically depend on the range selected. Generally Deviations from Avrami relationship: • a) Data fits portions of an Avrami plot with integer values, but deviates at high conversion. b) Avrami type plots show a linear fit over all conversions but have non-integer values of slope • Type 'a' deviations can be explained by having at least two different kinds of crystal growth. 1) different nucleation mechanisms 2) different kinds of spherulite 3) rod to disk to spherulite conversion Type 'b' deviations are inconsistent with theory.**
Aspect ratio by SEM	10% error
XRD	There are uncertainly about the measuring of the crystallinity percentage by XRD.
DMA	E_a : ±35 kJ/mol , T_g : ±5 ℃

*: UN Environment, 2017, available online at: http://www.rona.unep.org/un-declares-war-ocean-plastic Accessed at 23/2/2017

** Pen state, Available online at: http://www.personal.psu.edu/irh1/PDF/Kinetics.pdf

Poster presented at the Graduate School Poster conference 2013, Brunel University - Vice Chancellor's prize

Viva examination panel: (from left) Prof. Paul A. Sermon, Dr. Noreen Thomas, Me, Prof. Jack Silver